YTTRIUM AMIDATE COMPLEXES: FUNDAMENTAL REACTIVITY AND
APPLICATIONS IN CATALYSIS AND POLYMERIZATION

by

Louisa Janet Easton Stanlake

B.Sc. (Honours), University of Victoria, 2003

A THESIS SUBMITTED IN PARTIAL FULFILLMENT OF
THE REQUIREMENTS FOR THE DEGREE OF

DOCTOR OF PHILOSOPHY

in

The Faculty of Graduate Studies

(Chemistry)

THE UNIVERSITY OF BRITISH COLUMBIA
(Vancouver)

October 2008

Abstract

Rare-earth complexes are attractive catalyst systems due to their low cost, low toxicity and high reactivity. Modular ligand sets are ideal for complex formation since the steric and electronic properties of the resultant metal complexes can be easily varied. This thesis explores the structure and reactivity of new yttrium amidate complexes, which combine the highly reactive metal with the modular amidate ligand set. A library of tris, bis and mono(amidate) yttrium complexes have been directly synthesized from yttrium tris(trimethylsilyl)amidate and simple amide proligands.

The tris(amidate) yttrium complexes are highly active initiators of ring-opening polymerization of ε-caprolactone, yielding some of the largest molecular weight values for poly(ε-caprolactone) reported. The initiation of this polymerization is proposed to be ligand initiated; however, a side-reaction is postulated where formation of a ε-caprolactone-enolate yttrium complex results in broad polydispersity values of the resultant polymers.

The bis(amidate) yttrium complexes are also excellent precatalysts for the hydroamination of aminoalkenes. Simple modification to the amidate backbone to include electron-withdrawing groups was found to significantly enhance reaction efficiency. These catalysts can mediate cyclohydroamination with both primary and secondary amine containing substrates.

The mono(amidate) yttrium complexes were also investigated as novel precursors for the synthesis of the elusive terminal yttrium imido complex. Mixed anilido/amidate yttrium complexes were synthesized in high yield and α-H abstraction and deprotonation reactions were attempted in the hopes of isolating a crystalline compound. The addition of

monodentate and neutral donors was required for isolation and characterization of the key reactive intermediates.

This new family of yttrium complexes has proven to be very successful in preliminary catalytic studies. The ease with which the complexes can be synthesized and their steric and electronic properties make these complexes ideal for further catalytic investigations.

Table of Contents

List of Tables

List of Figures

List of Abbreviations

[M]/[I]	Monomer to initiator ratio
~	Approximately
>	Greater than
°	Degree symbol
° C	Degrees Celsius
‡	Transition state
Å	Angstrom
acac	Acetylacetonate
Anal.	Analysis
Ar	Aryl
atm	Atmosphere
b	Broad (NMR or IR spectrum)
bipy	2,2'-Bipyridine
Calcd.	Calculated
cat.	Catalyst
cm^{-1}	Wavenumber
conv.	Conversion
Cp	Cyclopentadienyl
Cp*	Pentamethylcyclopentadienyl
Cp'	Methylcyclopentadienyl
Cy	Cyclohexyl
δ	*Delta*, chemical shift
d	Doublet
DCM	Dichloromethane
ΔG	Gibbs Free Energy
Dipp	Diisopropylphenyl
Dmp	Dimethylphenyl
dr	Diastereomeric ratio
E	Energy

ε	Molar absorptivity
EI	Electron impact
equiv.	Equivalents
g	Gram
gem	Geminal
GPC	Gel permeation chromatography
h	Hours
HSAB	Hard-Soft Acid-Base Theory
Hz	Hertz, s^{-1}
I	Initiator
iPr	*iso*-propyl
IR	Infrared
J	Coupling constant
K	Kelvin
kcal	Kilocalorie
kJ	Kilojoules
L	Ligand
LLCT	Ligand to ligand charge-transfer
LLS	Laser-light scattering
λ_{max}	Maximum wavelength
LMCT	Ligand to metal charge-transfer
Ln	Lanthanide
m	multiplet (NMR spectroscopy)
M	Metal
M	Molar
M	Metal
m/z	Mass to charge ratio
M^+	Molecular ion
Me	Methyl
mg	Milligrams
MHz	Megahertz

min	Minute
mL	Millilitres
μL	Microlitre
MLCT	Metal-ligand charge transfer
mmol	Millimole
M_n	Number-average molecular weight
mol	Mole
mol%	Mole percent
MS	Mass spectrometry
M_w	Weight-average molecular weight
n	Number (integer)
ν	Frequency
Nap	Naphthyl
n-Bu	*n*-Butyl
nm	Nanometre
NMR	Nuclear magnetic resonance
NR	No reaction
o	*Ortho*
ORTEP	Oakridge Thermal Ellipsoid Program
p	*Para*
P	Polymer
PDI	Polydispersity Index
Ph	Phenyl
ppm	Parts per million
R	Aryl or alkyl substituent
R	*Rectus* (Configurational)
RDS	Rate-determining step
ROP	Ring-opening polymerization
rt	Room temperature
s	Strong (IR spectrum)

s	Singlet (NMR spectroscopy)
sec-butyl	Secondary-butyl
sh	Sharp, Shoulder (IR spectrum)
t	Triplet (NMR spectroscopy)
tBu	*tert*-Butyl
temp.	Temperature
THF	Tetrahydrofuran
TPPO	Triphenylphosphine oxide
™	Trademark
w	Weak (IR spectrum)
Xy	Xylide

Foreword

The work reported in this thesis involves the investigation of novel yttrium amidate complexes. This thesis is a manuscript-based thesis, where each chapter is considered as a stand-alone document. Consequently, there will be some reiteration of introductory information within separate chapters. Furthermore, there are several compounds that are used throughout the entire thesis; however, numbering is consistent within each chapter and therefore some compounds will be linked to more than one number in this thesis.

Acknowledgements

First and foremost I would like to thank Dr. Laurel Schafer for all the support over the years. I truly appreciate that she always treated me like an equal, and always made me believe in my abilities. The Schafer lab is one of the best environments that I have ever worked in and I owe great gratitude to the Schafer group members, past and present. I especially have to thank Dave for the great chemistry discussions, the introduction into quality music, and for spending the time to read this thesis.

I would like to thank the mechanical shop, the electronics shop, the glassblower, the NMR staff and the analytical staff; especially Ken Love for spending countless hours helping fix a troublesome glovebox. I would also like to thank Brian Patrick, Rob Thomson, and Neal Yonson for assistance with X-ray crystallography. Also, thank you to the chemistry department and MEC for funding during my Ph. D. studies.

Girlfriends, wine, and ANTM are a great stress reliever, so thanks to "team models" (Ali, Bronwyn, Courtney, Jenn, Jackie and Shiva) for taking the edge off, and always being there over the years. Thanks to Howie, for always making your "appearance" and to Mark, for always keeping me entertained.

I would like to thank my parents, who were right when they told me that graduate school would be the best time of my life. I also appreciate their great support, financially and psychologically throughout my Ph. D. I have to thank my brother and his family, Mel and K-Dub, for believing in me. Also, thank you to Jesse, for all your love and support and for trying really hard to understand what I do.

Co-Authorship Statement

All of the work contained herein was performed by Louisa J. E. Stanlake, except for the synthesis of compound **2.17** in Chapter 2, which was synthesized by J. David Beard. Consequently, J. David Beard is a co-author on the published paper, Rare-Earth Amidate Complexes. Easily Accessed Initiators For ε-Caprolactone Ring-Opening Polymerization. Louisa J. E. Stanlake, J. David Beard and Laurel L. Schafer, *Inorg. Chem.* **2008**, *47*, 8062. Laurel L. Schafer is the principle investigator for this work and assisted with identification and design of the research program, data analyses, and manuscript preparation; however, she did not assist in any experimental research within this thesis.

Chapter 1. Amidates as Tunable Ligand Set for Group 3 Metals

1.1 Ligand Design for Group 3 Metal Catalysts

In 1893 Alfred Werner postulated the "coordination theory" for bonding to explain the structure of a cobalt ammine complex, $CoCl_3 \cdot 6NH_3$. He proposed an octahedral cobalt complex with six NH_3 "ligands" at the vertices, and the chloride groups as counter ions (**1.1**, Figure 1.1). This theory garnered him the Nobel Prize in Chemistry in 1913. Since then, the term "ligand" has been synonymous with coordination chemistry.[1,2]

$$\left[\begin{array}{c} NH_3 \\ H_3N,,,\underset{Co}{\overset{|}{}} ,,NH_3 \\ H_3N^{\blacktriangleleft}\overset{|}{}^{\blacktriangleright}NH_3 \\ NH_3 \end{array} \right]^{3+}$$

1.1
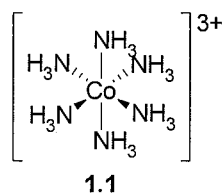
Figure 1.1. The cobalt ammine coordination complex proposed by Werner.

A ligand (L) is any molecule or atom that is bound to a central metal centre. A ligand can be monodentate, bridging or chelating. A chelating ligand has more than one atom bound to a metal centre. The bonding to the metal can be more ionic, or more covalent in nature depending upon the metal and ligands involved. Ligands that contain "hard" atoms, such as oxygen, tend to bind to hard metal centres, while the opposite is true for low oxidation state late transition metals that are best described as "soft" metals. These trends are in accordance with hard-soft acid base (HSAB) theory.[3]

Group 3 metals are hard metals and tend to bind hard donors. Furthermore, group 3 catalysts are almost exclusively in the 3+ oxidation state, and are best described as having an ionic bonding motif.[4-6] This 3+ oxidation state is the major difference between group 3 metals and the rest of the transition metal block. Most transition metals have a range of

oxidation states, whereas group 3 only exhibits the +3 (d^0) oxidation state. Yttrium is very similar in reactivity to the lanthanide metals and is often referred to as a "rare-earth" (a term used to include group 3 and the lanthanide metals in one group). Yttrium has a similar ionic radius to some lanthanides (for example, Y^{3+} = 1.04 Å, Nd^{3+} = 1.12 Å, Gd^{3+} = 1.07 Å, Er^{3+} = 1.00 Å, Lu^{3+} = 0.977 Å),[7] and is frequently included in reviews of lanthanide chemistry.[8-13] Group 3 or rare-earth complexes are very attractive catalyst systems due to their low toxicity, low cost and high reactivity,[14] and are often used in catalysis and are used in reactions such as, hydroamination,[15] hydrogenation,[5,6] hydrosilylation,[16-18] aldol condensation[10,11] as well as polymerization of olefins,[19] lactones and lactides.[20,21]

Like the lanthanides, yttrium often has very high coordination numbers, up to 9.[22-24] Complex formation and reactivity between yttrium and the smaller lanthanides also are very similar. However, one significant difference is that yttrium is diamagnetic, which renders NMR spectroscopy useful in the ch aracterization of compounds, and the monitoring of catalytic reactions. Early research into yttrium complexes was dominated by cyclopentadienyl complexes,[15-34] but easily accessed and modular ligand sets are becoming more common for the optimization of catalytic activity.[25] In this introduction only easily varied complexes of yttrium that have been exploited in various catalytic applications will be reviewed.

1.2   Non-cyclopentadienyl Ligand Systems for Group 3 Metals

Yttrium complexes containing cyclopentadienyl-based ancillary ligands are very common.[8,26-58] The chemistry involving these complexes has been explored extensively for mainly olefin polymerization,[29,32,39,40,49,52] but also polar monomer polymerization,[38,57] and

other catalytic processes such as hydrosilylation[28,42,50] and hydroamination.[15] However, the cyclopentadienyl ligand is not a modular ligand set, and can be synthetically difficult to functionalize. Due to limited synthetic flexibility, ligand sets that allow for easy modification of steric and electronic properties are attractive in group 3 complex synthesis. An auxiliary ligand that can be varied for tunable reactivity in the resultant complex is an ideal feature for catalyst design. There is a wide variety of ligand sets that are used in the synthesis of yttrium complexes that include monodentate ancillary ligands such as amido,[59-62] alkoxides,[63-65] bidentate (*vide infra*), tridentate and tetradentate ligands.[66-74] Bidentate modular ligand sets are common and include aminotroponimates (**1.2**),[75-77] aminotroponates (**1.3**),[78] β-diketiminates (**1.4**),[79-86] acetylacetonates (**1.5**),[87-90] bisoxazolinates (**1.6**)[91,92] alkoxydimethylsilylamides (**1.7**),[93,94] phosphoramidates (**1.8**),[95-97] amidinates (**1.9**),[98-109] guanidinates (**1.10**),[110-118] and salicylaldiminates (**1.11**)[80,119-122] (Figure 1.2). This thesis explores the synthesis and reactivity of yttrium amidate (**1.12**) complexes; however, up until now, these complexes have never been systematically explored for their reactivity in either stoichiometric or catalytic investigations.
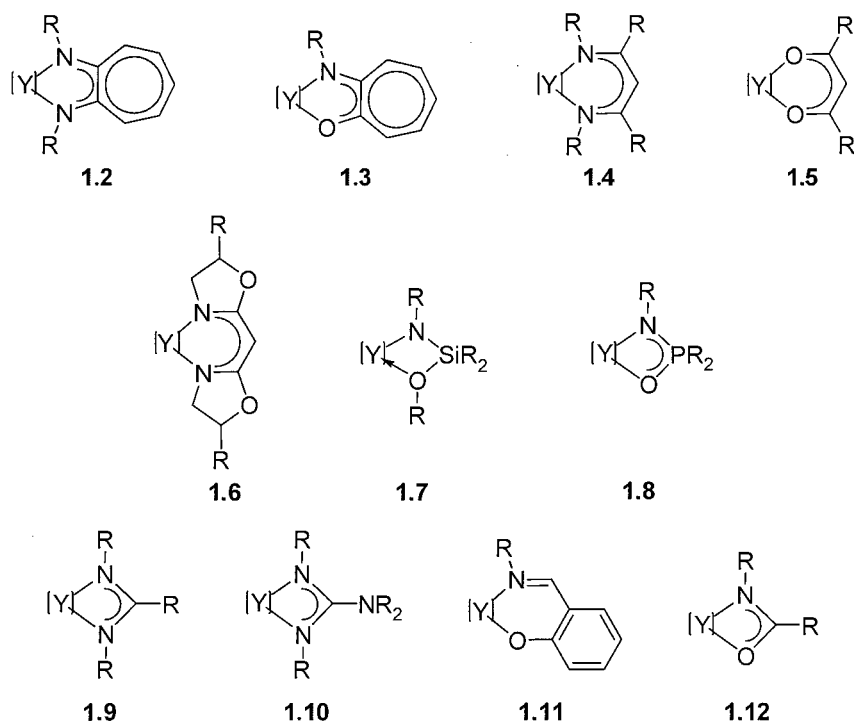
Figure 1.2. Selected examples of ligands that have been used in yttrium complex synthesis. (R = aryl or alkyl substituent)

The ligands shown in Figure 1.2 are all monoanionic ligand sets and many of these ligand sets are modular, where the R groups can be easily changed during the synthesis of the ligand. Most of these ligand sets use N and O donors, because of the desirable hard-hard match with yttrium. Furthermore, examples of four (**1.7, 1.8, 1.9, 1.10** and **1.12**), five (**1.2** and **1.3**) and six-membered (**1.4, 1.5, 1.6** and **1.11**) rings are observed in the yttrium metallacycles formed upon chelation. There is a vast number of ligand sets and recent reviews of this field are available.[10,15,19,25,123,124] Yttrium amidinate (**1.9**), guanidinate (**1.10**) and salicylaldiminate (**1.11**) complexes are known and display important structural similarities to the proposed amidate complexes. Previous to the work of this thesis, there were no examples of yttrium amidate complexes for comparison; however, these similar ligand sets provide useful benchmarks for reactivity trends. In particular, the amidinate and

4

guanidinate ligand sets have been studied for yttrium complex formation, and provide useful comparisons to the work presented in this thesis because they have a similar binding motif to the amidate. The salicylaldiminate ligand will also be reviewed because it is a popular N,O chelate for yttrium, and shares the asymmetric N,O donor atoms of the proposed amidate ligand.

1.3   Amidinate Complexes of Yttrium

Although amidinate complexes of yttrium can be formed *in situ*, by insertion of a carbodiimide into a reactive Y-C bond,[108] a direct route where the amidinate lithium salt is first isolated is more commonly used. The amidinate ligand is directly synthesized from a carbodiimide (R-N=C=N-R) (Figure 1.3) and a lithium reagent, alkyl, aryl or silyl. The amidinate salt can be reacted directly in a salt metathesis reaction with yttrium trichloride. The amidinate salt can also be protonated with water to form the amidine to yield the corresponding proligand for a protonolysis reaction with various yttrium starting materials to give the yttrium amidinate complexes. The protonolysis route was used in the synthesis of mono(amidinate) complexes **1.13** and **1.15**. These complexes were fully characterized and explored for their application in olefin polymerization[99] (for complex **1.13**) and hydrosilylation[103] (for complex **1.15**) (*vide infra*). Furthermore, Hessen and coworkers found that the ligand in complexes **1.13** and **1.15** is able to support cationic complexes for a range of group 3 and lanthanide metals (Sc, Lu, Y, Gd, Nd, and La).[100]
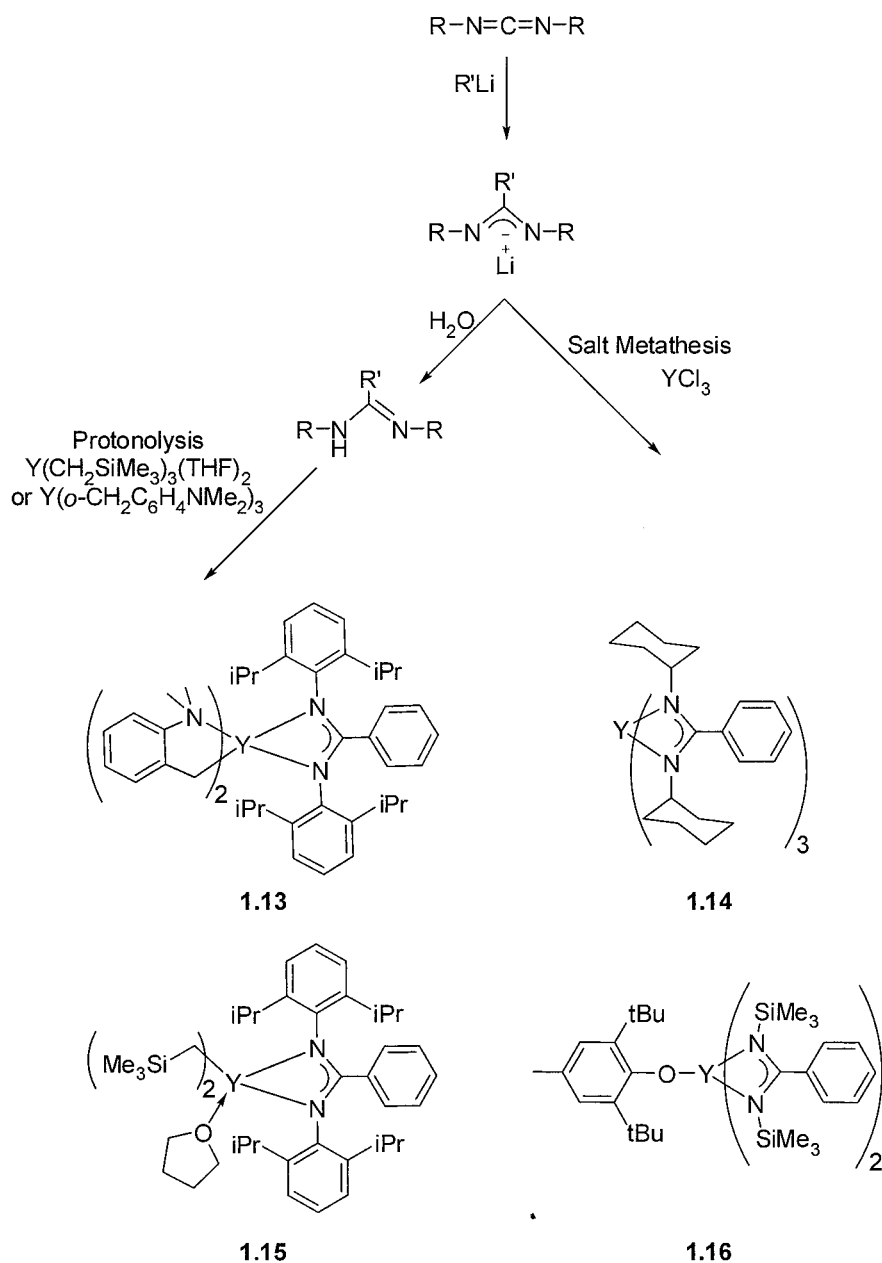
Figure 1.3. Synthesis of selected amidinate yttrium complexes.

The salt metathesis route was used in the formation of yttrium amidinate complexes **1.14**

and **1.16**. In the case of complex **1.16**, the bis(amidinate)mono(chloro) complex was first

synthesized and then used in a metathesis reaction with phenoxide salt to form complex

1.16.[98] Both complexes **1.14** and **1.16** have been explored for the ring-opening polymerization of lactones (*vide infra*).[98,105]

Hessen and coworkers have synthesized variations of tethered amidinate ligands for complex synthesis with yttrium (Figure 1.4).[101,102] The tethered bis(amidinate) ligand in complex **1.18** changes the orientation of the amidinate groups in the resultant complex giving it a more open metal coordination sphere in comparison to un-tethered bis(amidinate) complexes.[102] Shen and coworkers[107] used complex **1.18**, first synthesized by Hessen and coworkers, to form the bridged yttrium dimer **1.19**. This complex was studied for its ability to initiate the ring-opening polymerization of ε-caprolactone (*vide infra*). An alternative tethered ligand motif, the amino-amidinate ancillary ligand in complex **1.20** gives additional electronic stabilization to a highly electropositive metal centre.[101] Without this extra stabilization, a mono(amidinate) complex was difficult to synthesize due to ligand redistribution side-reactions.[101]
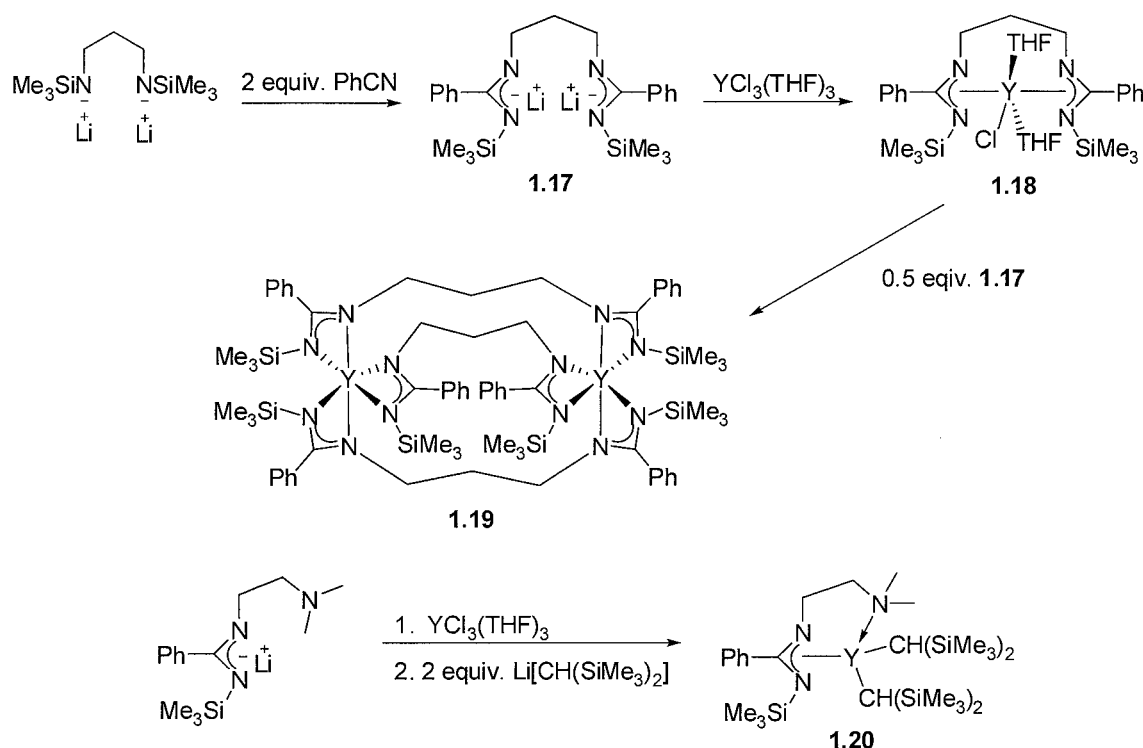
Figure 1.4. Synthesis of yttrium amidinate complexes with either a bridging amidinate or amido donor.[101,102]

These selected examples illustrate that mono, bis and tris(amidinate) complexes of yttrium can be synthesized directly with varying substituents. Tethered amidinate ligands can be used to isolate either monomeric or dimeric species. Furthermore, by modifying the amidinate ligand to include an amino donor, isolation of a solvent free alkyl yttrium complex is possible (complex **1.20**). The yttrium amidinate complexes presented here have been studied for hydrosilylation, as well as olefin and ring-opening polymerization.

Hydrosilylation is the addition of an Si-H bond across a C-C unsaturation and can be mediated by a wide range of transition and lanthanide metals including yttrium complexes.[16-18] For example, only 2 mol% of mono(amidinate) bis(alkyl) yttrium complex **1.13** (Figure 1.5)[103] in the reaction of phenylsilane with a variety of alkenes (R = butane, hexane,

8

cyclohexyl, cyclohexene, *tert*-butyl) results in nearly 100% yield of the linear hydrosilylation product in less than 5 minutes at 23 °C. Complex **1.13** has a notably higher turnover rate (> 600 h^{-1}) for this transformation when compared to other rare-earth or early transition metal catalysts.[103]
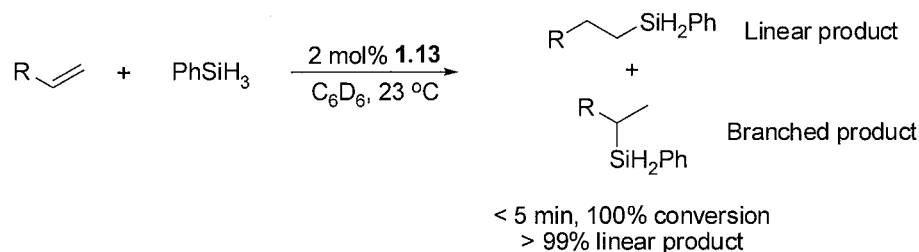
Figure 1.5. Hydrosilylation using complexes **1.13** as catalyst.[103]

The polymerization of substituted alkenes, such as isoprene, is not as well-developed for rare-earth catalysts as ethylene polymerization.[109] Interestingly, alkyl amidinate complexes have been explored for the polymerization of isoprene.[109] Complex **1.14** can be activated by [Ph$_3$C][B(C$_6$F$_5$)$_4$] and reacted with isoprene to give greater than 90% selectivity of *iso*-3,4-poly(isoprene). This polymerization at room temperature results in 100% yield of *iso*-3,4-poly(isoprene), and narrow polydispersity values (1.30). Interestingly, if complex **1.14** is first reacted with trimethylaluminum and then [Ph$_3$C][B(C$_6$F$_5$)$_4$] is added, polymerization of isoprene results in greater than 90% selective formation of *cis*-1,4-poly(isoprene). This polymerization at room temperature also results in 100% yield, and narrow polydispersity values (1.50 − 1.70). By a small change in the activation step, two different types of poly(isoprene) can be selectively formed using the same yttrium amidinate complex.
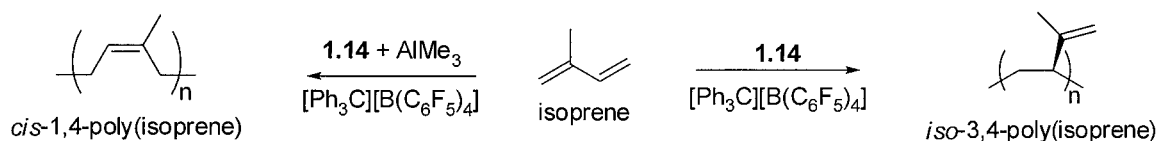
Figure 1.6. Isoprene polymerization using amidinate yttrium complex **1.14**.[109]

Another popular application of rare-earth complexes is the initiation of the ring-opening polymerization (ROP) of lactones. The most used monomers are lactide and ε-caprolactone, which both produce biodegradable polyester after ROP. Phenoxide amidinate yttrium complex **1.15** and bridging amidinate yttrium dimer **1.19** have been explored for the ROP of D,L-lactide and ε-caprolactone, respectively (Figure 1.7).[98,107] Both complexes give high-yielding polymer with very high molecular weights and moderate polydispersity indices. A more detailed overview of ROP using a range of yttrium complexes will be presented in Chapter 3.
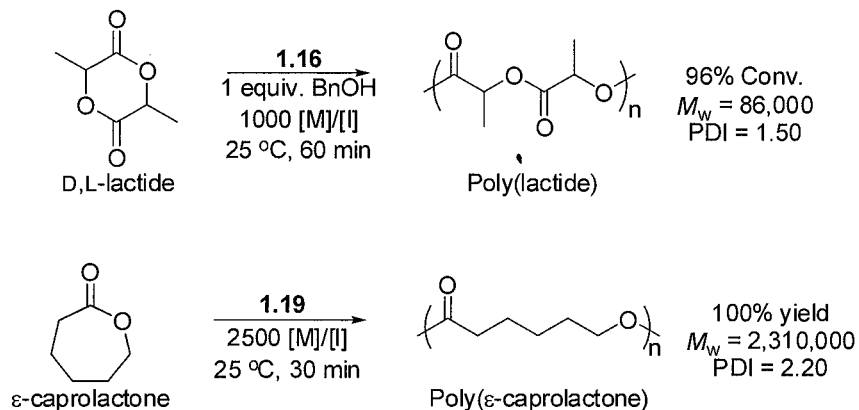
Figure 1.7. Lactone ring-opening polymerization examples.

Amidinate complexes of yttrium can be synthesized in two different ways starting from carbodiimides, salt metathesis or protonolysis. Selective formation of mono, bis or tris

amidinate yttrium complexes is readily achieved through control of reaction stoichiometry. Modifications to form tethered amidinates are reported to give a range of monomeric and bridged bimetallic complexes.

The amidinate complexes of yttrium have been used in multiple catalytic applications including, hydrosilylation of alkenes, polymerization of isoprene and the ROP of lactones. These results demonstrate the usefulness of a readily accessed, modular, ancillary ligand set for yttrium. Furthermore, they illustrate that 4-membered metallacyclic complexes formed upon chelation are sufficiently robust for a range of catalytic reactions.

1.4 Guanidinate Complexes of Yttrium

The guanidinate ligand is very similar to the amidinate ligand, except for the addition of a NR_2 group to the backbone (Figure 1.8). The synthesis starts from a carbodiimide molecule, and a lithium amide reagent is added to obtain the guanidinate lithium salt. Synthesis of complexes is most often performed via the salt metathesis route. It is evident that the guanidinate ligand can support different types of yttrium complexes including chloro (**1.21**),[114,115] aryl (**1.22**),[114] alkyl (**1.23**),[114] alkoxide (**1.24**)[110] and amido (**1.25**) complexes.[116]

R
|
N
‖
C
‖
N
|
R

$\xrightarrow{\text{LiNR'}_2}$

R
|
N
R'$_2$N—C(—⁺Li)
N
|
R

$\xrightarrow{\text{YCl}_3}$

1.21 R = Cl
1.22 R = Ph
1.23 R = tBu

R—Y[N⟩—N(SiMe$_3$)$_2$]$_2$

1.24 R = OiPr
1.25 R = NiPr$_2$

R—Y[N(iPr)⟩—N(SiMe$_3$)$_2$]$_2$
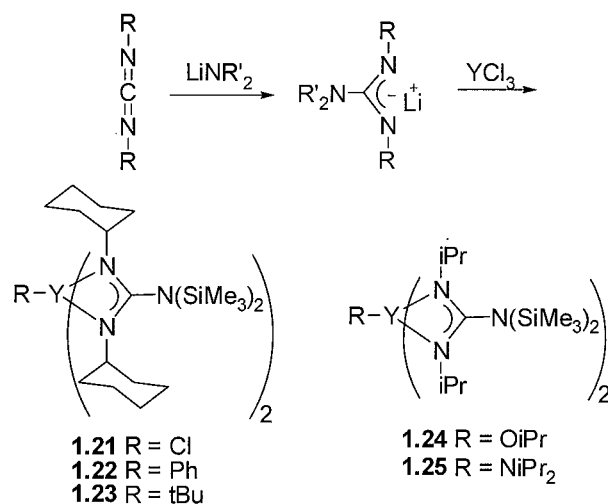
Figure 1.8. Synthesis of selected guanidinate yttrium complexes.

These complexes can be used as starting materials for a variety of catalytic investigations. For example, complex **1.21** can be used in a metathesis reaction to form an yttrium alkyl complex **1.26** (Figure 1.9). This alkyl complex can then be reacted with a hydride source to form the guanidinate supported yttrium hydrido complex **1.27**.[112] This is a rare example of a well-characterized non-cyclopentadienyl hydrido complex of yttrium,[112] and shows that the guanidinate ligand set is capable of providing the steric and electronic environment that is comparable to the cyclopentadienyl ligand. Furthermore, preliminary experiments with hydrido yttrium complex **1.27** show it can be used as a moderately active ethylene polymerization catalyst.[112]

As in the case of amidinate yttrium complexes, guanidinate yttrium complexes can be used in a vast range of catalytic reactions, including the ROP of lactones.
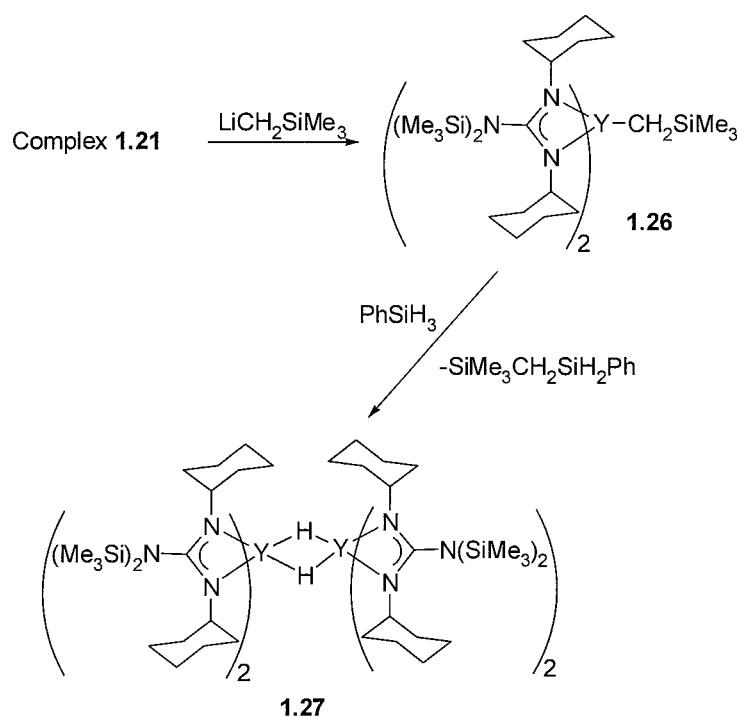
Figure 1.9. Synthesis of yttrium hydrido complex supported by guanidinate ligands.

Selected recent examples of ROP of D,L-lactide[110] and ε-caprolactone[116] are shown in Figure 1.10. The alkoxide complex **1.24** produces poly(lactide) in high yield with narrow polydispersity values in mild conditions. The amido complex **1.25** produces poly(ε-caprolactone) in high yield with very large molecular weights. Interestingly, in comparison with amidinate yttrium complexes, guanidinate examples show reduced poly(lactide) polymer molecular weights yet comparable poly(ε-caprolactone) molecular weights. These selected examples provide a useful point of reference for comparing and contrasting the amidate yttrium complexes investigated here.

1.24
100 [M]/[I]
20 °C, 3 h

98% Yield
M_w = 14,500
PDI = 1.50

D,L-lactide

Poly(lactide)

1.25
1000 [M]/[I]
15 °C, 5 min

100% yield
M_w = 2,430,000
PDI = 2.36

ε-caprolactone

Poly(ε-caprolactone)
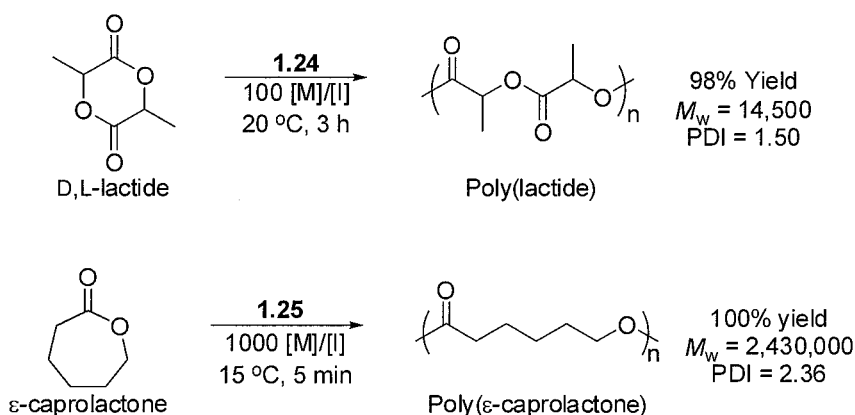
Figure 1.10. ROP of lactones using guanidinate supported yttrium complexes.

In Summary, guanidinate ligands are similar to the amidinate ligand set, but have -NR$_2$ group in the backbone. Yttrium guanidinate complexes are typically synthesized via salt metathesis and a wide range of bis(guanidinate) yttrium complexes can be synthesized, such as chloro, alkyl, aryl, alkoxide and amido species. Interestingly, yttrium hydrido complexes have been reported for this class of complexes. Another major application of guanidinate yttrium complexes is the ring-opening polymerization of selected lactones.

1.5 Salicylaldiminate and Dialkoxy-Diimino Complexes of Yttrium

Another N,O-chelating ligand for yttrium chelation is the salicylaldiminate. This ligand motif has the similar N,O-asymmetric binding motif to the amidate ligand. In contrast to the amidinate and guanidinate ligands, the salicylaldiminate ligand forms a 6-membered ring upon chelation, and has much less bulk close to the metal centre after binding (resulting from the binding of an O instead of NR group) than either amidinate or guanidinate complexes. The salicylaldiminate proligands can be synthesized from the condensation reaction between hydroxyl substituted benzaldehyde and substituted aniline compounds.[125] Salicylaldiminate

proligand **1.28** has been extensively used by Piers and coworkers for the synthesis of new yttrium salicylaldiminate compounds (Figure 1.11).[119]
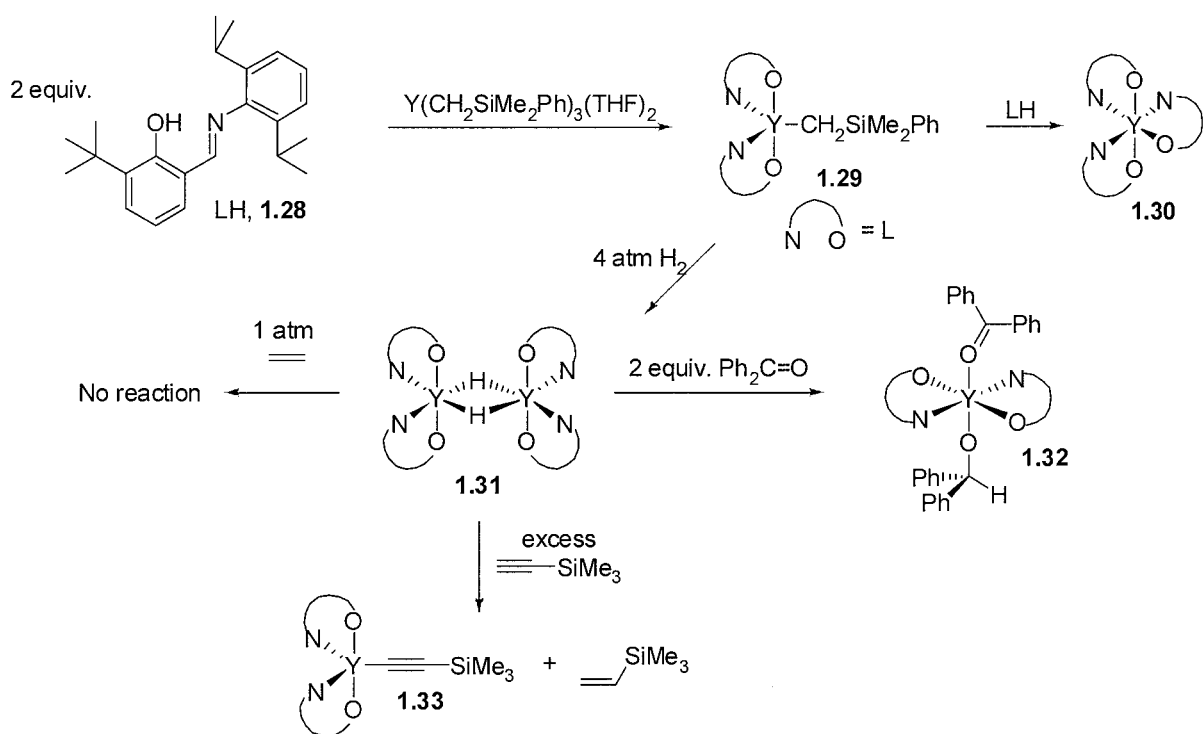
Figure 1.11. Synthesis and reactivity of yttrium salicylaldiminate complexes.[119]

Bis(salicylaldiminate) mono(alkyl) yttrium complex **1.29** can easily be formed via a protonolysis reaction. Also, a tris(salicylaldiminate) yttrium complex (**1.30**) can be synthesized in the same manner. A salicylaldiminate supported yttrium hydrido complex (**1.31**) can be formed directly from the yttrium alkyl complex and hydrogen gas. Hydrido complex **1.31** did not catalyze the polymerization of ethylene, but did hydrogenate stoichiometric amounts of alkyne, and diphenylketone. Notably, complex **1.31** is not catalytic and was only investigated for stoichiometric chemistry.

A similar ligand set to the salicylaldiminate that has been recently synthesized is the dialkoxy-diimino ligand **1.34** (Figure 1.12).[122,126] In a similar reaction to the salicylaldiminate proligand, the dialkoxy-diimino proligand **1.34** is synthesized from the condensation of β-hydroxy ketones and a bridging primary diamine. The CF$_3$ groups result in a tethered ligand where the tendency to form oligomers is reduced,[122] and thus a monomeric yttrium complex **1.35** can be synthesized in high yield.
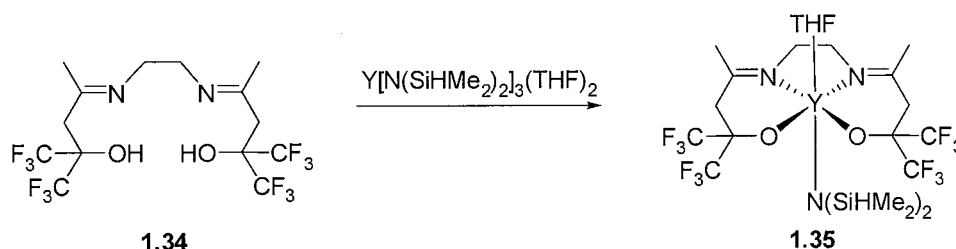
Figure 1.12. Synthesis of fluorous dialkoxy-diimino yttrium complex **1.35**.

The electron-withdrawing CF$_3$ groups in complex **1.35** promote higher reactivity for lactide polymerization (Figure 1.13). Complex **1.35** initiates the ROP of lactide obtaining poly(lactide) in high yield, with a narrow polydispersity value and is thought to be a living catalyst for the ROP of D,L-lactide.
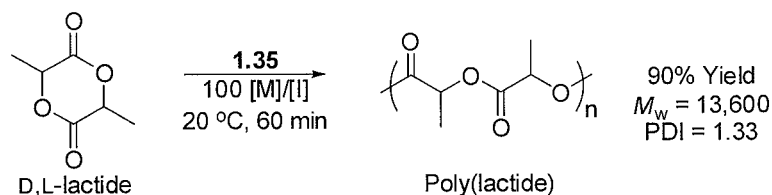
Figure 1.13. Lactide ring-opening polymerization using complex **1.35**.

N,O-chelates such as salicylaldiminate and dialkoxy-diimino ligands have been shown to form yttrium complexes in high yield. Proligand **1.28** was used in the synthesis of bis-ligated and tris-ligated yttrium complexes, and bis(salicylaldiminate) yttrium complex **1.29** can be reacted with hydrogen gas to give a hydrido complex that can reduce silylalkyne and diphenyl ketone stoichiometrically. The dialkoxy-diimino proligand **1.34** gives the monometallic yttrium complex **1.35**. This complex was found to be a controlled initiator for the ROP of lactide. Comparing the smaller amidate N,O-chelate with the salicylaldiminate reactivity trends in various catalytic and stoichiometric reactions provides insight into the effect of the metallacycle ring size.

1.6   Scope of Thesis

Previous work on yttrium complexes supported by amidinate, guanidinate, salicylaldiminate and the dialkoxy-diimino ligands, show that these complexes can be used in a range of applications. However, previous to the work of this thesis, no yttrium amidate complexes have been directly synthesized using either salt metathesis or protonolysis routes. The amidate ligand (**1.12**, Figure 1.2) is similar in many ways to the presented ligand sets in that it would chelate to give a 4-membered metallacycle of yttrium (as in amidinate and guanidinate yttrium complexes) and it is an N,O-chelate as in salicylaldiminate and dialkoxy-diimino complexes. The literature precedent established suggests that amidate ligands will be suitable for supporting reactive yttrium complexes. Furthermore, in the Schafer group, amidate complexes of group 4 metals have been synthesized in high-yield.[127-131]

In this thesis the extension of this work to yttrium, a group 3 metal, is investigated. Fundamental coordination modes, structure, bonding and stability investigations are

performed in the synthesis of novel tris, bis and mono(amidate) complexes of yttrium (Chapter 2). The catalytic applications of these yttrium amidate complexes will be explored in the ROP of ε-caprolactone (Chapter 3) and the hydroamination reaction (Chapter 4). Finally, stoichiometric reactivity investigations in the pursuit of a terminal yttrium imido complex will also be presented (Chapter 5).

1.7 References

(1)   Marusak, R. A.; Doan, K.; Cummings, S. D. *Integrated Approach to Coordination Chemistry*; John Wiley & Sons, Inc.: Hoboken, New Jersey, **2007**, 1-21.

(2)   Rayner-Canham, G.; Overton, T. *Descriptive Inorganic Chemistry*; 3rd ed.; W. H. Freeman and Company: New York, NY, **2002**, 448-474, 570-583.

(3)   Housecroft, C. E.; Sharpe, A. G. *Inorganic Chemistry*; Pearson Education Limited, **2001**.

(4)   Lachgar, A.; Dudis, D. S.; Dorhout, P. K.; Corbett, J. D. *Inorg. Chem.* **1991**, *30*, 3321.

(5)   Corbett, J. D. *Acc. Chem. Res.* **1981**, *14*, 239.

(6)   Di Salvo, F. J.; Waszczak, J. V.; Walsh, W. M.; Rupp, L. W.; Corbett, J. D. *Inorg. Chem.* **1985**, *24*, 4624.

(7)   Shannon, R. D. *Acta Crystallogr., Sect. A: Cryst. Phys., Diffr., Theor. Gen. Cryst.* **1976**, *32*, 751.

(8)   Arndt, S.; Okuda, J. *Chem. Rev.* **2002**, *102*, 1953.

(9)   Deacon, G. B.; Shen, Q. *J. Organomet. Chem.* **1996**, *506*, 1.

(10)   Gottfriedsen, J.; Edelmann, F. T. *Coord. Chem. Rev.* **2006**, *250*, 2347.

(11)   Kobayashi, S.; Sugiura, M.; Kitagawa, H.; Lam, W. W. L. *Chem. Rev.* **2002**, *102*, 2227.

(12)   Li, H. X.; Zhu, Y. J.; Cheng, M. L.; Ren, Z. G.; Lang, J. P.; Shen, Q. *Coord. Chem. Rev.* **2006**, *250*, 2059.

(13)   Molander, G. A.; Romero, J. A. C. *Chem. Rev.* **2002**, *102*, 2161.

(14)   Yao, Y.; Ma, M.; Xu, X.; Zhang, Y.; Shen, Q.; Wong, W.-T. *Organometallics* **2005**, *24*, 4014.

(15)   Hong, S.; Marks, T. J. *Acc. Chem. Res.* **2004**, *37*, 673.

(16)   Voskoboynikov, A. Z.; Shestakova, A. K.; Beletskaya, I. P. *Organometallics* **2001**, *20*, 2794.

(17)   Molander, G. A.; Romero, J. A. C.; Corrette, C. P. *J. Organomet. Chem.* **2002**, *647*, 225.

(18)   Fu, P.-F.; Brard, L.; Li, Y.; Marks, T. J. *J. Am. Chem. Soc.* **1995**, *117*, 7157.

(19)   Hou, Z.; Wakatsuki, Y. *Coord. Chem. Rev.* **2002**, *231*, 1.

(20)   Okada, M. *Prog. Polym. Sci.* **2002**, *27*, 87.

(21)   Yasuda, H. *J. Organomet. Chem.* **2002**, *647*, 128.

(22)   Evans, W. J.; Fujimoto, C. H.; Ziller, J. W. *Organometallics* **2001**, *20*, 4529.

(23)   Harrowfield, J. M.; Kepert, D. L.; Patrick, J. M.; White, A. H. *Aust. J. Chem.* **1983**, *36*, 483.

(24)   Wang, J.; Wang, Y.; Zhang, Z. H.; Zhang, X. D.; Tong, J.; Liu, X. Z.; Liu, X. Y.; Zhang, Y.; Pan, Z. J. *J. Struct. Chem.* **2005**, *46*, 895.

(25)   Edelmann, F. T.; Freckmann, D. M. M.; Schumann, H. *Chem. Rev.* **2002**, *102*, 1851.

(26)   Damrau, W.-E.; Paolucci, G.; Zanon, J.; Siebel, E.; Fischer, R. D. *Inorg. Chem. Commun.* **1998**, *1*, 424.

(27)   Deelman, B.-J.; Stevels, W. M.; Teuben, J. H.; Lakin, M. T.; Spek, A. L. *Organometallics* **1994**, *13*, 3881.

(28)   Douglass, M. R.; Ogasawara, M.; Hong, S.; Metz, M. V.; Marks, T. J. *Organometallics* **2002**, *21*, 283.

(29)   Evans, W. J.; Champagne, T. M.; Giarikos, D. G.; Ziller, J. W. *Organometallics* **2005**, *24*, 570.

(30)   Evans, W. J.; Davis, B. L.; Nyce, G. W.; Perotti, J. M.; Ziller, J. W. *J. Organomet. Chem.* **2003**, *677*, 89.

(31)   Evans, W. J.; Fujimoto, C. H.; Johnston, M. A.; Ziller, J. W. *Organometallics* **2002**, *21*, 1825.

(32)   Evans, W. J.; Kozimor, S. A.; Brady, J. C.; Davis, B. L.; Nyce, G. W.; Seibel, C. A.; Ziller, J. W.; Doedens, R. J. *Organometallics* **2005**, *24*, 2269.

(33)   Fryzuk, M. D.; Jafarpour, L.; Kerton, F. M.; Love, J. B.; Rettig, S. J. *Angew. Chem., Int. Ed.* **2000**, *39*, 767.

(34)   Fryzuk, M. D.; Love, J. B.; Rettig, S. J. *J. Am. Chem. Soc.* **1997**, *119*, 9071.

(35)   Gamer, M. T.; Roesky, P. W. *J. Organomet. Chem.* **2002**, *647*, 123.

(36)   Haar, C. M.; Stern, C. L.; Marks, T. J. *Organometallics* **1996**, *15*, 1765.

(37)   Halterman, R. L.; Schumann, H.; Dubner, F. *J. Organomet. Chem.* **2000**, *604*, 12.

(38)   Hultzsch, K. C.; Spaniol, T. P.; Okuda, J. *Organometallics* **1997**, *16*, 4845.

(39)   Ihara, E.; Yoshioka, S.; Furo, M.; Katsura, K.; Yasuda, H.; Mohri, S.; Kanehisa, N.; Kai, Y. *Organometallics* **2001**, *20*, 1752.

(40) Klimpel, M. G.; Eppinger, J.; Sirsch, P.; Scherer, W.; Anwander, R. *Organometallics* **2002**, *21*, 4021.

(41) Lewin, J. L.; Woodrum, N. L.; Cramer, C. J. *Organometallics* **2006**, *25*, 5906.

(42) Molander, G. A.; Dowdy, E. D.; Noll, B. C. *Organometallics* **1998**, *17*, 3754.

(43) Okuda, J.; Amor, F.; Du Plooy, K. E.; Eberle, T.; Hultzsch, K. C.; Spaniol, T. P. *Polyhedron* **1998**, *17*, 1073.

(44) Paolucci, G.; Vignola, M.; Formenti, S.; Massa, W. *Eur. J. Inorg. Chem.* **2005**, 3472.

(45) Qian, C.; Zhu, D. *J. Chem. Soc., Dalton Trans.* **1994**, 1599.

(46) Qian, C.; Zou, G.; Gao, L. *J. Organomet. Chem.* **1996**, *525*, 23.

(47) Qian, C.; Zou, G.; Sun, J. *J. Organomet. Chem.* **1998**, *566*, 21.

(48) Qian, C.-T.; Zou, G.; Nie, W.-L.; Sun, J.; Lemenovskii, D. A.; Borzov, M. V. *Polyhedron* **2000**, *19*, 1955.

(49) Rodrigues, A.-S.; Kirillov, E.; Roisnel, T.; Razavi, A.; Vuillemin, B.; Carpentier, J.-F. *Angew. Chem., Int. Ed.* **2007**, *46*, 7240.

(50) Roesky, P. W.; Denninger, U.; Stern, C. L.; Marks, T. J. *Organometallics* **1997**, *16*, 4486.

(51) Roesky, P. W.; Stern, C. L.; Marks, T. J. *Organometallics* **1997**, *16*, 4705.

(52) Saendig, N.; Koch, W. *Organometallics* **2002**, *21*, 1861.

(53) Schumann, H.; Erbstein, F.; Weimann, R.; Demtschuk, J. *J. Organomet. Chem.* **1997**, *536/537*, 541.

(54) Schumann, H.; Rosenthal, E. C. E.; Demtschuk, J.; Molander, G. A. *Organometallics* **1998**, *17*, 5324.

(55) Schumann, H.; Zietzke, K.; Weimann, R.; Demtschuk, J.; Kaminsky, W.; Schauwienold, A.-M. *J. Organomet. Chem.* **1999**, *574*, 228.

(56) Woodrum, N. L.; Cramer, C. J. *Organometallics* **2006**, *25*, 68.

(57) Yasuda, H. *J. Organomet. Chem.* **2002**, *647*, 128.

(58) Yoder, J. C.; Day, M. W.; Bercaw, J. E. *Organometallics* **1998**, *17*, 4946.

(59) Burgstein, M. R.; Berberich, H.; Roesky, P. W. *Chem. Eur. J.* **2001**, *7*, 3078.

(60) Kim, Y. K.; Livinghouse, T.; Bercaw, J. E. *Tetrahedron Lett.* **2001**, *42*, 2933.

(61) Tredget, C. S.; Lawrence, S. C.; Ward, B. D.; Howe, R. G.; Cowley, A. R.; Mountford, P. *Organometallics* **2005**, *24*, 3136.

(62)   Arnold, P. L.; Mungur, S. A.; Blake, A. J.; Wilson, C. *Angew. Chem., Int. Ed.* **2003**, *42*, 5981.

(63)   Bradley, D. C.; Chudzynska, H.; Hursthouse, M. B.; Motevalli, M. *Polyhedron* **1993**, *12*, 1907.

(64)   Evans, W. J.; Sollberger, M. S. *Inorg. Chem.* **1988**, *27*, 4417.

(65)   Evans, W. J.; Sollberger, M. S.; Hanusa, T. P. *J. Am. Chem. Soc.* **1988**, *110*, 1841.

(66)   Matsuo, Y.; Mashima, K.; Tani, K. *Organometallics* **2001**, *20*, 3510.

(67)   Meyer, N.; Kuzdrowska, M.; Roesky, P. W. *Eur. J. Inorg. Chem.* **2008**, 1475.

(68)   Xiang, L.; Wang, Q.; Song, H.; Zi, G. *Organometallics* **2007**, *26*, 5323.

(69)   Yang, Y.; Li, S.; Cui, D.; Chen, X.; Jing, X. *Organometallics* **2007**, *26*, 671.

(70)   Zi, G.; Xiang, L.; Song, H. *Organometallics* **2008**, *27*, 1242.

(71)   Pernin, C. G.; Ibers, J. A. *Inorg. Chem.* **1999**, *38*, 5478.

(72)   Pernin, C. G.; Ibers, J. A. *Inorg. Chem.* **2000**, *39*, 1222.

(73)   Fryzuk, M. D.; Haddad, T. S.; Rettig, S. J. *Organometallics* **1992**, *11*, 2967.

(74)   Fryzuk, M. D.; Yu, P.; Patrick, B. O. *Can. J. Chem.* **2001**, *79*, 1194.

(75)   Roesky, P. W. *Eur. J. Inorg. Chem.* **1998**, 593.

(76)   Roesky, P. W. *Chem. Soc. Rev.* **2000**, *29*, 335.

(77)   Roesky, P. W.; Buergstein, M. R. *Inorg. Chem.* **1999**, *38*, 5629.

(78)   Dehnen, S.; Burgstein, M. R.; Roesky, P. W. *J. Chem. Soc., Dalton Trans.* **1998**, 2425.

(79)   Avent, A. G.; Caro, C. F.; Hitchcock, P. B.; Lappert, M. F.; Li, Z.; Wei, X.-H. *Dalton Trans.* **2004**, 1567.

(80)   Hayes, P. G.; Welch, G. C.; Emslie, D. J. H.; Noack, C. L.; Piers, W. E.; Parvez, M. *Organometallics* **2003**, *22*, 1577.

(81)   Liddle, S. T.; Arnold, P. L. *Dalton Trans.* **2007**, 3305.

(82)   Sanchez-Barba, L. F.; Hughes, D. L.; Humphrey, S. M.; Bochmann, M. *Organometallics* **2005**, *24*, 3792.

(83)   Sanchez-Barba, L. F.; Hughes, D. L.; Humphrey, S. M.; Bochmann, M. *Organometallics* **2006**, *25*, 1012.

(84)   Vitanova, D. V.; Hampel, F.; Hultzsch, K. C. *Dalton Trans.* **2005**, 1565.

(85)   Vitanova, D. V.; Hampel, F.; Hultzsch, K. C. *J. Organomet. Chem.* **2005**, *690*, 5182.

(86)   Wei, X.; Cheng, Y.; Hitchcock, P. B.; Lappert, M. F. *Dalton Trans.* **2008**, 5235.

(87)   Barash, E. H.; Coan, P. S.; Lobkovsky, E. B.; Streib, W. E.; Caulton, K. G. *Inorg. Chem.* **1993**, *32*, 497.

(88)   Liu, W.; Zhu, Y.; Tan, M. *J. Coord. Chem.* **1991**, *24*, 107.

(89)   Plaziak, A. S.; Zeng, C. H.; Costello, C. E.; Lis, S.; Elbanowski, M. *Inorg. Chim. Acta* **1991**, *184*, 229.

(90)   Wang, R.; Song, D.; Seward, C.; Tao, Y.; Wang, S. *Inorg. Chem.* **2002**, *41*, 5187.

(91)   Dagorne, S.; Bellemin-Laponnaz, S.; Maisse-Francois, A. *Eur. J. Inorg. Chem.* **2007**, 913.

(92)   Gorlitzer, H. W.; Spiegler, M.; Anwander, R. *J. Chem. Soc., Dalton Trans.* **1999**, 4287.

(93)   Duchateau, R.; Brussee, E. A. C.; Meetsma, A.; Teuben, J. H. *Organometallics* **1997**, *16*, 5506.

(94)   Wong, E. W. Y.; Das, A. K.; Katz, M. J.; Nishimura, Y.; Batchelor, R. J.; Onishi, M.; Leznoff, D. B. *Inorg. Chim. Acta* **2006**, *359*, 2826.

(95)   Platel, R. H.; White, A. J. P.; Williams, C. K. *Inorg. Chem.* **2008**, *47*, 6840.

(96)   Platel, R. H.; Hodgson, L. M.; White, A. J. P.; Williams, C. K. *Organometallics* **2007**, *26*, 4955.

(97)   Platel, R. H.; White, A. J. P.; Williams, C. K. *Inorg. Chem.* **2008**, *47*, 6840.

(98)   Aubrecht, K. B.; Chang, K.; Hillmyer, M. A.; Tolman, W. B. *J. Polym. Sci., Part A: Polym. Chem.* **2000**, *39*, 284.

(99)   Zhang, L.; Nishiura, M.; Yuki, M.; Luo, Y.; Hou, Z. *Angew. Chem., Int. Ed.* **2008**, *47*, 2642.

(100)   Bambirra, S.; Bouwkamp, M. W.; Meetsma, A.; Hessen, B. *J. Am. Chem. Soc.* **2004**, *126*, 9182.

(101)   Bambirra, S.; Brandsma, M. J. R.; Brussee, E. A. C.; Meetsma, A.; Hessen, B.; Teuben, J. H. *Organometallics* **2000**, *19*, 3197.

(102)   Bambirra, S.; Meetsma, A.; Hessen, B.; Teuben, J. H. *Organometallics* **2001**, *20*, 782.

(103)   Ge, S.; Meetsma, A.; Hessen, B. *Organometallics* **2008**, *27*, 3131.

(104)   Hill, M. S.; Hitchcock, P. B.; Mansell, S. M. *Dalton Trans.* **2006**, 1544.

(105)   Luo, Y.; Yao, Y.; Shen, Q.; Sun, J.; Weng, L. *J. Organomet. Chem.* **2002**, *662*, 144.

(106) Schmidt, J. A. R.; Arnold, J. *Chem. Commun.* **1999**, 2149.

(107) Wang, J.; Sun, H.; Yao, Y.; Zhang, Y.; Shen, Q. *Polyhedron* **2008**, *27*, 1977.

(108) Zhang, J.; Ruan, R.; Shao, Z.; Cai, R.; Weng, L.; Zhou, X. *Organometallics* **2002**, *21*, 1420.

(109) Zhang, L.; Nishiura, M.; Yuki, M.; Luo, Y.; Hou, Z. *Angew. Chem., Int. Ed.* **2008**, *47*, 2642.

(110) Ajellal, N.; Lyubov, D. M.; Sinenkov, M. A.; Fukin, G. K.; Cherkasov, A. V.; Thomas, C. M.; Carpentier, J.-F.; Trifonov, A. A. *Chem. Eur. J.* **2008**, *14*, 5440.

(111) Lu, Z.; Yap, G. P. A.; Richeson, D. S. *Organometallics* **2001**, *20*, 706.

(112) Lyubov, D. M.; Bubnov, A. M.; Fukin, G. K.; Dolgushin, F. M.; Antipin, M. Y.; Pelce, O.; Schappacher, M.; Guillaume, S. M.; Trifonov, A. A. *Eur. J. Inorg. Chem.* **2008**, 2090.

(113) Lyubov, D. M.; Fukin, G. K.; Trifonov, A. A. *Inorg. Chem.* **2007**, *46*, 11450.

(114) Trifonov, A. A.; Lyubov, D. M.; Fedorova, E. A.; Fukin, G. K.; Schumann, H.; Muhle, S.; Hummert, M.; Bochkarev, M. N. *Eur. J. Inorg. Chem.* **2006**, 747.

(115) Trifonov, A. A.; Lyubov, D. M.; Fukin, G. K.; Baranov, E. V.; Kurskii, Y. A. *Organometallics* **2006**, *25*, 3935.

(116) Yao, Y.; Luo, Y.; Chen, J.; Zhang, Z.; Zhang, Y.; Shen, Q. *J. Organomet. Chem.* **2003**, *679*, 229.

(117) Zhang, J.; Cai, R.; Weng, L.; Zhou, X. *Organometallics* **2004**, *23*, 3303.

(118) Zhang, W.-X.; Nishiura, M.; Hou, Z. *Synlett* **2006**, 1213.

(119) Emslie, D. J. H.; Piers, W. E.; MacDonald, R. *J. Chem. Soc., Dalton Trans.* **2002**, 293.

(120) Emslie, D. J. H.; Piers, W. E.; Parvez, M. *Dalton Trans.* **2003**, 2615.

(121) Emslie, D. J. H.; Piers, W. E.; Parvez, M.; McDonald, R. *Organometallics* **2002**, *21*, 4226.

(122) Grunova, E.; Kirillov, E.; Roisnel, T.; Carpentier, J. F. *Organometallics* **2008**, ASAP.

(123) Amgoune, A.; Thomas, C. M.; Carpentier, J. F. *Pure Appl. Chem.* **2007**, *79*, 2013.

(124) Piers, W. E.; Emslie, D. J. H. *Coord. Chem. Rev.* **2002**, *233*, 131.

(125) Kang, M.; Sen, A. *Organometallics* **2005**, *24*, 3508.

(126) Marquet, N.; Grunova, E.; Kirillov, E.; Bouyahyi, M.; Thomas, C. M.; Carpentier, J.-F. *Tetrahedron* **2008**, *64*, 75.

(127) Zhang, Z.; Schafer, L. L. *Org. Lett.* **2003**, *5*, 4733.

(128) Wood, M. C.; Leitch, D. C.; Yeung, C. S.; Kozak, J. A.; Schafer, L. L. *Angew. Chem., Int. Ed.* **2007**, *46*, 354.

(129) Thomson, R. K.; Zahariev, F. E.; Zhang, Z.; Patrick, B. O.; Wang, Y. A.; Schafer, L. L. *Inorg. Chem.* **2005**, *44*, 8680.

(130) Thomson, R. K.; Bexrud, J. A.; Schafer, L. L. *Organometallics* **2006**, *25*, 4069.

(131) Li, C. Y.; Thomson, R. K.; Gillon, B.; Patrick, B. O.; Schafer, L. L. *Chem. Commun.* **2003**, 2462.

Chapter 2. Synthesis, Structure and Stability of Yttrium Amidate Complexes[1]

2.1   Introduction

Substantial research with group 3 and lanthanide complexes containing ancillary nitrogen donor ligands such as amido (2.1)[1-4] β-diketiminate (2.2),[5-13] amidinate (2.3),[14-17] guanidinate (2.4),[18-24] and ureate (2.5)[25] ligand sets has been conducted (Figure 2.1). These are all attractive ligands that can be assembled using a modular strategy to vary steric and electronic properties.
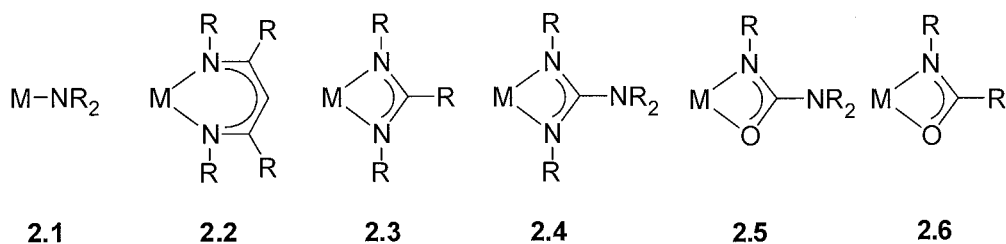
Figure 2.1. N-containing ancillary ligand sets.

The synthesis of discrete rare earth complexes can be difficult due to low energy ligand redistribution pathways. The high Lewis acidity of these rare earth metals, in combination with their larger radii means that synthetic approaches using multidentate ligands often results in dimer formation or even higher aggregates.[26-28] Typically, the formation of discrete species is most commonly controlled by creating a sterically demanding ligand. Furthermore, facile modification of steric and electronic properties of the ancillary ligand of new complexes is desirable for tuning reactivity profiles.

A similar ancillary ligand set to those shown in Figure 2.1 is the amidate ligand (2.6). Amidates have been largely overlooked as an auxiliary ligand set capable of providing selective metal complex reactivity. The research presented here focuses on new high-yielding preparative methods to access crystalline, discrete yttrium amidate complexes that will be investigated for catalytic activity.

Due to the facile synthesis of organic amides, from acid chlorides and primary amines, the amide proligands can be easily varied for desired steric and electronic properties. Previous examples of amidate complexes of the rare-earth metals have been synthesized via isocyanate insertion into a reactive M-C bond of rare-earth alkyl complexes (Figure 2.2).[29-31] This preparative approach typically yields amidate bridged bimetallic complexes (2.7), which have been fully characterized.[30] The corresponding tetrahydrofuran (THF) adduct (2.8) could not be analyzed by X-ray crystallography, but was characterized by elemental analysis, mass spectrometry and IR spectroscopy. Moreover, a decomposition product of an attempted isocyanate insertion reaction led to the only previous report of a homoleptic lanthanide amidate complex,[30] a $Ho[(n-Bu)[OCN]Ph]_3$ complex, which was characterized by elemental analysis and IR spectroscopy; no structural information was provided.[30] While the isocyanate insertion method is well established, the requisite lanthanide alkyl starting materials are non-trivial to synthesize and handle and often result in complex or ill-defined species. Furthermore, this route has been typically exploited for the reactivity of M-C bonds, rather than using the resultant amidate complexes as potential tunable catalytic systems.

Cp'₂LnCl →(n-BuLi, -30 °C / THF)→ Cp'₂Ln(n-Bu)(THF)

$Cp'_2LnCl \xrightarrow[THF]{n\text{-}BuLi,\ -30\ ^\circ C} Cp'_2Ln(n\text{-}Bu)(THF)$

Cp' = C₅H₄CH₃

PhCNO, -10 °C
THF

2.7

+THF / −THF

Ln = Sm, Dy, Er

2.8
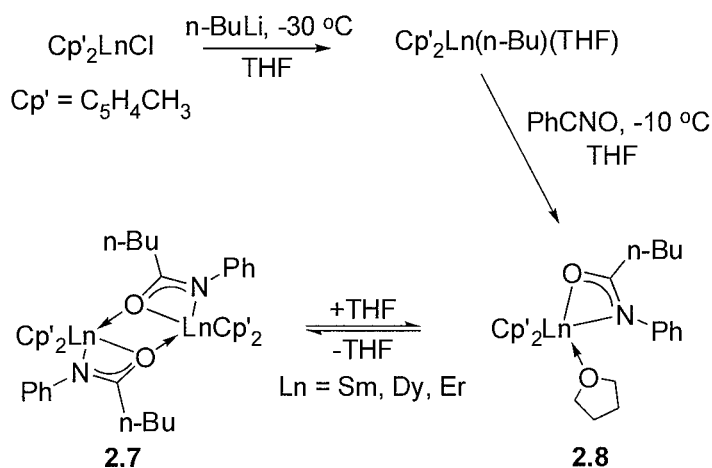
Figure 2.2. Isocyanate insertion into a Ln-C bond.[30]

To date, there are no examples of molecular structures of yttrium amidate complexes. However, there is a reported solid-state structure of a similar ureate complex (MeC₅H₄)₂Y(THF)(N(iPr)₂[O,N]Ph).[25] For purposes of this thesis, this monoureate yttrium complex will be used for comparison to the yttrium amidate complexes synthesized here.

As an alternative synthetic protocol, this work has focused on using organic amides as proligands in the direct preparation of yttrium amidate complexes. Using a high-yielding protonolysis reaction between organic amides and commercially available yttrium tris(bis(trimethylsilyl))amide (Y[N(SiMe₃)₂]₃), the first examples of monomeric crystalline tris, bis and mono(amidate) complexes of yttrium can be obtained. The structural properties and reactivity of these easily isolable complexes have also been investigated.

2.2   Amide Proligands

2.2.1   Introduction

Ligand design is a crucial aspect of catalyst synthesis. A ligand backbone needs to be tunable in order to vary the steric and electronic properties of the synthesized complexes. The amide proligand is an ideal candidate for catalyst preparation, since the synthesis is short, high-yielding and modular. Section 2.2 shows that a broad range of substituents, and electron-withdrawing groups can easily be installed on the amidate backbone. When bound to a metal centre, the substituent on the nitrogen is placed close to the metal centre, in contrast to the carbonyl substituent, which is further removed. As mentioned previously, rare-earth complexes are prone to dimerization or oligomerization; however, with sufficient steric bulk on the N-substituent, dimerization can be disfavoured, if not eliminated. In the Schafer group, the majority of monomeric group 4 bis(amidate)bis(amido) complexes that have been crystallographically determined contain either Dipp or dimethylphenyl (Dmp) as the N-substituent.[32-34]   Consequently, electronic properties of the amide proligands are typically varied by modifying the carbonyl substituent.

Another practical advantage to the amide proligand is the diagnostic N-*H* signal in the ^{1}H NMR spectrum (a singlet between δ 6.1 and 6.6 ppm) and the broad N-H stretch absorption in the IR spectrum ($\sim$ 3300 cm^{-1}). The progress of the protonolysis reaction can be monitored by the disappearance of these signals. The ease in synthesis, variability and characterization of the amide proligands make them ideal candidates for investigating yttrium complex formation.

2.2.2 Results and Discussion

As mentioned before, the amide proligands can be easily synthesized from acid chlorides and primary amines (Figure 2.3) in a dichloromethane (DCM) solution with triethylamine (NEt_3) as a base. After workup a pale yellow solid is isolated that can be recrystallized from hot toluene and hexanes to give amide product in high yield (76 - 91%). These proligands must be thoroughly dried by heating under vacuum before use in metal complexation reactions.
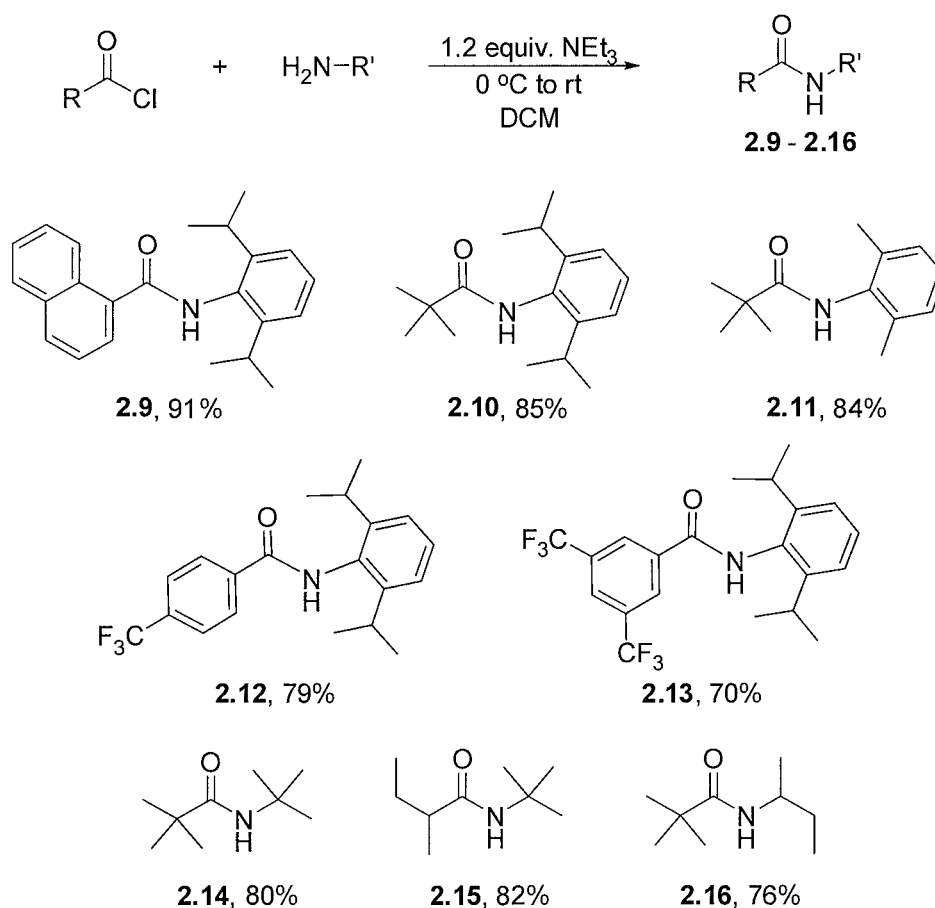
Figure 2.3. Synthesis of amide proligands.

As shown in Figure 2.3, the series of proligands have a broad range of the steric and electronic properties. Amide **2.9** (which is extensively used throughout this thesis, *vide*

infra) contains a naphthyl substituent, which has a diagnostic doublet signal in the ^{1}H NMR spectrum at δ 8.86 ppm for the naphthyl *ortho*-proton. Amide proligands **2.12** and **2.13** include trifluoromethyl groups that result in a more electron-withdrawing amidate backbone. Furthermore, yttrium complexes resulting from these proligands are expected to be more Lewis acidic. Amides **2.14**, **2.15** and **2.16** contain alkyl substituents, in contrast to the aryl substituents on all the other proligands. The advantage of using alkyl groups is increased solubility, lower melting points, and a lower molecular weight. The lower melting point may allow sublimation to be used as a purification technique.

The library of compounds shown in Figure 2.3 illustrates the variety of amide proligands that have been investigated during the course of this work. Formation of yttrium complexes using these proligands results in complexes with variable reactivity (*vide infra*). Synthesis of tris, bis and mono(amidate) complexes using this library of amide proligands will be presented, as well as their structural features, stability and reactivity.

2.3   Tris(amidate) Yttrium Complexes

2.3.1 Introduction

The importance of ligand design is evident in the synthesis of new, discrete, monometallic yttrium compounds as amidate ligands are known to promote the formation of ligand bridged species. The proligand library shown in Figure 2.3 explores a range of steric and electronic environments in this new class of complexes. Initial results show that placing larger groups (e.g. 2,6-diisopropylphenyl, Dipp) on the N-substituent had a positive effect in the isolation of the desired pure monomeric yttrium amidate species. Using amide proligands with smaller substituents (as in compounds **2.14**, **2.15** and **2.16**) resulted in uncharacterizable

yttrium species (as indicated by complex ^{1}H NMR spectra and inconclusive mass spectra). This is most likely due to a lack of steric bulk close to the metal centre, resulting in oligomerization. To date, the results of complex formation using amides **2.14**, **2.15** and **2.16** are inconclusive and consequently, this chapter will focus on complexes of amides **2.9** - **2.13**. Notably, resultant complexes of **2.9** - **2.13** all have sterically bulky aryl groups on the N and the Dipp or Dmp (2,6-dimethylphenyl) groups were found to be essential in synthesis of pure, monomeric yttrium tris(amidate) complexes.

2.3.2 Results and Discussion

In the Schafer group, the protonolysis route for complex formation has been used to make crystalline bis(amidate) complexes of group 4 metals.[32,35,36] Traditional salt metathesis routes, which are very useful for group 3 amidinate complex formation,[37] do not work well for preparing group 4 amidate complexes, often resulting in amorphous material. Initial preparative efforts by J. D. Beard toward yttrium amidate complexes using salt metathesis revealed the propensity for amidate ligands to promote the formation of bridged dimeric or ill-defined multi-metallic species.[38] However, one example of a bridged amidate complex (**2.17**) can be formed in low yield by salt metathesis using the sodium amidate salt of *N*-2′,6′-dimethylphenyl(*tert*-butyl)amide (**2.11**), formed from deprotonation with (Na(N(SiMe₃)₂), in a 3:1 molar ratio with yttrium trichloride. This material can be recrystallized from hexanes, and a solid-state molecular structure of complex **2.17** was obtained.[38] Unfortunately full characterization was not possible as this low yielding crystalline sample was not representative of the bulk material which had complex NMR spectra consistent with a highly fluxional species of ill-defined structure in the solution phase.[38] Figure 2.4 shows the solid-

state molecular structure of **2.17**, which is a centrosymmetric dimer, with each yttrium atom having three amidate ligands. One amidate ligand is bridging to another yttrium atom through the amidate oxygen. Notably, the use of the large sodium counter-ion and bulky base were found to be necessary, as deprotonation of **2.11** with *n*-butyllithium and subsequent reaction with yttrium trichloride resulted in the formation of completely insoluble materials.[38]
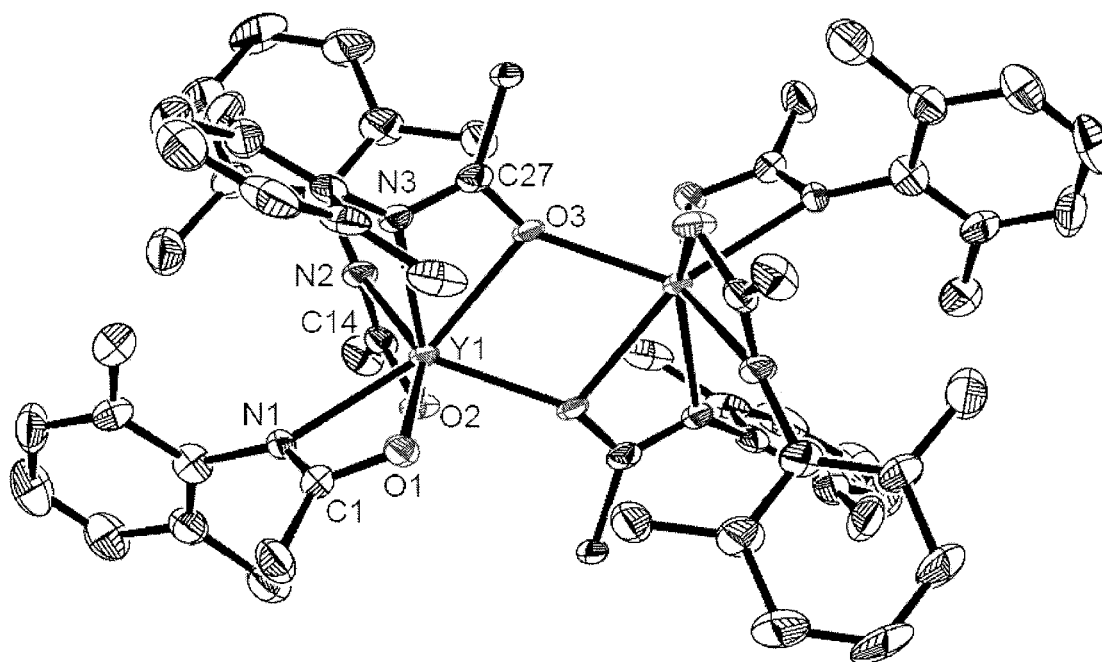
Figure 2.4. ORTEP of [Y{tBu[O,N]Me₂Ph}₃]₂ (**2.17**) with the probability ellipsoids drawn at the 50% level. *tert*-Butyl groups omitted for clarity.[38]

Table 2.1. Selected bond lengths (Å) and angles (°) for complex **2.17**.

	Bond Length (Å)		Bond Angle(°)
Y1-O1	2.260(4)	Y1-O1-C1	99.6(4)
Y1-N1	2.449(5)	O1-C1-N1	115.0(6)
O1-C1	1.286(8)	C1-N1-Y1	90.3(4)
N1-C1	1.299(9)	N1-Y1-O1	54.99(17)
Y1-O2	2.270(4)	Y1-O2-C14	99.8(4)
Y1-N2	2.492(5)	O2-C14-N2	116.3(6)
O2-C14	1.286(8)	C14-N2-Y1	88.9(4)
N2-C14	1.309(9)	N2-Y1-O2	54.90(18)
Y1-O3	2.384(4)	Y1-O3-C27	97.2(4)
Y1-N3	2.483(5)	O3-C27-N3	114.8(6)
O3-C27	1.327(8)	C27-N3-Y1	93.4(4)
N3-C27	1.302(9)	N3-Y1-O3	54.08(16)

Since salt metathesis preparation of yttrium amidate complexes has been difficult, and protonolysis is effective in formation of bis(amidate) complexes of group 4, protonolysis preparative methods were extended to yttrium in hopes of making crystalline, monomeric yttrium amidate species. Furthermore, Livinghouse and coworkers[39] discovered that chelating bis(thiophosphinic amidate) yttrium complexes can be formed cleanly from thiophosphinic amide proligands and yttrium tris(bis(trimethylsilyl)amide). The bis(thiophosphinic amidate) yttrium complexes have a similar 3-member chelate ring (N-P-S) as the amidate complexes (N-C-O). Also, these complexes are highly active for intramolecular hydroamination of aminoalkenes when formed *in situ*.

Homoleptic yttrium complexes can be made from proligands **2.9**, **2.10**, **2.11**, **2.12** and **2.13** using a simple protonolysis reaction (Figure 2.5). The starting material Y[N(SiMe$_3$)$_2$]$_3$, which is commercially available or can be easily synthesized,[40] is dissolved in tetrahydrofuran (THF) at room temperature. Separately, the amide proligand is dissolved in THF and is added dropwise to a stirring solution of Y[N(SiMe$_3$)$_2$]$_3$ in THF. The reaction

mixture is stirred at 60 °C for 2 hours, and after work-up pale yellow solids (**2.18**, **2.19**, and

2.20) or yellow oils that solidify over time (**2.21**, **2.22**) are obtained. The complexes formed

are recrystallized from hexanes to give colourless crystals in high yield (Figure 2.5). These

moisture sensitive complexes have been fully characterized and are soluble in all common

hydrocarbon solvents.
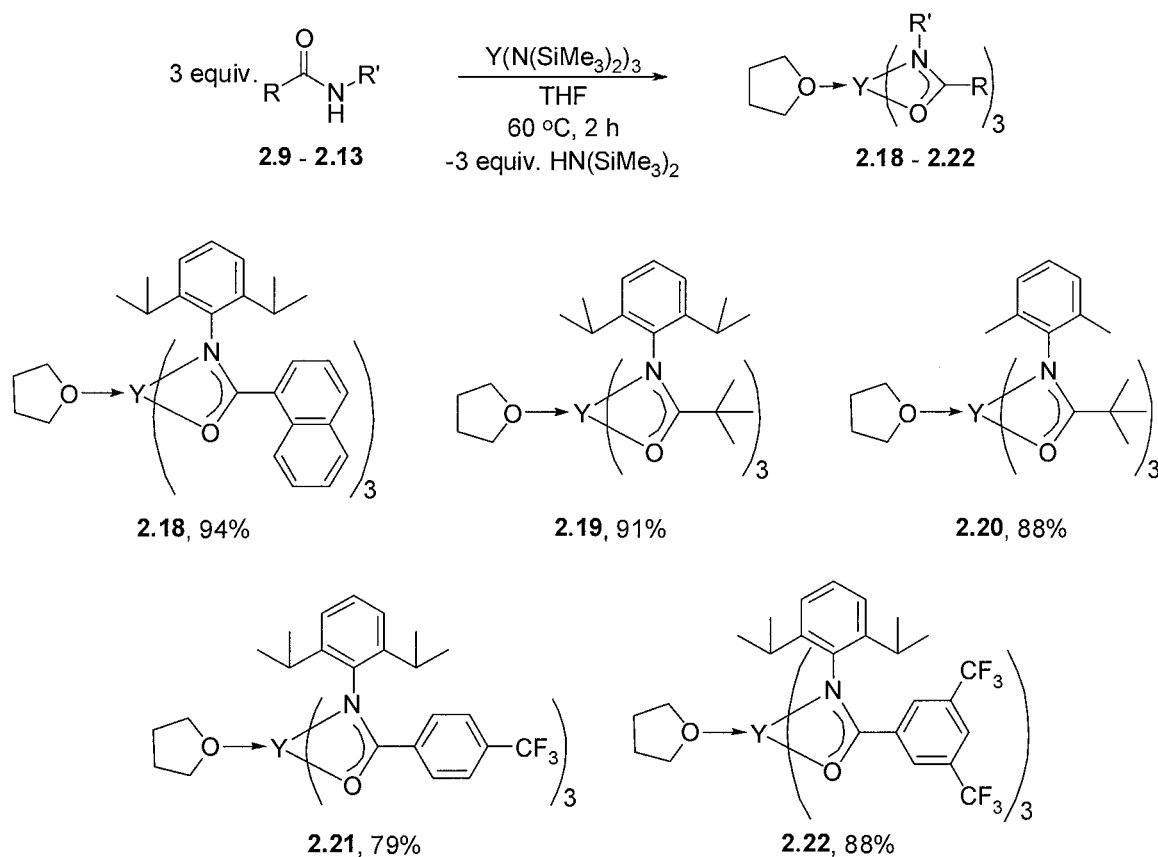
Figure 2.5. Synthesis of tris(amidate) complexes.

The ^{1}H NMR spectra of complexes **2.18**, **2.19**, **2.20**, **2.21** and **2.22** have very similar

characteristics, and all spectra show time averaged C_3 symmetric structures in the solution

phase and bind one equivalent of THF. Interestingly, the ^{1}H NMR spectrum of complex **2.19**

at room temperature contains broad signals compared to the other tris(amidate) complexes.

The signals in the ^{1}H NMR spectrum of **2.19** sharpened at higher temperatures (77 °C, in

C_7D_8) and maintained C_3 symmetry. In complexes **2.18**, **2.20**, **2.21** and **2.22**, the signals observed for the THF methylene protons are shifted (δ 4.08 ppm and 1.41 ppm for **2.18**, δ 3.46 ppm and 1.46 ppm for **2.19**, δ 3.89 ppm, and 1.42 ppm for **2.20**, δ 3.71 ppm and 1.32 ppm for **2.22**) and broadened from typical residual THF solvent signals (δ 3.57 ppm and 1.40 ppm).[41] This data is consistent with labile, coordinated THF that is rapidly exchanging on the NMR time scale. Variable temperature NMR spectroscopic experiments on complex **2.18** failed to yield any energetic parameters for this exchange, as no line-broadening was observed, even at -45 °C. Furthermore, the overall C_3 symmetry of this complex is maintained at these lower temperatures, also with no observable line broadening, consistent with either a highly fluxional complex, or a static structure. A key feature of the ^1H NMR spectrum for complex **2.18** is the diagnostic doublet signal at δ 9.26 ppm for the *ortho*-proton of the naphthyl substituent, which can be used to differentiate between tris, bis and mono(amidate) complexes (*vide infra*).

The THF ligand of complexes **2.18**, **2.19**, **2.21** and **2.22** is retained even after extended exposure to high vacuum, as evidenced by ^1H NMR spectroscopy and combustion analysis. However, this is not the case for complex **2.20**, which retains THF after exposure to vacuum overnight at 25 °C, but after exposure for more than three days, the THF can be partially removed, as evidenced by the decreased integration of the THF proton signals. Complex **2.20** has less steric bulk around the metal centre, and potentially converts to complex **2.17** under extensive vacuum.

IR spectroscopy is very diagnostic for the formation of these complexes as the disappearance of the N-H stretch absorption from proligands and a shift of the C=O stretch absorption bands are consistently observed. For example, from proligand **2.9** to the

formation of complex **2.18**, the disappearance of the N-H stretch band (3253 cm^{-1} for **2.9**) and the shifting of the C=O stretch band from 1643 cm^{-1} to 1513 cm^{-1} is observed. This weakening of the C=O bond is consistent with both amidate delocalization and metal complexation. Furthermore, the appearance of a weak C=N stretch absorption at 1406 cm^{-1} supports the formation of the desired complex with the delocalized monoanionic ligand. These IR trends are mirrored in complexes **2.19**, **2.20**, **2.21** and **2.22** (C=O v: 1647 cm^{-1} to 1618 cm^{-1} for **2.10** to **2.19**, 1650 cm^{-1} to 1541 cm^{-1} for **2.11** to **2.20**, 1648 cm^{-1} to 1528 cm^{-1} for **2.12** to **2.21**, and 1647 cm^{-1} to 1534 cm^{-1} for **2.13** to **2.22**). Finally, mass spectrometry of **2.18**, **2.19**, **2.20**, **2.21** and **2.22** results in molecular ion peaks corresponding to the complex without THF in all cases. As well, the fragmentation patterns for these complexes show signals for the loss of one ligand and for the free ligand itself.

X-ray quality crystals of complex **2.18** can be grown from hexanes at -35 °C and the solid-state molecular structure is shown in Figure 2.6. The 7-coordinate C_1 symmetric structure of **2.18** confirms electron delocalization through the κ^2-amidate backbone as indicated by the similar C-O and C-N bond lengths (average C-O is 1.290 Å and average C-N is 1.310 Å) (Table 2.2). The average Y-O (amidate) and Y-N (amidate) bond length are 2.303 and 2.411 Å, respectively. It is reasonable for the Y-O bond to be slightly shorter than the Y-N bond length, as shown in the previously mentioned and a structurally similar ureate complex of yttrium (MeC$_5$H$_4$)$_2$Y(THF)(N(iPr)$_2$[O,N]Ph).[25] This may be attributed to greater anionic charge density on oxygen and the oxophilic nature of yttrium. Also, there is a lack of steric bulk around the oxygen relative to the nitrogen making it sterically more favourable for O to approach the metal centre. Since there are no previous structurally characterized yttrium amidate complexes, the solid-state molecular structure of the monoureate yttrium

complex will be used for comparison. This monoureate complex, (MeC$_5$H$_4$)$_2$Y(THF)(N(iPr)$_2$[O,N]Ph), has similar Y-O and Y-N bond lengths to **2.18** (2.285(2) Å and 2.401(2) Å). Interestingly, in **2.18** one amidate metallacycle is further removed from the yttrium metal than the others, as evidenced by the much longer Y1-O3 and Y1-N3 bond lengths. This is likely due to the presence of the bulky groups on nitrogen. The average amidate bite angle (O-Y-N) for complex **2.18** is 55.90°, which is similar to (MeC$_5$H$_4$)$_2$Y(THF)(N(iPr)$_2$[O,N]Ph) (55.96(9)°).[25] The average sum total of the four angles of each amidate metallacycle is 359.5°, indicating the yttrium and amidate N-C-O backbone are all in the same plane.

Complexes **2.19**, **2.20**, **2.21** and **2.22** can be synthesized easily in high yield, but X-ray quality structure determinations have proven to be difficult. The composition and proposed structure of these complexes was based upon other characterization techniques, such as ^{1}H and ^{13}C NMR spectroscopy, IR spectroscopy, mass spectrometry, and elemental analysis. These data are then compared to those of complex **2.18**.
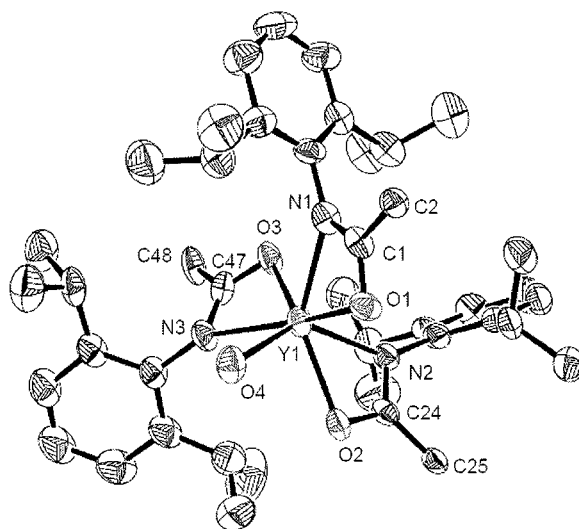
Figure 2.6. ORTEP diagram of the solid-state molecular structure of [(THF)Y{Nap[O,N](*i*Pr)₂Ph}₃]₂ (**2.18**) with the probability ellipsoids drawn at the 50% level. Naphthyl groups (except for *ipso*-carbon) and the carbons of the THF groups omitted for clarity.[42]

Table 2.2. Selected bond lengths (Å) and bond angles (°) for complex **2.18**.

	Bond Length (Å)		Bond Angle(°)
Y1-O1	2.334(3)	Y1-O1-C1	95.8(3)
Y1-N1	2.386(4)	O1-C1-N1	115.5(4)
O1-C1	1.292(5)	C1-N1-Y1	93.0(3)
N1-C1	1.304(5)	N1-Y1-O1	55.44(12)
Y1-O2	2.307(3)	Y1-O2-C24	94.8(3)
Y1-N2	2.369(3)	O2-C24-N2	117.0(4)
O2-C24	1.272(5)	C24-N2-Y1	90.8(3)
N2-C24	1.318(5)	N2-Y1-O2	56.38(11)
Y1-O3	2.268(3)	Y1-O3-C47	97.6(3)
Y1-N3	2.479(4)	O3-C47-N3	118.5(4)
O3-C47	1.293(6)	C47-N3-Y1	87.8(3)
N3-C47	1.304(6)	N3-Y1-O3	55.87(12)
Y1-O4	2.332(3)		

In an attempt to prepare a 6-coordinate (THF free), monomeric tris(amidate) complex, three equivalents of proligand **2.9** were reacted with Y[N(SiMe₃)₂]₃ in a non-coordinating solvent at 60 °C. The resultant moisture sensitive microcrystalline product (**2.23**) was

isolated from warm toluene in poor yield (12%). The residual material from the reaction was insoluble in common organic solvents, consistent with the formation of aggregate species. Complex **2.23** could not be fully characterized, although the data from the X-ray crystallographic studies of a poor quality crystal were satisfactory for establishing connectivity (Figure 2.7). Two of the ligands are bound as bidentate amidates, as seen previously, while one monodentate amidate ligand, bound through the oxygen only, displays the hemi-labile coordination mode that can be adopted by this ligand framework. Finally, the fourth ligand is a neutral amide, also bound through the oxygen. It is evident by ^{1}H NMR spectroscopy that one neutral amide is incorporated as a donor ligand, as the amide N-H signal can be seen as a highly deshielded broad singlet at approximately δ 11. Also in the ^{1}H NMR spectrum, the methyl groups and the methine protons for all diisopropylphenyl substituents are broad singlets or multiplets respectively, indicating the rapid exchange of proton and coordination modes between all the ligands on the NMR timescale.
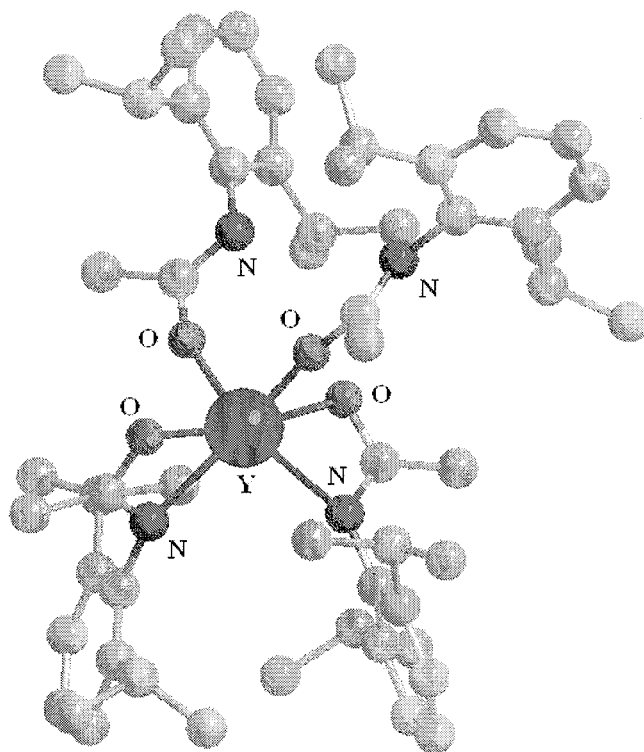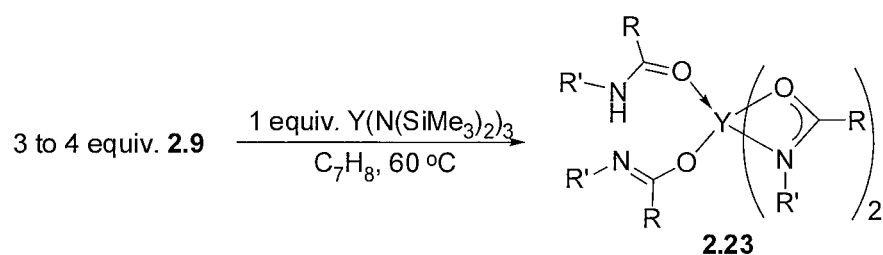
Figure 2.7. Synthesis of complex 2.23 and ball and stick representation of molecular solid-state structure of complex 2.23. Naphthyl groups (except for *ipso*-carbon) are omitted for clarity.

In non-coordinating solvent, even strict control of the reaction stoichiometry (3 proligands to 1 Y) consistently gave evidence (signal at δ 11 in the ^{1}H NMR spectrum) for formation of product 2.23 in poor yield. Interestingly, product 2.23 can also be prepared *in situ* on NMR tube scale by addition of one further equivalent of proligand 2.9 to complex 2.18, via THF displacement by the neutral amide group. Furthermore, pyridine has also been shown to add to complex 2.18, also resulting in displacement of coordinated THF.

As demonstrated by NMR spectroscopic investigations, the ancillary amidate ligands in complex **2.18** are highly fluxional and additional donors can be easily introduced to the metal center. Thus, when complex **2.18** was reacted with complex **2.19**, a rapid redistribution of the ligands occurred, as seen by ^{1}H NMR spectroscopy. The signals for the methylene protons of the THF molecules shifted from δ 4.08 ppm to δ 3.57 ppm, indicating free THF, and multiple signals were observed for the diisopropyl substituents, as well as naphthyl aryl signals. This reaction occurred immediately at room temperature, and no further change in the ^{1}H NMR spectrum was seen when the solution was heated to 110 °C. Attempts to isolate a mixed amidate yttrium complex have been unsuccessful. In solution phase, it is apparent that the amidate ligands are rapidly exchanging and are thought to exchange through a mechanism that takes advantage of the potential bridging mode of the ligand as seen in complex **2.17** and ligand hemi-lability as observed in complex **2.23**.

2.4   Bis(amidate) Yttrium Complexes

2.4.1 Introduction

The direct synthesis of tris(amidate) complexes using the protonolysis reaction is very successful in forming crystalline, monomeric complexes. However, the tris(amidate) complexes lack a reactive ligand (such as $N(SiMe_3)_2$) at the metal centre during catalytic processes.[43,44] With the success of the bis(amidate) complexes of group 4 as hydroamination precatalysts, synthesis of group 3 analogues are desirable. Furthermore, hydroamination precatalysts of group 3 are typically formed *in situ*, and are not fully characterized.[39,43] Without adequate steric protection about the metal centre oligomerization can occur and/or group 3 mixed-ligand complexes have the tendency to undergo ligand redistribution.[7]

However, the protonolysis route used in formation of tris(amidate) complexes of yttrium can also be used successfully for the preparation of bis(amidate) complexes.

2.4.2 Results and Discussion

The first example of a fully characterized bis(amidate) yttrium complex has been synthesized using amide **2.9** and $Y(N(SiMe_3)_2)$ in THF at room temperature. The amide proligand **2.9** was dissolved in THF and added dropwise to a stirring solution of $Y[N(SiMe_3)_2]_3$ in THF. The reaction mixture was stirred at 25 °C, and after work-up, concentrated in *vacuo* to obtain a pale yellow solid. As mentioned previously, the signal corresponding to the *ortho*-proton on the naphthyl substituent is very useful, and as shown in Figure 2.8 there are two separate *ortho*-proton doublets in the ^1H NMR spectrum (signal 'a' and 'b' in Figure 2.8) for the crude compound. This indicates that there are two discrete compounds in solution that contain the naphthyl substituent. There are no N-H signals at approximately δ 6.6 ppm (free proligand) or ~11 ppm (coordinated proligand) in the ^1H NMR spectrum, so these two discrete compounds are both amidate complexes. Furthermore, there is a singlet at approximately δ 0.3 ppm for the methyl protons in residual $Y[N(SiMe_3)_2]_3$ or $LY(N(SiMe_3)_2)_2$ (where L = amidate ligand). The doublet at δ 9.26 ppm matches the chemical shift for the *ortho*-proton on the naphthyl substituent in the analogous tris(amidate) complex **2.18**. The same reaction was repeated in THF at 60 °C for 2 hours, and the amount of tris(amidate) was decreased (as evidenced by the decrease in integration of the doublet 'a' compared to doublet 'b' in the ^1H NMR spectrum of the crude material). Heating the crude mixture dissolved in toluene to 90 °C resulted in clean bis(amidate)

complex formation. This was verified by the full removal of peak 'a' in the ^{1}H NMR spectrum of the product.
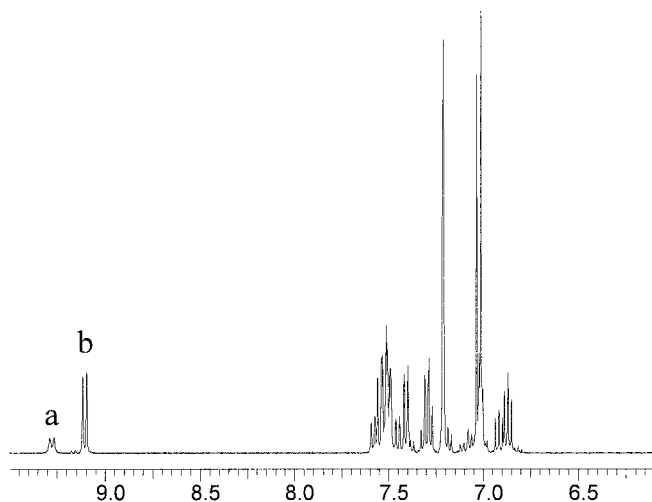
Figure 2.8. ^{1}H NMR spectrum (from δ 6.0 ppm to 9.5 ppm) in C_6D_6 of crude product after synthesis of complex 2.20 in THF at room temperature.

The discovery that heating the crude sample dissolved in toluene at 90 °C leads to the clean formation of bis(amidate) complex **2.24**, resulted in a synthetic protocol that gives the compound in high yield (82%) (Figure 2.9). This synthetic approach can also be used in the formation of bis(amidate) complexes **2.25**, and **2.26**, in 80% and 84% yield respectively. Initial reaction with $Y[N(SiMe_3)_2]_3$ and proligands **2.12** and **2.13** respectively in THF at 60 °C results in bis(amidate) formation as well as tris(amidate) by-product (as evidenced by the crude ^{1}H NMR spectra). As in the formation of complex **2.24**, heating the crude material dissolved in toluene at 90 °C and subsequent recrystallization gives clean crystalline bis(amidate) complexes **2.25**, and **2.26**.
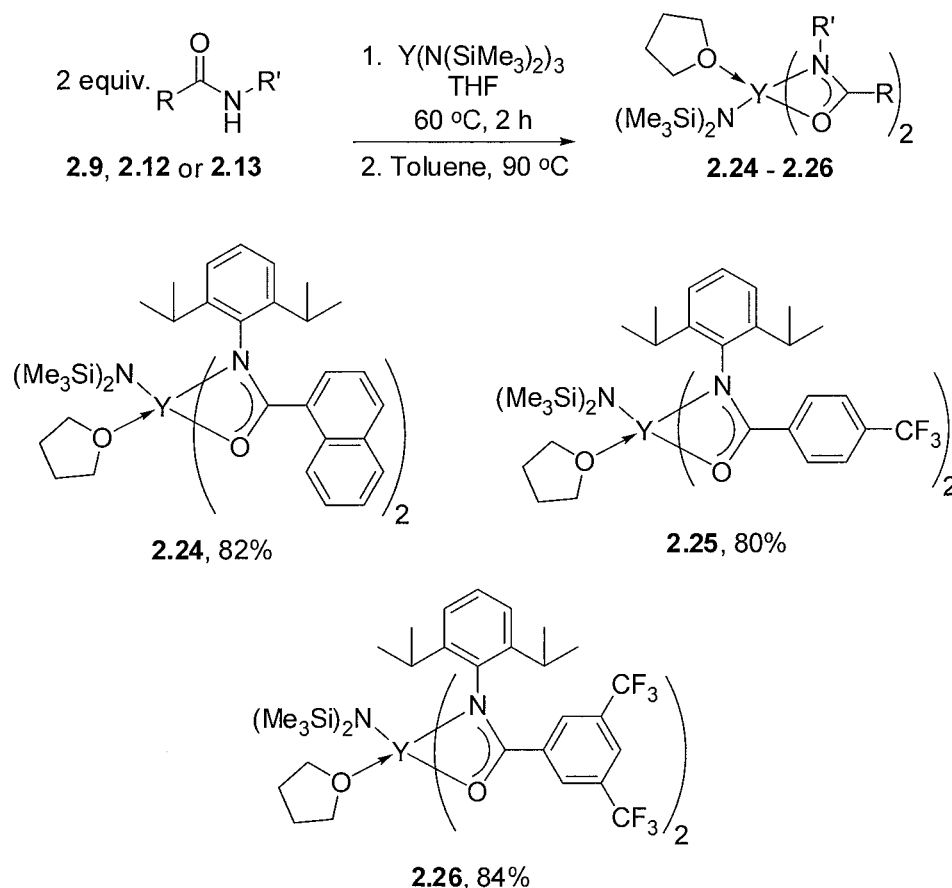
Figure 2.9. Synthesis of bis(amidate) complexes.

When the same reaction is carried out using a proligand with a less sterically bulky substituent on the N, such as dimethylphenyl instead of diisopropylphenyl, single product formation is not observed. Isolation of the bis(amidate) product proved very difficult in these cases and was subsequently abandoned. This shows that it is necessary to have the steric bulk of the diisopropylphenyl substituent on the N of the amidate when synthesizing high-yielding crystalline, monomeric bis(amidate) complexes of yttrium.

The complexes are moisture sensitive, and in the solid-state can be stored at -30 °C for more than 4 months. Furthermore, these complexes are stable in solution at 110 °C for an extended period of time, but after 16 hours at 145 °C, solid precipitates out of solution and degradation of product signals are seen in the ^{1}H NMR spectrum. The ^{1}H NMR spectra of all

the bis(amidate) complexes at room temperature are consistent with C_2 symmetric compounds in solution. No line broadening is evident by ^{1}H NMR spectroscopy when a solution of complex **2.24** is cooled to -50 °C, indicating no loss in symmetry at these lower temperatures. As in the case for the tris(amidate) complexes, the bis(amidate) complexes all have one molecule of THF bound to the metal centre. It is evident that the THF is bound from the shift of the methylene signals of THF in the ^{1}H NMR spectra (δ 3.94 and 1.23 ppm for **2.24**, δ 3.94 and 1.15 ppm for **2.25** and δ 3.90 and 1.05 ppm for **2.26**). These proton signals are broad due to the fluxionality of the chemical environment. The THF molecule remains bound even after exposing the bis(amidate) complexes to full vacuum overnight, since the ^{1}H NMR signals for the THF methylene protons maintain the same integration.

Complex formation and amidate delocalization is confirmed in the IR spectroscopic data for the bis(amidate) complexes. In all cases, the loss of the N-H stretching band from the proligand, and the shift of the C=O stretching band is evident (C=O ν: 1643 cm^{-1} to 1511 cm^{-1} for **2.9** to **2.24**, 1648 cm^{-1} to 1626 cm^{-1} for **2.12** to **2.25**, and 1647 cm^{-1} to 1623 cm^{-1} for **2.13** to **2.26**). The weakening of the C=O bond is not as drastic in the complexes that contain the electron-withdrawing trifluoromethyl group. This suggests that the anionic charge density is retained by the amidate ligand for complexes **2.25** and **2.26**.

The mass spectra of compounds **2.24**, **2.25** and **2.26** each have molecular ion peaks associated with their respective complexes without THF; the fragmentation pattern shows an initial loss of the N(SiMe$_3$)$_2$ group.

X-ray quality crystals of complexes **2.24** and **2.25** were grown at -35 °C from hexanes with a few drops of toluene. Their respective solid-state molecular structures are shown in Figure 2.10. Complexes **2.24** and **2.25** are six-coordinate, C_l symmetric, pseudo pentagonal

pyramidal complexes with the amido ligand as the axial group. There is electron delocalization through the κ^2-amidate backbone as indicated by the C-O and C-N bond lengths (average C-O, C-N for **2.24** is 1.291 Å, 1.312 Å and for **2.25** is 1.294 Å, 1.301 Å, respectively). The Y-O(amidate) and Y-N(amidate) average bond lengths are 2.282 and 2.444 Å for complex **2.24** and 2.286 and 2.428 Å for complex **2.25**. The binding of the amidate ligand is more distorted in the bis(amidate) complexes than the tris(amidate) complex **2.18**, as the Y-O bond is shorter and the Y-N bond longer. As in the tris(amidate) complex, this is attributed to the greater electronegativity of the oxygen in combination with steric bulk around the nitrogen. The Y-N(SiMe$_3$)$_2$ bond length for both **2.24** (2.255(3) Å) and **2.25** (2.235(3) Å) are very similar to the reported value for the pentamethyl cyclopentadienyl yttrium complex Cp$^*_2$Y(N(SiMe$_3$)$_2$ (Cp* = C$_5$Me$_5$) (2.255 Å).[45] The bite angles of the amidate ligand (O-Y-N) are 55.71 ° and 55.98 ° for **2.24** and **2.25**, respectively. These values are very similar to the tris(amidate) complex **2.18**. The average sum of the angles of the amidate metallacycles is 359.5° for **2.24** and 359.7° for **2.25**, indicating the yttrium and amidate backbone are in the same plane.
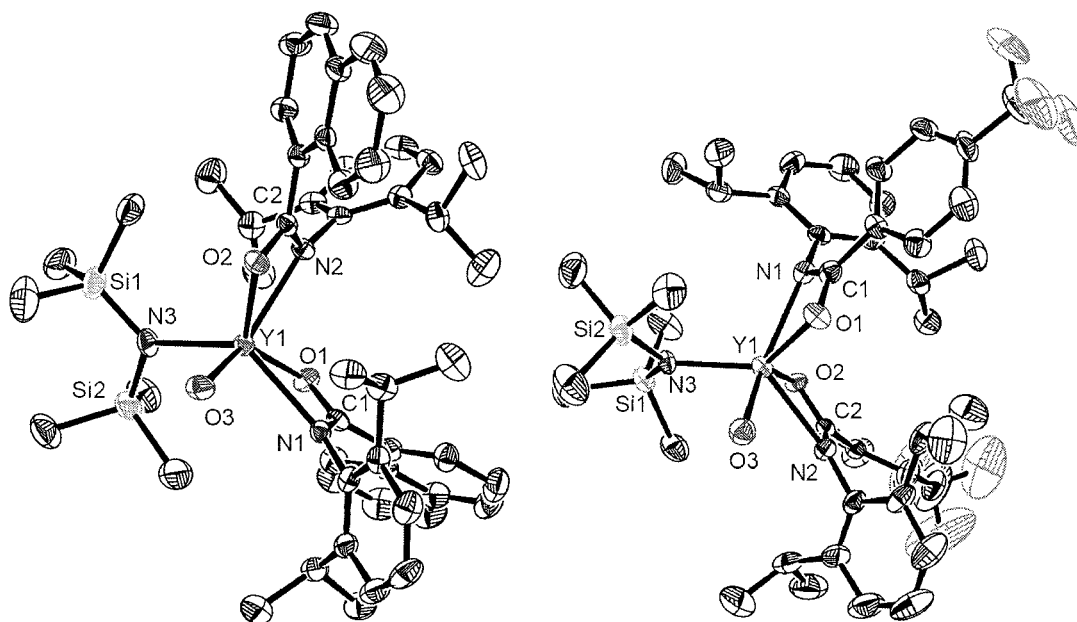
Figure 2.10. ORTEP structure of complex **2.24** and **2.25** with the probability ellipsoids drawn at the 50% level. For both structures the THF ring carbons have been omitted for clarity, and from the structure of **2.24**, two molecules of toluene were also omitted.

Table 2.3. Selected bond lengths and angles for complex **2.24**, and **2.25**.

Complex	**2.24**	**2.25**	Complex	**2.24**	**2.25**
	Bond Length (Å)	Bond Length (Å)	Bond Angle(°)	Bond Angle(°)	Bond Angle(°)
Y1-O1	2.285(3)	2.313(2)	Y1-O1-C1	97.6(2)	95.1(2)
Y1-N1	2.450(3)	2.391(3)	O1-C1-N1	116.8(3)	117.0(4)
O1-C1	1.288(4)	1.294(4)	C1-N1-Y1	89.4(2)	91.2(3)
N1-C1	1.313(5)	1.306(5)	N1-Y1-O1	55.65(10)	56.19(10)
Y1-O2	2.279(3)	2.259(3)	Y1-O2-C2	97.6(2)	97.9(3)
Y1-N2	2.437(3)	2.464(3)	O2-C2-N2	116.2(3)	117.8(4)
O2-C2	1.293(4)	1.294(5)	C2-N2-Y1	89.9(2)	88.5(3)
N2-C2	1.310(5)	1.295(5)	N2-Y1-O2	55.77(10)	55.77(11)
Y1-O3	2.350(3)	2.352(3)	Y1-N3-Si1	124.58(17)	121.50(18)
Y1-N3	2.255(3)	2.235(3)	Y1-N3-Si2	116.62(17)	115.07(16)
			Si1-N3-Si2	118.75(18)	122.87(19)

It was found with the tris(amidate) complexes that the amidate ligands were highly fluxional. The solution NMR spectra of the crystalline bis(amidate) complexes maintain the appearance of C_2 symmetry, even at cooler temperatures (-50 °C). This suggests that the amidate ligand is also highly fluxional in the bis(amidate) compounds. To further probe this, complex **2.24** and **2.25** were dissolved separately in C_6D_6 and combined in a J-Young NMR tube. Immediately, ligand redistribution occurs, as indicated by multiple aryl, methylene, and methyl signals in the ^1H NMR spectrum. These new signals do not match the signals associated with complex **2.24** or **2.25**. This redistribution occurs further when the sample is heated to 65 °C, and at 110 °C. After overnight at 110 °C, no further change occurs but isolation and characterization of a mixed complex was not possible. This indicates that the amidate ligands in the bis(amidate) complexes are as fluxional as they are in the tris(amidate) complexes.

2.5 Mono(amidate) Complexes of Yttrium

2.5.1 Results and Discussion

An efficient route for the formation of tris and bis(amidate) complexes has been determined, and to further study the reactivity of amidate complexes of yttrium, mono(amidate) complexes were synthesized. Initially, proligand **2.9** was used to synthesize a mono(amidate) complex so the progress of reaction could be monitored using the diagnostic *ortho*-naphthyl signal in the ^1H NMR spectrum (*vide supra*). The reaction was performed using the same protonolysis route as the tris and bis(amidate) complex synthesis, but at room temperature. The proligand was dissolved in THF, and added very slowly to a stirring solution of the starting material $Y[N(SiMe_3)_2]_3$ dissolved in THF. After stirring,

filtering and concentrating in *vacuo*, a pale yellow solid was obtained. The crude ^{1}H NMR

spectrum shows two separate *ortho*-naphthyl peaks, a major signal at δ 9.16 ppm, and a very

minor signal at δ 9.09 ppm, indicating a small amount of bis(amidate) product present. If the

same reaction is repeated with more dilute solutions (each in 10 mL THF instead of 5 mL),

after workup the crude ^{1}H NMR spectrum contains only one signal for the *ortho*-naphthyl

signal at δ 9.16 ppm. Thus, an effective synthetic route to mono(amidate) complexes of

yttrium has been developed (Figure 2.11).
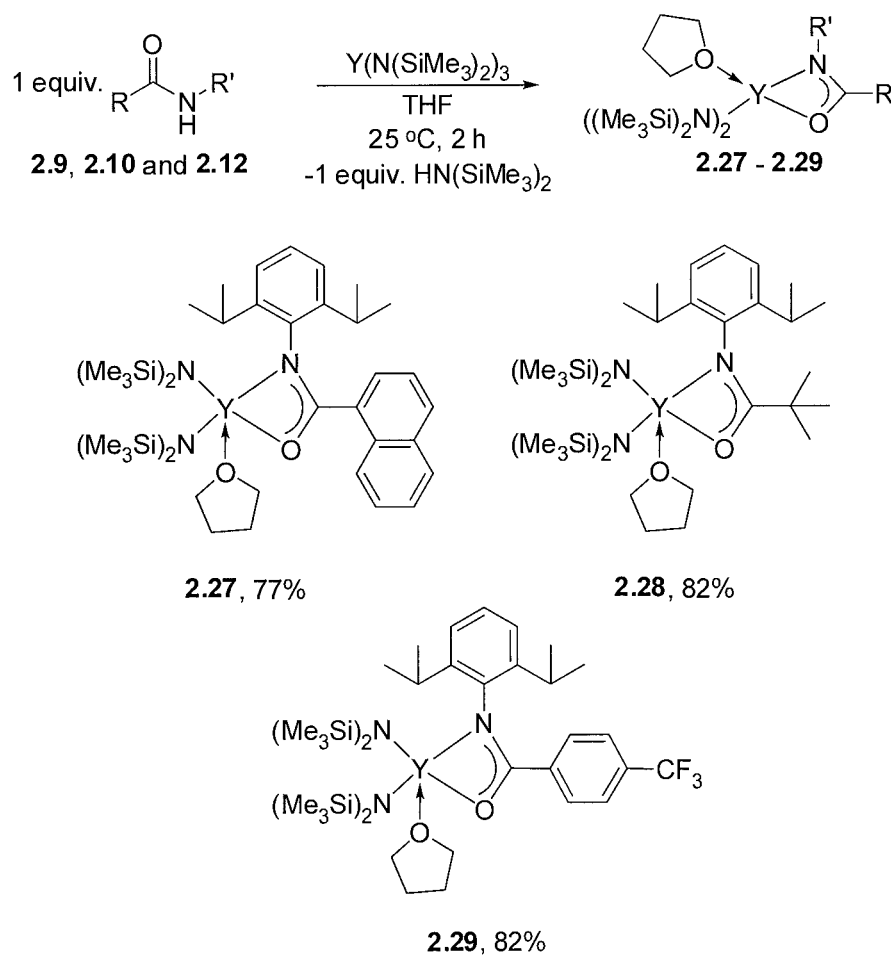
Figure 2.11. Synthesis of mono(amidate) complexes.

Mono(amidate) complexes **2.27**, **2.28** and **2.29** can be easily recrystallized from a minimum amount of hexanes at -35 °C to yield colourless plate-like crystals in high yield. These compounds are soluble in all common hydrocarbon solvents, and are very moisture sensitive. The solid samples can be stored at -30 °C for greater than 4 months without decomposition; however, these compounds undergo ligand redistribution in solution at higher temperatures. For example, heating a solution of complex **2.27** to 65 °C results in no change of the *ortho*-naphthyl signal at δ 9.16 ppm, in the ^{1}H NMR spectrum, but at 110 °C after even a short amount of time a doublet appears at δ 9.09 ppm (matching that of bis(amidate) complex **2.24**). After overnight at 110 °C the intensity of the doublet at δ 9.09 ppm increases and the doublet at δ 9.16 ppm decreases. This indicates that heating the mono(amidate) will cause selective formation of the bis(amidate) complex with no evidence for tris(amidate) formation. At a lower temperature (65 °C) it is evident that the mono(amidate) complex is stable in solution, and on the NMR timescale the proton signals for the $-N(Si(CH_3)_3)_2$ groups are rendered equivalent. This is postulated to occur by exchange of the $-N(Si(CH_3)_3)_2$ groups on the NMR timescale through a mono dentate amidate intermediate. The observed symmetry of the $-N(Si(CH_3)_3)_2$ groups is maintained at lower temperatures (-70 °C), suggesting a highly fluxional structure.

Interestingly, complex **2.28** displays dramatically different solution phase behaviour at room temperature. In the ^{1}H NMR spectrum, all signals are very broad and when the sample is warmed to 65 °C it is apparent that there are two species in solution, as evidenced by two separate broad septet signals at δ 3.39 and 3.25 ppm in a 1:2 integration ratio. This is similar to the tris(amidate) complex **2.19**, with the same amidate ligand, which also displays broadened signals in the ^{1}H NMR spectrum. Unfortunately, heating this sample past 65 °C

causes ligand redistribution, so a higher temperature ^{1}H NMR spectrum could not be obtained. It is known that in the solid-state, the molecular structure of complex **2.28** is a monomeric mono(amidate) complex (*vide infra*), and isolation of another species has not been possible to date. It is postulated that the two species are different geometric isomers (*vide infra*).

The mono(amidate) complexes are similar to the tris(amidate) and bis(amidate) complexes in that there is one molecule of bound THF on the yttrium centre indicated by ^{1}H NMR spectroscopy. The IR spectra of the mono(amidate) complexes **2.27**, **2.28** and **2.29** shows a loss of N-H stretch band, a shifted C=O stretch band and a new C=N stretch band. The electron-impact mass spectra of the mono(amidate) samples all show a typical fragmentation pattern, including the molecular ion peak (without THF) followed by [M$^+$ - CH$_3$] and [M$^+$ - N(SiMe$_3$)$_2$] fragments.

X-ray quality crystals can be obtained at -35 °C for the mono(amidate) complexes **2.27** and **2.28** (from a minimum amount of hexanes) (Figure 2.12). The mono(amidate) complexes formed crystals much more readily than the tris and bis(amidate) complexes. Both **2.27** and **2.28** are isostructural, 5-coordinate, C_1 symmetric and pseudo square-based pyramidal structures with one amido ligand as the axial group. This low coordination number is rare for yttrium due to the previously discussed ligand redistribution pathways, although the steric bulk of the –N(SiMe$_3$)$_2$ ligand stabilizes this species.[40] Electron delocalization is evident through the amidate backbone since the C-O and C-N bond lengths are 1.280(4) Å, 1.316(4) Å for **2.27** and 1.295(6) Å, 1.310(6) Å for **2.28**, respectively) (Table 2.4 and Table 2.5). The Y-O(amidate) bond lengths are slightly shorter than those for the analogous tris and bis(amidate) complexes (2.215(2) Å for complex **2.27** and 2.222(4) Å for

complex **2.28**), whereas the Y-N(amidate) bond length is much longer (2.519(3) Å for complex **2.27** and 2.540(3) Å for complex **2.28**) consistent with the asymmetry seen in amidate bonding. The average Y-N(SiMe₃)₂ bond length for both **2.27** (2.223 Å) and **2.28** (2.242 Å) are very similar to the bis(amidate) complexes **2.24** and **2.25**. The amidate bite angle in complexes **2.27** and **2.28** are also similar to the tris and bis(amidate) complexes at 55.52(8) ° and 54.62(12) °, respectively.

The mono(amidate) complexes were studied by ^{1}H NMR spectroscopy to explore the degree of ligand redistribution. It is evident that ligand redistribution occurs for a solution sample of **2.27** at 110 °C, but not at room temperature or 65 °C. Interestingly, when complexes **2.27** and **2.29** were combined in solution, no ligand redistribution occurred at room temperature or 65 °C, as evidenced by no change in the ^{1}H NMR spectrum of each respective complex. However, at 110 °C ligand redistribution is clear by formation of new naphthyl *ortho*-proton signals at δ 9.07 and 9.02 ppm. These signals do not match the bis(amidate) complex **2.24** *ortho*-naphthyl proton signal and therefore must be an indication of mixed compound formation. This result is in contrast to the tris and bis(amidate) complexes of yttrium that show ligand redistribution between complexes occurring immediately at room temperature. This indicates that ligand redistribution between mono(amidate) yttrium complexes is less favoured than in tris or bis(amidate) complexes, possibly due to the more sterically protecting –N(SiMe₃)₂ ligand blocking the approach of potential bridging amidate ligands.

The mono(amidate) yttrium complexes may be less stable than the tris and bis(amidate) counterparts (such as the ligand redistribution above 65 °C), but the ease of isolation and

crystallization of these compounds makes them ideal for reactivity investigations and catalytic applications.
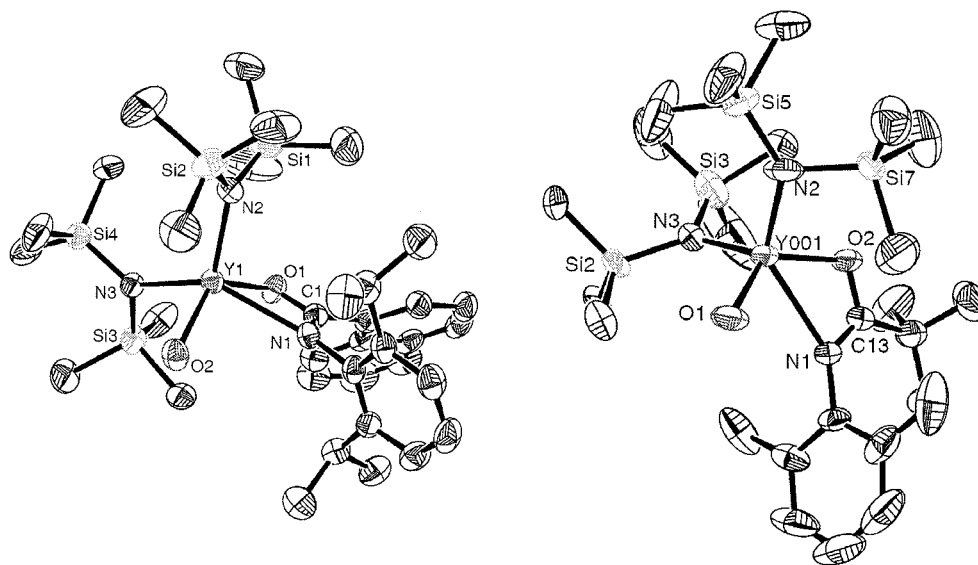
Figure 2.12. ORTEP structure of complex **2.27** and **2.28**, with the probability ellipsoids drawn at the 50% and 30% level, respectively. THF ring carbons omitted for clarity in both structures, and isopropyl methyl substituents omitted in **2.28**.

Table 2.4. Selected bond lengths and bond angles for complex **2.27**.

	Bond Length (Å)		Bond Angle(°)
Y1-O1	2.215(2)	Y1-O1-C1	100.65(18)
Y1-N1	2.519(3)	O1-C1-N1	117.6(3)
O1-C1	1.280(4)	C1-N1-Y1	85.80(19)
N1-C1	1.316(4)	N1-Y1-O1	55.52(8)
Y1-O2	2.343(2)	Y1-N2-Si1	120.56(14)
Y1-N2	2.214(2)	Y1-N2-Si2	119.90(15)
Y1-N3	2.231(2)	Si1-N2-Si2	119.48(15)
		Y1-N3-Si3	112.36(13)
		Y1-N3-Si4	126.58(13)
		Si3-N3-Si4	120.85(15)

Table 2.5. Selected bond lengths and bond angles for complex **2.28**.

	Bond Length (Å)		Bond Angle(°)
Y001-O2	2.222(4)	Y001-O2-C13	102.5(3)
Y001-N1	2.540(3)	O2-C13-N1	115.5(4)
O2-C13	1.295(6)	C13-N1-Y001	87.3(3)
N1-C13	1.310(6)	N1-Y001-O2	54.62(12)
Y001-O1(THF)	2.388(4)	Y001-N2-Si5	135.6(3)
Y1-N2	2.259(4)	Y001-N2-Si7	113.7(3)
Y1-N3	2.224(5)	Si5-N2-Si7	110.5(3)
		Y001-N3-Si2	118.6(3)
		Y001-N3-Si3	116.6(2)
		Si2-N3-Si3	123.8(3)

2.6   Comparison of Yttrium Amidate Complexes

These first examples of yttrium amidate complexes bearing the same naphthyl derivatized ligand (tris(amidate) complex **2.18**, bis(amidate) complex **2.24** and mono(amidate) complex **2.27**) lend themselves to a comparison within this family of compounds (Table 2.6).   These complexes may all have the same amidate ligand, but structural and stability trends are noticeable due to the different ligand stoichiometries.   A decrease in substitution from 3 amidate ligands to 1 amidate ligand, results in a coordination number decrease from 7 to 5.   Furthermore, the yield, the chemical shift of the *ortho*-naphthyl proton signal, the C-N IR stretching frequency, the Y-O and C-N bond lengths and the amidate bite angle all decrease with decreasing amidate coordination.

Table 2.6. Comparison table of reaction data, ^{1}H NMR, IR and X-ray crystallographic data for tris, bis and mono(amidate) complexes **2.18**, **2.24** and **2.27**.

Complex	2.18	2.24	2.27
Number of amidate ligands	3	2	1
Coordination number	7	6	5
Yield	94%	82%	77%
Chemical shift of *ortho*-naphthyl ^{1}H signal (in C_6D_6)	δ 9.26 ppm	δ 9.09 ppm	δ 9.16 ppm
C-O, C-N IR stretch	1513, 1406 cm^{-1}	1511, 1400 cm^{-1}	1516, 1399 cm^{-1}
Average* Y-O bond length	2.303 Å	2.282 Å	2.215(2) Å
Average* Y-N bond length	2.411 Å	2.444 Å	2.519(3) Å
Average* C-O bond length	1.290 Å	1.291 Å	1.280(4) Å
Average* C-N bond length	1.310 Å	1.312 Å	1.316(4) Å
Y-O(THF) bond length	2.332(3) Å	2.350(3) Å	2.343(2) Å
Average* Y-N(SiMe$_3$)$_2$ bond length	-	2.255(3) Å	2.223 Å
Average* N-Y-O bond angle	55.90 °	55.71 °	55.52(8) °

* Calculated averages do not include errors.
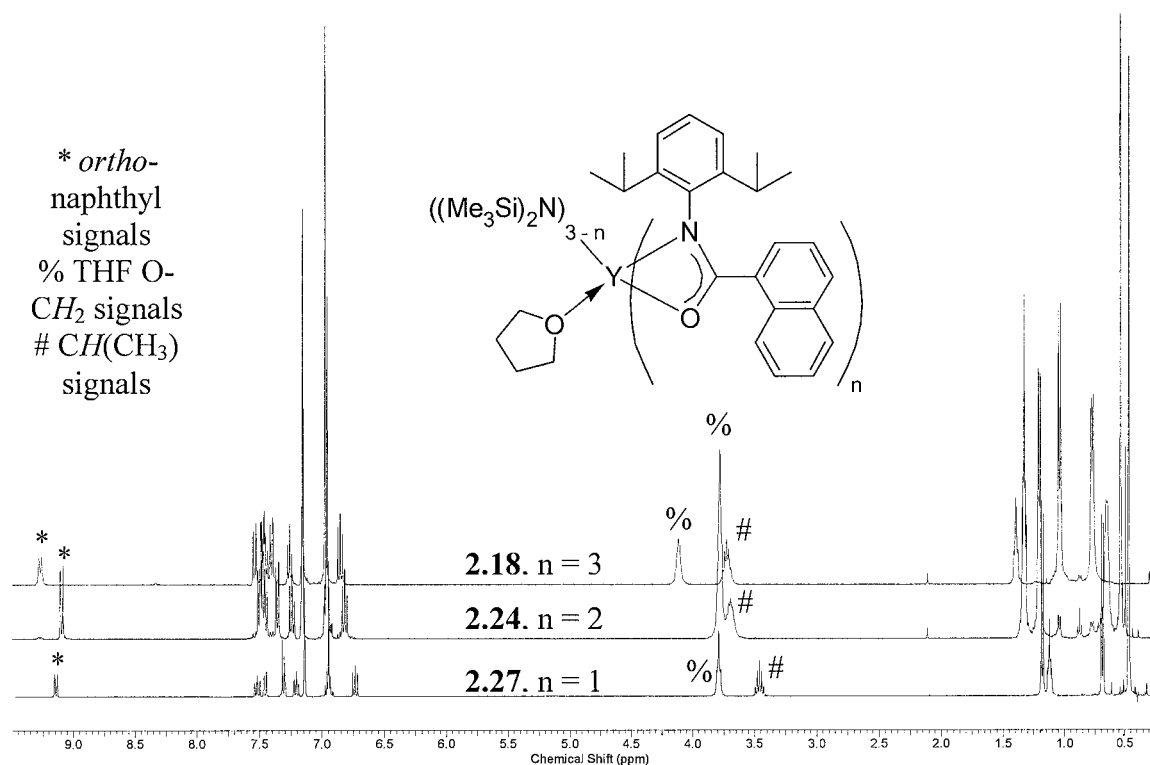
Figure 2.1. ¹H NMR (400 MHz, C₆D₆, 25 °C) of tris(amidate) complex **2.18**, bis(amidate) complex **2.24**, and mono(amidate) complex **2.27** in C₆D₆ at room temperature.

Figure 2.13 shows the ¹H NMR spectra for tris(amidate) complex **2.18**, bis(amidate) complex **2.24** and mono(amidate) complex **2.27** overlaid. The major differences are seen in the *ortho*-naphthyl signal (* in Figure 2.13), the THF chemical shifts (% in Figure 2.13), and the methine peak of the isopropyl groups (# in Figure 2.13). These diagnostic signals are critical in the interpretation of spectra with multiple species.

Both the tris(amidate) and bis(amidate) complexes were found to have very labile amidate ligands, and underwent ligand redistribution when another amide or complex was introduced into a reaction mixture. Also, the mono(amidate) complex undergoes ligand redistribution to form small amounts of bis(amidate) when heated above 65 °C. Interestingly, when one equivalent of tris(amidate) complex **2.18** is added to mono(amidate) complex **2.27** in solution, immediate redistribution is noted in the ¹H NMR spectrum.

Immediately there are three separate doublets for the *ortho*-naphthyl substituent at δ 9.26 ppm, 9.16 ppm and a minor doublet at 9.09 ppm. The first two signals match those of a tris(amidate) complex **2.18** and mono(amidate) complex **2.27**, and the minor doublet is form the bis(amidate) complex **2.24**. When the solution was heated to 65 °C for 48 hours, the same *ortho*-naphthyl signals were still evident, and the *ortho*-naphthyl signal matching that of the bis(amidate) complex grew in intensity. After 48 hours at 110 °C, the bis(amidate) complex is the major product (doublet at δ 9.09 ppm), and there is no evidence of mono(amidate) complex, but a small doublet associated with the tris(amidate) complex at δ 9.26 ppm is still present in the ^{1}H NMR spectrum. This may be due to a small difference in stoichiometry when the initial reaction was prepared. This confirms that the bis(amidate) complex is the thermodynamic product for this system.

All the complexes are soluble in common hydrocarbon solvents, but vary in their thermal stability. The tris(amidate) complexes are known to be stable up to 110 °C in solution and are highly fluxional. The bis(amidate) complexes are stable in solution up to 110 °C, but at 145 °C decomposition is noted as evidenced by degradation of signals in the ^{1}H NMR spectrum. The bis(amidate) complex in solution maintains C_2 symmetry, and is also fluxional. The mono(amidate) complexes on the other hand are stable only to 65 °C in solution, and were determined to be less fluxional than the corresponding tris or bis(amidate) complexes.

The asymmetry of the amidate binding increases from tris to mono(amidate) complex formation, meaning the Y-O bonds get shorter and the Y-N bonds get longer. The mono(amidate) yttrium complex has two bulky trimethylsilylamide groups that sterically repel the Dipp substituent on the N, causing the elongation of the Y-N bond. To compensate

for this, more charge is localized on the O of the amidate, causing a shorter Y-O bond in the mono(amidate) complex. The Y-O(THF) bond length is quite similar for all three complexes, not displaying any notable trends. In the mono(amidate) complex, the Y-N(SiMe$_3$)$_2$ are on average shorter than the corresponding bis(amidate) complex **2.24**. This structural data correlates with the observed solution phase behaviour for these complexes.

2.7 Summary and Conclusions

A direct synthesis of amidate complexes of yttrium has been accomplished using amide proligands and Y[N(SiMe$_3$)$_2$]$_3$. The amide proligands are easily synthesized from acid chlorides and primary amines in high yield and large quantities. Also, variations to the substituents on the amide proligand, such as adding steric bulk or electron-withdrawing groups, is incredibly straightforward. Ligand design was an important aspect of this chapter and the amide proligands used were designed to include steric bulk on the N substituent, as this was found to be essential in the formation of pure, isolable yttrium amidate complexes. Minor modifications, mainly stoichiometry, temperature and dilution, to the simple protonolysis reaction with Y[N(SiMe$_3$)$_2$]$_3$ allows selective formation and high-yielding preparations of crystalline tris, bis and mono(amidate) complexes. It is ideal to use coordinating solvent for synthesis, since one molecule of THF is bound to all yttrium amidate complexes and early attempts to exclude exogenous donors were unsuccessful. However, it should be noted the synthesis of bis and mono(amidate) complexes were not attempted in non-coordinating solvents.

Solid-state molecular structures of tris, bis and mono(amidate) complexes were obtained and trends in bond lengths were evident. From the tris(amidate) complexes to the

mono(amidate) complexes, the Y-O bond length decreases and the Y-N bond length increases.

The amidate ligand was found to be very fluxional in the tris and bis(amidate) complexes. When two tris or bis(amidate) complexes were combined in solution, ligand redistribution was immediately evident at room temperature. This was not the case for mono(amidate) complexes as ligand redistribution did not occur at room temperature or 65 °C. This is possibly due to the –N(SiMe$_3$)$_2$ ligand providing more steric protection from an approaching complex.

The hemi-lability of the amidate scaffold, and the ease with which the donor ligand can be displaced led us to consider tris, bis and mono(amidate) complexes of yttrium as being sterically accessible Lewis acids for a range of potential Lewis basic donors. Consequently, amidate complexes of yttrium have been investigated as initiators in ε-caprolactone ring-opening polymerization and compared with other known yttrium ε-caprolactone polymerization initiators (Chapter 3).

The bis and mono(amidate) complexes have reactive amido groups (-N(SiMe$_3$)$_2$) and are ideal candidates for hydroamination catalysis (Chapter 4). The different amidate ligands can be compared for their reactivity rates during hydroamination.

The mono(amidate) complexes can be used in mixed amidate/anilido complex formation. These complexes are studied and tested for possible yttrium imido formation in Chapter 5.

2.8 Experimental

2.8.1 Starting Materials and Reagents

All operations were performed under an inert atmosphere of nitrogen using standard Schlenk-line or glovebox techniques. THF, toluene, pentane, and hexanes were all purified by passage through an alumina column and sparged with nitrogen. $Y[N(SiMe_3)_2]_3$ was synthesized as described in literature,[40] or purchased from Aldrich and recrystallized from hexanes before use. All other chemicals were commercially available and used as received unless otherwise stated. ^1H and ^{13}C NMR spectra were recorded on Bruker AV300, AV400 or AV600 spectrometers. Shifts are reported in parts per million (ppm) relative to tetramethylsilane (TMS) and calibrated against residual solvent signal, coupling constants J are given in Hertz (Hz) (all couplings are ^3J unless otherwise stated). $^1J_{CF}$ coupling for some CF_3 groups could not be reported due to the complicated aryl region of the ^{13}C NMR spectrum. Infrared spectra were measured on a Nicolet 4700 spectrometer using KBr pellets and IR bands ν are reported in cm^{-1}. Elemental analyses and mass spectra were performed by the microanalytical laboratory of the Department of Chemistry at the University of British Columbia. Some elemental analyses gave low carbon content for yttrium complexes, possibly due to carbide formation.[46] X-ray crystallography was conducted at the University of British Columbia by Dr. Brian Patrick, Dr. Rob Thomson, or Neal Yonson. Compounds **2.9, 2.10, 2.11, 2.14, 2.15,** and **2.16** have been previously synthesized, but complete characterization data were not provided.[47-52]

2.8.2 Synthesis

Synthesis of *N*-(diisopropylphenyl)naphthyl amide (2.9)

To a 250 mL round-bottom flask was added 2,6-diisopropylaniline (4.95 mL, 26.2 mmol) dissolved in 125 mL of dichloromethane. The reaction mixture was cooled to 0 °C, and triethylamine (8 mL) was added dropwise by syringe. The resulting solution was stirred for 5 minutes with subsequent dropwise addition of 1-naphthoyl chloride (3.95 mL, 26.2 mmol). The reaction was stirred overnight and then was washed with 1 M aqueous HCl (3 x 50 mL), followed by 1M aqueous NaOH (30 mL), and brine (30 mL). The organic layer was dried over $MgSO_4$, filtered, and then concentrated under reduced pressure to obtain a beige solid. The solid was recrystallized twice from hot toluene to obtain a white powder. Yield: 7.94 g, 91%. ^1H NMR (C_6D_6, 400 MHz, 293 K) δ 8.86 (d, ^3J = 6 Hz, 1H, 9-naphthyl-*H*), 7.62 (overlapping d, ^3J = 6 Hz, 2H, 6-naphthyl-*H* and 4-naphthyl-*H*), 7.52 (d, ^3J = 5 Hz, 1H, 2-naphthyl-*H*), 7.32 (m, 3H, 8,7,3-naphthyl-*H*), 7.24 (t, ^3J = 6 Hz, 1H, 4-diisopropylphenyl-*H*), 7.11 (m, ^3J = 6 Hz, 2H, 3,5-diisopropylphenyl-*H*), 6.60 (s, 1H, N-*H*), 3.25 (septet, ^3J = 5 Hz, 2H, C*H*(CH$_3$)$_2$), 1.25 (d, ^3J = 5 Hz, 12H, CH(C*H$_3$*)$_2$). ^{13}C NMR (CDCl$_3$, 75.5 MHz, 293K) δ 170.4 (*C*=O), 147.8, 135.6, 135.3, 132.5, 132.2, 131.9, 130.1, 129.8, 128.8, 128.0, 126.8, 126.2, 126.1, 125.0 (aryl *C*), 30.4 (*C*H(CH$_3$)$_2$), 25.2(CH(*C*H$_3$)$_2$). IR data (KBr, cm^{-1}): 3253 (br), 3047 (w), 2961 (s), 2865 (w), 1643 (s), 1591 (w), 1517 (s), 1297 (w), 913 (w), 785 (w), 734 (w), 654 (w). EIMS (*m/z*): 331 [M]$^+$. Anal. Found (calcd for C$_{23}$H$_{25}$NO): C 83.74% (83.34%), N 4.55% (4.23%), H 7.54% (7.60%).
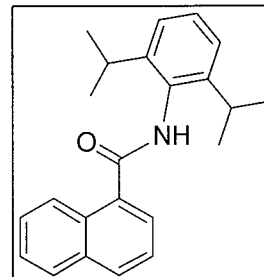
Synthesis of *N*-(2,6-diisopropylphenyl)*tert*-butyl amide (2.10)

The experimental method described for **2.9** was used in the preparation of

2.10 using 2,6-diisopropylaniline (5.00 mL, 0.027 mol) and

trimethylacetyl chloride (3.26 mL, 0.027 mol). Yield: 5.86 g, 85%. ^{1}H
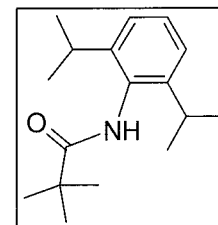
NMR (C_6D_6, 400 MHz, 293 K) δ 7.23 (m, 1H, phenyl-*H*), 7.11 (m, 2H,

phenyl-*H*), 6.26 (s, 1H, N-*H*), 3.07 (septet, ^3J = 7 Hz, 2H, C*H*(CH$_3$)$_2$), 1.21 (d, ^3J = 7 Hz,

12H, CH(C*H*$_3$)$_2$), 1.13 (s, 9H, C(C*H*$_3$)$_3$). ^{13}C NMR (C_6D_6, 100 MHz, 293K) δ 177.3 (*C*=O),

147.5, 133.2, 124.3 (aryl *C*'s), 39.8 (*C*(CH$_3$)$_3$), 29.8 (*C*H(CH$_3$)$_2$), 28.5 (CH(*C*H$_3$)$_2$), 24.5

(C(*C*H$_3$)$_3$). IR data (KBr, cm^{-1}): 3317 (s), 2962 (s), 2865 (w), 1647 (s), 1508 (s), 1498 (s),

790 (s), 736 (w). ESI (*m/z*): 284 [M + Na]$^+$, 262 [M + H]$^+$. Anal. Found (calcd for

$C_{17}H_{27}NO$): C 77.93% (78.11%), N 5.47% (5.36%), H 10.59% (10.41%).

Synthesis of *N*-(2,6-dimethylphenyl)*tert*-butyl amide (2.11)

The experimental method described for **2.9** was used in the preparation of

2.11 using 2,6-dimethylaniline (5.10 mL, 0.041 mol) and trimethylacetyl

chloride (5.05 mL, 0.041 mol). Yield: 7.07 g, 84%. ^{1}H NMR (C_6D_6, 400
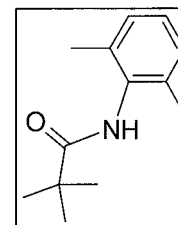
MHz, 293 K) δ 7.05 (m, 1H, phenyl-*H*), 6.95 (m, 2H, phenyl-*H*), 6.17 (s,

1H, N-*H*), 2.09 (s, 6H, C*H$_3$*), 1.08 (s, 9H, C(C*H$_3$*)$_3$). ^{13}C NMR (C_6D_6, 100 MHz, 293K) δ

175.6 (*C*=O), 135.6, 135.1, 127.7, 126.6 (phenyl *C*), 38.7 (*C*(CH$_3$)$_3$), 27.3 (C(*C*H$_3$)$_3$), 18.0

(*C*H$_3$). IR data (KBr, cm^{-1}): 3295 (br), 3021 (w), 2956 (s), 2921 (w), 1650 (s), 1593 (w),

1506 (s), 1278 (w), 1221 (m) 938 (w), 768 (s), 722 (w), 647 (w). EIMS (*m/z*): 205 [M]$^+$.

Anal. Found (calcd for $C_{13}H_{19}NO$): C 76.12% (76.06%), N 7.00% (6.82%), H 9.09%

(9.33%).

Synthesis of *N*-(2,6-diisopropylphenyl)*p*-(trifluoromethyl)phenyl amide (2.12)

The experimental method described for **2.9** was used in the

preparation of **2.12** using 2,6-diisopropylaniline (6.30 mL, 33.4

mmol) and *p*-(trifluoromethyl)benzoyl chloride (5.00 mL, 33.6

mmol). Yield: 9.24 g, 79%. ^{1}H NMR (C_6D_6, 600 MHz, 293 K)
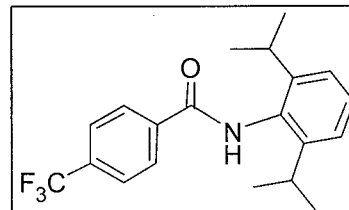
δ 7.47 (d, ^3J = 12 Hz, 2H, aryl-*H*), 7.25 (m, 2H, aryl-*H*), 7.14 (m, 3H, aryl-*H*), 6.68 (s, 1H,

N-*H*), 3.08 (septet, ^3J = 6 Hz, 2H, C*H*(CH$_3$)$_2$), 1.21 (d, ^3J = 6 Hz, 12H, CH(C*H*$_3$)$_2$). ^{13}C

NMR (C_6D_6, 375 MHz, 293K) δ 164.1 (*C*=O), 146.10, 137.2, 132.5, 130.8, 128.3, 125.1,

123.2 (aryl *C*), 28.6 (*C*H(CH$_3$)$_2$), 23.2 (CH(*C*H$_3$)$_2$). IR data (KBr, cm^{-1}): 3300 (br), 2966 (s),

2929 (s) 1648 (s), 1580 (w), 1530 (s), 1500 (s), 1330 (m), 1317 (w), 1158 (w), 1116 (w), 862

(w), 801 (w). EIMS (*m/z*): 349 [M]$^+$. Anal. found (calcd for $C_{20}H_{22}F_3NO$): C 68.75%

(68.75%), N 4.30% (4.01%), H 6.64% (6.35%).

Synthesis of *N*-(2,6-diisopropylphenyl)(*3,5-bis*(trifluoromethyl))phenyl amide (2.13)

To a 250 mL round-bottom flask were added 2,6-

diisopropylaniline (3.50 mL, 18.5 mmol) and 125 mL of

dichloromethane. The reaction mixture was cooled to 0 °C

using an ice bath, and triethylamine (3.20 mL, 23.0 mmol) was
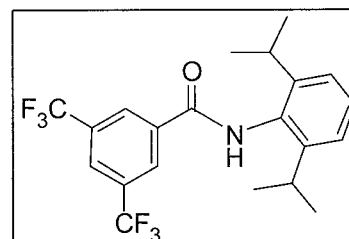
added dropwise by syringe. The resulting solution was stirred for 5 minutes with subsequent

dropwise addition of 3,5-bis(trifluoromethyl)benzoyl chloride (5.00 mL, 18.0 mmol), which

fumed upon addition. The reaction was stirred overnight in which time a white solid

precipitated from the solution. The solid was isolated by filtration and recrystallized by

dissolving in warm dichloromethane, with subsequent addition of hexanes and then cooling

to 0 °C. A white fibrous solid was isolated by filtration. Yield: 5.29 g, 70%. ^{1}H NMR

(C$_6$D$_6$, 600 MHz, 293 K) δ 8.14 (s, 2H, aryl-H), 7.73 (s, 1H, aryl-H), 7.23 (t, J = 6Hz, 1H,

aryl-H), 7.11 (d, J = 6 Hz, 2H, aryl-H), 6.49 (s, 1H, N-H), 2.95 (septet, J = 6 Hz, 2H,

CH(CH$_3$)$_2$), 1.18 (d, J = 6 Hz, 12H, CH(CH_3)$_2$). ^{13}C NMR (C$_6$D$_6$, 375 MHz, 293K) δ 162.59

(C=O), 146.0, 136.3, 131.6 (q, J = 86 Hz, CCF$_3$), 130.4, 128.5, 126.9, 124.5, 123.2(aryl C's),

28.6 (CH(CH$_3$)$_2$), 23.1 (CH(CH$_3$)$_2$). IR data (KBr, cm^{-1}): 3306 (br), 2967 (s), 2930 (s) 1647

(s), 1589 (w), 1525 (s), 1465 (s), 1374 (m), 1333 (w), 1274 (s), 1193 (s), 1140 (s), 911 (w),

797 (w). EIMS (m/z): 417 [M]$^+$. Anal. found (calcd for C$_{21}$H$_{21}$F$_6$NO): C 60.52% (60.43%),

N 3.60% (3.36%), H 5.28% (5.07%).

Synthesis of *N*-(*tert*-butyl)*tert*-butyl amide (2.14)

The experimental method described for **2.9** was used in the preparation of

2.14 using *tert*-butylamine (2.63 mL, 25.0 mmol) and trimethylacetyl

chloride (3.08 mL, 25.0 mmol). Yield: 3.14 g, 80%. ^{1}H NMR (C$_6$D$_6$, 400MHz, 293K) δ

5.10 (s, 1H, N-H), 1.26 (s, 9H, C(CH_3)$_3$), 1.05 (s, 9H, C(CH_3)$_3$). EIMS (m/z): 157 [M]$^+$.

Anal. found (calcd for C$_9$H$_{19}$NO): C 68.86% (68.74%), N 8.95% (8.91%), H 12.20%

(12.18%). Melting Point: 112-113 °C.
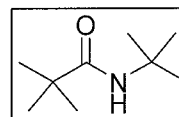
Synthesis of *N*-(*tert*-butyl)*sec*-butyl amide (2.15)

The experimental method described for **2.9** was used in the preparation of

2.15 using *tert*-butylamine (1.32 mL, 12.6 mmol) and *sec*-butyl acid

chloride (1.56 mL, 12.6 mmol). Yield: 1.63 g, 82%. ^{1}H NMR (C$_6$D$_6$, 400MHz, 293K) δ 4.84

(s, 1H, N-H), 1.80 (m, 1H, CH(CH$_3$)CH$_2$CH$_3$), 1.62 (m, 2H, CH(CH$_3$)CH_2CH$_3$), 1.38 (m, 2H,
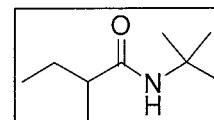
CH(CH$_3$)CH_2CH$_3$), 1.35 (s, 9H, C(CH_3)$_3$), 1.16 (d, J = 6 Hz, 3H, CH(CH_3)CH$_2$CH$_3$), 0.95 (t,

J = 6 Hz, 3H, CH(CH$_3$)CH$_2$CH_3). IR data (KBr, cm^{-1}): 3306 (s), 2963 (s), 1646 (s), 1547

(w), 1451 (s), 1390 (w), 1272 (m), 1250 (w), 1228 (w), 1109 (s), 967 (s), 676 (w). EIMS

(m/z): 157 [M]$^+$. Anal. found (calcd for C$_9$H$_{19}$NO): C 68.88% (68.74%), N 8.99% (8.91%),

H 12.22% (12.18%). Melting Point: 108-109 °C.


Synthesis of *N*-(*tert*-butyl)*sec*-butyl amide (2.16)

The experimental method described for **2.9** was used in the preparation of

2.16 using *sec*-butylamine (2.53 mL, 25.0 mmol) and trimethylacetyl

chloride (3.08 mL, 25.0 mmol). Yield: 2.99 g, 76%. ^{1}H NMR (C$_6$D$_6$, 400MHz, 293K) δ

5.48 (s, 1H, N-H), 4.04 (m, 1H, CH(CH$_3$)CH$_2$CH$_3$), 1.29 (m, 2H, CH(CH$_3$)CH_2CH$_3$), 1.13 (s,

9H, C(CH_3)$_3$), 0.98 (d, J = 6 Hz, 3H, CH(CH_3)CH$_2$CH$_3$), 0.79 (t, J = 6 Hz, 3H,

CH(CH$_3$)CH$_2$CH_3). ^{13}C NMR (C$_6$D$_6$, 150 MHz, 293K) δ 177.2 (C=O), 46.8, 38.9, 30.2,

28.2, 20.9, 11.0. IR data (KBr, cm^{-1}): 3336 (s), 2967 (s), 1634 (s), 1534 (w), 1478 (s), 1459

(w), 1210 (m), 669 (w). EIMS (m/z): 157 [M]$^+$. Anal. found (calcd for C$_9$H$_{19}$NO): C

68.91% (68.74%), N 8.94% (8.91%), H 12.26% (12.18%). Melting Point: 96-97 °C.
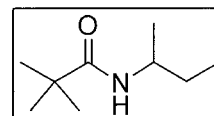
Synthesis of tris(*N*-2',6'-diisopropylphenyl(naphthyl)amidate)yttrium mono(tetrahydrofuran) (2.18)

Inside a nitrogen filled glovebox, a vial was charged

yttrium tris(bis(trimethylsilyl)amide) (0.118 g, 0.206

mmol) and a stirbar. To this, 5 mL of tetrahydrofuran

(THF) was transferred to the reaction vessel at room
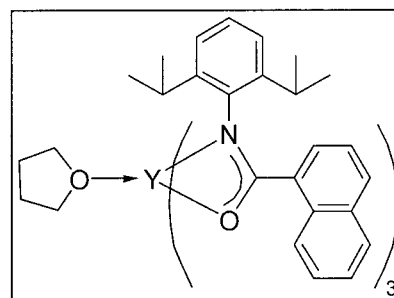
temperature. Amide **2.9** (0.205 g, 0.618 mmol) was dissolved in 5 mL THF and transferred dropwise to the stirring solution of yttrium tris(bis(trimethylsilyl)amide in THF. The solution was stirred within the glovebox for 2 hours at 60 °C, and then filtered through Celite™ and concentrated under reduced pressure to a pale yellow powder. The product was recrystallized by dissolving in a minimum amount of hexanes and then left at -30 °C to yield colorless crystals. Yield: 0.223 g, 94%. Refer to Figure 2.6, Table 2.2 and Appendix I for crystallographic data. ^{1}H NMR (300 MHz, C_6D_6) δ 9.26 (d, J = 9 Hz, 3H, aryl-H), 7.53 (d, J = 8 Hz, 3H, aryl-H), 7.49-7.43 (m, 10H, aryl-H), 7.38 (d, J = 8 Hz, 3H, aryl-H), 7.26 (t, J = 8 Hz, 3H, aryl-H), 6.98 (s, 5H, aryl-H), 6.85 (t, J = 7 Hz, 3H, aryl-H), 4.08 (broad m, 4H, O-CH_2), 3.73 (septet, J = 7 Hz, 6H, CH(CH$_3$)$_2$), 1.41 (m, 4H, O-CH$_2$CH_2), 1.04 (d, J = 7 Hz, 18H, CH(CH_3)$_2$), 0.77 (d, J = 7 Hz, 18H, CH(CH_3)$_2$). ^{13}C NMR (100.6 MHz, C_6D_6) δ 180.1 (C=O), 142.3, 141.6, 134.3, 132.1, 132.0, 130.1, 129.4, 128.3, 127.8, 127.5, 127.4, 127.3, 126.3, 125.4, 124.3, 123.9, 123.6, 123.5 (aryl-C), 69.6 (O-CH$_2$), 28.1 (O-CH$_2$$CH_2$), 25.0 ($C$H(CH$_3$)$_2$), 23.5 (CH($CH_3$)$_2$). IR data (KBr, cm^{-1}): 3052 (w), 2960 (s), 2860 (w), 1573 (w), 1513 (vs), 1406 (vs), 1382 (vs), 1318 (w), 1251 (s), 1191 (s), 1024 (s), 915 (s), 840 (w), 800 (w), 779 (s), 761 (w), 657 (w), 621 (w), 564 (w), 506 (w), 459 (w) cm^{-1}. EIMS (m/z): 1079 [M$^+$], 952 [M$^+$-Nap], 749 [M$^+$-Nap[O,N]Dipp], 331 [M$^+$-Y(Nap[O,N]Dipp)$_2$]. Anal. found (calcd. for $C_{73}H_{80}N_3O_4Y$): C 75.70% (76.09%), H 6.61% (7.00%); N 3.68% (3.65%).

Synthesis of tris(*N*-2',6'-diisopropylphenyl(*tert*-butyl)amidate)yttrium mono(tetrahydrofuran) (2.19)

The experimental method described for **2.18** was used in the preparation of **2.19** using **2.10** (0.200 g, 0.766 mmol) and yttrium tris(bis(trimethylsilyl)amide) (0.146 g, 0.256 mmol) to give a pale yellow solid. The product was recrystallized by dissolving in a minimum amount of pentane and then left at -30 °C to give a white crystalline solid. Yield: 0.207 g, 91%. ^{1}H NMR (600 MHz, C_6D_6, 25 °C) δ 7.07 (broad m, 9H, aryl-*H*), 3.46 (broad s, 4H, O-C*H*$_2$), 3.07 (broad m, 6H, C*H*(CH$_3$)$_2$), 1.46 (broad s, 4H, O-CH$_2$C*H*$_2$), 1.34 (d, *J* = 6 Hz, 18H, CH(C*H*$_3$)$_2$), 1.12 (overlapping d and s, 27H, CH(C*H*$_3$)$_2$ and C(C*H*$_3$)$_3$). ^{1}H NMR (400 MHz, C_7D_8, 77 °C) δ 6.98 (broad m, 9H, aryl-*H*), 3.48 (broad s, 4H, O-C*H*$_2$), 3.31 (septet, *J* = 7 Hz, 6H, C*H*(CH$_3$)$_2$), 1.36 (broad s, 4H, O-CH$_2$C*H*$_2$), 1.30 (d, *J* = 7 Hz, 18H, CH(C*H*$_3$)$_2$), 1.14 (overlapping d and s, *J* = 7 Hz, 27H, CH(C*H*$_3$)$_2$ and C(C*H*$_3$)$_3$). ^{13}C NMR (100.6 MHz, C_6D_6, 25 °C) δ 186.3 (*C*=O), 140.7, 124.7, 122.8, 121.5 (aryl-*C*), 69.2 (O-*C*H$_2$), 41.6 (O-CH$_2$*C*H$_2$), 25.0 (*C*H(CH$_3$)$_2$), 28.7 (*C*(CH$_3$)$_3$), 25.0 (*C*H$_3$), 23.0 (*C*H$_3$). IR data (KBr, cm^{-1}): 2961 (s), 2861 (w), 1618 (s), 1508 (s), 1474 (s), 1395 (w), 1351 (w), 1213 (w), 931 (w), 805 (w) cm^{-1}. EIMS (*m/z*): 869 [M$^+$], 686 [M$^+$- *t*Bu[O,N]Dipp], 261 [*t*Bu[O,N]Dipp]. Anal. found (calcd for $C_{55}H_{86}N_3O_4Y$): C 69.19% (70.11%), N 4.52% (4.46%), H 9.20% (9.26%).

Synthesis   of   tris(*N*-2',6'-dimethylphenyl(*tert*-butyl)amidate)yttrium mono(tetrahydrofuran) (2.20)

The experimental method described for **2.18** was used in the preparation of **2.20** using **2.11** (0.201 g, 0.981 mmol) and yttrium tris(bis(trimethylsilyl)amide) (0.187 g, 0.327 mmol) to give a pale yellow solid. The product was recrystallized by dissolving in a minimum amount of hexanes and then left at -30 °C to give a white crystalline

solid. Yield: 0.223 g, 88%. ^{1}H NMR (300 MHz, C_6D_6) δ 6.88 (m, 9H, aryl-*H*), 3.67 (m, 4H, O-C*H₂*), 2.24 (s, 18H, C*H₃*), 1.28 (m, 4H, O-CH₂C*H₂*), 1.08 (s, 27H, C(C*H₃*)₃). ^{13}C NMR (100.6 MHz, C_6D_6) δ 185.2 (*C*=O), 145.8, 130.8, 127.4, 122.7 (aryl-*C*), 68.7 (O-CH₂), 41.2 (O-CH₂*C*H₂), 28.0 (*C*(CH₃)₃), 25.0 (*C*H₃), 19.2 (*C*H₃). IR data (KBr, cm^{-1}): 2986 (w), 2951 (s), 2904 (w), 1541 (s), 1522 (s), 1477 (s), 1398 (s), 1352 (w), 1219 (s), 1183 (s), 927 (s), 759 (s), 605 (w) cm^{-1}. EIMS (*m/z*): 701 [M$^+$], 686 [M$^+$-CH₃], 644 [M$^+$-*t*Bu], 497 [M$^+$-(*t*Bu[O,N]Dmp]. Anal. found (calcd for $C_{43}H_{62}N_3O_4Y$): C 66.70% (66.75%), N 6.25% (5.99%), H 7.89% (7.76%).

Synthesis of tris(*N*-2',6'-diisopropylphenyl(*p*-(trifluoromethylphenyl) amidate)yttrium mono(tetrahydrofuran) (2.21)

The experimental method described for **2.18** was used in the preparation of **2.21** with amide **2.12** (0.401 g, 1.15 mmol) and yttrium tris(bis(trimethylsilyl)amide) (0.220 g, 0.386 mmol) to give a yellow oil which solidified over time. The product was recrystallized by dissolving in a minimum amount of

hexanes and then left at -30 °C to give a white crystalline solid. Yield: 0.365 g, 79%. ^{1}H

NMR (400 MHz, C$_6$D$_6$) δ 7.65 (d, J = 8 Hz, 6H, aryl-H), 7.20 (m, 6H, aryl-H), 7.12 (m, 9H,

aryl-H), 3.89 (m, 4H, O-CH_2), 3.46 (septet, 6H, J = 7 Hz, CH(CH$_3$)$_2$), 1.41 (m, 4H, O-

CH$_2$CH_2), 1.12 (d, 18H, J = 7 Hz, CH(CH_3)$_2$), 0.89 (d, 18H, J = 7 Hz, CH(CH_3)$_2$). ^{13}C NMR

(100.6 MHz, C$_6$D$_6$) δ 175.7 (C=O), 142.5, 141.2, 137.6, 132.4 (q, J = 32 Hz, C(CF$_3$)), 130.5,

125.4, 124.7, 124.3 (aryl-C), 71.5 (O-CH$_2$), 28.5 (CH(CH$_3$)$_2$), 25.4 (O-CH$_2$$CH_2$), 24.6
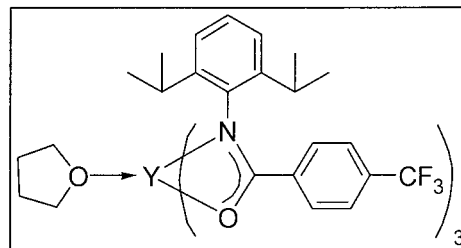
(CH(CH$_3$)$_2$), 24.0 (CH(CH$_3$)$_2$). IR data (KBr, cm^{-1}): 2964 (w), 1617 (s), 1528 (s), 1503 (s),

1409 (s), 1325 (s), 1167 (w), 1129 (s), 1066 (s), 925 (w), 858 (s), 764 (w), 697 (w) cm^{-1}

EIMS (m/z): 1133 [M$^+$], 785 [M$^+$- pCF$_3$phenyl[O,N]Dipp], 349 [pCF$_3$phenyl[O,N]Dipp].

Anal. found (calcd for C$_{64}$H$_{71}$F$_9$N$_3$O$_4$Y): C 62.36% (63.73%), N 3.43% (3.48%), H 6.16%

(5.93%).

Synthesis of tris(N-2′,6′-diisopropylphenyl((3,5-bis(trifluoromethyl) phenyl)amidate)yttrium mono(tetrahydrofuran) (2.22)
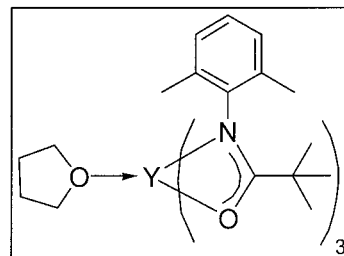
The experimental method described for **2.18** was used in the preparation of **2.22** with amide **2.13** (0.200 g, 0.479 mmol) and yttrium tris(bis(trimethylsilyl)amide) (0.0918 g, 0.161 mmol) to give a yellow oil which solidified over
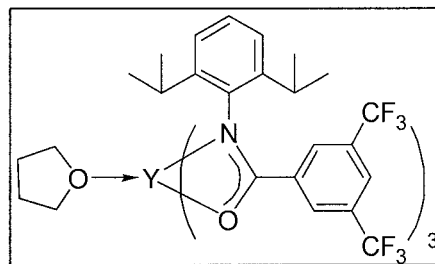
time. The product was recrystallized by dissolving in a minimum amount of hexanes and

then left at -30 °C to give a white crystalline solid. Yield: 0.200 g, 88%. ^{1}H NMR (400

MHz, C$_6$D$_6$) δ 8.05 (s, 6H, aryl-H), 7.61 (d, J = 8 Hz, 3H, aryl-H), 7.10 (m, 3H, aryl-H), 7.04

(m, 6H, aryl-H), 3.71 (broad s, 4H, O-CH_2), 3.38 (broad m, 6H, CH(CH$_3$)$_2$), 1.32 (m, 4H, O-

CH$_2$CH_2), 1.04 (broad s, 18H, CH(CH_3)$_2$), 0.83 (d, 18H, J = 7 Hz, CH(CH_3)$_2$). IR data (KBr,

cm^{-1}): 2966 (w), 1534 (s), 1459 (s), 1351 (s), 1278 (s), 1187 (w), 1137 (s), 1066 (s), 909 (w), 847 (s), 800 (w), 702 (w) cm^{-1}. EIMS (*m/z*): 1337 [M$^+$], 925 [M$^+$- 3,5-bis(CF$_3$)phenyl[O,N]Dipp], 417 [3,5-bis(CF$_3$)phenyl[O,N]Dipp]. Anal. found (calcd for C$_{67}$H$_{68}$F$_{18}$N$_3$O$_4$Y): C 56.90% (57.07%), N 3.16% (2.98%), H 4.82% (4.86%).

Synthesis of tris(*N*-2',6'-diisopropylphenyl(naphthyl)amidate)mono(*N*-2',6'-diisopropylphenyl(naphthyl)amide) yttrium (2.23)

Note: Only partial characterization data could be obtained, due to difficulty in recrystallization.

Inside a nitrogen filled glovebox, a 500 mL round bottomed Schlenk flask was charged with amide **2.9** (0.501g, 1.51 mmol), yttrium tris(bis(trimethylsilyl)amide) (0.317g, 0.550 mmol) and a stirbar. To this, 100 mL of toluene was transferred to the reaction vessel at room temperature. The solution was stirred overnight at 65 °C, and then filtered through Celite and concentrated under reduced pressure to a white powder. The product was recrystallized by dissolving in a minimum amount of hot toluene, layered with pentane and then left at -30 °C. Yield: 0.093g, 12%. Poor quality crystals were grown from warm toluene/pentane mixture. ^{1}H NMR (400 MHz, CDCl$_3$) δ 11.1 (s, 1H, bound amide N-*H*), 8.47 (d, *J* = 8 Hz, 3H, aryl-*H*), 7.97 (d, *J* = 8 Hz, 1H, aryl-*H*), 7.89 (d, *J* = 8 Hz, 1H, aryl-*H*), 7.83 (d, *J* = 8 Hz, 1H, aryl-*H*), 7.66-7.60 (m, 8H, aryl-*H*), 7.53 (m, 6H, aryl-*H*), 7.34-6.94 (m, 20H, aryl-*H*), 3.90 (broad m, 8H, C*H*(CH$_3$)$_2$), 0.65 (broad s, 24H, CH(C*H$_3$*)$_2$), 0.42 (broad s, 24H, CH(C*H$_3$*)$_2$). IR data (KBr, cm^{-1}): 3266 cm^{-1} (br, N-H), 3058 (w), 2961 (s), 2866 (s), 1629 and 1615 (s, C=O), 1490 (w), 1319 (s), 1253 (s), 1911 (s), 920 (s), 841 (s), 800 (s), 779 (s), 760 (s) cm^{-1}.

Synthesis of bis(*N*-2′,6′-diisopropylphenyl(naphthyl)amidate) mono(trimethylsilyl amido) yttrium mono(tetrahydrofuran) (2.24)

Inside a glovebox, a parallel synthetic apparatus tube was charged with yttrium tris(bis(trimethylsilyl)amide) (0.345 g, 0.605 mmol) 5 mL of tetrahydrofuran and a stirbar. The reaction mixture was stirred until all solid was dissolved and *N*-(diisopropylphenyl)naphthyl amide **2.9** (0.401 g, 1.21 mmol) dissolved in 5 mL of tetrahydrofuran was added dropwise. The solution was stirred within the glovebox for 2 hours at 60 °C, and then filtered through a pipette plug of Celite™ and concentrated under reduced pressure to a pale yellow solid. This solid was redissolved in toluene and stirred at 90 °C for a subsequent 2 hours. The product was then concentrated again to a pale yellow solid and recrystallized by dissolving in hexanes with a few drops of toluene to dissolve all solid and then left at -30 °C to give a white crystalline solid. Yield: 0.450 g, 82%. Refer to Figure 2.10, Table 2.3 and Appendix I for crystallographic data. ^{1}H NMR (300 MHz, C_6D_6) δ 9.09 (d, *J* = 9 Hz, 2H, aryl-*H*), 7.49 (m, 4H, aryl-*H*), 7.36 (d, *J* = 8 Hz, 2H, aryl-*H*), 7.24 (m, 2H, aryl-*H*), 7.14 (m, 2H, aryl-*H*), 7.03 (m, 2H, aryl-*H*), 6.96 (m, 4H, aryl-*H*), 6.81 (t, *J* = 8 Hz, 2H, aryl-*H*), 3.94 (broad t, *J* = 6 Hz, 4H, O-C*H*$_2$), 3.67 (broad septet, 4H, *J* = 7 Hz, C*H*(CH$_3$)$_2$), 1.23 (overlapping t and d, 16H, O-CH$_2$C*H*$_2$ and CH(C*H*$_3$)$_2$), 0.65 (d, *J* = 6 Hz, 12H, CH(C*H*$_3$)$_2$), 0.53 (s, 18H, N(Si(C*H*$_3$)$_3$)$_2$). ^{13}C NMR (100.6 MHz, C_6D_6) δ 179.6 (d, *J* = 2 Hz, *C*=O), 141.9, 141.4, 137.5, 134.3, 131.9, 131.5, 130.4, 128.9, 128.4, 126.8, 126.3, 125.5, 125.3, 124.5, 123.8, 123.6 (aryl-*C*'s), 69.9 (O-*C*H$_2$), 28.0 (*C*H(CH$_3$)$_2$), 25.4 (O-CH$_2$*C*H$_2$), 24.9 (CH(*C*H$_3$)$_2$), 23.5 (CH(*C*H$_3$)$_2$), 4.6 (N(Si(*C*H$_3$)$_3$)$_2$). IR data (KBr, cm^{-1}): 2962 (w), 1511 (s), 1496 (s), 1400 (s), 1382 (s), 1245
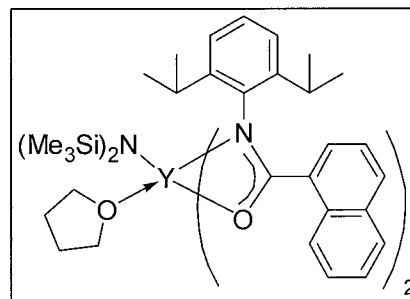
(s), 964 (w), 842 (w), 828 (w), 779 (w) cm^{-1}. EIMS (m/z): 909 [M$^+$], 749 [M$^+$ - N(Si(CH$_3$)$_3$)$_2$], 331 [naphthyl[O,N]Dipp]. Anal. found (calcd for C$_{56}$H$_{74}$N$_3$O$_3$Si$_2$Y): C 68.15% (68.47%), N 4.65% (4.28%), H 7.97% (7.59%).

Synthesis of bis(*N*-2',6'-diisopropylphenyl(*p*-(trifluoromethylphenyl)amidate) mono(trimethylsilyl amido) yttrium mono(tetrahydrofuran) (2.25)

The experimental method described for **2.24** was used in the preparation of **2.25** using **2.12** (0.400 g, 1.15 mmol) and yttrium tris(bis(trimethylsilyl)amide) (0.326 g, 0.572 mmol) to give a pale yellow solid.
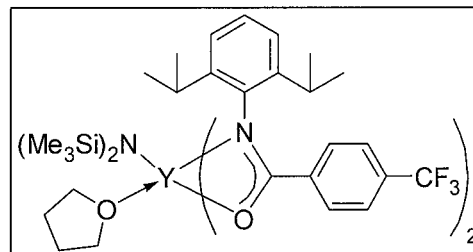
The product was recrystallized by dissolving in a minimum amount of hexanes, with a few drops of toluene, and then left at -30 °C to give a white crystalline solid. Yield: 0.432 g, 80%. Refer to Figure 2.10, Table 2.3 and Appendix I for crystallographic data. ^{1}H NMR (400 MHz, C$_6$D$_6$) δ 7.48 (d, J = 8 Hz, 4H, aryl-*H*), 7.10 (m, 6H, aryl-*H*), 7.01 (d, 4H, aryl-*H*), 3.94 (broad s, 4H, O-C*H$_2$*), 3.40 (septet, J = 7 Hz, 4H, C*H*(CH$_3$)$_2$), 1.18 (d, J = 7 Hz, 12H, CH(C*H$_3$*)$_2$), 1.15 (m, 4H, O-CH$_2$C*H$_2$*), 0.81 (d, J = 7 Hz, 12H, CH(C*H$_3$*)$_2$), 0.47 (s, 18H, N(Si(C*H$_3$*)$_3$)$_2$). ^{13}C NMR (100.6 MHz, C$_6$D$_6$) δ 175.0 (*C*=O), 141.4, 140.4, 136.5, 131.8 (q, J = 32 Hz, *C*(CF$_3$)), 129.8, 125.2, 124.1, 123.7 (aryl-*C*'s), 69.9 (O-*C*H$_2$), 27.8 (*C*H(CH$_3$)$_2$), 24.4 (O-CH$_2$*C*H$_2$), 24.0 (CH(*C*H$_3$)$_2$), 23.4 (CH(*C*H$_3$)$_2$). IR data (KBr, cm^{-1}): 2964 (w), 1626 (s), 1528 (s), 1503 (s), 1410 (s), 1325 (s), 1170 (w), 1132 (s), 1067 (s), 1016 (w), 857 (s), 786 (w), 764 (w) cm^{-1}. EIMS (m/z): 945 [M$^+$], 784 [M$^+$-N(SiMe$_3$)$_2$], 639 [M$^+$- N(SiMe$_3$)$_2$ - *p*CF$_3$phenyl[O,N]Dipp], 349 [*p*CF$_3$phenyl[O,N]Dipp]. Anal. found (calcd for C$_{50}$H$_{68}$F$_6$N$_3$O$_3$Si$_2$Y): C 58.33% (58.98%), N 4.00% (4.13%), H 6.56% (6.73%).

Synthesis of bis(N-2′,6′-diisopropylphenyl((3,5-bis(trifluoromethyl) phenyl)amidate) mono(trimethylsilyl amido) yttrium mono(tetrahydrofuran) (2.26)

The experimental method described for **2.24** was used in the preparation of **2.26** using **2.13** (0.201 g, 0.481 mmol) and yttrium tris(bis(trimethylsilyl)amide) (0.138 g, 0.242 mmol) to give a pale yellow solid. The
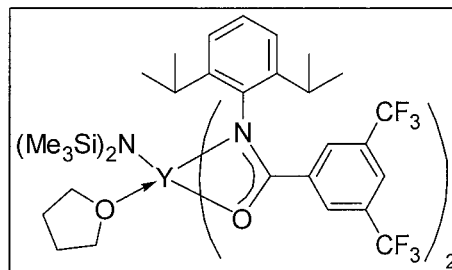
product was recrystallized by dissolving in a minimum amount of hexanes, with a few drops

of toluene, and then left at -30 °C to give a white crystalline solid. Yield: 0.219 g, 84%. ^{1}H

NMR (600 MHz, C_6D_6) δ 8.00 (s, 4H, aryl-H), 7.60 (s, 2H, aryl-H), 7.06 (m, 2H, aryl-H),

7.02 (d, J = 6 Hz, 4H, aryl-H), 3.91 (broad s, 4H, O-CH_2), 3.38 (broad septet, 4H, J = 6 Hz,

CH(CH$_3$)$_2$), 1.16 (d, J = 6 Hz, 12H, CH(CH_3)$_2$), 1.05 (broad s, 4H, O-CH$_2$CH_2) 0.78 (d, 12H,

J = 6 Hz, CH(CH_3)$_2$), 0.40 (s, 18H, N(Si(CH_3)$_3$)$_2$). ^{13}C NMR (150.9 MHz, C_6D_6) δ 173.0

(C=O), 140.7, 140.3, 135.3, 130.8 (q, J = 33 Hz, C(CF$_3$)), 129.7, 127.6, 127.2, 125.6, 124.0,

123.5, 122.7 (q, J = 270 Hz, C(CF$_3$)) (aryl-C's), 69.9 (O-CH$_2$), 27.7 (CH(CH$_3$)$_2$), 24.2 (O-

CH$_2$$CH_2$), 23.9 (CH($CH_3$)$_2$), 23.2 (CH($CH_3$)$_2$), 4.1 (N(Si($CH_3$)$_3$)$_2$). IR data (KBr, cm^{-1}): 2963

(w), 1623 (w), 1529 (s), 1463 (w), 1400 (s), 1349 (s), 1279 (s), 1185 (s), 1136 (s), 961 (w),

908 (w), 839 (w), 801 (w), 702 (w), 682 (w) cm^{-1}. EIMS (m/z): 1082 [M$^+$], 1066 [M$^+$ -

CH$_3$], 921 [M$^+$ - N(Si(CH_3)$_3$)$_2$], 665 [M$^+$ - N(Si(CH_3)$_3$)$_3$)$_2$ and 3,5-bisCF$_3$(phenyl)[O,N]Dipp],

416 [3,5-bisCF$_3$[O,N]Dipp]. Anal. found (calcd for C$_{52}$H$_{66}$F$_{12}$N$_3$O$_3$Si$_2$Y): C 54.50%

(54.11%), N 3.75% (3.64%), H 5.81% (5.76%).

Synthesis of mono(N-2',6'-diisopropylphenyl(naphthyl)amidate)bis(trimethylsilyl amido) yttrium mono(tetrahydrofuran) (2.27)

Inside a glovebox, a parallel synthetic apparatus tube was charged with yttrium tris(bis(trimethylsilyl)amide) (0.401 g, 0.701 mmol) 10 mL of tetrahydrofuran and a stirbar. The reaction mixture was stirred until all solid was dissolved and **2.9** (0.401 g, 1.21 mmol) dissolved in 10 mL of
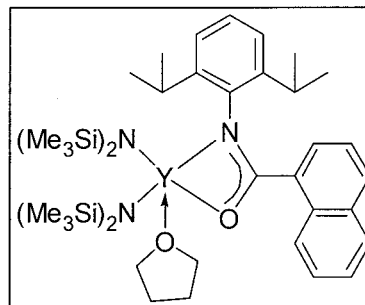

tetrahydrofuran was added very slowly (approximately over 10 minutes) to the stirring solution of yttrium tris(bis(trimethylsilyl)amide) at room temperature. The solution was stirred within the glovebox for 2 hours and then filtered through a pipette plug of Celite and concentrated under reduced pressure to a white solid. The product was recrystallized by dissolving in minimum amount of hexanes and then left at -30 °C to give colourless plates. Yield: 0.443 g, 77%. Refer to Figure 2.12, Table 2.3 and Appendix I for crystallographic data. ^{1}H NMR (600 MHz, C_6D_6) δ 9.16 (d, J = 6 Hz, 1H, aryl-H), 7.54 (t, J = 6 Hz, 1H, aryl-H), 7.48 (d, J = 6 Hz, 1H, aryl-H), 7.33 (t, J = 6 Hz, 2H, aryl-H), 7.23 (t, 1H, J = 6 Hz, aryl-H), 6.97 (m, 3H, aryl-H), 6.75 (t, J = 6 Hz, 1H, aryl-H), 3.81 (broad t, J = 6 Hz, 4H, O-CH_2), 3.48 (septet, 4H, J = 6 Hz, CH(CH$_3$)$_2$), 1.20 (d, 6H, J = 6 Hz, CH(CH_3)$_2$), 1.13 (broad t, J = 6 Hz, 4H, O-CH$_2$CH_2), 0.70 (d, J = 6 Hz, 6H, CH(CH_3)$_2$), 0.49 (s, 32H, N(Si(CH_3)$_3$)$_2$). ^{13}C NMR (150.9 MHz, C_6D_6) δ 179.9 (C=O), 142.8, 141.9, 135.1, 132.7, 132.0, 131.9, 131.2, 129.2, 128.7, 128.6, 127.6, 127.3, 126.4, 125.5, 125.0, 124.2 (aryl-C's), 72.4 (O-CH$_2$), 28.3 (CH(CH$_3$)$_2$), 26.2 (O-CH$_2$CH$_2$), 25.2 (CH(CH$_3$)$_2$), 24.5 (CH(CH$_3$)$_2$), 6.1 (N(Si(CH$_3$)$_3$)$_2$). IR data (KBr, cm^{-1}): 2963 (w), 1516 (s), 1497 (s), 1399 (s), 1379 (s), 1245 (s), 956 (w), 863 (w), 844 (w), 668 (w) cm^{-1}. EIMS (m/z): 739 [M$^+$], 724 [M$^+$ - CH$_3$], 578 [M$^+$ - N(Si(CH$_3$)$_3$)$_2$].

Anal. found (calcd for $C_{39}H_{68}N_3O_2Si_4Y$): C 57.82% (57.67%), N 5.46% (5.17%), H 8.38% (8.44%).

Synthesis of mono(*N*-2′,6′-diisopropylphenyl(*tert*-butyl)amidate)bis(trimethylsilyl amido)yttrium mono(tetrahydrofuran) (2.28)

The experimental method described for **2.27** was used in the preparation of **2.28** using **2.10** (0.100 g, 0.384 mmol) and yttrium tris(bis(trimethylsilyl)amide) (0.219 g, 0.384 mmol) to give a pale yellow solid. The product was recrystallized by dissolving in minimum amount of pentane and then left at -30
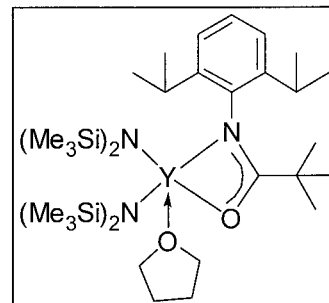
°C to give a colourless plates. Yield: 0.234 g, 82%. Refer to Figure 2.12, Table 2.5 and Appendix I for crystallographic data. ^{1}H NMR (400 MHz, C_6D_6, 65 °C, mixture of two compounds **a** and **b** in a ~ 1:2 ratio) δ 7.08 (s, 1H, aryl-*H*, compound **a**), 7.01 (s, 2H, aryl-*H*, compound **a**), 7.00 (s, 2H, aryl-*H*, compound **b**), 6.70 (m, 1H, aryl-*H*, compound **b**), 3.81 (broad s, 4H, O-C*H₂*), 3.39 (septet, 2H, *J* = 6 Hz, C*H*(CH₃)₂, compound **a**), 3.25 (septet, 2H, *J* = 6 Hz, C*H*(CH₃)₂, compound **b**), 1.42 (d, 6H, *J* = 6 Hz, CH(C*H₃*)₂, compound **a**), 1.34 (d, 6H, *J* = 6 Hz, CH(C*H₃*)₂, compound **a**), 1.31 (d, 10H, *J* = 6 Hz, CH(C*H₃*)₂ for compound **b** overlapping with O-CH₂C*H₂*), 1.22 (d, 15H, *J* = 6 Hz, CH(C*H₃*)₂ for compound **b** overlapping with C(C*H₃*)₃ for compound **a**), 1.10 (s, 9H, C(C*H₃*)₃ for compound **b**), 0.36 (s, 36H for **a**, 36H for **b**, N(Si(C*H₃*)₃)₂ for both compound **a** and **b**). ^{13}C NMR (150.9 MHz, C_6D_6, 25 °C, broad and complicated) δ 186.3 (*C*=O), 140.7, 140.6, 124.7, 124.2, 123.1 (br), 121.4 (br), 121.4 (br), 120.5 (br) (aryl-*C*'s), 71.2 (O-*C*H₂), 41.7 (O-CH₂*C*H₂), 29.5 (br), 28.6 (br), 27.9, 27.6 (br), 25.4 (br), 24.9 (br), 24.1 (br) 23.6 (br), 22.9 (br), 21.6 (br) (*C*H(CH₃)₂

and $C(CH_3)_3$), 5.12 (br), 4.34 (br) ($N(Si(CH_3)_3)_2$). IR data (KBr, cm^{-1}): 2961 (s), 1513 (s), 1477 (s), 1399 (s), 1348 (s), 1313 (w), 1246 (s), 1176 (w), 942 (s), 830 (s), 767 (w) cm^{-1}. EIMS (*m/z*): 669 [M$^+$], 654 [M$^+$ - CH$_3$], 509 [M$^+$ - N(Si(CH$_3$)$_3$)$_2$]. Anal. found (calcd for $C_{33}H_{70}N_3O_2Si_4Y$): C 52.35% (53.40%), N 5.48% (5.66%), H 9.11% (9.51%).

Synthesis of mono(*p*-(trifluoromethylphenyl)amidate)bis(trimethylsilylamido) yttrium mono(tetrahydrofuran) (2.29)

The experimental method described for **2.27** was used in the preparation of **2.29** using **2.12** (0.100 g, 0.287 mmol) and yttrium tris(bis(trimethylsilyl)amide) (0.163 g, 0.286 mmol) to give a pale yellow solid. The product was recrystallized by dissolving in minimum amount of
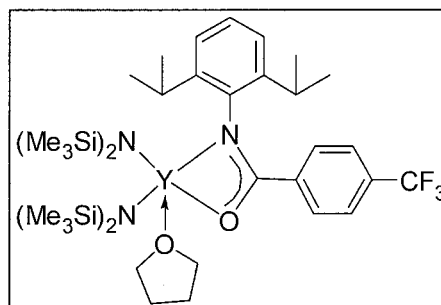
pentane and then left at -30 °C to give a white solid. Yield: 0.194 g, 82%. ^{1}H NMR (600 MHz, C$_6$D$_6$) δ 7.50 (d, *J* = 6 Hz, 2H, aryl-*H*), 7.07 (m, 3H, aryl-*H*), 6.96 (d, *J* = 6 Hz, 2H, aryl-*H*), 3.69 (broad s, 4H, O-C*H*$_2$), 3.31 (septet, *J* = 6 Hz, 2H, C*H*(CH$_3$)$_2$), 1.17 (d, *J* = 6 Hz, 6H, CH(C*H*$_3$)$_2$), 1.11 (broad s, *J* = 6 Hz, 4H, O-CH$_2$C*H*$_2$), 0.82 (d, *J* = 6 Hz, 6H, CH(C*H*$_3$)$_2$), 0.46 (s, 36H, N(Si(C*H*$_3$)$_3$)$_2$). ^{13}C NMR (150.9 MHz, C$_6$D$_6$) δ 174.6 (*C*=O), 143.1, 141.6, 137.5, 132.8 (q, *J* = 33 Hz, *C*(CF$_3$)), 131.0, 126.2, 125.5, 125.4 (q, *J* = 169 Hz, C(*C*F$_3$)), 125.2, 124.9 (aryl-*C*'s), 72.1 (O-*C*H$_2$), 28.5 (*C*H(CH$_3$)$_2$), 25.2 (overlapping O-CH$_2$*C*H$_2$ and CH(*C*H$_3$)$_2$), 24.4 (CH(*C*H$_3$)$_2$), 6.0 (N(Si(*C*H$_3$)$_3$)$_2$). IR data (KBr, cm^{-1}): 2962 (w), 1528 (s), 1501 (s), 1410 (s), 1327 (s), 1247 (s), 1132 (s), 1067 (w), 833 (s), 668 (w) cm^{-1}. EIMS (*m/z*): 742 [M$^+$ - CH$_3$], 596 [M$^+$ - N(Si(CH$_3$)$_3$)$_2$]. Anal. found (calcd for C$_{36}$H$_{65}$F$_3$N$_3$O$_2$Si$_4$Y): C 51.74% (52.08%), N 4.86% (5.06%), H 7.49% (7.89%).

2.9   References

(1)   Burgstein, M. R.; Berberich, H.; Roesky, P. W. *Chem. Eur. J.* **2001**, *7*, 3078.

(2)   Kim, Y. K.; Livinghouse, T.; Bercaw, J. E. *Tetrahedron Lett.* **2001**, *42*, 2933.

(3)   Tredget, C. S.; Lawrence, S. C.; Ward, B. D.; Howe, R. G.; Cowley, A. R.; Mountford, P. *Organometallics* **2005**, *24*, 3136.

(4)   Arnold, P. L.; Mungur, S. A.; Blake, A. J.; Wilson, C. *Angew. Chem., Int. Ed.* **2003**, *42*, 5981.

(5)   Yao, Y. M.; Zhang, Z. Q.; Peng, H. M.; Zhang, Y.; Shen, Q.; Lin, J. *Inorg. Chem.* **2006**, *45*, 2175.

(6)   Xue, M. Q.; Yao, Y. M.; Shen, Q.; Zhang, Y. *J. Organomet. Chem.* **2005**, *690*, 4685.

(7)   Sanchez-Barba, L. F.; Hughes, D. L.; Humphrey, S. A.; Bochmann, M. *Organometallics* **2005**, *24*, 3792.

(8)   Sanchez-Barba, L. F.; Hughes, D. L.; Humphrey, S. M.; Bochmann, M. *Organometallics* **2006**, *25*, 1012.

(9)   Chai, J.; Jancik, V.; Singh, S.; Zhu, H.; He, C.; Roesky, H. W.; Schmidt, H.-G.; Noltemeyer, M.; Hosmane, N. S. *J. Am. Chem. Soc.* **2005**, *127*, 7521.

(10)   Avent, A. G.; Caro, C. F.; Hitchcock, P. B.; Lappert, M. F.; Li, Z.; Wei, X.-H. *Dalton Trans.* **2004**, 1567.

(11)   Luo, Y.; Yao, Y.; Zhang, Y.; Shen, Q.; Yu, K. *Chin. J. Chem.* **2004**, *22*, 187.

(12)   Neculai, D.; Roesky, H. W.; Neculai, A. M.; Magull, J.; Herbst-Irmer, R.; Walfort, B.; Stalke, D. *Organometallics* **2003**, *22*, 2279.

(13)   Hitchcock, P. B.; Lappert, M. F.; Tian, S. *J. Chem. Soc., Dalton Trans.* **1997**, 1945.

(14)   Bambirra, S.; Bouwkamp, M. W.; Meetsma, A.; Hessen, B. *J. Am. Chem. Soc.* **2004**, *126*, 9182.

(15)   Bambirra, S.; Brandsma, M. J. R.; Brussee, E. A. C.; Meetsma, A.; Hessen, B.; Teuben, J. H. *Organometallics* **2000**, *19*, 3197.

(16)   Bambirra, S.; Meetsma, A.; Hessen, B.; Teuben, J. H. *Organometallics* **2001**, *20*, 782.

(17)   Zuyls, A.; Roesky, P. W.; Deacon, G. B.; Konstas, K.; Junk, P. C. *Eur. J. Org. Chem.* **2008**, 693.

(18)   Luo, Y.; Yao, Y.; Shen, Q.; Yu, K.; Weng, L. *Eur. J. Inorg. Chem.* **2003**, 318.

(19)   Zhang, J.; Cai, R.; Weng, L.; Zhou, X. *Organometallics* **2004**, *23*, 3303.

(20)   Heitmann, D.; Jones, C.; Junk, P. C.; Lippert, K. A.; Stasch, A. *Dalton Trans.* **2007**, 187.

(21)   Lyubov, D. M.; Bubnov, A. M.; Fukin, G. K.; Dolgushin, F. M.; Antipin, M. Y.; Pelce, O.; Schappacher, M.; Guillaume, S. M.; Trifonov, A. A. *Eur. J. Inorg. Chem.* **2008**, 2090.

(22)   Skvortsov, G. G.; Yakovenko, M. V.; Fukin, G. K.; Cherkasov, A. V.; Trifonov, A. A. *Russ. Chem. Bull.* **2007**, *56*, 1742.

(23)   Trifonov, A. A.; Lyubov, D. M.; Fedorova, E. A.; Skvortsov, G. G.; Fukin, G. K.; Kurskii, Y. A.; Bochkarev, M. N. *Russ. Chem. Bull.* **2006**, *55*, 435.

(24)   Zhou, L. Y.; Yao, Y. M.; Zhang, Y.; Xue, M. Q.; Chen, J. L.; Shen, Q. *Eur. J. Inorg. Chem.* **2004**, 2167.

(25)   Mao, L.; Shen, Q.; Xue, M. *Organometallics* **1997**, *16*, 3711.

(26)   Piers, W. E.; Emslie, D. J. H. *Coord. Chem. Rev.* **2002**, *233*, 131.

(27)   Kerton, F. M.; Whitwood, A. C.; Willans, C. E. *Dalton Trans.* **2004**, 2237.

(28)   Westmoreland, I.; Arnold, J. *Dalton Trans.* **2006**, 4155.

(29)   Zhou, X. G.; Zhu, M. *J. Organomet. Chem.* **2002**, *647*, 28.

(30)   Zhou, X. G.; Zhang, L. B.; Zhu, M.; Cai, R. F.; Weng, L. H.; Huang, Z. X.; Wu, Q. J. *Organometallics* **2001**, *20*, 5700.

(31)   Hsieh, K.-C.; Lee, W.-Y.; Lai, C.-L.; Hu, C.-H.; Lee, H. M.; Huang, J.-H.; Peng, S.-M.; Lee, G.-H. *J. Organomet. Chem.* **2004**, *689*, 3362.

(32)   Thomson, R. K.; Zahariev, F. E.; Zhang, Z.; Patrick, B. O.; Wang, Y. A.; Schafer, L. L. *Inorg. Chem.* **2005**, *44*, 8680.

(33)   Bexrud, J. A.; Li, C. Y.; Schafer, L. L. *Organometallics* **2007**, *26*, 6366.

(34)   Zhang, Z.; Leitch, D. C.; Lu, M.; Patrick, B. O.; Schafer, L. L. *Chem. Eur. J.* **2007**, *13*, 2012.

(35)   Li, C. Y.; Thomson, R. K.; Gillon, B.; Patrick, B. O.; Schafer, L. L. *Chem. Commun.* **2003**, 2462.

(36)   Thomson, R. K.; Patrick, B. O.; Schafer, L. L. *Can. J. Chem.* **2005**, *83*, 1037.

(37)   Li, C.; Wang, Y. R.; Zhou, L. Y.; Sun, H. M.; Shen, Q. *J. Appl. Polym. Sci.* **2006**, *102*, 22.

(38)   Beard, J. D. *M.Sc. thesis, University of British Columbia, Vancouver, BC* **2004**.

(39)   Kim, Y. K.; Livinghouse, T.; Horino, Y. *J. Am. Chem. Soc.* **2003**, *125*, 9560.

(40)   Bradley, D. C.; Ghotra, J. S.; Hart, F. A. *J. Chem. Soc., Dalton Trans.* **1973**, 1021.

(41)   Gottlieb, H. E.; Kotlyar, V.; Nudelman, A. *J. Org. Chem.* **1997**, *62*, 7512.

(42)   Data was processed using the SQUEEZE function of the PLATON software to remove disordered hexanes. Speck, A. L. *J. Appl. Cryst.* **2003**, *36*, 7.

(43)   Hong, S.; Marks, T. J. *Acc. Chem. Res.* **2004**, *37*, 673.

(44)   Bambirra, S.; Tsurugi, H.; van Leusen, D.; Hessen, B. *Dalton Trans.* **2006**, 1157.

(45)   Hultzsch, K. C.; Spaniol, T. P.; Okuda, J. *Organometallics* **1997**, *16*, 4845.

(46)   Vitanova, D. V.; Hampel, F.; Hultzsch, K. C. *Dalton Trans.* **2005**, 1565.

(47)   Callens, E.; Burton, A. J.; Barrett, A. G. M. *Tetrahedron Lett.* **2006**, *47*, 8699.

(48)   Gowda, B. T.; Usha, K. M.; Jyothi, K. *Z. Natur. A.: Phys. Sci.* **2004**, *59*, 69.

(49)   Pettersson, I.; Sandstroem, J. *Acta. Chem. Scand. B: Org. Chem. Biochem.* **1984**, *B38*, 397.

(50)   Joergensen, K. A.; Ghattas, A. B.; Lawesson, S. O. *Bull. Chem. Soc. Chim. Fra.* **1984**, 204.

(51)   Budzelaar, P. H. M.; van Oort, A. B.; Orpen, G. *Eur. J. Inorg. Chem.* **1998**, *10*, 1485.

(52)   Leonard, N. J.; Nommensen, E. W. *J. Am. Chem. Soc.* **1949**, *71*, 2808.

Chapter 3. Yttrium Amidate Complexes as Effective Initiators for the Ring-Opening Polymerization of ε-Caprolactone[1]

3.1   Introduction

Plastic products have become essential to the modern economy, being utilized in everything from packaging to electronic devices. Currently, most plastics are made from petroleum sources, meaning fossil fuel consumption. A more sustainable option is the utilization of biodegradable polymers, which can re-enter the carbon cycle upon decomposition. Synthetic biodegradable polymers (green plastics) can be used for a variety of consumer needs such as biomedical applications and plastic substitutes.[1-5] The most common synthetic green polymers are variations of polyesters, which can be synthesized in multiple ways. Polycondensation of diols and dicarboxylic acids is one method, but usually requires high temperatures and long reaction times to obtain high molecular weight polymer.[6] A more efficient method for high molecular weight polyester formation is ring-opening polymerization (ROP) of lactones or lactides, since the chain length can be controlled and the reactions are typically done at modest temperatures.[6] The ring-opening polymerization of ε-caprolactone (3.1) is widely used, and the resulting polyester (3.2) is already used extensively in the biomedical industry (eg. surgical sutures, drug delivery media) (Figure 3.1).[7]

ε-caprolactone
3.1

poly(ε-caprolactone)
3.2
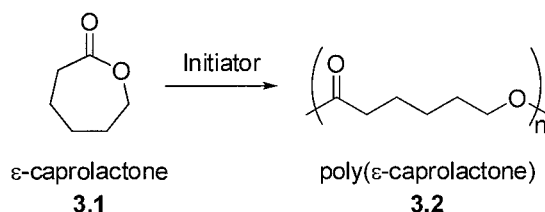
Figure 3.1. Ring-opening polymerization of ε-caprolactone.

Generally, polymerization can be explained in three different steps, initiation, propagation and finally, termination. Specifically for ring-opening polymerization of ε-caprolactone, the initiation step is believed to involve the ring-opening of one molecule of ε-caprolactone, which is promoted by the coordination of the second molecule of ε-caprolactone (Figure 3.2).[8] Propagation begins when the third equivalent of ε-caprolactone coordinates and concurrently another molecule of ε-caprolactone is inserted into the growing polymer chain. The metal complex is known as an initiator (I) because its presence is required to begin the polymerization.
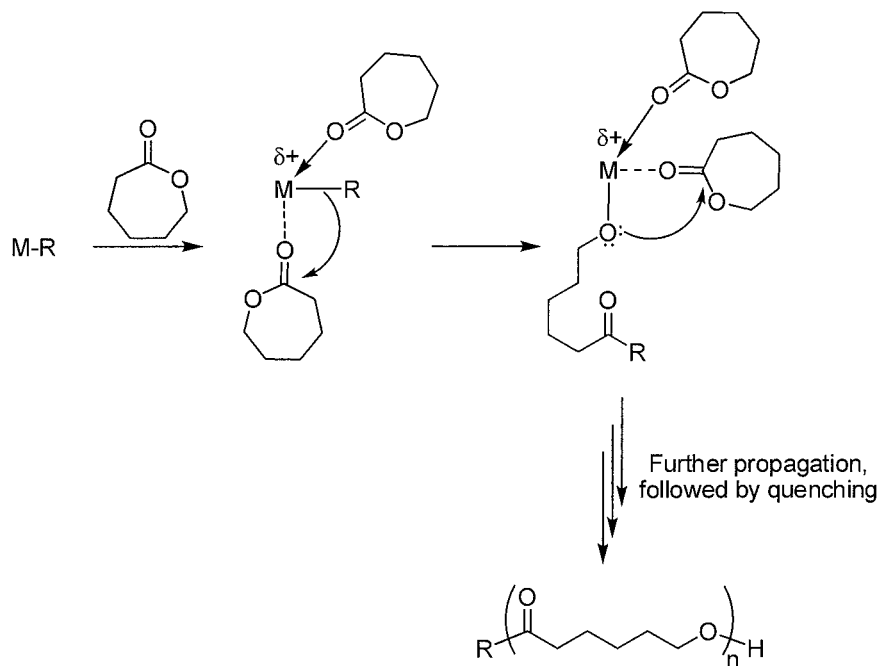
Figure 3.2. Proposed mechanism for the ring-opening polymerization of ε-caprolactone.[8]

Many rare-earth initiators of ROP of ε-caprolactone are "living" initiators,[9-17] denoting that the rate of initiation is much larger than the rate of propagation. Furthermore, the termination step is insignificant, which results in a well-behaved catalyst that can generate block copolymers,[18-24] and produce polymer with controlled molecular weights paired with

low molecular weight distributions as measured by the polydispersity index, PDI. For the purposes of this thesis, the latter properties represent what will be referred to as a "controlled" polymerization (where PDI is close to one). Most often the molecular weight values of poly(ε-caprolactone) correlate very well with calculated values which arise from the molecular weight of ε-caprolactone (114 gmol^{-1}) multiplied by the monomer to initiator ratio ([M]/[I]). Living initiators typically have a linear relationship between 1) percent conversion and time of the reaction and 2) molecular weight (of polymer obtained) and the monomer to initiator ratio.[25]

Many metal-based initiators have been used in the synthesis of poly(ε-caprolactone) such as tin,[26-28] aluminum,[29,30] and rare-earth metals (lanthanides, and group 3 metals).[4,13,31-37] Tin and aluminum compounds are very successful in this transformation, but due to their acute toxicity they are not ideal for commercial use.[38,39] Rare-earth complexes are very attractive catalyst systems due to their low toxicity, low cost and high activity.[40] These features make group 3 and the lanthanides popular for use as initiators in ε-caprolactone ROP.

Interestingly, homoleptic amidinate complexes (**3.3**), and bis(guanidinate) complexes (**3.4**) of the lanthanides and group 3 metals have been modestly successful in ROP of ε-caprolactone (Figure 3.3).[41-43] An example is the homoleptic neodymium amidinate complex, [CyNC(Me)NCy]$_3$Nd that forms poly(ε-caprolactone) of a moderate molecular weight (7.98 x 10^4 gmol^{-1}) with a PDI value of 1.81.[41] Also, aryloxo lanthanide compounds (**3.5**) supported by β-diketiminato ligands were found to be living initiators for this transformation.[11]
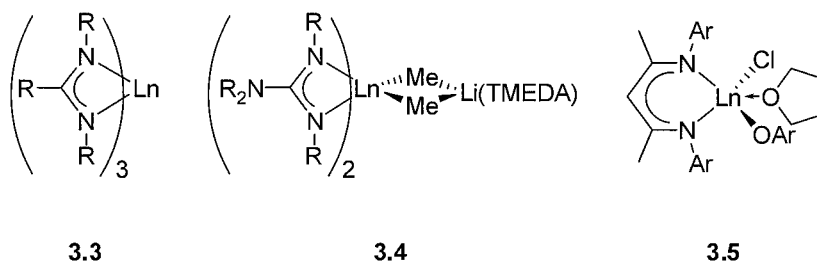
Figure 3.3. Initiators for ε-caprolactone ring-opening polymerization. (Ln = Y or the lanthanides).

Selected examples of known yttrium complexes that initiate the ring-opening polymerization of ε-caprolactone are shown in Figure 3.4, and some polymerization results are shown in Table 3.1. Polymer characteristics are very dependant on polymerization conditions (temperature, concentration, [M]/[I] ratio, rate of addition of monomer etc.), so the reported examples provide a guide for yttrium initiator ability for ROP of ε-caprolactone.

Compounds **3.7**[25] and **3.8**[44] are variations of yttrium metallocenes, where one is an yttrium alkoxide (**3.7**), and the other contains a linked amido-cyclopentadienyl ligand (**3.8**). Both **3.7** and **3.8** gave reasonable polydispersity values (< 2) and molecular weights typical for group 3 complexes (Table 3.1, Entry 1 and 2). The isopropoxy yttrium diethyl acetoacetate complex **3.9** is shown to be a well-controlled living polymerization catalyst with molecular weights that match calculated values, and a polydispersity value very close to one (Table 3.1, Entry 3). The bis(phosphinimino) methanide yttrium complex **3.10** (Table 3.1, Entry 4) produced higher molecular weight polymer with larger polydispersity values than complex **3.7**, **3.8** or **3.9**. Interestingly, the yttrium pyrrolyl complex **3.6**, the only homoleptic complex described here, was unable to initiate polymerization (Table 3.1, Entry 5), which Matsuo and co-workers attribute to the Y-N(pyrrolyl) bond being too strong to initiate polymerization.[15]
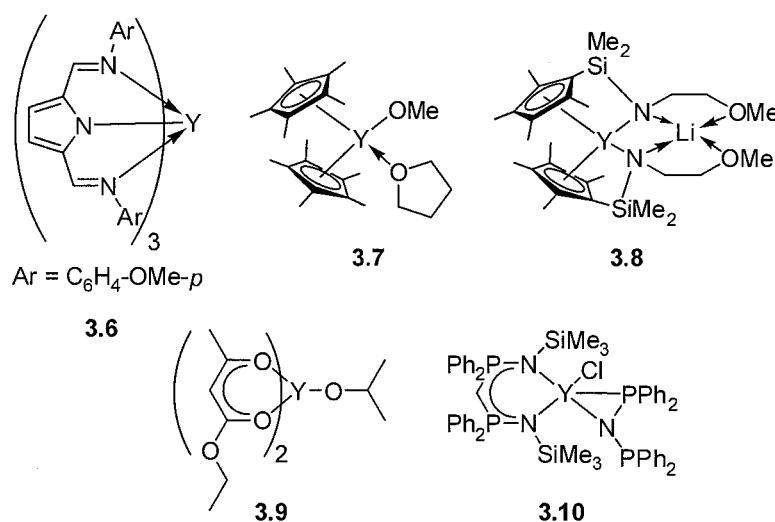
Figure 3.4. Known yttrium complexes of varying ligands that have been used as initiators for ε-caprolactone ROP.

Table 3.1. Comparison of yttrium initiators for the ROP of ε-caprolactone.

Entry	Initiator	[M]/[I]	Temp. (°C)	Time (h)	Yield (%)[a]	M_w[b] (x 10^4 gmol^{-1})	PDI [b]
5[15]	**3.6**	100	20	5	trace	-	-
1[25]	**3.7**	20	0	10	90	9.97	1.12
2[44]	**3.8**	197	25	1.5	92	7.20	1.80
3[23]	**3.9**	200	20	0.5	94	2.48	1.08
4[45]	**3.10**	289	25	2	94	10.2	2.10

[a] Yield = weight of polymer obtained/weight of monomer used. [b] Measured by GPC calibrated with standard polystyrene samples.

Taking a look at the above rare-earth complexes it is apparent that vastly different metal complexes can mediate this desirable reaction. It has been realized that the ligand can influence the molecular weight, polydispersity values, and yield of resultant polymers.[40,41,46-74] Therefore, easily accessed and modular ligand sets suitable for rare-earth complexation are also ideal targets for the optimization of the synthesis of requisite metal complexes and their inherent catalytic activity.

3.1.1 Mechanistic Introduction

The mechanism for the ROP of ε-caprolactone using rare-earth initiators (Figure 3.2) is thought to proceed *via* a coordination-insertion mechanism which involves formation of a metal-alkoxide species by cleavage of the oxygen-acyl bond that then regenerates a metal-alkoxide species and promotes further polymerization. The mechanism involves coordination of one molecule of ε-caprolactone, and subsequently a second incoming equivalent promotes the ring-opening. Also, the terminus of the growing polymer contains the ligand that was originally bound to the metal centre. The coordination-insertion route is most probable for rare-earth metal centres, as compounds can be isolated with ε-caprolactone as a donor molecule through its carbonyl oxygen[14,75] and end-group analysis most often determines that the ligand terminates the polymer.[10,48,82,83] Furthermore, this mechanism was calculated to be favoured over the route where ring-opening occurs at the oxygen-alkyl position on ε-caprolactone.[1]

To further elucidate the ROP mechanism, Yasuda and co-workers studied the initiation step with a living initiator yttrium cyclopentadienyl alkoxide complex **3.7** (Figure 3.5).[25] Complex **3.7** reacted with one equivalent of ε-caprolactone to give a coordination complex where ε-caprolactone can initially bind as a monodentate ligand (**3.11**).[75] After quenching, ε-caprolactone was re-isolated. If two equivalents of ε-caprolactone are reacted with complex **3.7** and then quenched, one equivalent of ε-caprolactone is returned and one equivalent of ring-opened ester alcohol (**3.13**) is produced. This indicates that the intermediate species after initiation is complex **3.12**. Therefore, polymerization is perceived to start with the coordination of ε-caprolactone to form the 2:1 complex. In the initiation step, the alkoxide

attacks to C=O group to generate the ring-opened complex with ε-caprolactone coordinated.[14]
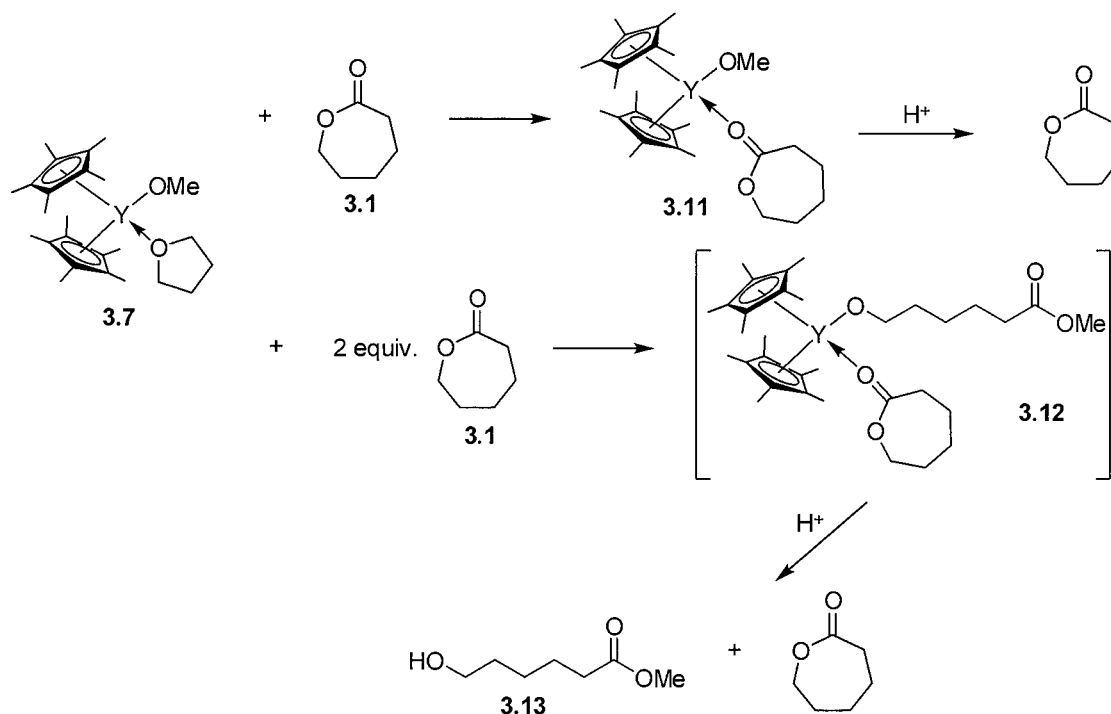
Figure 3.5. Initiation of ROP of ε-caprolactone using complex 3.7.[25]

To emphasize the importance of coordination of ε-caprolactone as the initial step, a samarium tris(β-diketiminate) complex (Figure 3.6, **3.14**) was found to be inactive for the polymerization of ε-caprolactone. Barbier-Baudry and coworkers interpret the solid-state molecular structure of **3.14** as having no open coordination site for monomer coordination.[16]
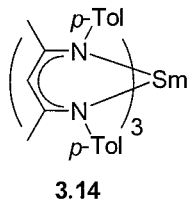
Figure 3.6. Samarium tris(β-diketiminate) complex **3.14**.

Another potential initiation mechanism has been proposed for the ROP of ε-caprolactone using as Zr(acac)₄ (**3.15**, acac = acetylacetonate) (Figure 3.7).[39] The polymer obtained using Zr(acac)₄ as an initiator contained no evidence of acetylacetonate derivatives at the chain end. Additionally Dobrzynski observed enolate formation in the ^{1}H NMR spectrum as indicated by signals arising at δ 4.05 and 3.63, corresponding to the CH_2O, and $CH=C(O)$ protons in deprotonated ε-caprolactone, as well as diagnostic peaks associated with protonated acetylacetonate ligand (**3.18**). The ROP of ε-caprolactone using Zr(acac)₄ was found to have an almost linear relationship between conversion of monomer and time of reaction, and slightly higher than calculated molecular weights of poly(ε-caprolactone) were obtained with quite low polydispersity values (< 1.50).
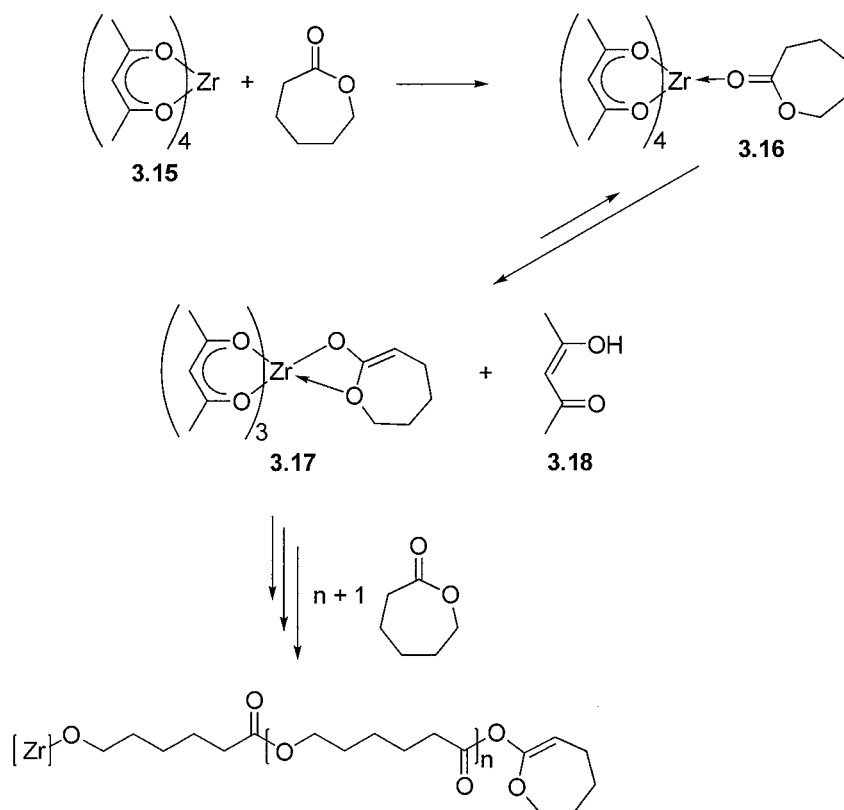
Figure 3.7. Initiation of ε-caprolactone ROP using Zr(acac)₄ (**3.15**).[39]

Another potential enolate mechanism has been described using rare-earth phenyl compounds.[38,76] These complexes are believed to initiate by enolization of the ε-caprolactone monomer, followed by insertion into the lanthanide-oxygen bond by another molecule of ε-caprolactone. The evidence for the proposed mechanism presented by Deng and coworkers is the lack of aryl signals in the end-group analysis, indicating that the ligand is not terminating the polymer.

In all investigated cases, rare-earth ROP of ε-caprolactone started by coordination of ε-caprolactone. It was shown in Chapter 2 that the THF molecule in complex **3.19** is easily displaced by multiple donors making it an intriguing potential initiator for ROP of ε-caprolactone.

3.1.2 Scope of Chapter

Similarities can be drawn between the reported yttrium initiators and the yttrium amidate complexes that were introduced in Chapter 2. The rare earth amidate complex replaces one nitrogen donor for an oxygen donor when compared to the amidinate complexes (**3.3**), and bis(guanidinate) complex (**3.4**). Stevels and coworkers propose that a hard oxygen donor can stabilize the highly electropositive nature of the rare earth metal centre, thereby reducing the possibility of acid-base type side reactions that can occur with substrates containing activated hydrogen atoms.[32] Tetrahydrofuran (THF) occupies a seventh coordination site in **3.5** as well as **3.19**, and as shown in Chapter 2, the THF molecule can be displaced by a range of Lewis base donors. The modifiability of the amidate scaffold, and the ease with which the donor THF is displaced led us to consider the amidate complexes of yttrium as ε-caprolactone ring-opening initiators. As shown in Section 3.1, varying stoichiometries of

ligands can be used to give rare-earth complexes that are initiators in the ROP of ε-caprolactone. For this reason, tris, bis and mono(amidate) complexes of yttrium (**3.19**, **3.20** and **3.21**, respectively, Figure 3.8) are explored as ε-caprolactone ring-opening initiators. The desirable amidate ligand features are determined by varying substituents on the amidate backbone and testing the initiator ability of the varied yttrium complexes. Furthermore, this chapter will include the results for mechanistic investigations for ROP of ε-caprolactone.

3.19   **3.20**   **3.21**
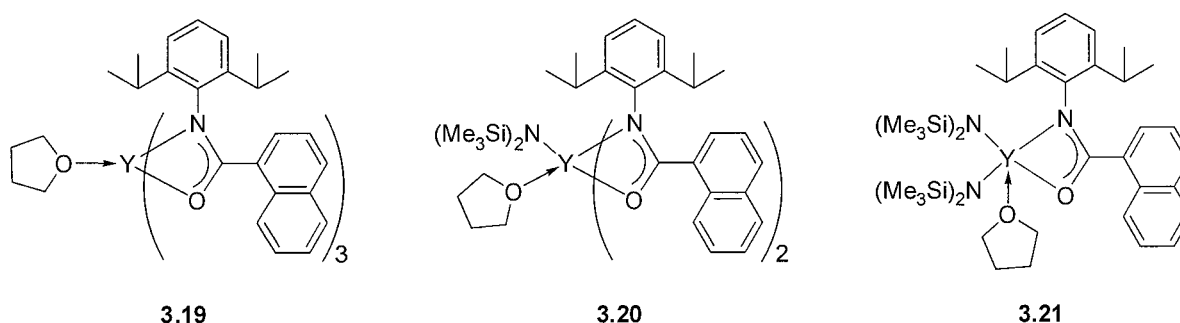
Figure 3.8. Tris, bis and mono(amidate) complexes of yttrium.

3.2 Yttrium Amidate Complexes as Initiators

3.2.1 Results and Discussion

Research on ROP of ε-caprolactone is very dependant on the characterization of the resultant polymer. The polymer is characterized by yield, molecular weight and polydispersity indices, where the latter two results are obtained from gel permeation chromatography (GPC). It should be noted that the molecular weight (M_w) and polydispersity indices (PDI) are reported two separate ways in this thesis 1) versus a polystyrene standard curve and 2) using a triple-detection laser-light scattering (LLS) detector. Most literature values for M_w and PDI for rare-earth initiation of ε-caprolactone

ROP are reported versus a polystyrene standard curve (including selected results presented in Section 3.1), but this is known to give misleading results for M_w and PDI due to the very different nature of the two polymers.[77] Results in this thesis for M_w using a polystyrene standard curve are typically twice the value received for M_w using triple-detection laser-light scattering results. Using the triple-detection LLS technique molecular weights can be determined directly without a standard curve. These results are more accurate than using a standard curve, but in order to compare results to literature values, both the polystyrene standard curve results and the LLS results will be reported.

Furthermore, it must be emphasized that all results have good reproducibility and are averaged values from duplicate, or presented triplicate polymerization runs. Polymerizations were initially done in duplicate, and if there was more than ± 5% difference in yield, M_w or PDI values, further polymerization runs were performed until the data was precise.

3.2.1.1   Comparison of Tris, Bis and Mono(amidate) Complexes

Amidate   complexes   tris(N-2',   6'-diisopropylphenyl(naphthyl)amidate)yttrium mono(tetrahydrofuran)   (3.19),   bis(N-2',   6'-diisopropylphenyl(naphthyl)amidate) mono(trimethylsilyl amido) yttrium mono(tetrahydrofuran) (3.20), and mono(N-2', 6'-diisopropylphenyl(naphthyl)amidate)   bis(trimethylsilyl   amido)   yttrium mono(tetrahydrofuran) (3.21), were found to have similarities to known ε-caprolactone ring-opening polymerization initiators. Since they have the same amidate ligand, a direct comparison between tris, bis and mono(amidate) complexes was undertaken to see which complex would be the ideal initiator for the ROP of ε-caprolactone.

Initial experiments for the ROP of ε-caprolactone were carried out using complexes **3.19**, **3.20** and **3.21** as initiators. The experimental procedure was adapted from literature results[78] with an optimized [M]/[I] of 225 (*vide infra*). Under an inert atmosphere, ε-caprolactone was added directly to a stirring solution of initiator in 10 mL dry toluene. The reactions were stirred vigorously for 15 min, subsequently exposed to air, quenched with 1 M aqueous hydrochloric acid (HCl) and the polymer can be isolated by precipitation with cold petroleum ether. The polymerization data of initiators **3.19**, **3.20** and **3.21** are shown in Table 3.2. As shown in chapter two, these complexes were directly synthesized from yttrium tris(trimethylsilyl) amide (**3.22**), which is a known ε-caprolactone polymerization initiator. Thus polymerization results are also compared to **3.22** to note the effect of the amidate ligand on polymerization. Furthermore, a control experiment, where the sodium salt of *N*-(diisopropylphenyl)naphthyl amide was isolated and used as an initiator has been completed. This control experiment tests the possibility that the anionic amidate ligand is sufficient to mediate polymerization on its own. This control experiment only produced trace amounts of polymer, indicating the presence of the yttrium centre is required for effective polymerization.

Table 3.2. Comparison of initiators for the ROP of ε-caprolactone using a [M]/[I] of 225.

Entry	Initiator	Yield (%)[b]	M_w[c] (x 10^4 gmol^{-1})	PDI[c]	M_w[d] (x 10^4 gmol^{-1})	PDI[d]
1	**3.19**	91	32.5	2.12	10.7	1.28
2	**3.20**	99	12.8	3.8	6.33	2.04
3	**3.21**	99	11.8	2.43	5.81	1.86
4	**3.22**	94	16.0	3.214	9.6	2.46

[a] General polymerization conditions: in toluene, 15 min. of stirring, 25 °C. [b] Yield = weight of polymer obtained/weight of monomer used. [c] Measured by GPC calibrated with standard polystyrene samples. [d] Measured by GPC (triple detection) equipped with differential refractometer (Waters), viscometer, and laser-light scattering detectors (Wyatt).

Although the yield using the tris(amidate) complex **3.19** is somewhat lower than its bis and mono(amidate) counterparts, the M_w value is much larger. Also the PDI values for complex **3.19** are narrower in comparison to complexes **3.20** and **3.21**. It is well established that a more shielded active site on the metal centre can block transesterification, which is a major contribution to chain termination, and also molecular weight distribution broadening, which consequently results in larger PDI values.[2,79,62,80] The PDI enlargement is due in part to the randomization of the polymer, which can occur with intermolecular transesterification, or the formation of cyclic polymers from intramolecular transesterification reactions (Figure 3.9).[19] Another possible reason for molecular weight distribution broadening is that more than one active species may be present, with initiation and propagation occurring at different rates.[16]
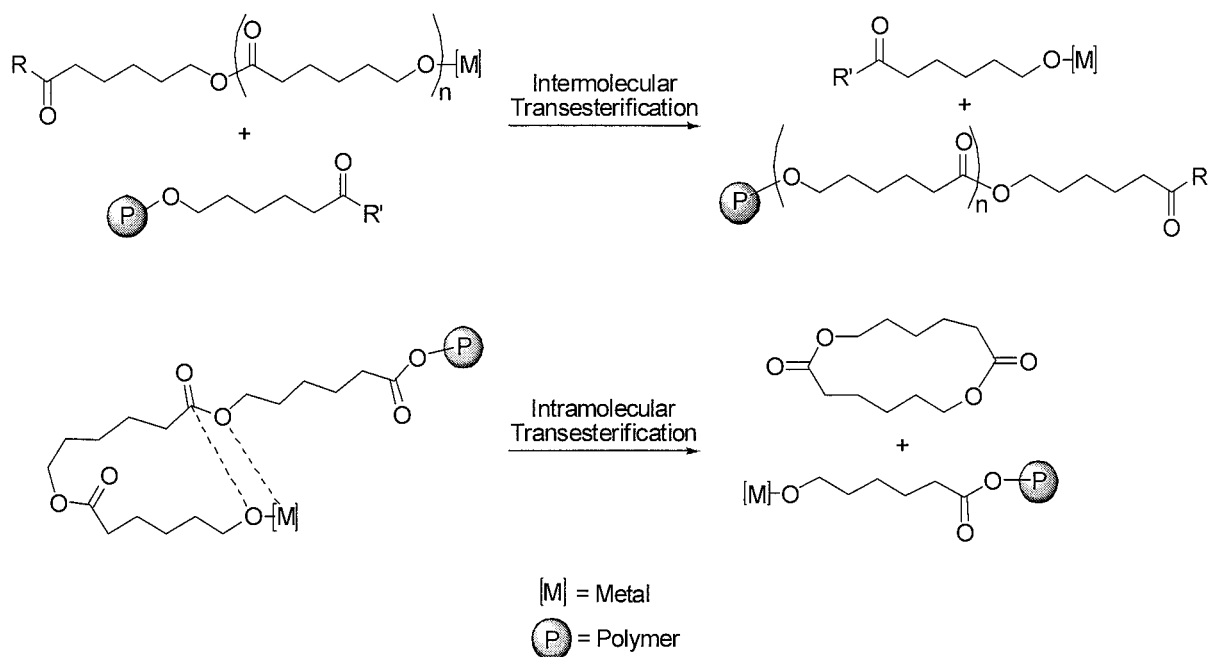
Figure 3.9. Intermolecular and intramolecular transesterification reactions for chain termination with poly(ε-caprolactone).[19]

Interestingly, using the same polymerization conditions as for initiators **3.19**, **3.20**, and **3.21**, complex **3.22** was found to produce polymers with a much larger PDI than any amidate complex, but a smaller molecular weight than that obtained with complex **3.19** (Table 3.2, Entry 4). Hultzch *et. al* hypothesize that the large molecular weights and broad PDI are due to the absence of an inert spectator ligand, as well as the monodentate nature of the amido ligands.[44,81]

The amidate ligands help influence the control over the polymerization as shown by the lower PDI values compared to complex **3.22**. The calculated molecular weight value for a [M]/[I] of 225:1 is 2.57×10^4 gmol^{-1}, which is much lower than the values in Table 3.2 for the amidate complexes. This indicates the amidate complexes are not polymerizing in a controlled manner. The tris(amidate) complex **3.19** had the lowest PDI value paired with the

highest molecular weight, and is thought to be the better initiator over the corresponding bis and mono(amidate) complexes.

Compared to known rare-earth initiators (**3.7**, **3.8**, **3.9** and **3.10** (Figure 3.4)) for ROP of ε-caprolactone, complex **3.19** produces poly(ε-caprolactone) with some of the highest molecular weights with a fast reaction time of 15 min. The polydispersity values are similar to the values obtained by complexes **3.8**, and **3.10**, but are much higher than known living initiator **3.9**. Complex **3.19** produces polymer with a much higher molecular weight than neodymium amidinate complex [CyNC(Me)NCy]$_3$Nd, but has similar polydispersity values. Although the analogous yttrium amidinate complex was prepared, no polymerization results were reported. Polymerization reactivity of rare-earth metal derived initiators has been found to increase with increasing metal radii, since a less crowded coordination environment (resulting from a larger metal radius) facilitates monomer coordination and presumably faster insertion.[40,82] This indicates similar neodymium compounds should be more reactive than yttrium (since Nd is larger than Y). Thus, the tris(amidate) complex **3.19** compares very well to the neodymium complex, suggesting that the amidate scaffold can result in an increase in reactivity over the amidinate ligand set.

When used as an initiator, tris(amidate) complex **3.19** produces polymer with optimized properties (high molecular weight, narrow PDI) compared to the bis and mono(amidate) analogues **3.20** and **3.21**. Resultant polymer properties suggest that complex **3.19** has better control during polymerization than the starting material yttrium tris(bis(trimethylsilyl)amide) **3.22**. Also, complex **3.19** yields larger polymer molecular weights at room temperature than the other reported yttrium complexes (Table 3.1), as well as moderate PDI values. Improvements to this class of initiators could result in a more controlled polymerization,

which would be denoted by molecular weights that approach calculated values, as well as polydispersity values close to one. Further studies of ROP of ε-caprolactone were carried out using varying [M]/[I] ratios to find the optimized conditions. Additionally, modifications were made to the amidate ligand to vary the steric and electronic properties in order to evaluate the potential for tuning the activity of the polymerization initiator.

3.2.1.2 Effect of Monomer to Initiator Ratio

Varying monomer to initiator ratios can have a profound effect on the polymer produced. When an initiator is a living catalyst, the molecular weight of the obtained polymer will increase with increasing monomer to initiator ratio. Thus, initial experiments for varying the [M]/[I] ratio were carried out to explore complex **3.19** as a living catalyst, since complex **3.19** was found to be the optimal amidate complex for ring-opening polymerization of ε-caprolactone. The polymerization reactions were carried out with the same conditions as described in section 3.2.1.1 except the monomer to initiator ratios ([M]/[I]) were varied as shown in Table 3.3.

Table 3.3. Summary of ring-opening polymerization of ε-caprolactone for initiator **3.19**.

Entry	[M]/[I]	Yield (%)[b]	M_w^c (x 10^4 gmol^{-1})	PDI[c]	M_w^d (x 10^4 gmol^{-1})	PDI[d]
1	10	70	5.52	1.61	4.36	1.17
2	20	73	6.43	1.61	4.59	1.14
3	30	84	9.46	1.94	7.25	1.44
4	40	74	10.1	1.70	7.39	1.18
5	50	95	24.7	2.56	11.8	1.62
6	100	96	27.8	2.40	10.2	1.38
7	225	91	32.5	2.12	10.7	1.28
8	500	63	31.7	2.20	10.7	1.28

[a] General polymerization conditions: in toluene, 15 min. of stirring, 25 °C. [b] Yield = weight of polymer obtained/weight of monomer used. [c] Measured by GPC calibrated with standard polystyrene samples. [d] Measured by GPC (triple detection) equipped with differential refractometer (Waters), viscometer, and laser-light scattering detectors (Wyatt).
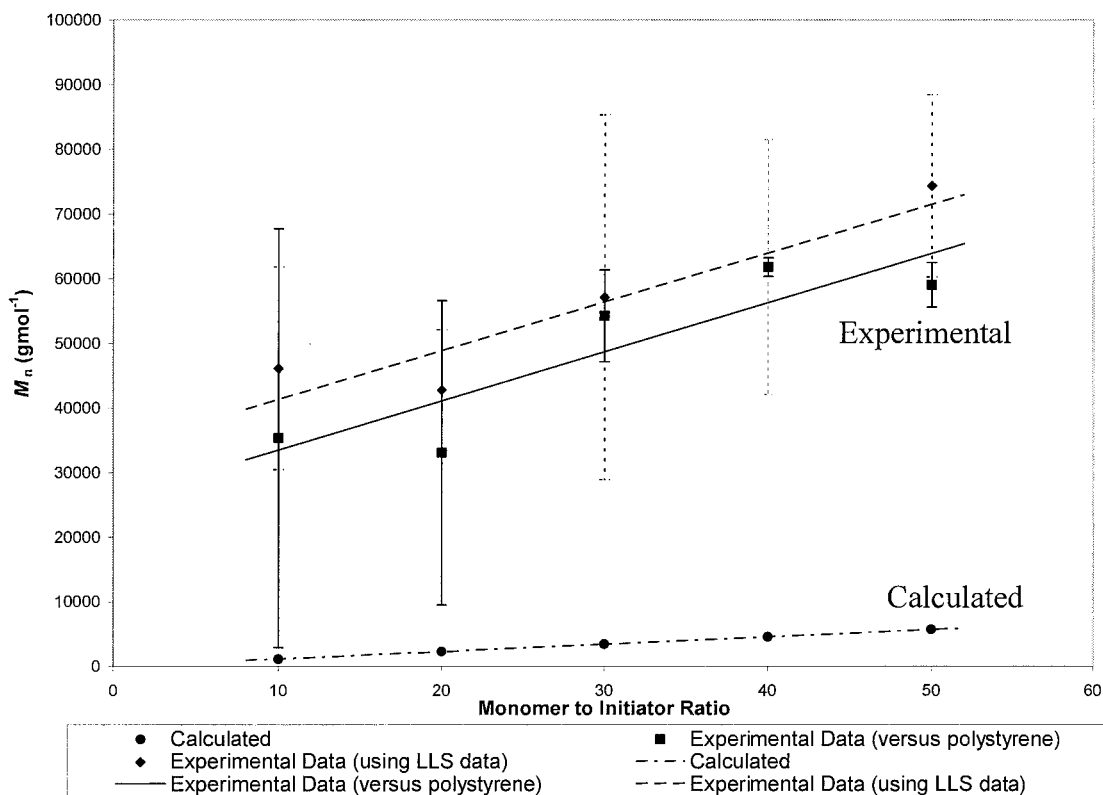
Figure 3.10. M_w values of poly(ε-caprolactone) at different [M]/[I] ratios using complex **3.19** as the initiator at room temperature.[a]

[a] Experimental plot uses averaged data, error bars are 2σ and trendline is in place to guide the eye.

Comparing entries 1-6, the yield of the polymer is increased as the [M]/[I] is increased to a maximum at [M]/[I] of 100, where the yield of polymer starts to decline at higher [M]/[I] ratios (Table 3.3, Entries 7 and 8). From the graph (Figure 3.10), the M_w values on average increase with increasing [M]/[I] ratio, but the relationship is much larger than calculated values (calculated line in Figure 3.10). The M_w and PDI values of polymer obtained when complex **3.19** was employed as an initiator is an indication of uncontrolled or slow initiation, or possible side-reactions. This may be due to an increase in chain termination/catalyst decomposition events as the concentration of monomer is increased.[83,84] The molecular weights obtained (against a polystyrene standard curve) in entries 5-8, are among the highest molecular weights observed for rare-earth metal initiated ε-caprolactone ring-opening polymerization.[12,63,64,85] However, the PDI values are typical for yttrium initiated ring-opening polymerization of ε-caprolactone. The [M]/[I] ratio of 225 was regarded as the optimized reaction conditions (as shown in entry 7 where polymer yield and molecular weight were maximized for compound **3.19**) and was used for comparison studies with other yttrium amidate complexes.

3.2.1.3   Effect of Amidate Ligand on Initiator

As mentioned before, the ligand can influence the molecular weight, polydispersity values, and yield of resultant polymers.[40,41,46-74] Thus, varying the substituents of the amidate ligand is expected to result in modified polymer properties. The advantage to the amidate backbone is the ease with which steric or electronic properties can be varied. Figure 3.11 shows four different yttrium complexes that have been synthesized using different amidate ligands. Complex **3.23** has a slightly more electron-donating group than complex **3.19** (*tert-*

butyl group versus naphthyl). Complex **3.24** has less bulk shielding the active site than any of the other yttrium amidate complexes (*vide supra*), which provides insight into the effect of sterically protecting the active site during polymerization. Both complexes **3.25** and **3.26** have electron-withdrawing groups on the amidate backbone, which results in more ligand charge localized on the ligand as opposed to donating to the yttrium centre. The outcome of this is the yttrium centre being more electropositive than in complex **3.23** or **3.24**, and being therefore more Lewis acidic.
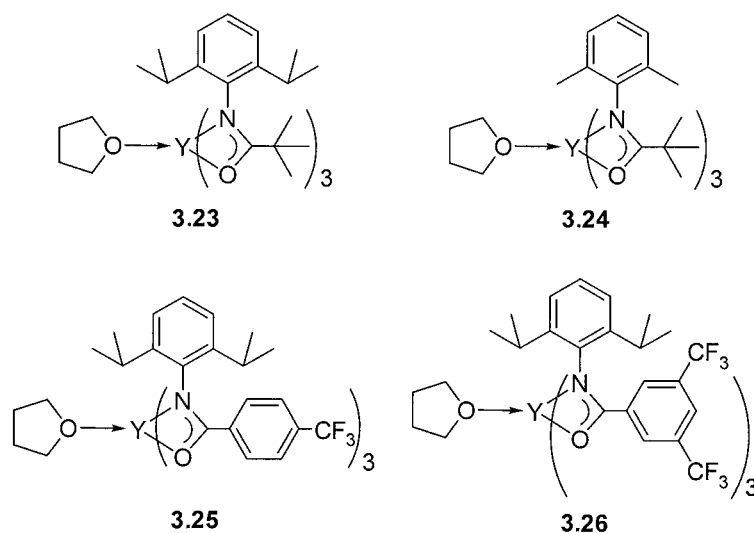
Figure 3.11. Yttrium amidate complexes containing varying amidate backbones.

Each of the complexes in Figure 3.11 are used in polymerization studies and the results are shown in Table 3.4. Complex **3.23** (Table 3.4, Entry 1) has a slightly more electron-donating group than complex **3.19** (*tert*-butyl group versus naphthyl) but similar steric bulk about the reactive metal centre, resulting in lower molecular weight values yet similar polydispersity values. The more sterically accessible complex **3.24** gave a reduced yield in comparison to **3.23** and **3.19**, but also a higher molecular weight and slightly broader PDI.

This is consistent with a more open active site that can lead to more side reactions, such as transesterification.[23]

When a more electron-withdrawing amidate ligand is installed, such as compounds **3.25** and **3.26**, the yields of polymer are reduced dramatically. The molecular weight of the polyester produced is also lower than when compound **3.19** is used as initiator, indicating a reduced efficiency of initiating the ROP of ε-caprolactone. Possibly the yttrium complexes **3.25** and **3.26** are too Lewis acidic resulting in sluggish initiation and/or propagation.

Modest variations to ligand structure investigated here result in notable changes in polymerization initiation activity. These results show that tris(amidate) complexes **3.19**, **3.23**, **3.24**, **3.25** and **3.26** are good initiators of ring-opening ε-caprolactone, with **3.19** giving the best combination of yield, high molecular weight and low PDI. A more sterically protected active site on the initiator, by using bulkier diisopropyl (Dipp) groups as opposed to dimethylphenyl (Dmp) groups on the amidate ligand, imparts a narrower molecular weight distribution in resultant poly(ε-caprolactone) (Entries 1 and 2). When using a more electropositive yttrium centre as an initiator, low molecular weights, and poor yield of polymer are produced (Entries 4 and 5). The ideal yttrium amidate initiator, in terms of sterics and electronics on the amidate ligand, was found to be complex **3.19**.

Table 3.4. Comparison of initiator ability for the ROP of ε-caprolactone for tris(amidate) complexes **3.23**, **3.24**, **3.25** and **3.26** using a [M]/[I] of 225.

Entry	Initiator	Yield (%)[b]	M_w[c] (x 10⁴ gmol⁻¹)	PDI[c]	M_w[d] (x 10⁴ gmol⁻¹)	PDI[d]
1	**3.19**	91	32.5	2.12	10.7	1.28
2	**3.23**	89	13.2	2.17	7.9	1.49
3	**3.24**	72	38.6	2.49	14.0	1.45
4	**3.25**	56	17.8	2.47	5.6	1.41
5	**3.26**	30	5.0	2.00	3.19	1.30

[a] General polymerization conditions: in toluene, 15 min. of stirring, 25 °C. [b] Yield = weight of polymer obtained/weight of monomer used. [c] Measured by GPC calibrated with standard polystyrene samples. [d] Measured by GPC (triple detection) equipped with differential refractometer (Waters), viscometer, and laser-light scattering detectors (Wyatt)

3.2.1.4 Effect of Temperature on Initiation

The M_w of the poly(ε-caprolactone) obtained by tris(amidate) complexes as initiators is much larger than calculated, and the PDI values show broad molecular weight distribution, suggesting slow initiation followed by rapid polymerization by small quantities of catalytically active species. Temperature was shown to have an effect on the polymerization (Table 3.5). Firstly, the ROP reaction using complex **3.19** as an initiator was performed at 0 °C, with a reaction time of 15 minutes. The polymerizations were carried out in Schlenk flasks containing the initiator in 10 mL of dry toluene, cooled to 0 °C using an ice bath. The monomer was syringed directly into the stirring solution of initiator, stirred for 1 hour, quenched with a few drops of 1 M aqueous hydrochloric acid, and then precipitated from cold petroleum ether. The polymer was isolated by vacuum filtration and dried in *vacuo* overnight at room temperature before GPC analysis. After 15 minutes of reaction time only trace amounts of polymer were obtained, however, once the reaction time was increased to 1 hour at 0 °C, polymer yield increased greatly for a [M]/[I] ratio of 225. The reported lower

yields for polymer with smaller [M]/[I] ratios is most likely due to the smaller scale on which the reaction is performed, which results in a challenging polymer isolation step.

At 0 °C, the polymerization produces polymer with lower molecular weights than the same study at room temperature, but the molecular weights are still substantially larger than calculated values (Figure 3.12). The PDI values are also slightly narrower than at room temperature, indicating that side reactions are less prevalent at lower temperatures. These results are all consistent with the observation that tris(amidate) complex **3.19** is not a living initiator at room temperature or at 0 °C. The effect of temperature on the initiation and propagation steps of the polymerization is further studied in section 3.3.

Table 3.5. Comparison of initiator ability for the ROP of ε-caprolactone at 0 °C for tris(amidate) complex **3.19**.

Entry	Temp. (°C)	[M]/[I]	Yield (%)[c]	M_w[d] (x 10^4 gmol^{-1})	PDI[d]	M_w[e] (x 10^4) gmol^{-1})	PDI[e]
1[a]	25	225	91	32.5	2.12	10.7	1.28
2[b]	0	225	93	6.24	1.77	3.32	1.34
3	0	10	55	3.219	1.55	1.82	1.19
4	0	20	54	5.15	1.62	2.63	1.42
5	0	30	48	5.17	1.96	2.58	1.24
6	0	40	42	6.02	1.78	3.08	1.43
7	0	50	55	4.65	1.65	2.43	1.53

[a] Conditions: in toluene, 15 min. of stirring. [b] Conditions: in toluene, 1 hour of stirring. [c] Yield = weight of polymer obtained/weight of monomer used. [d] Measured by GPC calibrated with standard polystyrene samples. [e] Measured by GPC (triple detection) equipped with differential refractometer (Waters), viscometer, and laser-light scattering detectors (Wyatt).
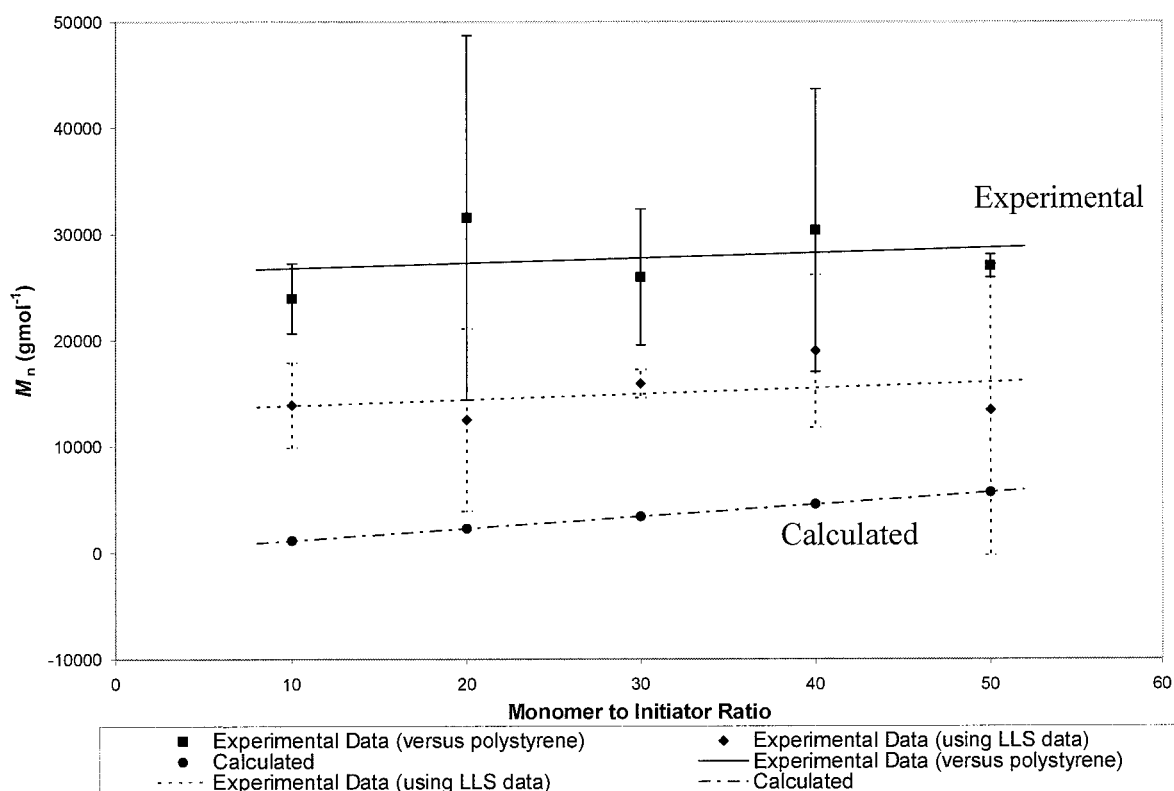
Figure 3.12. M_w values of poly(ε-caprolactone) at different [M]/[I] ratios using complex **3.19** as the initiator at 0 °C.[a]

[a] Experimental plot uses averaged data, error bars are 2σ and trendline is in place to guide the eye.

It has been shown that the tris(amidate) complex **3.19** was a better initiator than the analogous bis and mono(amidate) complexes **3.20** and **3.21**, at the optimized [M]/[I] ratio of 225. Variations on the amidate ligand of the initiator did have an effect on the polymerization results. When less bulk (complex **3.24**) or when electron-withdrawing groups (complexes **3.25** and **3.26**) were installed on the amidate ligand of the initiator, polymerization was less controlled than when complex **3.19** was used. Temperature was found to have an effect on the polymerization, and at 0 °C the polymerization results were closer to the calculated values than results obtained from room temperature experiments.

Overall, complex **3.19** was deemed to be the optimized initiator and is used for further investigation into the polymerization mechanism.

3.3 Mechanistic Investigations

3.3.1 Results and Discussion

From the results in Section 3.2, it is evident that tris(amidate) complexes are prone to promote uncontrolled ROP of ε-caprolactone (high molecular weights paired with moderate PDI values). The initiators formed *in situ* are highly active, but more insight into the mechanism is needed in order to better understand and improve upon these initiators.

Firstly, the terminus of the poly(ε-caprolactone) was identified in order to deduce which initiation mechanism is most likely involved for amidate complex **3.19**. The polymer produced using initiator **3.19** at 0 °C and a 10:1 monomer to initiator ratio was evaluated using end group analysis by ^{1}H NMR spectroscopy, as shown in Figure 3.13. The incorporation of one ligand in the polymer chain is observed, as evidenced by the signal at δ 3.66, (for the CH_2OH terminus of the polymer, signal 'a') that integrates for 2 protons, as does the multiplet at δ 3.33 for the methine protons of the ligand isopropyl substituents (also 2 protons, signal 'g'). This is consistent with the mechanism of polymerization proceeding through ligand promoted initiation to produce a polymer with *N*-(diisopropylphenyl)naphthyl amide as the terminus.
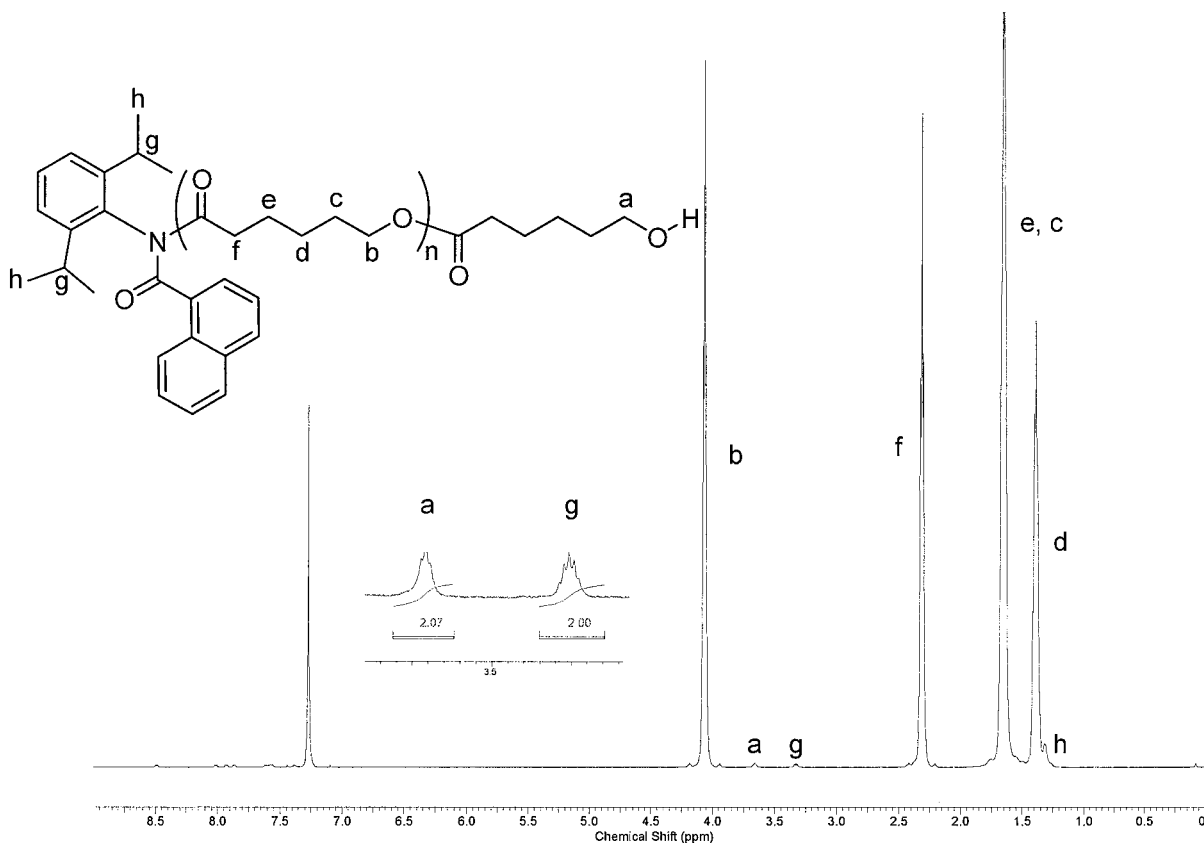
Figure 3.13. ^{1}H NMR (600 MHz, CDCl$_3$, 25 °C) spectrum of poly(ε-caprolactone) using initiator **3.19** at 0 °C with 10:1 [M]/[I] ratio.

As noted earlier, complex **3.19** does not display living catalyst behaviour, potentially due to small amounts of initiation occurring. To examine this, the progress of the reaction was studied. This was completed at 0 °C because the polymerization occurs too rapidly at room temperature (>90% yield after 4 minutes). Multiple polymerization reactions were carried out simultaneously and then quenched at varying times during the reaction. The yield of polymer was graphed against reaction time to monitor the course of polymerization (Figure 3.14). As indicated by the reaction profile there is a notable induction period (only trace amounts of polymer were obtained after 10 minutes). This induction period may be required to form the active initiator from complex **3.19**. Relatively slow initiation often results in a broad molecular weight distribution.[38] After the induction period, polymerization occurs

105

almost in a linear fashion to give greater than 90% yield. The inset confirms that the molecular weight of the polymer increases as the yield of reaction increases. The maximum molecular weight and maximum polymer yield were reached after 50 minutes of reaction time, indicating the reaction is proceeding throughout the entire hour. To understand the reason for the induction period, the initiation step using complex **3.19** was probed.
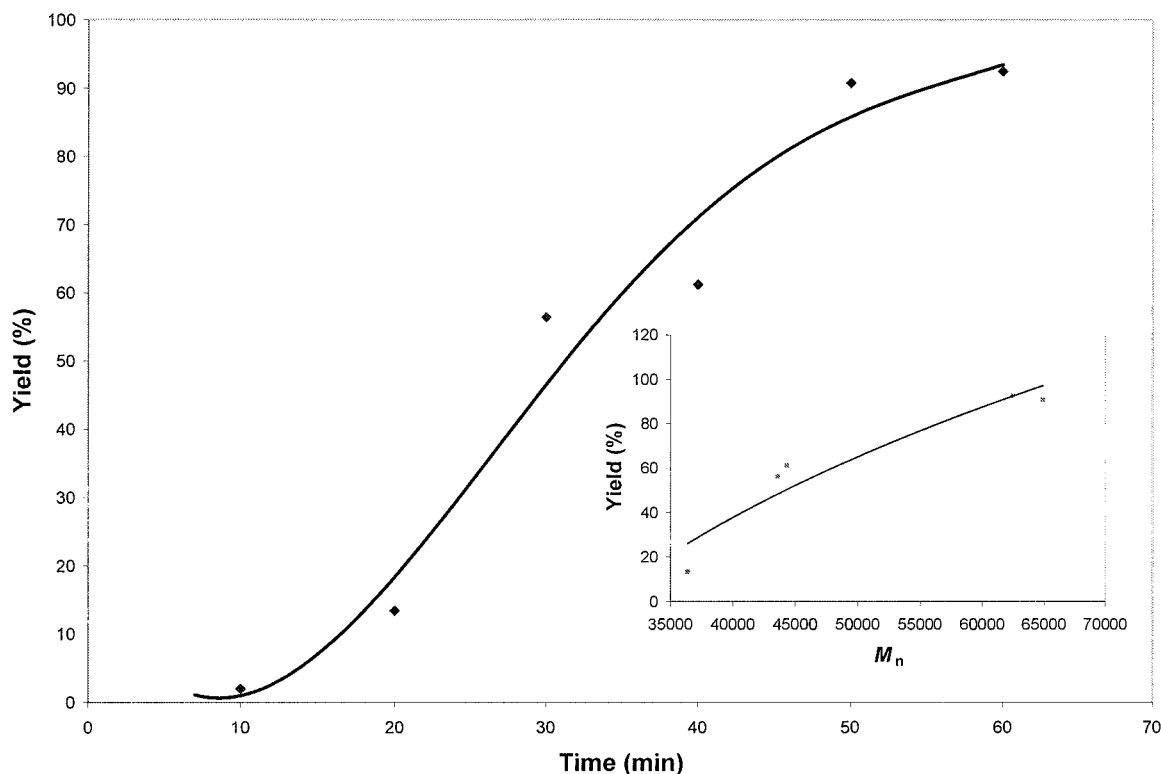
Figure 3.14. Yield of polymer during ROP of ε-caprolactone using initiator **3.19** ([M]/[I] = 225, 0 °C). Inset shows tendency of M_n values as yield increases.[a]

[a] Trendlines are only in place to guide the eye.

Following the method employed by Yasuda and co-workers,[25] one equivalent of ε-caprolactone was added slowly to a stirring solution of complex **3.19** in hexanes at room temperature (Figure 3.15). The product was dried in *vacuo* to give a ε-caprolactone yttrium tris(amidate) complex **3.27** as a white solid that is quite soluble in deuterated benzene. The coordination of ε-caprolactone is indicated in the ^{1}H NMR spectrum, which shows a shift in

signals from that of uncoordinated ε-caprolactone, and there is no evidence of the tetrahydrofuran present in **3.27** (Figure 3.16). The α-hydrogens $(CH_2C(O)OCH_2)$ and ε-hydrogens $(CH_2C(O)OCH_2)$ in ε-caprolactone are shifted from δ 3.46 and 2.12 ppm respectively in uncoordinated ε-caprolactone, to δ 3.44 and 2.50 ppm in complex **3.27**. This is in accordance to already published complexes where ε-caprolactone is bound monodentate through the carbonyl oxygen to yttrium.[14,75] The mass spectrum was the same as the parent complex **3.19** with a M^+ of 1079, indicating loss of bound ε-caprolactone during analysis just as the bound THF molecule is lost during analysis of complex **3.19**. Attempts at recrystallization from several solvents have been unsuccessful in producing crystalline **3.27** suitable for X-ray crystallographic analysis.
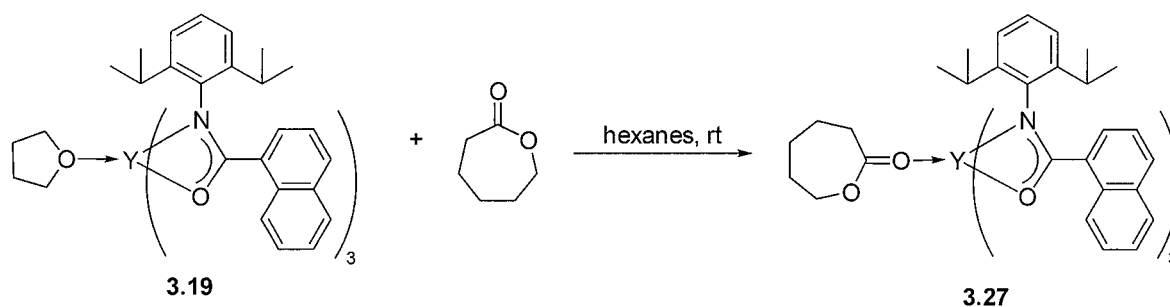
Figure 3.15. Formation of monodentate ε-caprolactone yttrium complex **3.27**.
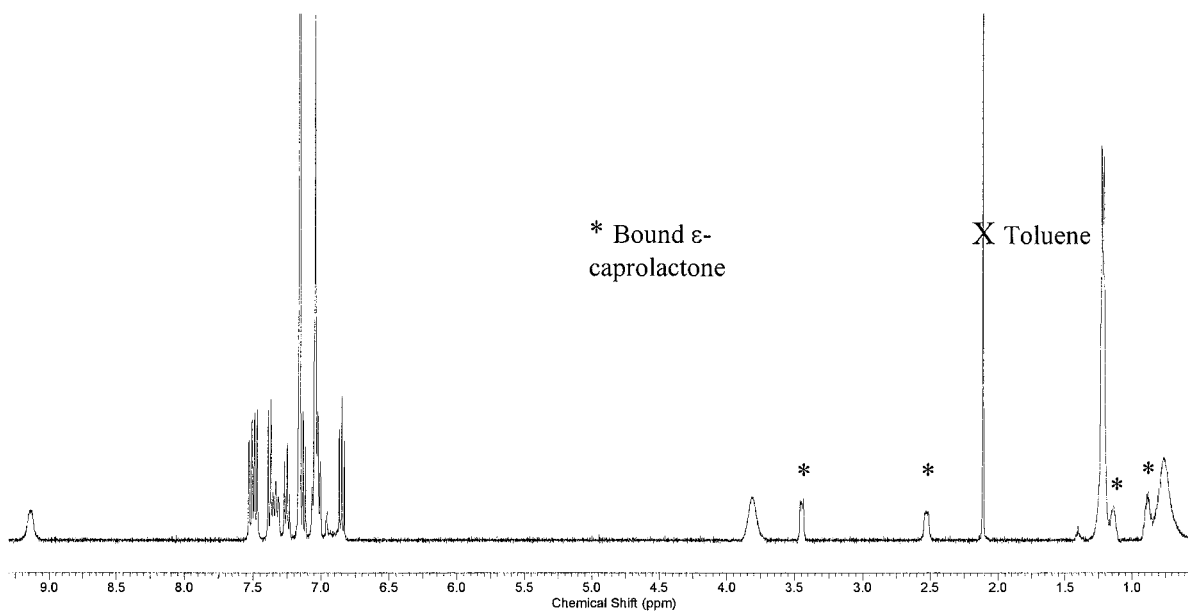
Figure 3.1. ^{1}H NMR spectrum (600 MHz, C_6D_6, 25 °C) of complex **3.27**.

The ^{1}H NMR spectrum of **3.27** showed quite broad signals (note broadened signals at δ 9.53, 3.81 and 0.75 for the *ortho*-naphthyl, C*H*(CH$_3$)$_2$ and CH(C*H*$_3$)$_2$ protons for complex **3.27**, respectively) in comparison to the parent complex **3.19**, but attempts to heat the sample (65 °C in a J-Young NMR tube) to sharpen signals caused decomposition, as indicated by precipitate forming, and two diagnostic proton signals at approximately δ 11 and 6.5 ppm resulting from protonated amide bound to the yttrium centre, and the N-H signal for the free amide proligand respectively (*vide supra*). The precipitate is thought to contain insoluble yttrium containing compounds that are not characterizable. Solid **3.27** also very slowly degrades in the same fashion at room temperature when stored in the inert atmosphere glovebox, but it is stable when stored at -30 °C for greater than a month.

When 2 equivalents of ε-caprolactone are reacted with **3.19** at room temperature, protonated amide is immediately apparent in the ^{1}H NMR spectrum of the crude sample.

108

When the crude sample is heated in solution at 65 °C overnight a solid precipitates, and in the ^{1}H NMR spectrum the only detectable species is amide proligand. Since the ε-caprolactone is extensively dried and does not have a deleterious effect upon **3.19** in significant excess (during polymerization runs), presumably decomposition is not originating from adventitious trace amounts of water. One possibility is that decomposition is due to the enolization of ε-caprolactone. The coordination of the second molecule of ε-caprolactone may somehow promote the enolization (Figure 3.16). The ^{1}H NMR spectrum of the crude reaction shown in Figure 3.16 does have similarities to a reported spectrum for the proposed enolization of ε-caprolactone using $Zr(acac)_4$. There are signals arising at δ 4.00 and 3.61 ppm, which are very similar to reported values of δ 4.05 and 3.63 ppm for the CH_2O, and $CH=C(O)$ protons in deprotonated ε-caprolactone using $Zr(acac)_4$.
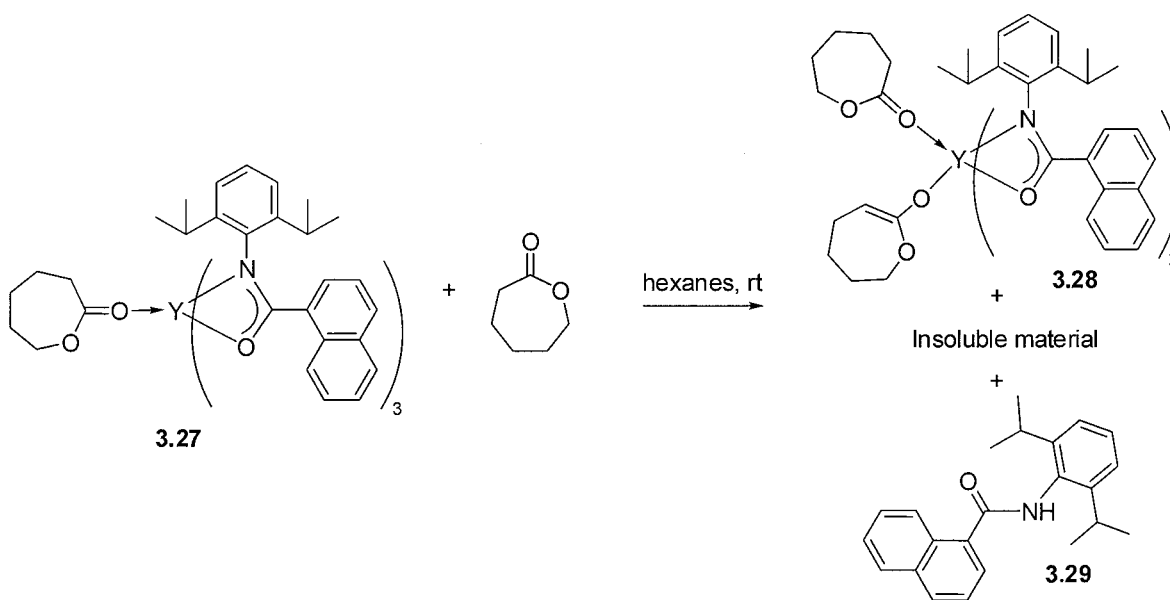
Figure 3.17. Possible reaction after second equivalent of ε-caprolactone is added.

Rare-earth enolate compounds are rarely isolated,[86,87] but are more typically formed in situ for catalytic reactions such as the aldol condensations.[88-95] Unfortunately, ε-caprolactone

is not used as a reagent in aldol reactions but other cyclic ketones, such as cyclohexanone, are very commonly used. For this reason, complex **3.19** was probed for its reactivity with cyclohexanone. The reaction was performed by adding two equivalents of cyclohexanone slowly to a stirring solution of complex **3.19** in hexanes at room temperature. A precipitate formed after 2 hours of stirring, and after drying in *vacuo*, the crude product was obtained as a white solid that was moderately soluble in aromatic hydrocarbon solvents. Attempts to fully characterize this material in the solid-state were unsuccessful due to its resistance to single crystal formation. The ^{1}H NMR spectrum of the crude material clearly shows evidence of protonated ligand bound to the yttrium centre by the diagnostic N-H signal at approximately δ 11.2 ppm (signal 'a', Figure 3.18). Signal b and c are indicative of the *ortho*-proton on the naphthyl substituent of the residual complex and the protonated ligand (**3.29**). Signal 'b' is very broad, potentially due to oligomeric yttrium species forming in solution that are sparingly soluble in deuterated benzene. If enolate is forming, and the bulky amidate ligand is lost, the resulting metal complexes will likely form proposed compound **3.30** and/or dimers or oligomers. Signal 'd' is proposed to be the C*H*=C(O) signal of the bound cyclohexanone enolate (**3.30**) and attempts to quench the enolization product using D_2O, and CF_3COOD have thus far been inconclusive. Using D_2O and CF_3COOD as quenching reagents did show incorporation of deuterium, indicated by a small broad triplet at approximately δ 3.56 ppm,[96,97] but incorporation was not quantitative and full characterization proved problematic.

110
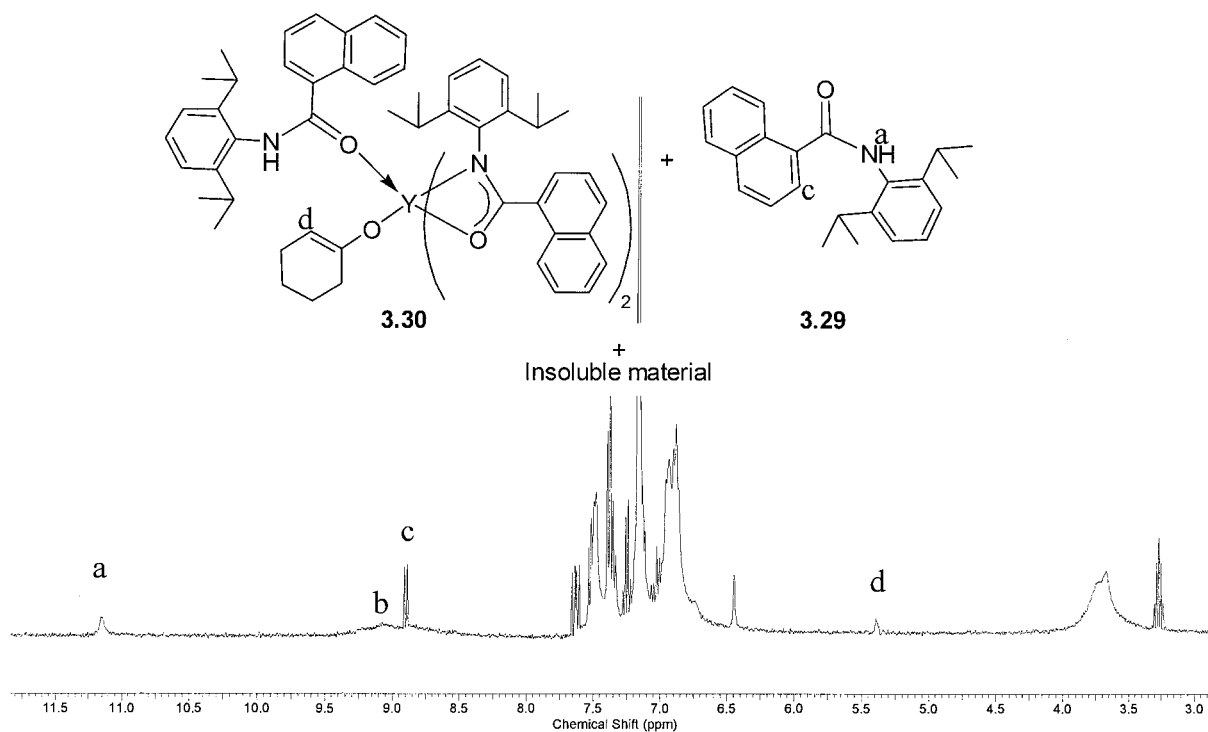
Figure 3.2. Proposed product formation (**3.30**, **3.29** and insoluble material) and ^{1}H NMR spectrum (400 MHz, C_6D_6, 25 °C) of the crude material obtained after direct reaction of complex **3.19** with cyclohexanone.

The aldol reaction using the proposed yttrium enolate compound **3.30** (formed using cyclohexanone) was attempted by quenching using benzaldehyde (**3.31**) (Figure 3.18). The expected initial product is 2-(hydroxyphenylmethyl)cyclohexan-1-one (**3.32**), which in the presence of a Lewis acid can easily dehydrate to form 2-benzylidenecyclohexanone (**3.33**).[98]
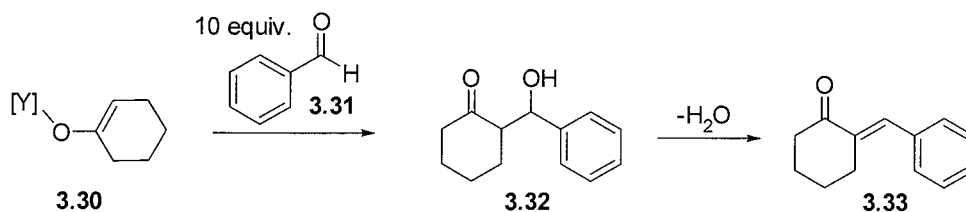
Figure 3.19. Formation of 2-(hydroxyphenylmethyl)cyclohexan-1-one (**3.32**) and 2-benzylidenecyclohexanone (**3.33**).

The proposed enolate complex was formed by stirring a solution of complex **3.19** dissolved in toluene inside an inert atmosphere glovebox and slowly adding dropwise two equivalents of cyclohexanone. This crude solution was transferred to a Schlenk flask and then cooled to -78 °C, where dry benzaldehyde was added dropwise by syringe. The resulting mixture was warmed to room temperature before quenching with 1 M aqueous HCl. The organic layer was isolated and dried *in vacuo* to give a crude mixture, which was analyzed by mass spectrometry and NMR spectroscopy. The electron-impact (EI) mass spectrum contained a fragmentation pattern of that for free proligand ($M^+ = 331$, 20%)[99], and a signal at 204 (mass for **3.32**, 5%) and a mass at 187 (mass for **3.33**, 5%). By comparing the literature values for the ^{1}H NMR spectrum of **3.32**[100] and **3.33**[101-103] there is evidence for compound **3.33** in the sample as indicated by a multiplet at δ 2.88 ppm for the γ-hydrogens, and a triplet at δ 2.50 ppm for the $CH_2C(O)$ hydrogens. However, isolation of the small amount of product in the presence of excess ligand and starting material proved problematic. Thus preliminary evidence supports formation of an enolate, which is presumably occurring during reaction of complex **3.19** with ε-caprolactone or cyclohexanone.

The enolization of ε-caprolactone is not thought to be an initiation step, since using end group analysis the polymer was found to be terminated by an amide proligand, but instead a competing side-reaction during polymerization initiation. To test this theory, the yttrium

enolate of ε-caprolactone product **3.28** was tested as an initiator for the ROP of ε-caprolactone (Table 3.6). The yield of polymer for **3.28** is much lower than for the parent complex **3.19**. Also, the resultant polymer has lower M_w values and larger polydispersity values than when complex **3.19** is used as an initiator. This gives an indication that the material **3.28** that is proposed to contain an enolate complex, is not as efficient an initiator as complexes **3.19** and may be involved in a competing process.

As mentioned before, initiation of ε-caprolactone ROP is proposed to begin with coordination of ε-caprolactone, such as in complex **3.27**. Therefore, complex **3.27** was also tested for its initiator ability for the ROP of ε-caprolactone. The polymer yield using **3.27** as an initiator was much lower than for the parent complex **3.19**. This could be due to complex **3.27** forming more complex **3.28** under the polymerization conditions. The M_w for the complex **3.27** are similar to the parent complex **3.19**, with comparable polydispersity values. Combining all the data presented above a proposed mechanism of ring-opening polymerization of ε-caprolactone using initiator **3.19** is shown in Figure 3.20.

Table 3.6. Comparison of initiator ability (225:1 [M]/[I]) for the ROP of ε-caprolactone at 0 °C for tris(amidate) complex **3.19**, the ε-caprolactone complex **3.27**, and the proposed enolate complex **3.28**[a].

Entry[b]	Initiator	Reaction Time (min)	Yield (%)[c]	M_w[d] (x 10^4 gmol[-1])	PDI[d]	M_w[e] (x 10^4 gmol[-1])	PDI[e]
1	3.19	30	56	4.36	2.24	3.48	1.59
2	3.19	60	93	6.24	1.77	3.32	1.34
3	3.27	30	28	4.36	2.13	2.17	1.32
4	3.27	60	50	5.76	2.18	3.42	1.24
5	3.28	30	15	3.201	2.55	1.86	1.47
6	3.28	60	36	3.225	3.7	1.92	1.68

[a] Crude material used, and molecular weight based on complex **3.28** [b] Conditions: in toluene, 1 hour of stirring, 0 °C. [c] Yield = weight of polymer obtained/weight of monomer used. [d] Measured by GPC calibrated with standard polystyrene samples. [e] Measured by GPC (triple detection) equipped with differential refractometer (Waters), viscometer, and laser-light scattering detectors (Wyatt).
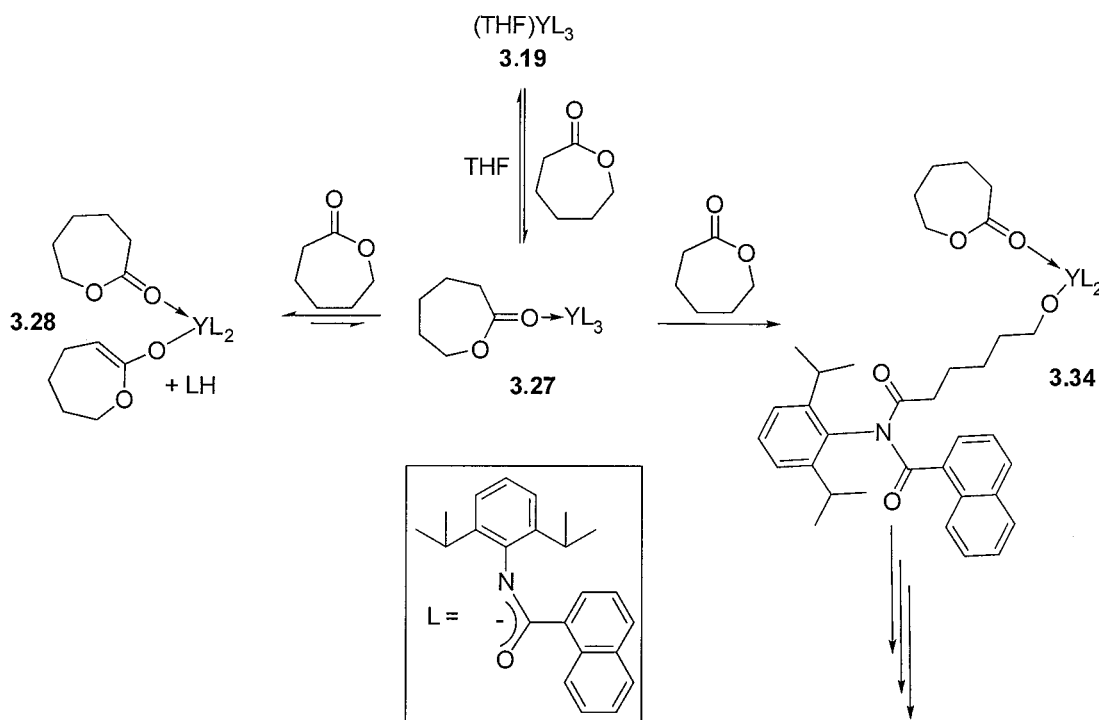
Figure 3.20. Proposed mechanism for ε-caprolactone ROP using complex **3.19** as initiator.

Initially, one molecule of ε-caprolactone displaces a THF molecule to form complex **3.27**. This complex can coordinate another molecule of ε-caprolactone and initiate the ring-

114

opening of the first molecule of ε-caprolactone (Complex **3.34**), or form an enolate complex **3.28** and consequently a protonated ligand is displaced. When the complex **3.27** is isolated and used as an initiator, perhaps it more easily forms more of complex **3.28** explaining the lower yield of polymer in Table 3.6 (Entry 3 and 4). Complex **3.28** is thought to reversibly form complex **3.27**, such as in Zr(acac)$_4$ initiated polymerization,[39] which competes with the formation of complex **3.34** and subsequent further propagation. This rationalizes the non-living character of complex **3.19** and the induction period observed for the polymerization. These competing reactions (formation of **3.28** and **3.34**) result in species polymerizing at different rates giving broader molecular weight distributions in the obtained polymers.

3.3.2 Mechanistic Investigation Summary

ROP of ε-caprolactone using yttrium amidate complex **3.19** was found to be an efficient initiator at room temperature and at 0 °C. By end group analysis, it was found that the amide proligand terminated the polymer. It was also found that alone, the anionic ligand (the sodium salt of *N*-(diisopropylphenyl)naphthyl amide) was incapable of efficient polymerization. The combination of both these results indicates polymerization occurs *via* the coordination-insertion mechanism. Studies of the progress of reaction indicated a slow initiation followed by an almost linear polymerization, with full conversion of monomer after 60 minutes of reaction at 0 °C. Further studies into the initiation step showed that complex **3.19** could coordinate one equivalent of ε-caprolactone easily, but was prone to possible enolization, to produce protonated amide ligand and uncharacterizable potential enolate complexes of yttrium. A possible mechanism for initiation proposes an equilibrium between the bound yttrium complex of ε-caprolactone, and an enolate complex, causing an induction

period during the initiation of polymerization. Despite the induction period, the yttrium amidate complex **3.19** is a highly active initiator for ROP of ε-caprolactone.

3.4   Conclusions

Amidate complexes of group 3 metals were found to be very active initiators for the ROP of ε-caprolactone. The tris(amidate) complexes were found to have more control over the polymerization compared to bis and mono(amidate) complexes. The polymer properties were varied by changing the substituents on the amidate scaffold of the initiating complex. The optimum amidate ligand for tris(amidate) complexes for desirable polymer properties (high molecular weight, moderate PDI values) combined steric bulk at the metal centre with slightly electron-withdrawing capabilities. Therefore, the optimum tris(amidate) complex investigated was complex **3.19**, which in comparison to other reported group 3 ε-caprolactone ROP initiators is highly active, but has moderate control over polymerization. Tris(amidate) complex **3.19** was found to be a non-living initiator with a significant induction period, leading to broader PDI values. The polymerization mechanism is thought to follow the coordination-insertion pathway, since by end group analysis the polymer was found to be terminated by an amide group and it is known that the anionic ligand is incapable of efficient initiation. Initiation studies indicate that a molecule of ε-caprolactone can coordinate the yttrium centre, supporting the coordination mechanism; however, the monomer has been observed to be enolizable, by us and others.[38,39,76] This may contribute to the non-living behaviour of the initiator, the induction period for initiation of polymerization, as well as broad polydispersity values.

Overall, rare-earth amidate complexes are highly active initiators for the ROP of ε-caprolactone. The ease with which the tris(amidate) complexes can be formed makes them ideal candidates for further study in ROP of other lactones as well as lactides. On-going research will take advantage of the tunable amidate ligand set to generate new rare-earth amidate complexes as optimized initiators for the ring-opening polymerization of a variety of cyclic lactones including ε-caprolactone and lactide.

3.5 Experimental

3.5.1 Starting Materials and Reagents

All operations were performed under an inert atmosphere of dinitrogen using standard Schlenk-line or glovebox techniques. Toluene was purified by passage through an alumina column and sparged with nitrogen. ε-Caprolactone was dried by stirring over CaH_2 for 4 days, allowed to settle for 2 days, decanted to a new flask and then distilled under reduced pressure, and stored over molecular sieves. $Y[N(SiMe_3)_2]_3$ was synthesized as described in the literature.[104] All other chemicals were commercially available and used as received unless otherwise stated. ^1H and ^{13}C NMR spectra were recorded on Bruker AV300, AV400 and AV600 spectrometers. Molecular weights were estimated by triple detection gel permeation chromatography (GPC - LLS) using a Waters liquid chromatograph equipped with a Waters 515 HPLC pump, Waters 717 plus autosampler, Waters Styragel columns (4.6 × 300 mm) HR5E, HR4 and HR2, Waters 2410 differential refractometer, Wyatt tristar miniDAWN (laser light scattering detector) and a Wyatt ViscoStar viscometer. A flow rate of 0.5 mL min^{-1} was used and samples were dissolved in THF (ca. 4 mg mL^{-1}). Molecular weights were determined by comparison to a polystyrene standard curve, and absolute molecular weights were determined using a dn/dc (change in refractive index/change in concentration) of 0.079 mL g^{-1}.[105,106] Elemental analyses and mass spectra were performed by the microanalytical laboratory of the Department of Chemistry at the University of British Columbia.

3.5.2 Synthesis

General Procedure for ε-caprolactone ring-opening polymerization (225:1 monomer to initiator ratio) at room temperature.

Inside a dinitrogen filled glovebox, complex **3.19** (13.5 mg, 0.0117 mmol) was dissolved in 10 mL toluene (measured by volumetric flask). The colorless solution was transferred to a 10 mL vial, equipped with a stir bar. ε-Caprolactone (0.28 mL, 0.3012 g, 2.64 mmol) was transferred by syringe directly into the vigorously stirring solution of complex **3.19**. The reaction was stirred for 15 minutes within the glovebox and then exposed to air and quenched with several drops of a 1 M aqueous HCl solution. The polymer was precipitated from cold petroleum ether. The polymer was isolated by vacuum filtration, and then dried overnight *in vacuo*. Yield: 0.274 g, 91%.

General Procedure for ε-caprolactone ring-opening polymerization (225:1 monomer to initiator ratio) at 0 °C.

Inside a dinitrogen filled glovebox, complex **3.19** (13.5 mg, 0.0117 mmol) was dissolved in 10 mL toluene (measured by volumetric flask). The colorless solution was transferred to a tube Schlenk flask, equipped with a rubber Suba™ stopper and a stir bar. The Schlenk flask was brought out of the glovebox and cooled in an ice bath for 15 minutes. ε-Caprolactone (0.28 mL, 0.3012 g, 2.64 mmol) was syringed directly into the vigorously stirring solution of complex **3.19**. The reaction was stirred for 1 hour at 0 °C, then exposed to air and quenched with several drops of a 1 M aqueous HCl solution. The polymer was precipitated from cold petroleum ether. The polymer was isolated by vacuum filtration, and then dried overnight *in vacuo*. Yield: 0.280 g, 93%.

General Procedure for ε-caprolactone ring-opening polymerization (10:1, 20:1, 30:1, 40:1, 50:1 monomer to initiator ratio) at room temperature.

Inside a dinitrogen filled glovebox, complex **3.19** (0.333 g, 0.289 mmol) was dissolved in 10 mL toluene (measured by volumetric flask) to make a stock solution (0.0289 M). The solution was transferred *via* syringe (10:1 (3.04 mL), 20:1 (1.52 mL), 30:1 (1.01 mL), 40:1 (0.76 mL), 50:1 (0.61 mL) to a 10 mL volumetric flask, diluted to 10.00 mL and then transferred to 20 mL vial, equipped with a stir bar. ε-Caprolactone (0.100 g, 0.876 mmol) was transferred by syringe directly into the vigorously stirring solution of complex **3.19**. The reaction was stirred for 15 minutes within the glovebox and then exposed to air and quenched with several drops of a 1 M aqueous HCl solution. The polymer was precipitated from cold petroleum ether. The polymer was isolated by vacuum filtration, and then dried overnight in *vacuo*. Yield: 10:1 (0.086 g, 86%), 20:1 (0.079 g, 80%), 30:1 (0.095 g, 94%), 40:1 (0.100 g, 100%), 50:1 (0.100 g, 100%).

Synthesis of tris(N-2', 6'-diisopropylphenyl(naphthyl)amidate)yttrium mono(ε-caprolactone) (3.27)

A solution of complex **3.19** (0.129 g, 0.112 mmol) was dissolved in 5 mL hexanes in a 20 mL glass vial equipped with a stir bar. ε-Caprolactone (12.7 mg, 0.111 mmol) was dissolved in 2 mL hexanes and added dropwise to a stirring solution of complex **3.19**. The reaction was stirred overnight at room temperature at which time a fine white solid precipitated out of the solution. The reaction was dried in *vacuo* to give a white solid. Yield: 0.109 g, 82%. ^{1}H NMR (600 MHz, C$_6$D$_6$) δ 9.53 (broad s, 3H, aryl-H), 7.48 (broad m, 6H, aryl-H), 7.23-7.40 (m, 12H, aryl-H), 7.05 (s, 6H, aryl-H), 6.83 (broad m, 3H, aryl-H), 3.211 (broad s, 6H,

CH(CH$_3$)$_2$), 3.44 (broad s, 2H, O-CH_2), 2.50 (broad s, 2H, OC(O)CH_2), 1.23 (d, J = 7 Hz, 18H, CH(CH_3)$_2$), 1.13 (broad s, 2H, O-CH$_2$CH_2), 0.88 (broad s, 4H, OC(O)CH$_2$CH_2CH_2), 0.75 (broad s, 18H, CH(CH_3)$_2$). ^{13}C NMR (150 MHz, C$_6$D$_6$) δ 180.7 (C=O), 142.7, 135.0, 133.4, 132.5, 130.4, 128.9, 128.7, 127.5, 126.7, 126.0, 125.1, 124.7, 124.4 (aryl-C), 71.7 (O-CH_2), 34.7 (CH(CH$_3$)$_2$), 28.9 (O-CH$_2$$CH_2$), 28.7 (CH($CH_3$)$_2$), 28.5 (OC(O)CH$_2$$CH_2$), 26.0 (CH($CH_3$)$_2$), 24.5 (OC(O)$CH_2$), 24.3 (OC(O)CH$_2CH_2$$CH_2$). MS (EI): 1079 (M$^+$), 952 (M$^+$-Nap), 749 (M$^+$-Nap[O,N]Dipp), 331 (M$^+$-Y(Nap[O,N]Dipp)$_2$). Anal. found (calcd. for C$_{75}$H$_{82}$N$_3$O$_5$Y): C 73.55% (75.42%), H 7.30% (6.92%); N 3.44% (3.52%).

General Procedure for quenching reaction with benzaldehyde.

Inside an inert atmosphere glovebox, at room temperature, complex **3.19** (0.142 g, 0.123 mmol) was dissolved in toluene in a 20 mL vial equipped with a stir bar. Cyclohexanone (24.2 mg, 0.247) was dissolved in toluene and added dropwise to the stirring solution of complex **3.19**. The crude solution was transferred to a Schlenk flask equipped with a Suba seal cap, and attached to a vacuum manifold and cooled to -78 °C. Dry benzaldehyde (0.13 mL, 1.28 mmol) was added dropwise by syringe. The resulting mixture was warmed to room temperature and stirred overnight before quenching with 1 M HCl. The organic layer was isolated, dried over MgSO$_4$, filtered and dried in *vacuo* to give a crude mixture (0.155 g). ^{1}H NMR (400 MHz, C$_6$D$_6$) Complicated, but notable peaks at δ 7.20-8.20 (aryl-H of **3.29**), 3.30 (septet, J = 6 Hz, 2H, CH(CH$_3$)$_2$ of **3.29**), 2.88 (m, γ-hydrogens of **3.33**), and 2.50 ppm (t, CH_2C(O) of **3.33**), 1.50-2.50 (multiple multiplets), 1.24 (d, J = 6 Hz, 12H, CH(CH_3)$_2$ of **3.29**). MS (EI): 331 (M$^+$) (**3.29**), 288 (M$^+$-iso-propyl) (**3.29**), 204 (M$^+$) (**3.31**), 188 (M$^+$ - OH) (**3.33**) 176 (M$^+$-ONap) (**3.29**), 155 (M$^+$- NDipp) (**3.29**).

3.6 References

(1)   Barros, N.; Mountford, P.; Guillaume, S. M.; Maron, L. *Chem. Eur. J.* **2008**, *14*, 5507.

(2)   Agarwal, S.; Mast, C.; Dehnicke, K.; Greiner, A. *Macromol. Rapid Commun.* **2000**, *21*, 195.

(3)   Xu, X.; Yao, Y. M.; Hu, M. Y.; Zhang, Y.; Shen, Q. *J. Polym. Sci. Part A: Pol. Chem.* **2006**, *44*, 4409.

(4)   Zhang, L.; Niu, Y.; Wang, Y.; Wang, P.; Shen, L. *J. Mol. Cat. A: Chem.* **2008**, *287*, 1.

(5)   Save, M.; Schappacher, M.; Soum, A. *Macromol. Chem. Phys.* **2002**, *203*, 889.

(6)   Okada, M. *Prog. Polym. Sci.* **2002**, *27*, 87.

(7)   Hayashi, T. *Prog. Polym. Sci.* **1994**, 663.

(8)   Sanchez-Barba, L. F.; Hughes, D. L.; Humphrey, S. A.; Bochmann, M. *Organometallics* **2005**, *24*, 3792.

(9)   Sheng, H. T.; Zhou, L. Y.; Zhang, Y.; Yao, Y. M.; Shen, Q. *J. Polym. Sci. Part A: Pol. Chem.* **2007**, *45*, 1210.

(10)   Sanchez-Barba, L. F.; Hughes, D. L.; Humphrey, S. M.; Bochmann, M. *Organometallics* **2006**, *25*, 1012.

(11)   Xue, M. Q.; Sun, H. M.; Zhou, H.; Yao, Y. M.; Shen, Q.; Zhang, Y. *J. Polym. Sci. Part A: Pol. Chem.* **2006**, *44*, 1147.

(12)   Luo, Y.; Yao, Y.; Shen, Q.; Yu, K.; Weng, L. *Eur. J. Inorg. Chem.* **2003**, 318.

(13)   Satoh, Y.; Ikitake, N.; Nakayama, Y.; Okuno, S.; Yasuda, H. *J. Organomet. Chem.* **2003**, *667*, 42.

(14)   Yasuda, H. *J. Organomet. Chem.* **2002**, *647*, 128.

(15)   Matsuo, Y.; Mashima, K.; Tani, K. *Organometallics* **2001**, *20*, 3510.

(16)   Barbier-Baudry, D.; Bouazza, A.; Brachais, C. H.; Dormond, A.; Visseaux, M. *Macromol. Rapid Commun.* **2000**, *21*, 213.

(17)   Penczek, S.; Cypryk, M.; Duda, A.; Kubisa, P.; Slomkowski, S. *Prog. Polym. Sci.* **2007**, *32*, 247.

(18)   Zhao, B.; Lu, C. R.; Shen, Q. *J. Appl. Polym. Sci.* **2007**, *106*, 1383.

(19)   Stridsberg, K. M.; Ryner, M.; Albertsson, A.-C. *Adv. Polym. Sci.* **2002**, *157*, 41.

(20)   Yasuda, H. *J. Polym. Sci. Part A: Polym. Chem.* **2001**, *39*, 1955.

(21)	Desurmont, G.; Li, Y.; Yasuda, H.; Maruo, T.; Kanehisa, N.; Kai, Y. *Organometallics* **2000**, *19*, 1811.

(22)	Nishiura, M.; Hou, Z.; Koizumi, S.; Imamoto, T.; Wakatsuki, Y. *Macromolecules* **1999**, *32*, 8245.

(23)	Shen, Y. Q.; Shen, Z. Q.; Zhang, Y.; Yao, K. *Macromolecules* **1996**, *29*, 8289.

(24)	Ihara, E.; Morimoto, T.; Yasuda, H. *Macromolecules* **1995**, *28*, 7886.

(25)	Yamashita, M.; Takemoto, Y.; Ihara, E.; Yasuda, H. *Macromolecules* **1996**, *29*, 1798.

(26)	Kalmi, M.; Lahcini, M.; Castro, P.; Lehtonen, O.; Belfkira, A.; Leskela, M.; Repo, T. *J. Polym. Sci. Part A: Pol. Chem.* **2004**, *42*, 1901.

(27)	Annunziata, L.; Pappalardo, D.; Tedesco, C.; Antinucci, S.; Pellecchia, C. *J. Organomet. Chem.* **2006**, *691*, 1505.

(28)	Qi, C. Y.; Wang, Z.-X. *J. Polym. Sci. Part A: Polym. Sci.* **2006**, *44*, 4621.

(29)	Tang, Z.; Pang, X.; Sun, J.; Du, H.; Chen, X. S.; Wang, X.; Jing, X. B. *J. Polym. Sci. Part A: Pol. Chem.* **2006**, *44*, 4932.

(30)	Yao, W.; Mu, Y.; Gao, A.; Gao, W.; Ye, L. *Dalton Trans.* **2008**, 3199.

(31)	Zhang, L. F.; Yu, C. P.; Shen, Z. Q. *Polym. Bull.* **2003**, *51*, 47.

(32)	Stevels, W. M.; Ankone, M. J. K.; Dijkstra, P. J.; Feijen, J. *Macromolecules* **1996**, *29*, 8296.

(33)	Nomura, N.; Taira, A.; Tomioka, T.; Okada, M. *Macromolecules* **2000**, *33*, 1497.

(34)	Palard, I.; Soum, A.; Guillaume, S. M. *Macromolecules* **2005**, *38*, 6888.

(35)	Sun, H. M.; Li, H. R.; Yao, C. S.; Yao, Y. M.; Sheng, H. T.; Shen, Q. *Chin. J. Chem.* **2005**, *23*, 1541.

(36)	Westmoreland, I.; Arnold, J. *Dalton Trans.* **2006**, 4155.

(37)	Kerton, F. M.; Whitwood, A. C.; Willans, C. E. *Dalton Trans.* **2004**, 2237.

(38)	Deng, X. M.; Yuan, M. L.; Xiong, C. D.; Li, X. H. *J. Appl. Polym. Sci.* **1999**, *71*, 1941.

(39)	Dobrzynski, P. *Polymer* **2007**, *48*, 2263.

(40)	Yao, Y.; Ma, M.; Xu, X.; Zhang, Y.; Shen, Q.; Wong, W.-T. *Organometallics* **2005**, *24*, 4014.

(41)	Luo, Y.; Yao, Y.; Shen, Q.; Sun, J.; Weng, L. *J. Organomet. Chem.* **2002**, *662*, 144.

(42)	Villiers, C.; Thuery, P.; Ephritikhine, M. *Eur. J. Inorg. Chem.* **2004**, 4624.

(43)   Luo, Y. J.; Yao, Y. M.; Shen, Q.; Yu, K. B.; Weng, L. H. *Eur. J. Inorg. Chem.* **2003**, 318.

(44)   Hultzsch, K. C.; Spaniol, T. P.; Okuda, J. *Organometallics* **1997**, *16*, 4845.

(45)   Gamer, M. T.; Rastatter, M.; Roesky, P. W.; Steffens, A.; Glanz, M. *Chem. Eur. J.* **2005**, *11*, 3165.

(46)   Villiers, C.; Thuery, P.; Ephritikhine, M. *Eur. J. Inorg. Chem.* **2004**, 4624.

(47)   Wang, Y.; Shen, Q. *Organometallics* **2000**, *19*, 357.

(48)   Yuan, F.-G.; Wang, H.-Y.; Zhang, Y. *Chin. J. Chem.* **2005**, *23*, 409.

(49)   Natrajan, L. S.; Blake, A. J.; Wilson, C.; Weinstein, J. A.; Arnold, P. L. *Dalton Trans.* **2004**, 3748.

(50)   Arnold, P. L.; Mungar, S. A.; Blake, A. J.; Wilson, C. *Angew. Chem., Int. Ed.* **2003**, *42*, 5981.

(51)   Gordon, J. C.; Giesbrecht, G. R.; Clark, D. L.; Hay, P. J.; Keogh, D. W.; Poli, R.; Scott, B. L.; Watkin, J. G. *Organometallics* **2002**, *21*, 4726.

(52)   Douglass, M. R.; Ogasawara, M.; Hong, S.; Metz, M. V.; Marks, T. J. *Organometallics* **2002**, *21*, 283.

(53)   Collin, J.; Giuseppone, N.; Jabor, N.; Domingos, A.; Maria, L.; Santos, I. *J. Organomet. Chem.* **2001**, *628*, 271.

(54)   Herrmann, W. A.; Munck, F. C.; Artus, G. R. J.; Runte, O.; Anwander, R. *Organometallics* **1997**, *16*, 682.

(55)   Wong, W.-K.; Zhang, L.; Xue, F.; Mak, T. C. W. *Polyhedron* **1997**, *16*, 345.

(56)   van den Hende, J. R.; Hitchcock, P. B.; Lappert, M. F. *J. Chem. Soc., Dalton Trans.* **1995**, 2251.

(57)   Tilley, T. D.; Anderson, R. A.; Zalkin, A. *Inorg. Chem.* **1984**, *23*, 2271.

(58)   Rizvi, S. S. A. *Bull. Chem. Soc. Ethiop.* **1992**, *6*, 115.

(59)   Bambirra, S.; Bouwkamp, M. W.; Meetsma, A.; Hessen, B. *J. Am. Chem. Soc.* **2004**, *126*, 9182.

(60)   Zuyls, A.; Roesky, P. W.; Deacon, G. B.; Konstas, K.; Junk, P. C. *Eur. J. Org. Chem.* **2008**, 693.

(61)   Bambirra, S.; Brandsma, M. J. R.; Brussee, E. A. C.; Meetsma, A.; Hessen, B.; Teuben, J. H. *Organometallics* **2000**, *19*, 3197.

(62)   Bambirra, S.; Meetsma, A.; Hessen, B.; Teuben, J. H. *Organometallics* **2001**, *20*, 782.

(63)   Yao, Y.; Zhang, Z.; Peng, H.; Zhang, Y.; Shen, Q.; Lin, J. *Inorg. Chem.* **2006**, *45*, 2175.

(64)   Xue, M.; Yao, Y.; Shen, Q.; Zhang, J. *J. Organomet. Chem.* **2005**, *690*, 4685.

(65)   Zhang, Z.-Q.; Yao, Y.-M.; Zhang, Y.; Shen, Q.; Wong, W.-T. *Inorg. Chim. Acta* **2004**, *357*, 3173.

(66)   Luo, Y.; Yao, Y.; Zhang, Y.; Shen, Q.; Yu, K. *Chin. J. Chem.* **2004**, *22*, 187.

(67)   Yao, Y.; Xue, M.; Luo, Y.; Zhang, Z.; Jiao, R.; Zhang, Y.; Shen, Q.; Wong, W.-T.; Yu, K.; Sun, J. *J. Organomet. Chem.* **2003**, *678*, 108.

(68)   Yao, Y.; Luo, Y.; Jiao, R.; Shen, Q.; Yu, K.; Weng, L. *Polyhedron* **2003**, *22*, 441.

(69)   Chai, J.; Jancik, V.; Singh, S.; Zhu, H.; He, C.; Roesky, H. W.; Schmidt, H.-G.; Noltemeyer, M.; Hosmane, N. S. *J. Am. Chem. Soc.* **2005**, *127*, 7521.

(70)   Neculai, D.; Roesky, H. W.; Neculai, A. M.; Magull, J.; Herbst-Irmer, R.; Walfort, B.; Stalke, D. *Organometallics* **2003**, *22*, 2279.

(71)   Sanchez-Barba, L. F.; Hughes, D. L.; Humphrey, S. M.; Bochmann, M. *Organometallics* **2005**, *24*, 3792.

(72)   Sanchez-Barba, L. F.; Hughes, D. L.; Humphrey, S. M.; Bochmann, M. *Organometallics* **2006**, *25*, 1012.

(73)   Avent, A. G.; Caro, C. F.; Hitchcock, P. B.; Lappert, M. F.; Li, Z.; Wei, X.-H. *Dalton Trans.* **2004**, 1567.

(74)   Hitchcock, P. B.; Lappert, M. F.; Tian, S. *J. Chem. Soc., Dalton Trans.* **1997**, 1945.

(75)   Evans, W. J.; Shreeve, J. L.; Doedens, R. J. *Inorg. Chem.* **1993**, *32*, 245.

(76)   Yuan, M. L.; Li, X. H.; Xiong, C. D.; Deng, X. M. *Eur. Polym. J.* **1999**, *35*, 2131.

(77)   Huang, Y.; Xu, Z.; Huang, Y.; Ma, D.; Yang, J.; Mays, J. W. *J. Polym. Anal. Charact.* **2003**, *8*, 383.

(78)   Luo, Y. J.; Yao, Y. M.; Shen, Q.; Sun, J.; Weng, L. H. *J. Organomet. Chem.* **2002**, *662*, 144.

(79)   Penczek, S.; Szymanski, R.; Duda, A.; Baran, J. *Macromol. Symp.* **2003**, *201*, 261.

(80)   Xu, X. P.; Yao, Y. M.; Hu, M. Y.; Zhang, Y.; Shen, Q. *J. Polym. Sci. Part A: Pol. Chem.* **2006**, *44*, 4409.

(81)   Evans, W. J.; Katsumata, H. *Macromolecules* **1994**, *27*, 2330.

(82)   Wang, J. F.; Sun, H.; Yao, Y. M.; Zhang, Y.; Shen, Q. *Polyhedron* **2008**, *27*, 1977.

(83)   Penczek, S.; Szymanski, R.; Duda, A.; Baran, J. *Macromol. Symp.* **2003**, *201*, 261.

(84)   Stridsberg, K. M.; Ryner, M.; Albertsson, A.-C. *Adv. Polym. Sci.* **2002**, *157*, 41.

(85)   When using polystyrene calibration curve.

(86)   Hitzbleck, J.; Okuda, J. *Organometallics* **2007**, *26*, 3227.

(87)   Zhang, C. M.; Liu, R. T.; Chen, Z. X.; Zhou, X. G. *Chin. J. Chem.* **2006**, *24*, 231.

(88)   Mikami, K.; Terada, M.; Matsuzawa, H. *Angew. Chem., Int. Ed.* **2002**, *41*, 3554.

(89)   Mlynarski, J.; Jankowsk, J.; Rakiel, B. *Tetrahedron: Asymmetry* **2005**, *16*, 1521.

(90)   Comelles, J.; Pericas, A.; Moreno-Manas, M.; Vallribera, A.; Drudis-Sole, G.; Lledos, A.; Parella, T.; Roglans, A.; Garcia-Granda, S.; Roces-Fernandez, L. *J. Org. Chem.* **2007**, *72*, 2077.

(91)   Kobayashi, S.; Hamada, T.; Nagayama, S.; Manabe, K. *Org. Lett.* **2001**, *3*, 165.

(92)   Hamada, T.; Manabe, K.; Ishikawa, S.; Nagayama, S.; Shiro, M.; Kobayashi, S. *J. Am. Chem. Soc.* **2003**, *125*, 2989.

(93)   Kobayashi, S.; Araki, M.; Yasuda, M. *Tetrahedron Lett.* **1995**, *36*, 5773.

(94)   Kobayashi, S.; Ishitani, H.; Komiyama, S.; Oniciu, D. C.; Katritzky, A. R. *Tetrahedron Lett.* **1996**, *37*, 3731.

(95)   Mascarenhas, C. M.; Miller, S. P.; White, P. S.; Morken, J. P. *Angew. Chem., Int. Ed.* **2001**, *40*, 601.

(96)   Nishibayashi, Y.; Takei, I.; Hidai, M. *Angew. Chem., Int. Ed.* **1999**, *38*, 3047.

(97)   Takei, I.; Nishibayashi, Y.; Ishii, Y.; Mizobe, Y.; Uemura, S.; Hidai, M. *J. Organomet. Chem.* **2003**, *679*, 32.

(98)   Enholm, E. J.; Whitley, P. E.; Xie, Y. *J. Org. Chem.* **1996**, *61*, 5384.

(99)   Percentages based on base peak arising from the fragment O-naphthyl (mass = 155, 100%).

(100) Huang, J.; Zhang, X.; Armstrong, D. W. *Angew. Chem., Int. Ed.* **2007**, *46*, 9073.

(101) Magnus, P.; Lacour, J.; Evans, A.; Rigollier, P.; Tobler, H. *J. Am. Chem. Soc.* **1998**, *120*, 12486.

(102) Takeishi, K.; Sugishima, K.; Sasaki, K.; Tanaka, K. *Chem. Eur. J.* **2004**, *10*, 5681.

(103) Falck, J. R.; He, A.; Reddy, L. M.; Kundu, A.; Barma, D. K.; Bandyopadhyay, A.; Kamila, S.; Akella, R.; Bejot, R.; Mioskowski, C. *Org. Lett.* **2006**, *8*, 4645.

(104)   Bradley, D. C.; Ghotra, J. S.; Hart, F. A. *J. Chem. Soc., Dalton Trans.* **1973**, 2228.

(105)   Knecht, M. R.; Elias, H.-G. *Die Makro. Chem.* **1972**, *157*, 1.

(106)   Dostal, J.; Simek, L.; Kasparkova, V.; Bohdanecky, M. *J. Appl. Polym. Sci.* **1998**, *68*, 1917.

Chapter 4. Yttrium Amidate Complexes as Effective Precatalysts for the Cyclohydroamination of Aminoalkenes[1]

4.1 Introduction

The synthesis of nitrogen-containing molecules is a much sought after process in the pharmaceutical and fine chemical industries.[1] A catalytic route to nitrogen-containing molecules is hydroamination, which is the formal addition of nitrogen and hydrogen atoms across a carbon-carbon unsaturation. The carbon-carbon multiple bond can include alkynes,[1,2] allenes,[3-10] or alkenes,[11-16] and the amine source can be either primary or secondary amines. Hydroamination is atom-economical, can occur in an inter- or intramolecular fashion, and excluding some highly active substrates,[17-20] requires a catalyst. Alkene hydroamination is a thermodynamically less favourable process than alkyne or allene hydroamination,[21] and therefore constitutes a greater challenge (Figure 4.1). The addition of ammonia to ethylene is described as virtually thermoneutral with $\Delta G°$ estimated at -14.7 kJ mol^{-1}.[21,22] However, this reaction has a high activation barrier arising from bringing two electron-rich molecules together and thus requires a catalyst to overcome this barrier.
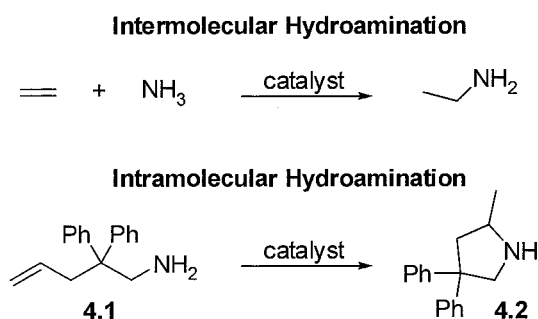

Figure 4.1. Examples of inter- and intramolecular alkene hydroamination.

Metal-based catalysts for alkene hydroamination include examples from across the periodic table, including calcium,[23,24] group 4 metals,[12,25-34] copper,[35-38] gold,[13,39,40] platinum,[41,42] palladium,[43] rhodium[16,44] and zinc.[14,45,46] The rare-earth metals are also attractive, as they are very active for the intra-[47-69] and intermolecular[22,70-72] hydroamination of alkenes. Although intermolecular hydroamination is the ultimate goal, intramolecular hydroamination allows preliminary investigation into catalyst efficiency to give nitrogen-containing heterocycles. *Geminally*-substituted aminoalkenes are most often used for intramolecular hydroamination (such as **4.1**, Figure 4.1) due to enhanced reactivity. This is known as the *gem*-disubstituent effect, which is a combination of the Thorpe-Ingold effect and the reactive rotamer hypothesis.[73] The substrate, 2,2-diphenyl-4-pentenylamine (**4.1**), is commonly used because its large phenyl substituents facilitate intramolecular hydroamination.
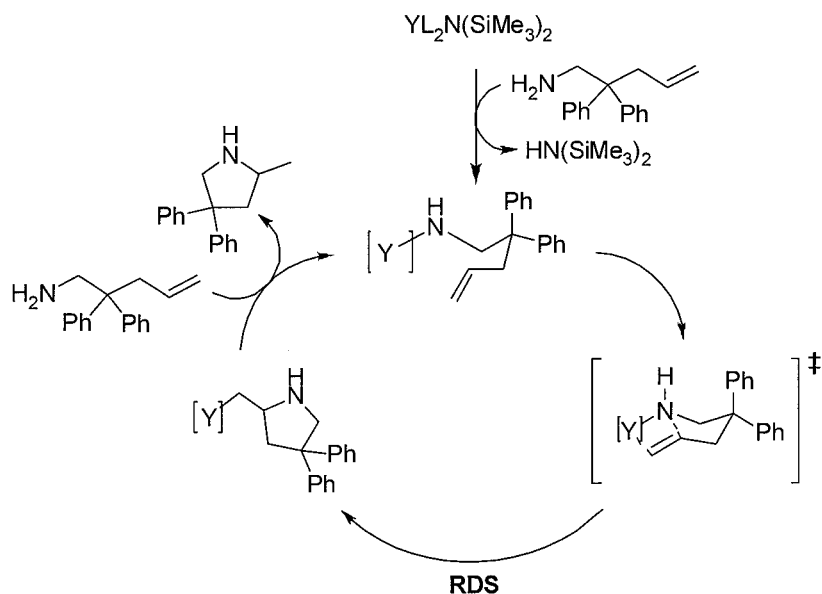
Figure 4.2. σ-Bond insertion mechanism for hydroamination of aminoalkenes using rare-earth catalysts.[57,72]

In contrast to group 4 metals which are proposed to catalyze the hydroamination of aminoalkenes through a metal-imido intermediate,[74,75] rare-earth catalysts are thought to proceed *via* a σ-bond insertion mechanism (Figure 4.2).[57,72] The insertion is thought to be the rate-determining step (RDS).[57,72] Ligand design is important to enhance the turnover rate of the reaction, and to this end, rare-earth catalyzed intramolecular hydroamination has been catalyzed by organometallic complexes, amido complexes and phenoxides. Also, hydroamination of aminoalkenes produces a chiral centre, which has led to research using chiral ligands,[61-69] for asymmetric catalysis. Examples of some well known yttrium complexes used as pre-catalysts for hydroamination are shown in Figure 4.3.
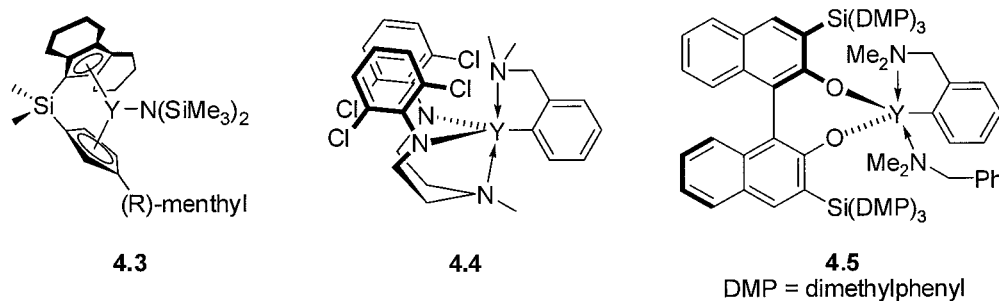
Figure 4.3. Known yttrium complexes used as catalysts for hydroamination.

ansa-Metallocene complex **4.3** has a labile (reactive) amido ligand, whereas **4.4** and **4.5** both employ labile aryl ligands, and all compounds have two auxiliary ligands. All complexes **4.3**, **4.4** and **4.5** are successful hydroamination pre-catalysts and their reactivity towards the cyclohydroamination of the substrate 4-pentenylamine (**4.6**) is shown in Table 4.1.

Table 4.1. Hydroamination of 4-pentenylamine (**4.6**)

Entry	Cat.	mol%	Temp [°C]	Time[a] [h]	Conv. [%]
1[72]	**4.3**	5	60	0.34	100
2[50]	**4.4**	3	60	60	97
3[64]	**4.5**	4	22	20	94
4[50]	Y[N(SiMe₃)₂]₃	3	80	216	6

[a] Time for conversion.

Substrate **4.6**, which lacks any substitution on the alkyl chain, is a challenging hydroamination substrate relative to **4.1**. Complex **4.3**, which contains a labile amido rather than an aryl, showed high reactivity with substrate **4.6** (Table 4.1, Entry 1), while complex **4.4** at the same temperature required drastically longer reaction times in order to obtain comparable conversion.[50,72] The binaphthol complex **4.5** catalyzed the hydroamination of **4.6**

at a lower temperature, but required a much longer reaction time than complex **4.3** (Table 4.1, Entry 3).[64] A common starting material for yttrium complexes, Y[N(SiMe$_3$)$_2$]$_3$ was a poor pre-catalyst for the hydroamination of substrate **4.6** (Table 4.1, Entry 4), obtaining only 6% conversion after 216 hours at 80 °C.[50]

In the Schafer lab, bis(amidate)bis(amido) complexes of group 4 have been shown to be active pre-catalysts in the cyclohydroamination of aminoalkenes[32,34] and the successful synthesis of amidate complexes has now been extended to group 3 (shown in Chapter 2). Interestingly, substrate **4.6** continues to be a challenging substrate for group 4 hydroamination catalysts. This chapter will involve studies of intramolecular hydroamination of aminoalkenes using amidate complexes of group 3.

4.1.1 Scope of Chapter

Due to the success of group 4 amidate complexes for the cyclohydroamination of aminoalkenes, it is of interest to investigate the reactivity of related group 3 complexes. As shown in Chapter 2, crystalline bis(amidate) complexes of yttrium can be synthesized in high yield. This is ideal, as synthesis of known rare-earth precatalysts for hydroamination can be lengthy and low-yielding.[51,54,66] Another advantage to the facile synthesis of group 3 amidates is the ease with which the substituents can be varied on the amidate backbone. It has been shown using group 4 amidate complexes that electron-withdrawing substituents on the amidate can shorten hydroamination reaction times.[29] It is of interest to compare and contrast reactivity trends in yttrium catalyzed cyclohydroamination of aminoalkenes. The three bis(amidate) complexes investigated in this Chapter are shown in Figure 4.4. For comparison, homoleptic **4.11** and mono(amidate) **4.12** were also tested for reactivity.
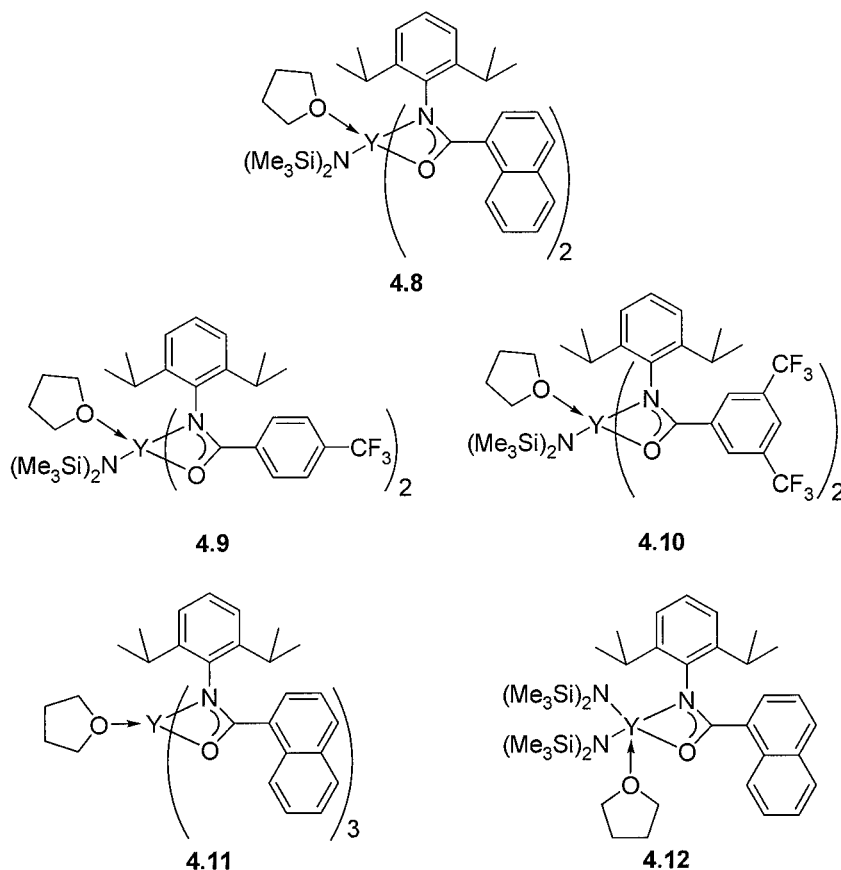
Figure 4.4. Yttrium amidate complexes as precatalysts for cyclohydroamination of aminoalkenes.
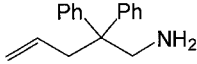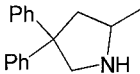
4.2 Yttrium Amidate Complexes as Precatalysts

4.2.1 Results and Discussion

Initially, to test the reactivity of the bis(amidate) complexes, the hydroamination of 2,2-diphenyl-4-pentenylamine (**4.1**) was performed (Table 4.2). The precatalyst, standard (1,3,5-trimethoxybenzene), and substrate were weighed out separately in an inert atmosphere glovebox, and dissolved in approximately 0.7 g of deuterated benzene. The reaction was monitored until greater than 99% conversion was observed in the ^{1}H NMR spectrum, indicated by complete depletion of substrate alkene proton multiplets at δ 5.73 and 5.10, and the appearance of product peaks at δ 2.47 (-CH$_2$C$\underline{H}$(CH$_3$)NH-) and 1.92 (-C$\underline{H}_2$CH(CH$_3$)NH-)

and 1.09 (-CH$_2$CH(C$\underline{H}_3$)NH-). After full conversion, NMR yields were obtained by comparison between the standard proton signals (aryl and methyl protons) and the product **4.2** proton signals in the ^{1}H NMR spectrum.
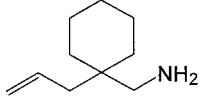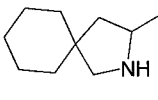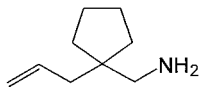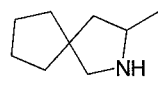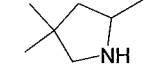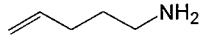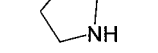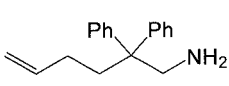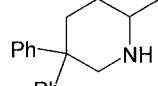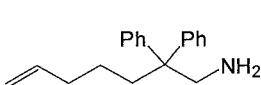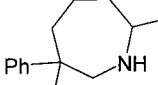
Table 4.2. Hydroamination of 2,2-diphenyl-4-pentenylamine (**4.1**).

Entry[a]	Aminoalkene	Product	Cat.[b]	Time[c] [h]	Yield[d] [%] (isolated)[e]
1			**4.8**	<0.25	>95 (95)
2			**4.9**	<0.25	>95 (94)
3			**4.10**	<0.25	>95 (93)

[a] All reactions performed at 25 °C [b] 10 mol% precatalyst [c] Time for >99% conversion. [d] Yield determined by ^{1}H NMR spectroscopy using 1,3,5-trimethoxybenzene as an internal standard.[e] Isolated yield.

The bis(amidate) complexes were highly efficient in the conversion of compound **4.1** to the heterocycle (**4.2**) (Entry 1-3, Table 4.2) at room temperature. These reactions resulting in high NMR yields of product, which correlated well to the isolated yields obtained.

Table 4.3. Hydroamination of various aminoalkenes using bis(amidate) complexes **4.8**, **4.9** and **4.10**.

Entry	Aminoalkene	Product	Cat.	Temp. [°C]	Time[a] [h]	Yield[b] [%]
1	**4.13**	**4.14**	**4.8**	25	<0.25	>95
			4.9		<0.25	>95
			4.10		<0.25	>95
2	**4.15**	**4.16**	**4.8**	25	1.8	96
			4.9		1	88
			4.10		1	>95
3	**4.17**	**4.18**	**4.8**	25	4.5	88
			4.9		2.5	88
			4.10		2.5	93
4	**4.6**	**4.7**	**4.8**	110	24	>95
			4.9		6	>95
			4.10		6	88[c]
5	**4.19**	**4.20**	**4.8**	65	1.8	>95
			4.9		0.8	>95
			4.10		0.8	>95
6	**4.21**	**4.22**	**4.8**	110	30	81
			4.9		21	85
			4.10		19	82

[a] Time for >99% conversion. [b] Yield determined by ^{1}H NMR spectroscopy using 1,3,5-trimethoxybenzene as an internal standard. [c] Percent conversion

In order to determine the substrate scope of the bis(amidate) precatalyst, a variety of aminoalkenes were tested (Table 4.3). Entries 1-4 contain substrates that have a decrease in geminal-substituent steric properties, from a cyclohexyl group (**4.13**) to no *gem*-disubstituents at all (**4.19**). The *gem*-disubstituent effect is evident when comparing entries 1-4, as an increase in reaction time is noted; in the case of entry 4, an increase in temperature is also needed to achieve full conversion. For the hydroamination of substrate **4.13**, all bis(amidate) complexes give high yield in less than 15 minutes. When the size of the ring in

the *gem*-position on the substrate is reduced to a cyclopentyl group (**4.15**), reaction time is increased to at least an hour, but still provides high yields. This reaction reveals a reactivity difference between the amidate complexes, with the CF_3 substituted bis(amidate) complexes **4.9** and **4.10** giving the fastest times (1 hr). The ring substituents in substrates **4.13** and **4.15** facilitate the transition state (shown in Fig. 4.2), more than the methyl substituents of **4.17**, because of the lack of the reactive rotamer effect. This is evidenced by the increase in reaction time (Entry 3, Table 4.3) for the cyclization of substrate **4.17**. The use of complex **4.8** as a precatalyst results in a reaction time 2 hours longer than the other bis(amidate) complexes (**4.9** and **4.10**). The substrate **4.19** contains no substituents and requires the use of higher temperatures (110 °C) in order to achieve full conversion (Entry 4, Table 4.3). Again, complexes **4.9** and **4.10** result in faster reaction times, compared to complex **4.8**. The same reaction using complex **4.8** as a precatalyst at 25 °C results in no evidence of reaction after 24 hours. Compared to the known yttrium catalysts (Figure 4.3, Table 4.1) amidate complexes **4.8**, **4.9**, and **4.10** are precatalysts for hydroamination of compound **4.19** at higher reaction temperatures. However, the amidate complexes have much shorter reaction times and good conversion compared to the starting material used to synthesize them, $Y[N(SiMe_3)_2]_3$.

For hydroamination of aminoalkenes, 5-membered ring formation is the most facile, but this can be extended to more challenging 6- and 7-membered rings (substrates **4.19** and **4.21**). As expected from hydroamination results presented above, the hydroamination of substrates **4.19**, and **4.21**, proceeded with a faster reaction time using precatalysts **4.9** and **4.10** (Entry 5 and 6, Table 4.3).

The same hydroamination reaction as in Entry 5 (Table 4.3, using precatalyst **4.8**) was also carried out with an *in situ* catalyst preparation. Firstly, 20 mol% of the ligand, *N*-2', 6'-diisopropylphenyl(naphthyl)amide, and 10 mol% of yttrium tris(bis(trimethylsilyl)amide) ($Y[N(SiMe_3)_2]_3$) were combined in approximately 0.7 g of deuterated benzene, and the substrate **4.19** was added after a 15 minute delay. After 1.8 hours the reaction was completed with greater than 95% conversion, as evidenced by the disappearance of alkene signals at δ 5.72 and 4.92 and the growth of product **4.20** proton signals at δ 3.75 (NHC*HH*) and 2.90 (NHC*HH*), 2.50 (C*H*(CH₃)NH), 2.43 (C*HH*CH₂CH(CH₃)NH) and 2.03 (CH*HH*CH₂CH(CH₃)NH), 1.33 (CH₂C*HH*CH(CH₃)NH) and 1.11 (CH₂CH*HH*CH(CH₃)NH) and 0.84 (CH(C*H₃*)NH) in the ¹H NMR spectrum. This result correlates well to the hydroamination outcome where precatalyst **4.8** was isolated prior to reaction (Entry 5, Table 4.3). This demonstrates that the reaction can be affected with the commercially available starting material ($Y[N(SiMe_3)_2]_3$), and an easily prepared amide with no need to isolate the bis(amidate) complex.

Another challenge is the hydroamination of substrates of internal alkenes. As mentioned before, the rate determining step of the hydroamination cycle is proposed to be the σ-bond insertion step. Thus, a substituent at the terminal end of the alkene sterically impedes this step (Figure 4.5).
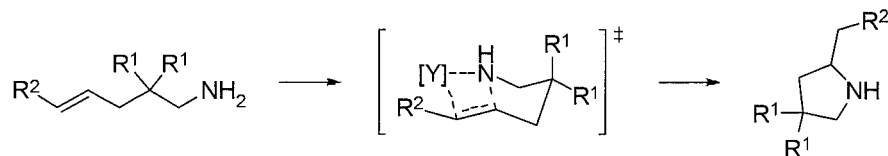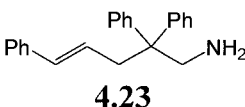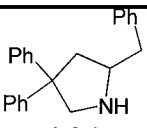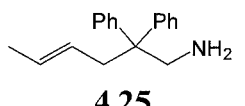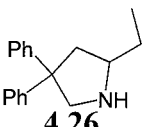

Figure 4.5. σ-Bond insertion step with terminal substitution on aminoalkene.

Substrates **4.23** and **4.25**, which both contain terminal substituents, were cyclized using complexes **4.8**, **4.9** and **4.10** as precatalysts and the results are shown in Table 4.4. For the substrate with a phenyl substituent on the terminus (**4.23**), reaction rates were very fast producing high yields for the CF_3 containing bis(amidate) complexes **4.9** and **4.10**. Much longer reaction times and higher temperatures are needed when the phenyl terminus is replaced with a methyl substituent (compound **4.25**). High yields are obtained for this reaction, and all amidate complexes give similar reaction times.

Table 4.4. Hydroamination of aminoalkenes with terminal substituents using bis(amidate) complexes **4.8**, **4.9** and **4.10**.

Entry	Aminoalkene	Product	Cat.	Temp. [°C]	Time[a] [h]	Yield[b] [%] (isolated)[c]
1	Ph, Ph, Ph, NH₂ **4.23**	Ph, Ph, Ph, NH **4.24**	**4.8**	25	6	>95 (99)
			4.9		<0.25	>95
			4.10		<0.25	>95
2	Ph, Ph, NH₂ **4.25**	Ph, Ph, NH **4.26**	**4.8**	65	18	>95 (85)
			4.9		18	>95 (81)
			4.10		17	>95 (82)

[a] Time for >99% conversion. [b] Yield determined by ^{1}H NMR spectroscopy using 1,3,5-trimethoxybenzene as an internal standard. [c] Isolated yield.

Hydroamination using rare-earth metals as catalysts can tolerate the use of secondary amine substrates. This is in contrast to neutral group 4 catalyzed hydroamination which requires a primary amine to form the proposed imido intermediate.[33] In a preliminary screen using substrate **4.27** and precatalyst **4.8** (Figure 4.6), reactivity was noticed by product methyl proton signals at δ 2.07 (N(C$\underline{H}_3$)) and 1.11 (CH(C$\underline{H}_3$)) and diastereotopic proton signals at δ 3.10 and 3.02 (C$\underline{H}_2$CH(CH₃)) and 2.35 and 2.03 (N(CH₃)C$\underline{H}_2$) in the ^{1}H NMR spectrum.
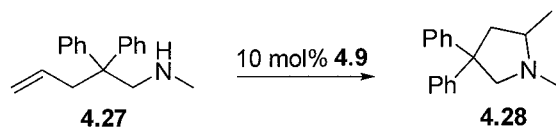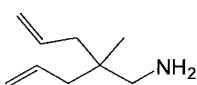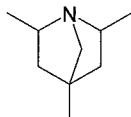
Figure 4.6. Preliminary screen of secondary amines for hydroamination.

The reactivity of secondary amines was then extended to a tandem reaction using the substrate 1-amino-2,2-diallylpropane (**4.29**), which contains two alkene groups Table 4.5).[58] Neutral group 4 catalyzed hydroamination generally stops at the formation of the 5-membered heterocycle, whereas rare-earth catalyzed hydroamination can instead do a tandem cyclization to form the tertiary amine **4.30**. The bis(amidate) complexes **4.8**, **4.9** and **4.10** were used in the hydroamination of **4.29** initially at 65 °C. After 11 hours, the conversion values using precatalysts **4.8**, **4.9** and **4.10** were 68%, 61% and 69%, respectively. In all cases, these conversion values were mostly achieved after only 6 hours at 65 °C. The reaction was repeated at 110 °C, and after 1 hour using precatalysts **4.8**, **4.9** and **4.10** the conversion values reached 86%, 71% and 71% respectively. After longer reaction times at 110 °C no further reactivity was noted; however, if more precatalyst was added the reaction would go to completion. This reaction "stalling" may be due to product inhibition.[57] In order to verify this, the product **4.30** was isolated by vacuum distillation and a small amount was purposely added to a hydroamination reaction to monitor the reaction rate in presence of the product.

Two hydroamination reactions were prepared concurrently using precatalyst **4.8** and substrate **4.29**, where one reaction had product **4.30** added. Both reactions were run at 110 °C concurrently for 1 hour. The normal hydroamination reaction with precatalyst **4.8** and substrate **4.29** resulted in a 96% conversion as noted by the appearance of ^{1}H signals at δ

139

3.22 and 3.15 for the two C$\underline{H}$(CH)$_3$ protons and δ 2.69 for the C$\underline{H_2}$N protons in the ^{1}H NMR

spectrum. The reaction that was spiked with the product **4.30** gave a conversion of 86%.

This shows that **4.30** does inhibit the hydroamination efficiency, most likely through

competitive binding to the yttrium centre. When comparing the different complexes, this

effect seems to be more of a problem for the precatalysts that contain the CF$_3$ groups on the

amidate backbone (complexes **4.9** and **4.10**). Complexes **4.9** and **4.10** are expected to be

more Lewis acidic, and therefore likely bind the product more tightly than the other

complexes.

Table 4.5. Hydroamination of 2-allyl-2-methyl-4-pentenylamine (**4.29**)

Entry	Aminoalkene	Product	Cat.	Temp. [°C]	Time^a [h]	Conversion [%]
1			**4.8**		7	95
			4.9	110	5	85
	4.29	**4.30**	**4.10**		5	77

^{a} Time for conversion value

Overall, complexes **4.9** and **4.10** were deemed the most active catalysts. Since some rare-

earth catalysts are known to catalyze the intermolecular hydroamination of alkenes and

amines,[22,70-72] complex **4.9** was used in a precatalyst screen to see if intermolecular

hydroamination was possible with bis(amidate) complexes of yttrium (Figure 4.7). All

reactions were attempted at 110 °C, since at higher temperatures degradation of catalyst was

noted after 24 hours. Attempts at intermolecular hydroamination employed styrene as the

alkene source, and aniline, 2,6-dimethylaniline, cyclohexylamine, and benzylamine as the

amine sources. Initially the reactions were prepared using a 1:1 stoichiometric ratio between

styrene and amine (10 mol% **4.9**, 30 mg styrene, 0.7 g C$_6$D$_6$). When no hydroamination

reaction was seen, as evidenced by no formation of product signals in the ^{1}H NMR spectrum after a week at 110 °C, the amine stoichiometry was varied from 1.1, 1.5 and 2 equivalents. Polystyrene formation was seen in these conditions as indicated by very broad proton signals between δ 5 and 6 ppm and precipitate forming in the NMR tube. These variations of amine stoichiometry still resulted in no reaction, but previous successful intermolecular alkene hydroamination reactions use 2 equivalents of alkene.[72] Using benzylamine as the amine source, the reactions were attempted again using styrene stoichiometry varied from 5, 2 and 1.5 equivalents. After a week at 110 °C for all experiments, no reaction was observed. This indicates that the bis(amidate) complexes presented here are not active for intermolecular hydroamination under these conditions. Future work will focus on changing the conditions, as well as catalyst development to obtain a amidate complex that will catalyze intermolecular hydroamination.
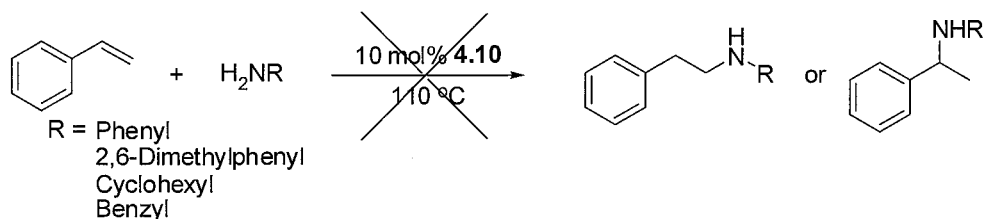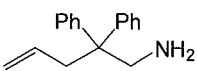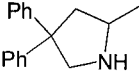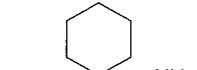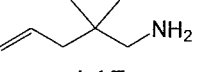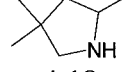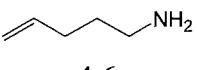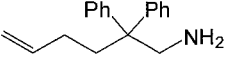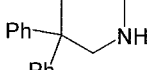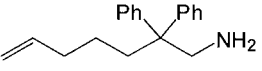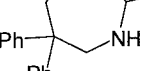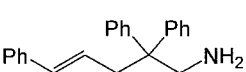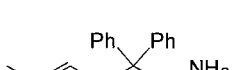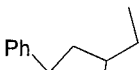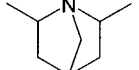
Figure 4.7. Intermolecular hydroamination using precatalyst 4.9.

The tris(amidate) complex 4.11 was determined to be a highly efficient initiator for the ring-opening polymerization of ε-caprolactone (Chapter 3) and although the tris(amidate) complex does not have any labile amido ligands, perhaps it can react in situ to give an active catalyst. Also, the analogous mono(amidate) complexes 4.12 was screened in hydroamination experiments and the results are shown in Table 4.6.

The tris(amidate) complex 4.11 does not catalyze the hydroamination of compound 4.1 (Entry 1, Table 4.6), even at elevated temperatures (65 °C, and 110 °C) for longer than 24

hours. The mono(amidate) complex **4.12** had comparable rates and yields to complexes **4.9** and **4.10**, as shown in Entries 1-7 (Table 4.6). Although it was shown in Chapter 2 that mono(amidate) complexes will undergo ligand redistribution at 110 °C and at this temperature, it is not known what the reactive species is in solution. For the hydroamination of internal alkene substrate **4.23**, mono(amidate) complex **4.12** effected the transformation much quicker than the analgous bis(amidate) complex **4.8**, but slightly slower than bis(amidate) complexes **4.9** and **4.10** (Entry 8, Table 4.6). When comparing the tandem cyclization reaction (Entry 10, Table 4.6) between the amidate complexes, the mono(amidate) complex **4.12** cyclized the fastest and with the highest conversion to product **4.28**.

Table 4.6. Hydroamination using complexes **4.11** and **4.12** as precatalysts (10 mol%).

Entry	Aminoalkene	Product	Cat.	Temp. [°C]	Time[a] [h]	Yield[b] (isolated)[c] [%]
1	**4.1**	**4.2**	**4.11**	25	NR[d]	–
			4.12		<0.25	94
2	**4.13**	**4.14**	**4.12**	25	<0.25	89
3	**4.15**	**4.16**	**4.12**	25	1.3	92
4	**4.17**	**4.18**	**4.12**	25	2.5	83
5	**4.6**	**4.7**	**4.12**	110	6.5	>95
6	**4.19**	**4.20**	**4.12**	65	0.8	86
7	**4.21**	**4.22**	**4.12**	110	16	91
8	**4.23**	**4.24**	**4.12**	25	0.8	94 (89)
9	**4.25**	**4.26**	**4.12**	65	17	86 (84)
10	**4.27**	**4.28**	**4.12**	110	3.5	>95[e]

[a] Time for >99% conversion. [b] Yield determined by ^{1}H NMR spectroscopy using 1,3,5-trimethoxybenzene as an internal standard. [c] Isolated yield. [d] No reaction. [e] Percent conversion.

143

The hydroamination of aminoalkenes produces a chiral centre, and since the amidate backbone in the bis and mono(amidate) complexes is achiral, no enantioselectivity is expected to result from this reaction; however, these complexes can induce diastereoselectivity. Using complexes **4.8** and **4.12**, for a direct comparison between bis and mono(amidate) complexes, the hydroamination of 1-methyl-4-pentenylamine (**4.31**) was carried out and the diastereomeric ratio (dr) determined (Figure 4.8). The bis(amidate) complex **4.8** results in a better dr after 99% conversion. Monitoring of the reaction showed that the diastereomeric ratio maintains a constant value throughout both reactions. Furthermore, presumably the bis(amidate) complex is not forming the mono(amidate) complex *in situ*, or the dr values would be the same as the result using complex **4.12**. Complex **4.10** gave the best dr value, and complex **4.9** obtained a slightly better dr value than the mono(amidate) complex **4.12**. This indicates that a bis(amidate) complex imparts more stereocontrol over the reaction as compared to the less sterically encumbered mono(amidate). This supports the future use of chiral bis(amidate) complexes for use in asymmetric hydroamination.

Precatalyst	Yield	trans 4.32	:	cis 4.33
4.8	94%	11	:	1
4.9	84%	7	:	1
4.10	81%	15	:	1
4.12	83%	5	:	1
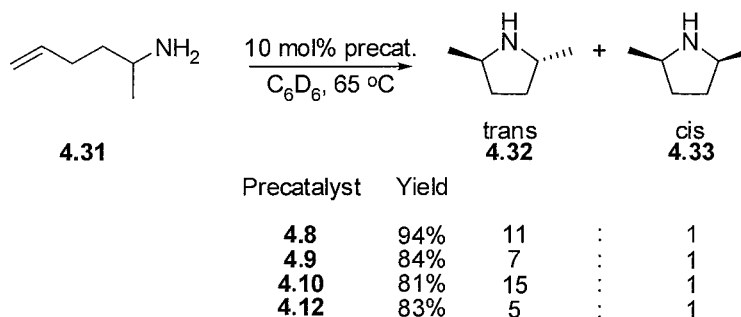
Figure 4.8. Hydroamination of 1-methyl-4-pentenylamine (**4.31**). Yield determined by ^{1}H NMR spectroscopy using 1,3,5-trimethoxybenzene as an internal standard and comparison of known values[76,77] for the HNC*H*Me ^{1}H signal in NMR spectrum of **4.32** and **4.33**.

4.2.2 Summary

Overall the bis(amidate) complexes of yttrium were shown to be good catalysts for the hydroamination of aminoalkenes. The reaction times for multiple substrates indicated that the bis(amidate) complexes that contain the electron-withdrawing group CF_3 on the amidate backbone (complexes **4.9** and **4.10**) are more reactive than the bis(amidate) **4.8**. One of the more reactive complexes, **4.9**, gave no reaction when tested for the ability to catalyze intermolecular hydroamination. The tris(amidate) complex **4.11** was inactive for the hydroamination of aminoalkenes, but the mono(amidate) complex **4.12** had comparable reactivity to complexes **4.9** and **4.10**. The bis(amidate) complex **4.8** proved to give better diastereoselectivity that related mono(amidate) complex **4.12**.

It was shown that adding electron-withdrawing groups on the amidate backbone could reduce reaction times. It is also known for forming bis(amidate) and mono(amidate) complexes that bulk on the *N*-substituent on the amidate is necessary for clean synthesis (Chapter 2). By combining these two structural features into the ligand set, the reaction rates and improved selectivity could be further enhanced.

4.3 Conclusions

Amidate complexes of group 3 are easily synthesized in high yield and are good candidates for hydroamination precatalysts. They show moderate activity in comparison to known yttrium precatalysts and adding electron-withdrawing groups onto the amidate backbone has a significant effect on reaction time, resulting in the identification of the most active amidate complexes as **4.9** and **4.10**. Mono(amidate) complex **4.12** was found to be a good precatalyst for the hydroamination of aminoalkenes, but gave reduced

diastereoselectivity than the analogous bis(amidate) complex (**4.8**). Modifications to the amidate backbone, including more electron-withdrawing groups while maintaining steric protection at the nitrogen, for the synthesis of bis(amidate) complexes increases reactivity rates in the hydroamination of aminoalkenes.

Future work will mainly focus on ligand design to increase reaction rates, and attempt to obtain reactivity in intermolecular hydroamination. Since the bis(amidate) complex **4.8** gave better diastereoselectivity than the analogous mono(amidate) complex **4.12**, further studies into enantioselective hydroamination will focus on versions of bis(amidate) complexes.

4.4   Experimental

4.4.1 Starting Materials and Reagents

All operations were performed under an inert atmosphere of nitrogen using standard Schlenk-line or glovebox techniques. THF, toluene, pentane, and hexanes were all purified by passage through an alumina column and sparged with nitrogen. The compounds 2,2-diphenyl-4-pentenylamine,[62] 4-pentenylamine,[78] 1-methyl-4-pentenylamine,[76] C-(1-allylcyclohexyl)-methylamine,[79] C-(1-allyl-cyclopentyl)-methylamine,[65] 2,2-dimethyl-pent-4-enylamine,[80] 2,2-diphenyl-5-hexenylamine,[81] 2,2-diphenyl-6-septenylamine, 2,2,5-triphenyl-4-pentenylamine,[81] 5-methyl-2,2-diphenyl-4-pentenylamine and 1-amino-2,2-diallylpropane[82] were made according to previously reported procedures and purified by distillation and storage over molecular sieves. Complexes **4.11**, **4.8**, **4.9**, **4.10**, and **4.12** were prepared as stated in Chapter 3. All other chemicals were commercially available and used as received unless otherwise stated. ^{1}H and ^{13}C NMR spectra were recorded on Bruker AV300, AV400 and AV600 spectrometers.

4.4.2 Synthesis

Typical procedure for hydroamination using amidate complexes. (For Entry 2, Table 4.2)

Inside a inert-atmosphere glovebox, complex **4.8** (24.11 mg, 0.025 mmol, 10 mol%), 1,3,5-trimethoxybenzene (14.2 mg, 0.084 mmol) and 2,2-diphenyl-4-pentenylamine (**4.1**) (60.0 mg, 0.253 mmol) were weighed out in separate vials, dissolved and combined in approximately 0.7 g of deuterated benzene inside a J-Young sealable NMR tube. The ^{1}H NMR spectrum was immediately obtained (approximately 15 minute delay) to monitor conversion (>99%). By comparison of the integration values for the proton signals of 1,3,5-trimethoxybenzene (δ 6.25 and 3.32 for aryl-H and $-O(CH_3)$ protons respectively) to the newly formed $CH(CH_3)$ signal (2.47 ppm) in the ^{1}H NMR spectrum, the NMR yield is obtained (>95%). The reaction was exposed to air and quenched with dichloromethane. The residual material was added to a small frit silica column and initially flushed with 200 mL of 1:1 solution of hexanes and ethyl acetate (to remove residual ligand). The column was then flushed with 200 mL of 10% methanol and 1% isopropylamine in dichloromethane, which was collected and dried in *vacuo* to give the product **4.2** (57.0 mg, 95% yield). NMR yield is typically larger than isolated yield, due to loss of product during the isolation procedure.

4.5   References

(1)   Severin, R.; Doye, S. *Chem. Soc. Rev.* **2007**, *36*, 1407.

(2)   Pohlki, F.; Doye, S. *Chem. Soc. Rev.* **2003**, *32*, 104.

(3)   Zhang, Z. B.; Bender, C. F.; Widenhoefer, R. A. *J. Am. Chem. Soc.* **2007**, *129*, 14148.

(4)   Nishina, N.; Yamamoto, Y. *Angew. Chem., Int. Ed.* **2006**, *45*, 3314.

(5)   Nishina, N.; Yamamoto, Y. *Synlett* **2007**, 1767.

(6)   LaLonde, R. L.; Sherry, B. D.; Kang, E. J.; Toste, F. D. *J. Am. Chem. Soc.* **2007**, *129*, 2452.

(7)   Ackermann, L.; Bergman, R. G.; Loy, R. N. *J. Am. Chem. Soc.* **2003**, *125*, 11956.

(8)   Yamamoto, Y.; Radhakrishnan, U. *Chem. Soc. Rev.* **1999**, *28*, 199.

(9)   Besson, L.; Gore, J.; Gazes, B. *Tetrahedron Lett.* **1995**, *36*, 3857.

(10)   Kinder, R. E.; Zhang, Z.; Widenhoefer, R. A. *Org. Lett.* **2008**, *10*, 3157.

(11)   Mueller, C.; Saak, W.; Doye, S. *Eur. J. Org. Chem.* **2008**, 2731.

(12)   Mueller, C.; Loos, C.; Schulenberg, N.; Doye, S. *Eur. J. Org. Chem.* **2006**, 2499.

(13)   Giner, X.; Najera, C. *Org. Lett.* **2008**, *10*, 2919.

(14)   Dochnahl, M.; Loehnwitz, K.; Pissarek, J.-W.; Roesky, P. W.; Blechert, S. *Dalton Trans.* **2008**, 2844.

(15)   Cheng, X.; Xia, Y.; Wei, H.; Xu, B.; Zhang, C.; Li, Y.; Qian, G.; Zhang, X.; Li, K.; Li, W. *Eur. J. Org. Chem.* **2008**, 1929.

(16)   Liu, Z.; Hartwig, J. F. *J. Am. Chem. Soc.* **2008**, *130*, 1570.

(17)   Le Blanc, M.; Santini, G.; Gallucci, J.; Riess, J. G. *Tetrahedron* **1977**, *30*, 2931.

(18)   Le Blanc, M.; Santini, G.; Riess, J. G. *Tetrahedron Lett.* **1975**, *47*, 4151.

(19)   Brunet, J. J.; Fixari, B.; Caubere, P. *Tetrahedron Lett.* **1974**, *30*, 2931.

(20)   Flowers, W. T.; Haszeldine, R. N.; Owen, C. R.; Thomas, A. *Chem. Commun.* **1974**, 134.

(21)   Muller, T. E.; Beller, M. *Chem. Rev.* **1998**, *98*, 675.

(22)   Hultzsch, K. C. *Adv. Synth. Catal.* **2005**, *347*, 367.

(23)   Crimmin, M. R.; Casely, I. J.; Hill, M. S. *J. Am. Chem. Soc.* **2005**, *127*, 2042.

(24)   Datta, S.; Roesky, P. W.; Blechert, S. *Organometallics* **2007**, *26*, 4392.

(25)   Marcsekova, K.; Loos, C.; Rominger, F.; Doye, S. *Synlett* **2007**, 2564.

(26)   Smolensky, E.; Kapon, M.; Eisen, M. S. *Organometallics* **2007**, *26*, 4510.

(27)   Smolensky, E.; Kapon, M.; Eisen, M. S. *Organometallics* **2005**, *24*, 5495.

(28)   Ackermann, L.; Kaspar, L. T.; Althammer, A. *Org. Biomol. Chem.* **2007**, *5*, 1975.

(29)   Bexrud, J. A.; Li, C. Y.; Schafer, L. L. *Organometallics* **2007**, *26*, 6366.

(30)   Lee, A. V.; Schafer, L. L. *Organometallics* **2006**, *25*, 5249.

(31)   Watson, D. A.; Chiu, M.; Bergman, R. G. *Organometallics* **2006**, *25*, 4731.

(32)   Thomson, R. K.; Bexrud, J. A.; Schafer, L. L. *Organometallics* **2006**, *25*, 4069.

(33)   Bexrud, J. A.; Beard, J. D.; Leitch, D. C.; Schafer, L. L. *Org. Lett.* **2005**, *7*, 1959.

(34)   Wood, M. C.; Leitch, D. C.; Yeung, C. S.; Kozak, J. A.; Schafer, L. L. *Angew. Chem., Int. Ed.* **2007**, *46*, 354.

(35)   Taylor, J. G.; Whittall, N.; Hii, K. K. *Org. Lett.* **2006**, *8*, 3561.

(36)   Sherman, E. S.; Fuller, P. H.; Kasi, D.; Chemler, S. R. *J. Org. Chem.* **2007**, *72*, 3896.

(37)   Munro-Leighton, C.; Delp, S. A.; Alsop, N. M.; Blue, E. D.; Gunnoe, T. B. *Chem. Commun.* **2008**, 111.

(38)   Munro-Leighton, C.; Delp, S. A.; Blue, E. D.; Gunnoe, T. B. *Organometallics* **2007**, *26*, 1483.

(39)   Kovacs, G.; Ujaque, G.; Lledos, A. *J. Am. Chem. Soc.* **2008**, *130*, 853.

(40)   Liu, X. Y.; Li, C. H.; Che, C. M. *Org. Lett.* **2006**, *8*, 2707.

(41)   Brunet, J. J.; Chu, N. C.; Rodriguez-Zubiri, M. *Eur. J. Inorg. Chem.* **2007**, 4711.

(42)   Brunet, J. J.; Chu, N. C.; Diallo, O. *Organometallics* **2005**, *24*, 3104.

(43)   Hartwig, J. F. *Pure Appl. Chem.* **2004**, *76*, 507.

(44)   Simpson, M. C.; ColeHamilton, D. J. *Coord. Chem. Rev.* **1996**, *155*, 163.

(45)   Dochnahl, M.; Lohnwitz, K.; Pissarek, J. W.; Biyikal, M.; Schulz, S. R.; Schon, S.; Meyer, N.; Roesky, P. W.; Blechert, S. *Chem. Eur. J.* **2007**, *13*, 6654.

(46)   Dochnahl, M.; Pissarek, J.-W.; Blechert, S.; Loehnwitz, K.; Roesky, P. W. *Chem. Commun.* **2006**, 3405.

(47)   Kim, Y. K.; Livinghouse, T.; Horino, Y. *J. Am. Chem. Soc.* **2003**, *125*, 9560.

(48)   Kim, Y. K.; Livinghouse, T. *Angew. Chem., Int. Ed.* **2002**, *41*, 3645.

(49)   Kim, J. Y.; Livinghouse, T. *Org. Lett.* **2005**, *7*, 4391.

(50)   Kim, Y. K.; Livinghouse, T.; Bercaw, J. E. *Tetrahedron Lett.* **2001**, *42*, 2933.

(51)   Tian, S.; Arredondo, V. M.; Stern, C. L.; Marks, T. J. *Organometallics* **1999**, *18*, 2568.

(52)   Ryu, J. S.; Marks, T. J.; McDonald, F. E. *Org. Lett.* **2001**, *3*, 3091.

(53)   Ryu, J. S.; Marks, T. J.; McDonald, F. E. *J. Org. Chem.* **2004**, *69*, 1038.

(54)   Panda, T. K.; Zulys, A.; Gainer, M. T.; Roesky, P. W. *Organometallics* **2005**, *24*, 2197.

(55)   Panda, T. K.; Zulys, A.; Gamer, M. T.; Roesky, P. W. *J. Organomet. Chem.* **2005**, *690*, 5078.

(56)   Lauterwasser, F.; Hayes, P. G.; Brase, S.; Piers, W. E.; Schafer, L. L. *Organometallics* **2004**, *23*, 2234.

(57)   Bambirra, S.; Tsurugi, H.; van Leusen, D.; Hessen, B. *Dalton Trans.* **2006**, 1157.

(58)   Hultzsch, K. C.; Hampel, F.; Wagner, T. *Organometallics* **2004**, *23*, 2601.

(59)   Molander, G. A.; Pack, S. K. *Tetrahedron* **2003**, *59*, 10581.

(60)   Molander, G. A.; Dowdy, E. D. *J. Org. Chem.* **1999**, *64*, 6515.

(61)   Gagne, M. R.; Brard, L.; Conticello, V. P.; Giardello, M. A.; Stern, C. L.; Marks, T. J. *Organometallics* **1992**, *11*, 2003.

(62)   Hong, S. W.; Tian, S.; Metz, M. V.; Marks, T. J. *J. Am. Chem. Soc.* **2003**, *125*, 14768.

(63)   Gribkov, D. V.; Hultzsch, K. C. *Chem. Commun.* **2004**, 730.

(64)   Gribkov, D. V.; Hultzsch, K. C.; Hampel, F. *J. Am. Chem. Soc.* **2006**, *128*, 3748.

(65)   Riegert, D.; Collin, J.; Meddour, A.; Schulz, E.; Trifonov, A. *J. Org. Chem.* **2006**, *71*, 2514.

(66)   Collin, J.; Daran, J. C.; Schulz, E.; Trifonov, A. *Chem. Commun.* **2003**, 3048.

(67)   Collin, J.; Daran, J. C.; Jacquet, O.; Schulz, E.; Trifonov, A. *Chem. Eur. J.* **2005**, *11*, 3455.

(68)   O'Shaughnessy, P. N.; Scott, P. *Tetrahedron: Asymmetry* **2003**, *14*, 1979.

(69)   Xiang, L.; Wang, Q. W.; Song, H. B.; Zi, G. F. *Organometallics* **2007**, *26*, 5323.

(70)   Li, Y. W.; Marks, T. J. *Organometallics* **1996**, *15*, 3770.

(71)   Li, Y. W.; Marks, T. J. *J. Am. Chem. Soc.* **1998**, *120*, 1757.

(72)   Hong, S.; Marks, T. J. *Acc. Chem. Res.* **2004**, *37*, 673.

(73)   Jung, M. E.; OPiizzi, G. *Chem. Rev.* **2005**, *105*, 1735.

(74)   Duncan, A. P.; Bergman, R. G. *Chem. Rec.* **2002**, *2*, 431.

(75)   Gott, A. L.; Clarke, A. J.; Clarkson, G. J.; Scott, P. *Chem. Commun.* **2008**, 1422.

(76)   Harding, K. E.; Burks, S. R. *J. Org. Chem.* **1981**, *46*, 3920.

(77)   Gagne, M. R.; Stern, C. L.; Marks, T. J. *J. Am. Chem. Soc.* **1992**, *114*, 275.

(78)   Gagne, M. R.; Stern, C. L.; Marks, T. J. *J. Am. Chem. Soc.* **1992**, *114*, 275.

(79)   Bender, C. F.; Widenhoefer, R. A. *J. Am. Chem. Soc.* **2005**, *127*, 1070.

(80)   Tamaru, Y.; Hojo, M.; Higashimura, H.; Yoshida, Z. *J. Am. Chem. Soc.* **1988**, *110*, 3994.

(81)   Kondo, T.; Okada, T.; Mitsudo, T. *J. Am. Chem. Soc.* **2002**, *124*, 186.

(82)   Quinet, C.; Jourdain, P.; Hermans, C.; Ates, A.; Lucas, I.; Markó, I. E. *Tetrahedron* **2008**, *64*, 1077.

Chapter 5. Yttrium Amidate Complexes as Imido Precursors[1]

5.1 Introduction

Terminal imido (=NR) complexes of group 4 are well known[1] and are proposed as intermediates in multiple catalytic processes such as imine metathesis,[2] transamidation,[3] and hydroamination of alkenes and alkynes.[3,4] The only amidate supported imido complex has been characterized in the Schafer lab (**5.1**, Figure 5.1).[4] It was found that in order to generate a terminal imido species, a bulky donor, triphenylphosphine oxide (O=PPh₃), was required to coordinatively saturate the metal centre.[4] Without an added donor this imido product is not isolable. The imido ligand is formally a dianionic ligand and considered to be a 6-electron donor to the zirconium metal centre.[4]
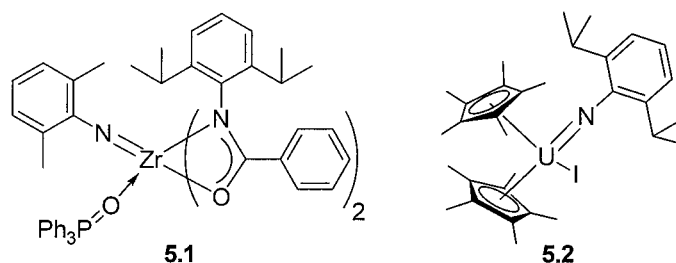
Figure 5.1. Examples of imido complexes.[4,6]

Imido complexes of the actinides have also been successfully isolated (**5.2**, Figure 5.1).[5,6,9] Isolation of actinide imido complexes is possible without the added bulky base; however, the imido substituent typically is a bulky group such as diisopropylphenyl (Dipp), 2,4,6-tri-*tert*-butylphenyl, or *tert*-butyl.[5,6] The imido in the uranium compound **5.2**, is also considered to be a dianionic ligand and a 6-electron donor.[5,6] A similarity between the two

---

examples in Figure 5.1, is the ionic radius of the metal centres ($Zr^{4+} = 0.72$ Å, $U^{5+} = 0.76$ Å).[7] In contrast to group 4 and actinide imido complexes, isolation of analogous terminal lanthanide or group 3 compounds has proven synthetically impossible to date.[8,9] Although, it has been calculated that a lanthanide imido is possible,[8] although it will most likely involve an optimized coordination environment.[8] In fact, only one example of a terminal imido lanthanide complex (**5.4**) has been suggested, but is depicted as a Lu-N single bond (2.122(2) Å, Figure 5.2) and is formally a monoanionic ligand.[10] However, DFT studies of complex **5.4** indicate that the bonding in Lu-N is described as $2\sigma,4\pi$-donor (6-electron), like previously mentioned terminal imido complexes. Interestingly, the ionic radius of Lu^{3+} (0.861 Å) is larger than Zr^{4+} and U^{5+}, but similar to Y^{3+} (0.90 Å).[7]
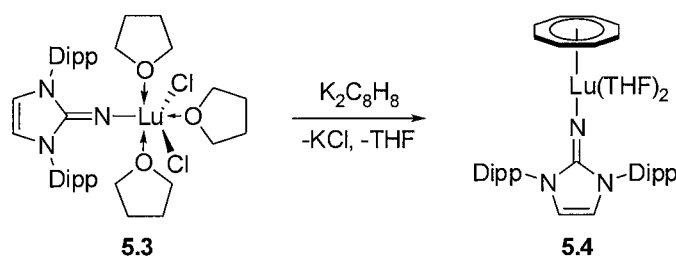
Figure 5.2. Formation of lanthanide imido complex **5.4**.

Typically, lanthanide imido complexes are formed where the imido nitrogen is bridging, or capping.[11-17] An example of a bridging imido is shown in the synthesis of Yb imido complexes **5.5** and **5.6** (Figure 5.3).[11]
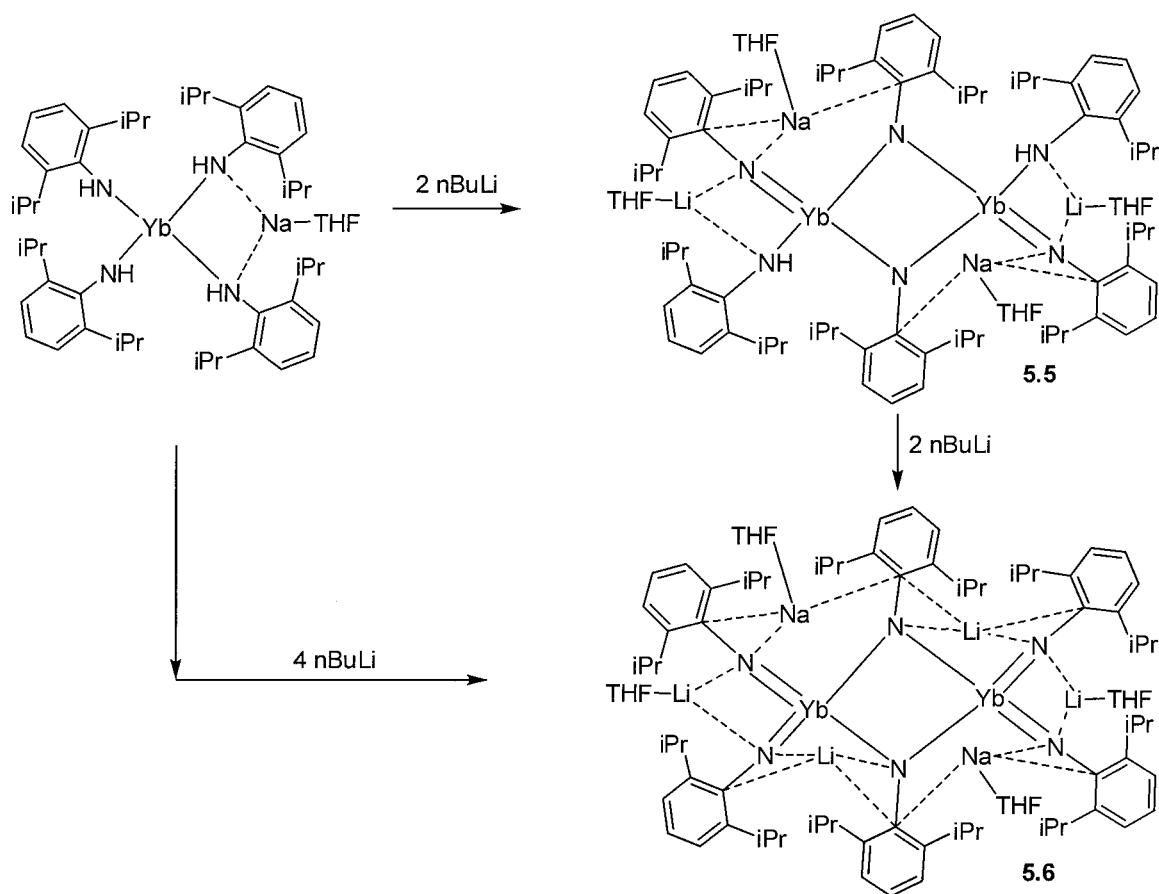
Figure 5.3. Synthesis of Yb bridging imido complexes **5.5** and **5.6**.

To date, no group 3 terminal imido complex has been characterized. Hessen *et al.* have proposed that a transition state in the formation of a bridging scandium imido dimer (**5.8**) is in fact a terminal scandium imido complex (Figure 5.4).[12] Piers *et al.* propose that with enough steric support, a terminal group 3 imido complex could indeed be isolable;[13] however, their attempts at deprotonation of a NHR group of a scandium β-diketiminato complex have thus far been unsuccessful.[13] It should be noted that analogous work on yttrium has not yet been reported.

154
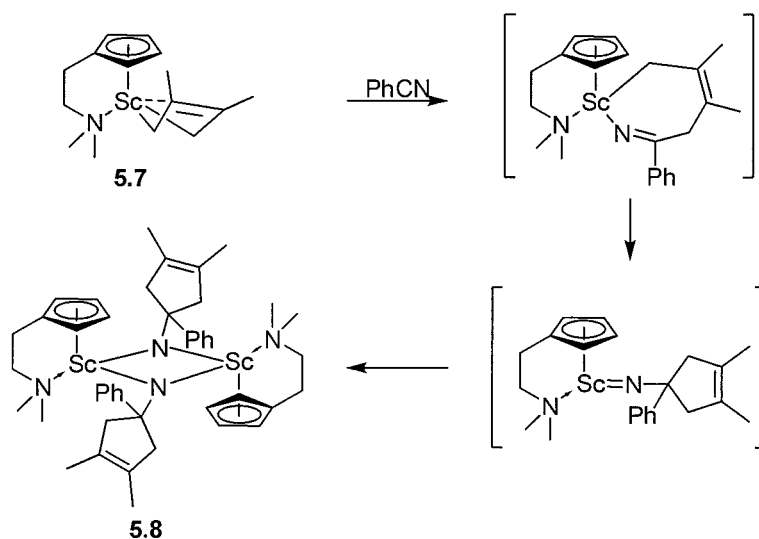
Figure 5.4. Postulated scandium imido intermediate.

Although there have been no reports of group 3 terminal imido complex formation, it is plausible that with the right steric support it can occur. It is also calculated to be possible to form a lanthanide imido complex[8] and since yttrium has a comparable size and reactivity to the lanthanides, which display some propensity for imido formation (Figure 5.3), yttrium is therefore thought to be able to form an imido as well. The amidate ligand, with its tunable nature, can incorporate sterically demanding groups easily. Since mono(amidate) complexes of yttrium can be formed in high yield with varying steric properties, they are ideal candidates to explore as imido precursors. This chapter will detail the synthesis of anilido yttrium complex precursors, and deprotonation investigations in an attempt to form yttrium imido compounds.

155

5.2 Anilido Complexes

5.2.1 Introduction

Literature precedence for imido formation, whether terminal, bridging or capping, usually involves a bulky substituent as the R group of the NR^{2-} moiety. The most extensively used substituent is diisopropylphenyl (Dipp).[5,8,14,15] Furthermore, the most commonly used synthetic route to form an imido complex using bulky R groups is deprotonation of previously formed anilido complexes.[11,14] Synthesis of anilido yttrium complexes is known in the literature,[15,16] and an anilido phosphinimine (**5.9**) and amino phosphine (**5.10**) supported yttrium bis(anilido) complexes are shown in Figure 5.5.[15] Evans and coworkers have reported a synthesis of tris(2,6-diisopropylanilido)yttrium, which exists as a dimer in the solid-state, but unfortunately the quality of the structure does not allow discussion of bond lengths and angles.[16]
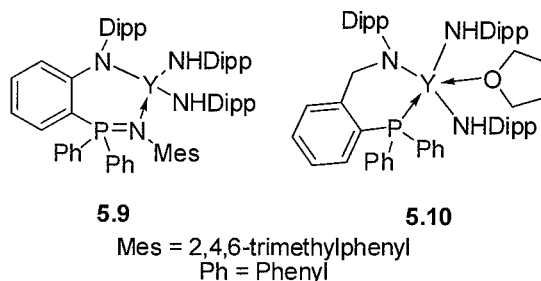
Figure 5.5. Anilido phosphinimine (**5.9**) and amino phosphine (**5.10**) supported yttrium bis(anilido) complexes.[15]

While anilido complexes of yttrium are known, there has been no success thus far in using them as precursors in the formation of imido complexes. For complex **5.9**, this may be due to the Y-N bond not being reactive enough to promote α-H abstraction. With this in mind, aryl yttrium complexes can be used as anilido precursors to exchange the Y-N bond for

a more reactive Y-C bond. A useful starting material for yttrium aryl compounds is complex 5.11.[17,18] This complex has been used extensively by Hultzsch and coworkers to synthesize new yttrium complexes.[18-20]

5.2.2 Results and Discussion

A mono(amidate)bis(aryl) yttrium complex was synthesized in 52% yield as shown in Figure 5.6. Yttrium aryl complex 5.11 was dissolved in tetrahydrofuran (THF) and stirred at room temperature. Proligand 5.12 was dissolved in THF and added dropwise slowly to the solution of 5.11. The crude product was redissolved in toluene, heated at 65 °C and then isolated by removal of the solvent in *vacuo*, and recrystallization from warm pentanes.
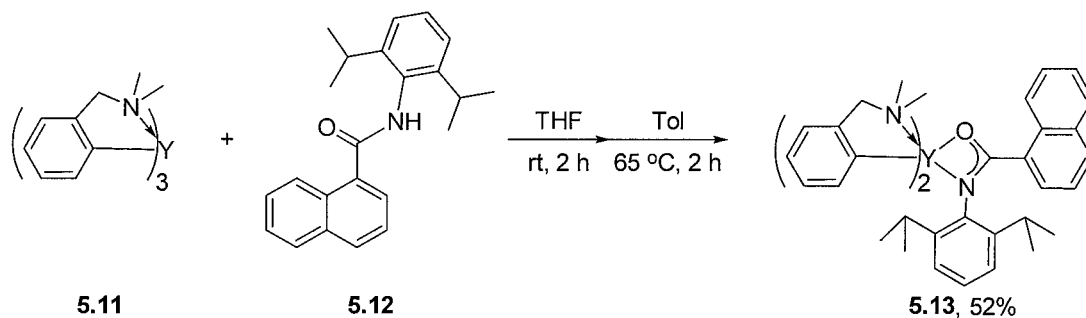
Figure 5.6. Synthesis of aryl/amidate yttrium complex 5.13.

Complex 5.13 is soluble in common hydrocarbon solvents but is resistant to X-ray quality crystal formation. Compound 5.13 is moisture sensitive, and is thermally sensitive and decomposes above 65 °C when in solution. This is evidenced by a colour change in solution from a colourless to a dark brown, as well as degradation of proton signals in the ^{1}H NMR spectrum.

The room temperature ^{1}H NMR spectrum of complex **5.13** is very similar to the analogous mono(amidate)bis(amido) complex introduced in Chapter 2. The diagnostic signal associated with the *ortho*-naphthyl proton is situated at δ 8.93 ppm. The proton signals for the isopropyl substituents are all broadened and no coupling is evident. Unfortunately, due to the thermal sensitivity of this compound high temperature NMR spectra could not be obtained. The proton signals associated with the aryl substituent are very diagnostic at δ 3.69 and 2.40 ppm for the CH_2N(CH$_3$) and CH$_2$N(CH_3), respectively, of the pendant amine donor. Notably, there is no THF donor molecule, unlike the analogous mono(amidate)bis(amido) complexes. This is most likely due to the pendant amine donor of the aryl substituent resulting in a potentially 6-coordinate yttrium complex. The integrations of the proton signals for the aryl ligands and the amidate ligand are in a 2:1 ratio, matching the proposed structure.

A mass spectrum of complex **5.13** was attempted, but due to the decomposition of the compound a spectrum was not obtained. Elemental analysis is consistent with the structure proposed for complex **5.13**.

With complex **5.13** in hand, preparation of an anilido complex was attempted. One equivalent of 2,6-diisopropylaniline (**5.15**) was diluted in toluene and added dropwise to a stirring solution of **5.13** dissolved in toluene. The reaction mixture turned a bright yellow colour after the full addition of **5.15**. The crude product was isolated by concentrating the sample in vacuo to obtain a red oil. The crude ^{1}H NMR spectrum of the product was very complicated, and did not change when heated at 65 °C overnight. The product was washed with pentanes to hopefully remove the expected amine by-product (N,N-dimethyl-1-phenylmethanamine). An orange sticky solid was obtained after drying by vacuum, which

was resistant to recrystallization from various organic solvents (toluene, diethylether). The ^{1}H NMR spectrum of the orange solid matched that of the crude product. To date, it is unclear whether an anilido complex was formed, and isolation of clean product has not been possible. Furthermore, the synthesis of the mixed aryl/amidate yttrium complex **5.13** is low yielding, and this aryl product is more difficult to work with in comparison to the previously discussed mono(amidate)bis(amido) yttrium complexes. Thus further attempts focused on using mono(amidate)bis(amido) complex **5.14** (same as complex **2.27** from Chapter 2) as a suitable starting material.

Mixed amidate/anilido complexes of yttrium were synthesized from 2,6-diisopropylaniline (**5.15**) and mono(amidate) yttrium complex **5.14** (Figure 5.7). Mono(amidate) complex **5.14** was chosen for these studies due to the ease of synthesis and existing structural data for comparison with proposed compounds here.

The synthesis of yttrium anilido complex **5.16** is easily achieved by stirring a solution of mono(amidate) complex **5.14** dissolved in 3 mL of tetrahydrofuran (THF), and adding one equivalent of aniline **5.15** dropwise. The reaction mixture turns pale yellow upon addition. The reaction is concentrated *in vacuo*, and recrystallized from a minimum amount of pentane or hexanes at -30 °C to give a yellow crystalline compound in 85% yield. Compound **5.16** is moisture sensitive, but can be stored in an inert atmosphere glovebox for greater than 4 months at -30 °C. Furthermore, compound **5.16** is thermally sensitive and will decompose above 65 °C when in solution. This is evidenced by a colour change in solution from a bright yellow to a dark brown, as well as degradation of proton signals in the ^{1}H NMR spectrum.
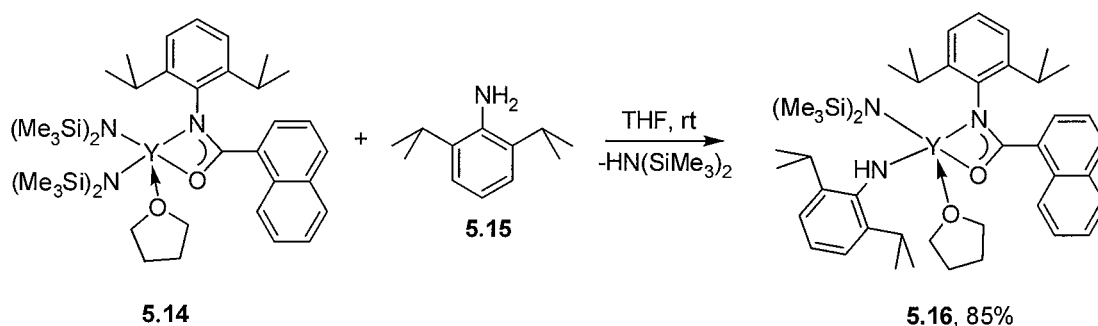
Figure 5.7. Synthesis of mixed amidate/anilido complex **5.16**.

The ^{1}H NMR spectrum of complex **5.16** is shown in Figure 5.8. The spectrum is similar to the parent mono(amidate) complex **5.14**, but with an new proton signal at δ 5.28 ppm for the N-H proton of the anilido ligand. Interestingly, this proton signal is a doublet, with a small coupling constant of 1.9 Hz, due to the ^{89}Y coupling. There is no previously reported anilido N-H signal for the ^{1}H NMR spectrum for the anilido phosphinimine yttrium complex (**5.9**); however, there is a reported broad singlet for the N-H anilido signal in the amino phosphine yttrium complex (**5.10**) at δ 4.72 (400 MHz).[15] An Y-H agostic interaction in a yttrium complex containing the –N(SiH(CH$_3$)$_2$ moeity, was found to have a J_{YH} of 5 Hz.[19] Also, the Y-N bond was found to have restricted rotation due to this agostic interaction.[19] Since the ^{89}Y coupling in complex **5.16** is comparatively small, it is postulated that no Y-H agostic interaction occurs.

In compound **5.16** there are also new proton signals associated with the isopropyl groups from the anilido ligand at δ 3.25 (CH(CH$_3$)$_2$) and 1.37 ppm (CH(CH_3)$_2$). Since there is only one methine proton signal, this indicates free rotation about the N-aryl bond. The diagnostic *ortho*-naphthyl proton signal shifts slightly from δ 9.16 ppm in the parent mono(amidate) complex **5.14**, to δ 9.13 ppm in complex **5.16**. Also, it is evident that there is a molecule of THF bound (δ 3.99 and 1.13 ppm) to yttrium. The THF signals are very broad, consistent

160

with it being a labile donor. The presence of one molecule of THF is also evident in the combustion analysis.
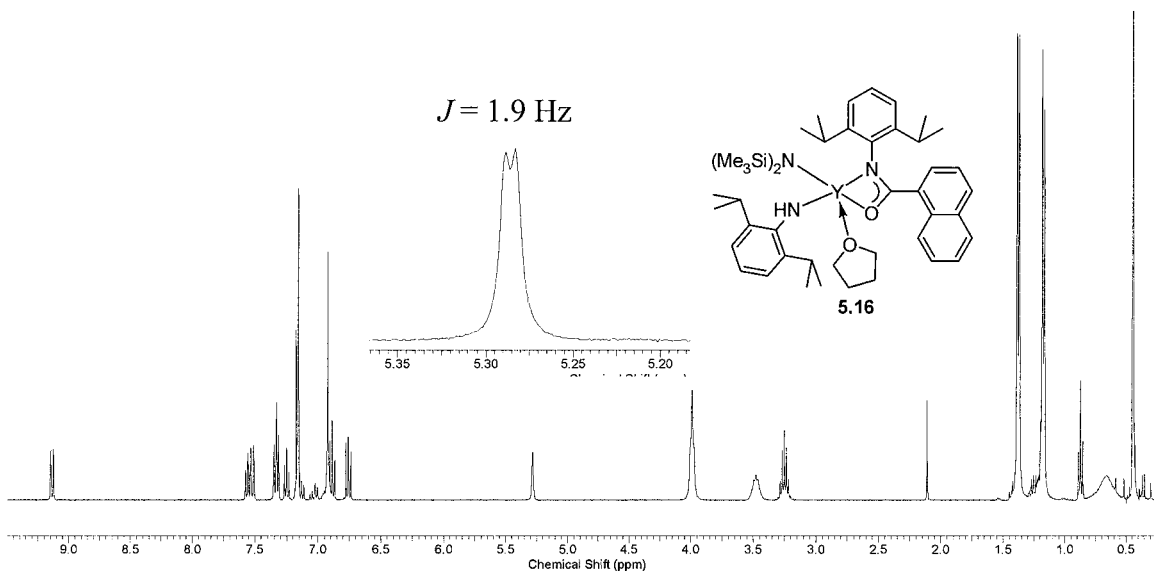
Figure 5.8. ^{1}H NMR spectrum (600 MHz, C_6D_6, 25 °C) of complex **5.16**.[a]
[a] Small amounts of toluene (singlet at δ 2.11 ppm) and pentane (triplet at δ 0.87 ppm, multiplet at δ 1.23 ppm) are evident in sample.

The IR spectrum of complex **5.16** clearly shows an N-H stretch band at 3295 cm^{-1} for the anilido ligand. The C-O and the C-N stretching frequency do not change compared to the parent mono(amidate) complex **5.14**. The mass spectrum of complex **5.16** gives a parent ion for the THF-free complex.

X-ray quality crystals of complex **5.16** can be grown at -30 °C from a minimum amount of pentanes and the solid-state molecular structure is shown in Figure 5.9; metrical parameters are in Table 5.1. The C_l symmetric structure displays a pseudo square-based pyramidal structure, with the -N(SiMe)$_3$)$_2$ as the axial group. Compared to the mono(amidate) complex **5.14**, the amidate Y-O bond length in complex **5.16** is longer (2.2841(16) Å versus 2.215(2) Å) but Y-N bond length is shorter (2.3767(19) Å versus

2.519(3) Å). This indicates that the steric congestion has decreased around the yttrium centre, allowing a shorter Y-N(amidate) bond. The amidate metallacycle angles equal 360.0°, indicating the amidate backbone is in the same plane as the yttrium centre. The Y-O(THF) is also shorter in complex **5.16** than complex **5.14**. The Y-N(anilido) bond length is 2.205(2) Å, with a Y-N-C bond angle of 145.26(19)°. The similar yttrium complex **5.9**, supported by an anilido phosphinimine ligand has similar Y-N(anilido) bond lengths (2.194(5) and 2.242(4) Å) and slightly more linear Y-N-C bond angles (139.5(4) and 139.1(4)°),[15] likely due to the different steric environment around the yttrium centre.
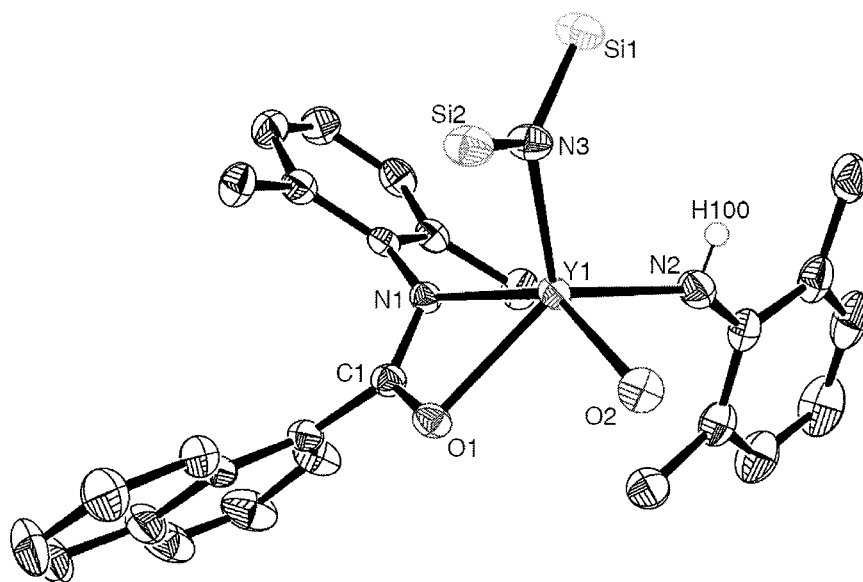
Figure 5.9. ORTEP diagram of the solid-state molecular structure of **5.16** with the probability ellipsoids drawn at the 50% level. Carbons of the THF, and methyl carbons of the isopropyl and trimethylsilyl groups omitted for clarity.[20]

162

Table 5.1. Selected bond length and bond angles for the solid-state molecular structure of **5.16.**

	Bond Length (Å)		Bond Angle(°)
Y1-O1	2.2841(16)	Y1-O1-C1	95.41(13)
Y1-N1	2.3767(19)	O1-C1-N1	117.1(2)
O1-C1	1.291(3)	C1-N1-Y1	90.80(14)
N1-C1	1.306(3)	N1-Y1-O1	56.70(6)
Y1-O2	2.3262(18)	Y1-N2-C24	145.26(19)
Y1-N2	2.205(2)	Y1-N3-Si1	116.84(10)
N2-C24	1.386(3)	Y1-N3-Si2	117.84(10)
Y1-N3	2.225(2)	N3-Y1-O2	96.20(7)
N3-Si1	1.710(2)	N2-Y1-N3	112.02(8)
N3-Si2	1.708(2)	O2-Y1-N2	90.88(7)

Interestingly, if two equivalents of diisopropylaniline are reacted with mono(amidate) complex **5.14**, an isolable crystalline compound cannot be obtained. The resultant yellow oil is also thermally sensitive, as is complex **5.16**. The ^{1}H NMR spectrum of the yellow oil does not show any clear diagnostic signals compared to complex **5.16**. This is possibly due to dimer or oligomeric species forming in solution and suggests that the steric bulk provided by the $-N(SiMe_3)_2$ moiety is necessary to form stable monomeric species.

In previous work in the group, amidate supported group 4 imido complexes can be formed from anilido precursors simply by adding a bulky donor.[4] In the next section, attempts to add sterically demanding neutral donors to complex **5.16** to induce α-H abstraction are discussed.

5.3   Attempted α-H Abstraction Routes to Imido Complexes

In the Schafer lab, successful isolation of crystalline imido complexes of group 4 generally requires the presence of a neutral donor, such as triphenylphosphine oxide (TPPO)[4] or pyridine.[21] It is already known that pyridine can displace the THF from yttrium in tris(amidate) complexes (Chapter 2); however, pyridine is sterically small. It is known that group 3 complexes have a high affinity to bind the bulkier 2,2'-bipyridine (**5.17**, bipy).[32-34] Therefore, one equivalent of bipy dissolved in hexanes was added to a hexanes solution of anilido complex **5.16** (Figure 5.10). Immediately, the solution becomes a deep purple and a red-orange precipitate forms (supernatant remains deep purple in colour), which can be isolated by filtration through a fritted funnel and rinsed with hexanes. This solid product can be recrystallized from a minimum amount of toluene and cooled to -30 °C to give complex **5.18** in 76% yield. This red-orange solid is moisture sensitive, and is soluble in toluene or benzene, but not hexanes or pentane. When dissolved in toluene or benzene, a dark purple solution is noted. The compound is also thermally sensitive, and will form a brown-black solid if heated.
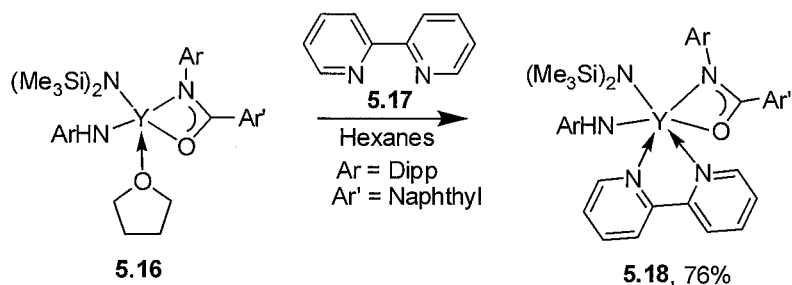
Figure 5.10. Synthesis of bipy complex **5.18**.

The ^{1}H NMR spectrum of complex **5.18** indicates that the bipy molecule displaces the THF of **5.16**, as evidenced by the disappearance of THF proton signals. Also, the chemical shift of bipy proton signals change, for example, there is a doublet signal in free bipy at δ 8.74 that shifts to δ 9.45 upon formation of complex **5.18**. There is still the presence of an N-*H* proton signal at δ 4.83 ($J_{YH} = 1.2$ Hz), which has shifted upfield compared to the parent complex **5.16** (δ 5.28 ppm). Another difference in the ^{1}H NMR spectrum between complex **5.16** and **5.18** is the *ortho*-naphthyl aryl signal, which has shifted from δ 9.13 ppm to δ 9.32 ppm.

The IR spectrum of complex **5.18** also changes from complex **5.16**. There is still the presence of an N-H stretching band, but it has shifted from 3295 cm^{-1} to 3449 cm^{-1}. Furthermore, the C=O stretching frequency of the amidate has shifted from 1589 cm^{-1} to 1600 cm^{-1}. The mass spectrum of complex **5.18** indicates a molecular ion of the complex without bipy; however, there was difficulty in obtaining the mass spectrum due to the thermal stability of the solid.

X-ray quality crystals of complex **5.18** were grown at -30 °C from a minimum amount of toluene and the solid-state molecular structure is given in Figure 5.11. The C_1 symmetric structure displays a pseudo-octahedral structure with -N(SiMe$_3$)$_2$ and the N-Dipp from the amidate backbone as axial ligands and the bipy, NHDipp, and O-amidate making up the equatorial plane. Compared to complex **5.16**, the amidate Y-O and Y-N bond lengths in complex **5.18** are both slightly longer (Y-O = 2.2841(16) Å versus 2.310(3) Å, Y-N = 2.3767(19) Å versus 2.484(4) Å) (Table 5.2). This indicates that the steric congestion has increased around the yttrium centre, resulting in the slight displacement of the amidate ligand. The amidate metallacycle angles equal 359.9°, indicating the amidate backbone

remains in the same plane as the yttrium centre. The Y-N(anilido) bond length is longer (2.275(4) Å) than in complex **5.16** (2.205(2) Å) and the Y-N-C bond angle has increased from 145.26(19)° in complex **5.16** to 154.3(4)° in complex **5.18**. This is most likely due to the greater steric congestion around the yttrium centre, when switching from a THF molecule to the bipy ligand. The bond lengths in the bipy ligand are all very similar (~ 1.37 Å) confirming no loss of aromaticity when bound to yttrium.
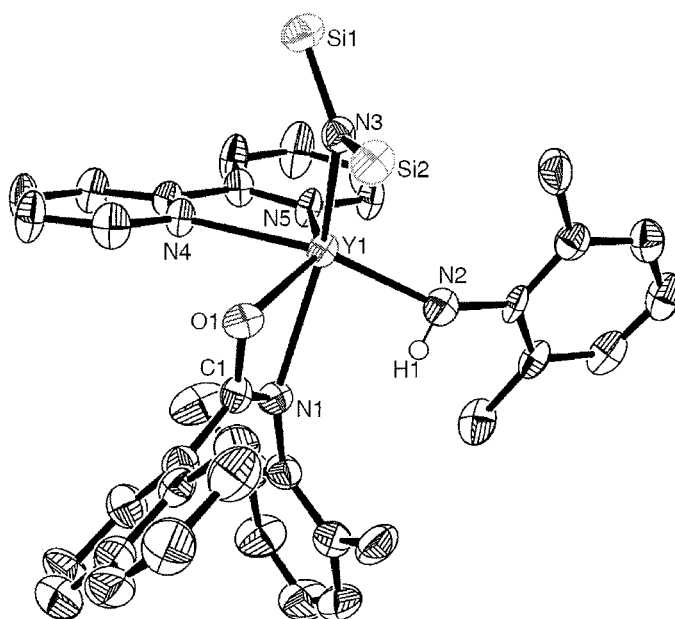
Figure 5.11. ORTEP diagram of the solid-state molecular structure of **5.18** with the probability ellipsoids drawn at the 50% level. Methyl carbons of the isopropyl and trimethylsilyl groups omitted for clarity.[22]

Table 5.2. Selected bond length and bond angles for the solid-state molecular structure of **5.18**.

	Bond Length (Å)		Bond Angle(°)
Y1-O1	2.310(3)	Y1-O1-C1	99.2(2)
Y1-N1	2.484(4)	O1-C1-N1	115.5(4)
O1-C1	1.294(5)	C1-N1-Y1	90.6(3)
N1-C1	1.312(5)	N1-Y1-O1	54.61(11)
Y1-N2	2.275(4)	Y1-N2-C24	154.3(4)
Y1-N3	2.263(3)	Y1-N3-Si1	125.31(17)
Y1-N4	2.482(3)	Y1-N3-Si2	111.98(17)
Y1-N5	2.496(3)		
N3-Si1	1.715(4)		
N3-Si2	1.712(3)		

Interestingly, the bis(anilido) yttrium complex **5.19** can be made directly from mono(amidate) complex **5.14** (Figure 5.12). As mentioned previously, the intermediate (presumably a bis(anilido) yttrium oligomer or dimer) could not be isolated as a solid. However, if one equivalent of bipy is added to the proposed bis(anilido) yellow oil redissolved in hexanes, complex **5.19** is obtained in 83% yield. As in the case of synthesizing complex **5.18**, the reaction mixture turns a dark red colour upon addition of bipy, and simultaneously complex **5.19** precipitates out of solution as a red solid. The solid can be isolated by filtration through a fritted filter, and rinsed with hexanes or pentane. Complex **5.19** can be recrystallized at -30 °C from a minimum amount of toluene; however, an X-ray crystallographic structural determination has not been successful. This compound has similar solubility properties as complex **5.18**; it is soluble in toluene or benzene, but not hexanes or pentane. It is also thermally sensitive, and will decompose above 100 °C to give a brown/black solid. It is for this reason that an EIMS analysis was unattainable. Interestingly, if complex **5.18** is synthesized in the same manner (by not isolating complex

167

5.16 first) clean formation does not occur, as evidenced by the ^{1}H NMR spectrum that indicates there is free bipy (doublet at δ 8.76 ppm).
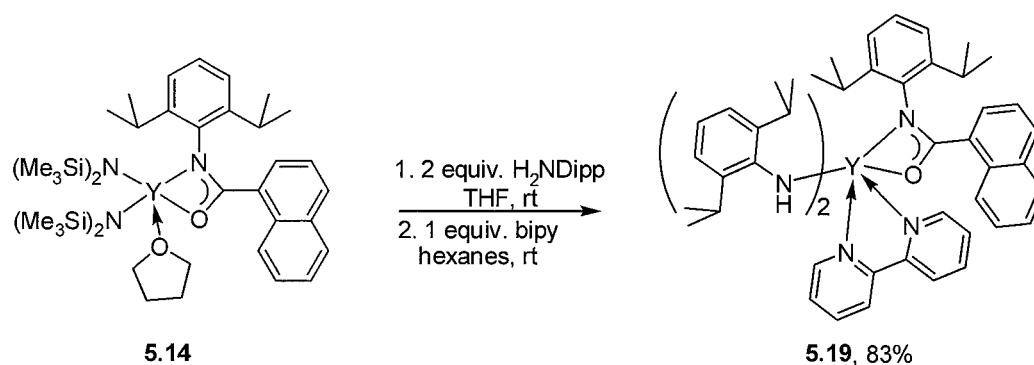
Figure 5.12. Synthesis of bis(anilido) yttrium complex **5.19**.

The ^{1}H NMR spectrum of complex **5.19** is very indicative of two bound anilido ligands (Figure 5.13). The diagnostic N-H signal at δ 5.42 ppm integrates to 2 protons, and has a J_{YH} of 1.4 Hz. This chemical shift is more downfield than compared to the mono(anilido) complex **5.18** (N-H signal at δ 4.83 ppm). Furthermore, the methine signal at δ 3.15 ppm for the isopropyl substituents on the anilido ligands integrates to 4 protons. An interesting feature of this ^{1}H NMR spectrum is the drastic shift in the *ortho*-naphthyl proton signal. In complex **5.18** this signal is at δ 9.32 ppm, and for all other amidate complexes this signal is between δ 9.10 and 9.30 ppm. However, for complex **5.19** the *ortho*-naphthyl proton signal has shifted upfield to δ 7.53 ppm, indicating a different chemical environment. There still is a proton signal associated with the bipy ligand at δ 9.15 ppm, which is shifted upfield compared to complex **5.18** (δ 9.45 ppm). The IR spectrum of complex **5.19** is very similar to that of complex **5.18**, and also has a broad N-H stretch band at 3449 cm^{-1}.
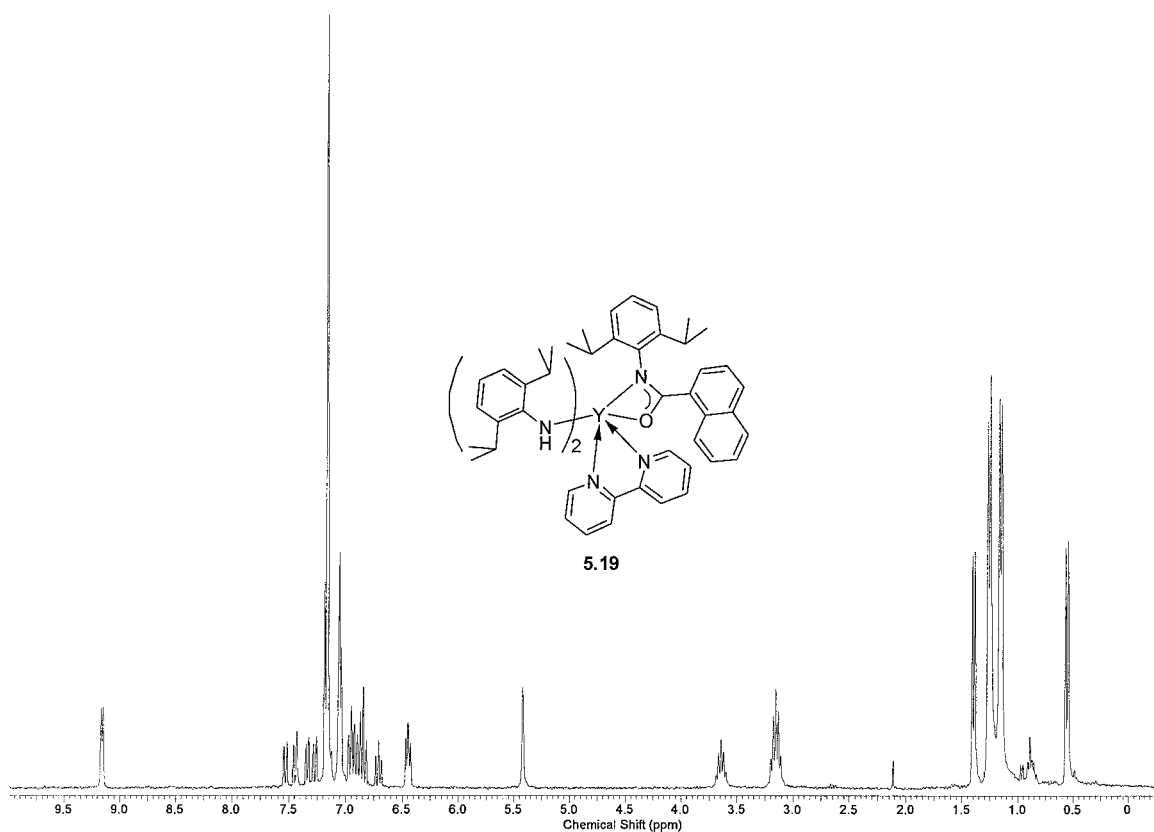
Figure 5.13. ^{1}H NMR spectrum (600 MHz, C_6D_6, 25 °C) of complex **5.19**.

Both complexes **5.18** and **5.19** are intensely coloured in the solid-state as well as in solution. Complexes **5.18** dissolved in toluene gives an intense purple (λ_{max} = 544 nm), whereas complex **5.19** dissolved in toluene results in red solution (λ_{max} = 514 nm). The calculated molar absorptivity values at the maximum wavelengths are ε_{544} = 292 dm^{3}mol$^-$ ^{1}cm^{-1} for **5.18** and ε_{514} = 262 dm^{3}mol^{-1}cm^{-1} for **5.19**. Presumably these highly coloured solutions are from charge-transfer bands associated with a ligand to metal charge-transfer (LMCT) or a ligand to ligand charge-transfer (LLCT). The yttrium centre is formally d^0, so a metal-ligand charge transfer (MLCT) band is not probable.

169

Bipy was found to have great donor ability to mixed amidate/anilido yttrium complexes. The initial hope was that binding bipy would induce a α-H abstraction from the anilido ligands to form a yttrium imido. So far, this strategy has been unsuccessful. Regardless, these are novel compounds that show interesting characteristics, such as intense colour. Successful ventures into group 3 or lanthanide imido formation have typically used deprotonation of an anilido N-H with a strong base. Complexes **5.18** and **5.19** can be formed in high yield and with high purity, and are ideal precursors for deprotonation attempts to form a yttrium imido complex.

5.4   Attempted Deprotonation Routes

Literature precedence for group 3 or lanthanide imido formation (where the imido is bridging or capping) have been formed by deprotonation of an anilido complex.[11,14] It has been shown that mixed amidate/anilido complexes of group 3 can be formed easily. These yttrium complexes can be coordinated readily by one molecule of bipy, which will create some steric protection around the yttrium centre as opposed to one molecule of THF (such as in complex **5.16**). Since the bipy yttrium complex **5.19** can be formed in high-yield in a one-pot synthesis, it was chosen for deprotonation studies.

Three bases were chosen to initially test the deprotonation of complex **5.19**, *n*-butyllithium (*n*-BuLi), sodium bis(trimethylsilyl)amide (Na(N(SiMe_3)_2), and potassium xylide (KXy). All these bases, once reacted, will form volatile products that can be removed *in vacuo*. Also, using a range of metal counterions (Li, Na, and K), will give an indication of the best counterion size for forming proposed deprotonated yttrium species. Unfortunately,

formation of single crystals is necessary in fully determining whether an imido is formed, and this can be counterion dependant.

The deprotonation studies have been carried out in the same manner for all bases, so a direct comparison can be obtained. Complex **5.19** can be dissolved in 5 mL toluene and stirred at room temperature. An equimolar amount of base is dissolved in 2 mL of toluene, was added dropwise to the stirring solution of complex **5.19** at room temperature. These reactions are performed with approximately 60 mg of complex **5.19**. In all cases, the reaction mixture changes colour from red to dark brown. The solvent is removed *in vacuo* to give a crude brown oil when using *n*-BuLi and Na(N((SiMe)$_3$)$_2$), but a brown solid when using KXy as the base. The ^{1}H NMR spectrum of the crude compound in all cases shows multiple N-H signals from δ 4.50 to 5.50 ppm and evidence of 2,6-diisopropylaniline formation (septet at δ 2.67 ppm, and doublet at δ 1.15 ppm). All the ^{1}H NMR spectra were complicated and contained multiple signals in the aryl and alkyl region that were not identifiable. Recrystallization of the products was only successful in forming amorphous solids. Since a solid was initially obtained from the reaction of complex **5.19** and KXy (instead of an oil) this reaction was further studied.

18-Crown-6 is known to coordinate potassium molecules, and also aid in crystallization of compounds.[31-33] With this in mind, KXy was reacted with 18-crown-6, and then subsequently added to a solution of complex **5.19**. After removing the solvent *in vacuo*, a dark brown solid was obtained. The ^{1}H NMR spectrum of this compound was similar to analogous reaction without the crown ether. The crown ether is thought to be coordinated since the proton signal for 18-crown-6 has shifted from δ 3.52 ppm (for free 18-crown-6) to δ 2.90 ppm. Again, diisopropylaniline was evident in the sample (septet at δ 2.67 ppm, and

doublet at δ 1.15 ppm) and there were multiple N-H signals between δ 5.00 ppm and 5.50 ppm. Presumably, the diisopropylaniline is formed by α-H abstraction of the anilido ligand of complex **5.19**. The multiple N-H signals could arise from a mix of different compounds (oligomers or dimers) that have bridging or capping imido ligands, and bridging anilido ligands. The deprotonation is most likely not going to completion. Heating the solution of the product to above 65 °C to force deprotonation causes solid to precipitate and the ^{1}H NMR spectrum becomes very complicated. Most likely, the compound obtained is a dimer or oligomer with bridging imido and/or amido compounds. Unfortunately, only amorphous solid has been obtained after recrystallization attempts. Scaling up the reaction (above 60 mg of **5.19**) also proved difficult, and only resulted in dark brown oils, with very complicated ^{1}H NMR spectra. Also, other characterization techniques, such as IR spectroscopy, mass spectrometry have been inconclusive. The IR spectroscopy still indicates an N-H stretch band at 3449 cm^{-1}, and the mass spectrometry analysis was unable to be performed due to decomposition of the sample on the instrument probe.

To test if there is an imido present, an insertion reaction with 2,6-dimethylphenyl isocyanate (**5.20**) was attempted. The insertion reaction with **5.20** would produce yttrium oxide species **5.21** (which are very insoluble) and carbodiimide **5.22** (Figure 5.14). Ideally, the yttrium oxide species would precipitate out of solution and the carbodiimide would be confirmed in the ^{13}C NMR spectrum by the diagnostic N=C=N signal. Since only small amounts of the proposed imido complex can be obtained at a time, this insertion reaction consequently was performed on small (NMR) scale. Upon addition of **5.20** to the proposed imido complex, the reaction mixture turned a darker brown colour and subsequently a solid precipitated out of solution. Unfortunately, due to the small scale of the reaction, the

experimental results were inconclusive. However, a precipitate did form, possibly indicating that yttrium oxide species are indeed forming.
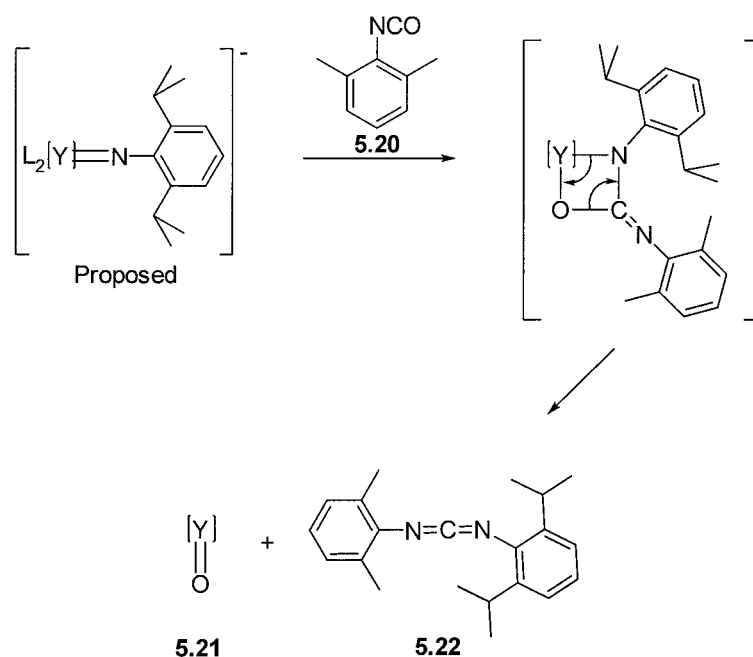
Figure 5.14. Insertion reaction into proposed imido complex.

Although a solid-state molecular structure of an yttrium imido species was not obtained, possibly α-H abstraction by a strong base may result in an imido-containing yttrium species. The complex formed is most likely not fully deprotonated (to form a monomeric terminal imido), but possibly an oligomer where there are bridging or capping imido groups mixed with bridging or terminal anilido ligands (as indicated by N-*H* proton signal and stretch band present in the ^{1}H NMR and IR spectrum) is formed. With the right chemical environment, and the correct choice of base, ideally a crystalline yttrium amidate/imido species can be formed.

5.5   Conclusions

Simple reactions with mono(amidate) yttrium complex **5.14** proved to be a route into yttrium imido precursors. The mono(anilido) complex **5.16** could be isolated in high-yield by addition of one equivalent of diisopropylaniline to complex **5.14**. Increasing the amount of diisopropylaniline to two equivalents resulted in a non-isolable species, presumably a bis(anilido) yttrium dimer or oligomer. Bipy was found to be an excellent donor for yttrium, but does not induce α-H abstraction of an anilido ligand to form an yttrium imido complex under these particular experimental conditions. Bipy mono(anilido) yttrium complex **5.18** can be formed in high yield from the reaction of mono(anilido) complex **5.16**, but can not be formed in one-pot from mono(amidate) complex **5.14**. In contrast, bis(anilido) bipy yttrium complex **5.19** can be formed in high yield in one-pot from mono(amidate) **5.14**. Both complexes are highly coloured, and thermally sensitive.

Deprotonation of complex **5.19** with a strong base to form an yttrium imido complex proved to be very difficult. This is not surprising since the target yttrium imido complex is a long-standing goal in group 3 chemistry. Reaction of complex **5.19** with the base KXy gave a solid as opposed to a dark oil (as is the case when using n-BuLi or Na(N(SiMe$_3$)$_2$)), which seems promising as suggested by spectroscopic studies and preliminary insertion reactions.

A crystalline yttrium imido complex, whether formed by α-H abstraction or by deprotonation methods, would be a remarkable discovery. Many more conditions, bipy derivatives, supporting ligands and deprotonating bases can be tested in the synthesis of the elusive yttrium imido complex. The efforts described in this Chapter are promising, but are just a starting point for further research in the Schafer group and the broader chemistry community.

5.6 Experimental

5.6.1 Starting Materials and Reagents

All operations were performed under an inert atmosphere of nitrogen using standard Schlenk-line or glovebox techniques. THF, toluene, pentane, and hexanes were all purified by passage through an alumina column and sparged with nitrogen. $Y[N(SiMe_3)_2]_3$ was synthesized as described in literature,[23] or purchased from Aldrich and recrystallized from hexanes before use. 2,6-Diisopropylaniline was purchased from Aldrich and distilled from CaH_2 before use. 18-crown-6 was purchased from Aldrich and sublimed under vacuum at 140 °C before use. All other chemicals were commercially available and used as received unless otherwise stated. ^1H and ^{13}C NMR spectra were recorded on Bruker AV300, AV400 and AV600 spectrometers. Shifts are reported in parts per million (ppm) relative to tetramethylsilane (TMS) and calibrated against residual solvent signal, coupling constants J are given in Hertz (Hz) (all couplings are ^3J unless otherwise stated). Infrared spectra were measured on a Nicolet 4700 spectrometer using KBr pellets and IR bands ν are reported in cm^{-1}. Elemental analyses and mass spectra were performed by the microanalytical laboratory of the Department of Chemistry at the University of British Columbia. Some elemental analyses gave low carbon content for yttrium complexes, possibly due to carbide formation.[24] X-ray crystallography was conducted at the University of British Columbia by Dr. Brian Patrick, Dr. Rob Thomson, or Neal Yonson.

5.6.2 Synthesis

Synthesis of mono(*N*-2',6'-diisopropylphenyl(naphthyl)amidate)bis(2-methyldimethylaminophenyl) yttrium (5.13)

Inside a glovebox, a 20 mL glass vial was charged with yttrium aryl complex **5.11** (0.297 g, 0.604 mmol), 5 mL of tetrahydrofuran and a stirbar. The reaction mixture was stirred until all solid was dissolved and *N*-2',6'-diisopropylphenyl(naphthyl) amide **5.12** (0.202 g, 0.605 mmol) was dissolved in 5 mL of tetrahydrofuran was added very slowly to the stirring reaction mixture at room temperature. The solution was stirred within the glovebox for 2 hours filtered through a pipette plug of Celite™ and then concentrated under reduced pressure to a pale yellow solid. The product was washed with 3 x 5 mL of pentanes to remove residual amine. The solid was redissolved in 5 mL toluene, heated to 65 °C for 2 hours and then concentrated in vacuo. The white solid was recrystallized by dissolving in minimum amount of warm pentane, with a few drops of toluene and then cooled to -30 °C to give a white solid. Yield: 0.216 g, 52%. ^{1}H NMR (600 MHz, C$_6$D$_6$) δ 8.93 (d, *J* = 12 Hz, 1H, *ortho*-naphthyl-*H*), 8.14 (d, *J* = 6 Hz, 2H, aryl-*H*), 7.51 (d, *J* = 12 Hz, 1H, aryl-*H*), 7.46 (t, *J* = 6 Hz, 1H, aryl-*H*), 7.37 (m, 3H, aryl-*H*), 7.28 (t, *J* = 6 Hz, 2H, aryl-*H*), 7.23 (t, *J* = 6 Hz, 1H, aryl-*H*), 7.03 (t, *J* = 6 Hz, 3H, aryl-*H*), 6.94 (s , 3H, aryl-*H*), 6.69 (t, *J* = 6 Hz, 1H, aryl-*H*), 3.69 (broad s, 4H, -C*H*$_2$N(CH$_3$)$_2$), 3.25 (broad s, 2H, C*H*(CH$_3$)$_2$), 2.40 (s, 12H, -CH$_2$N(C*H*$_3$)$_2$), 1.05 (broad s, 6H, CH(C*H*$_3$)$_2$), 0.45 (broad s, 6H, CH(C*H*$_3$)$_2$). ^{13}C NMR (150.9 MHz, C$_6$D$_6$) δ 184.0 (*C*=O), 183.7, 179.8, 146.5, 141.0, 140.8, 137.1, 133.9, 131.6, 131.3, 129.6, 127.9, 126.5, 126.3, 125.6, 125.5, 125.3, 124.5, 124.4, 124.3, 123.3, 123.2 (aryl-*C*'s), 68.5 (-*C*H$_2$N(CH$_3$)$_2$), 44.5 (-CH$_2$N(*C*H$_3$)$_2$), 28.0 (*C*H(CH$_3$)$_2$),
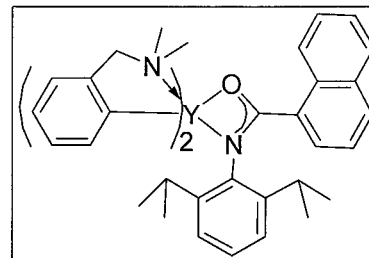
23.8 (CH(CH_3)$_2$), 22.7 (CH(CH_3)$_2$). Anal. found (calcd for $C_{39}H_{44}N_3OY$): C 71.40%

(71.01%), N 6.00% (6.37%), H 6.81% (6.72%).

Synthesis of mono(N-2′,6′-diisopropylphenyl(naphthyl)amidate)mono(trimethylsilyl

amido)mono(2,6-diisopropylanilido)mono(tetrahydrofuran)yttrium (5.16)

Inside a glovebox, a 20 mL glass vial was charged with

mono(amidate) complex **5.14** (0.203 g, 0.249 mmol), 5 mL

of tetrahydrofuran and a stirbar. The reaction mixture was
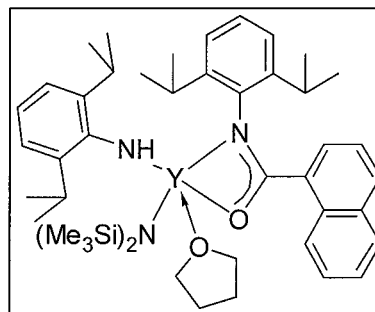
stirred until all solid was dissolved and 2,6-

diisopropylaniline (44.1 mg, 0.248 mmol) diluted in 2 mL of

tetrahydrofuran was added very slowly to the stirring reaction mixture at room temperature.

The solution was stirred within the glovebox for 2 hours and then concentrated under reduced

pressure to a yellow oil. The product was recrystallized by dissolving in minimum amount

of pentane and then cooled to -30 °C to give yellow crystals. Yield: 0.175 g, 85%. Refer to

Figure 5.9, Table 5.1 and Appendix II for crystallographic data. ^{1}H NMR (600 MHz, C_6D_6)

δ 9.13 (d, J = 9 Hz, 1H, aryl-H), 7.55 (m, 2H, aryl-H), 7.33 (t, J = 9 Hz, 2H, aryl-H), 7.25 (t,

J = 9 Hz, 2H, aryl-H), 7.18 (s, 2H, aryl-H), 6.93 (s, 2H, aryl-H), 6.89 (t, J = 6 Hz, 1H, aryl-

H), 6.76 (t, J = 6 Hz, 1H, aryl-H), 5.28 (d, J = 1.9 Hz, 1H, N-H), 3.99 (broad s, 4H, O-CH_2),

3.48 (broad septet, J = 6 Hz, 2H, CH(CH$_3$)$_2$), 3.25 (septet, J = 6 Hz, 2H, CH(CH$_3$)$_2$), 1.37 (d,

J = 6 Hz, 12H, CH(CH_3)$_2$), 1.17 (d, J = 6 Hz, 12H, CH(CH_3)$_2$), 1.13 (broad s, 4H, O-

CH$_2$CH_2), 0.44 (s, 18H, N(Si(CH_3)$_3$)$_2$). ^{13}C NMR (150.9 MHz, C_6D_6) δ 180.8 (C=O), 151.9,

142.1, 141.7, 134.9, 133.6, 132.3, 131.7, 131.0, 129.3, 128.7, 127.2, 127.0, 126.7, 126.3,

125.6, 125.4, 124.5, 123.4, 116.5 (aryl-C's), 71.8 (O-CH$_2$), 30.6 (CH(CH$_3$)$_2$), 28.4

(CH(CH$_3$)$_2$), 25.9 (O-CH$_2$$CH_2$), 25.5 (CH($CH_3$)$_2$), 24.4 (CH($CH_3$)$_2$), 5.9 (N(Si($CH_3$)$_3$)$_2$). IR

(KBr, cm^{-1}): 3295 (s), 3264 (w), 2958 (s), 1589 (w), 1517 (s), 1497 (s), 1422 (w), 1399 (s),

1379 (w), 1255 (s), 984 (s), 838 (s), 763 (w), 744 (w), 670 (w) cm^{-1}. MS (EI): 755 (M$^+$),

579 (M$^+$ - NHDipp). Anal. found (calcd for C$_{39}$H$_{68}$N$_3$O$_2$Si$_2$Y): C 65.60% (65.27%), N

4.78% (5.07%), H 8.41% (8.28%).

Synthesis of mono(*N*-2',6'-diisopropylphenyl(naphthyl)amidate) mono(trimethylsilyl amido) mono(2,6-diisopropylanilido)mono(2,2'-bipyridine)yttrium (5.18)

Inside a glovebox, a 20 mL glass vial was charged with complex **5.16** (0.240 g, 0.290 mmol), 5 mL of hexanes and a stirbar. The reaction mixture was stirred until all solid was dissolved and bipyridine (45.4 mg, 0.290 mmol) diluted in 2 mL of hexanes was added very slowly to the
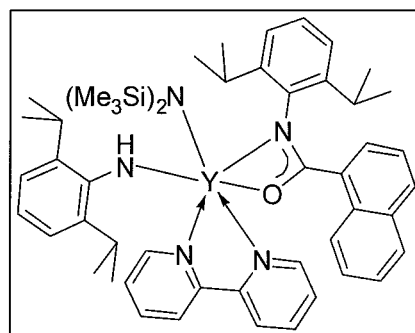

stirring reaction mixture at room temperature. Immediately the reaction mixture turns a dark

purple colour and an orange solid precipitates out of solution. The product was isolated by

filtration through a fritted funnel and rinsed with hexanes. The product was recrystallized by

dissolving in minimum amount of toluene and then cooled to -30 °C to give red-orange

crystals. Yield: 0.199 g, 76%. Refer to Figure 5.11, Table 5.2 and Appendix II for

crystallographic data. ^{1}H NMR (400 MHz, C$_6$D$_6$) δ 9.45 (d, J = 4.4 Hz, 2H, aryl-H (bipy)),

9.32 (d, J = 9 Hz, 1H, *ortho*-naphthyl-H), 7.53 (m, 2H, aryl-H), 7.40 (m, 1H, aryl-H), 7.25

(m, 4H, aryl-H), 7.13-7.01 (m, 8H, aryl-H), 6.94 (m, 4H, aryl-H), 6.89-6.80 (m, 4H, aryl-H),

6.73 (t, J = 8 Hz, 2H, aryl-H), 6.39 (t, J = 8 Hz, 2H, aryl-H), 4.83 (d, J = 1.2 Hz, 1H, N-H),

3.52 (broad s, 1H, CH(CH$_3$)$_2$), 3.33 (septet, J = 6 Hz, 2H, CH(CH$_3$)$_2$), 2.90 (broad s, 1H,

CH(CH$_3$)$_2$), 1.22 (overlapping d and broad s, J = 6 Hz, 18H, amidate CH(CH_3)$_2$) and anilido

CH(CH_3)$_2$), 1.17 (broad s, 6H, CH(CH_3)$_2$), 0.49 (s, 18H, N(Si(CH_3)$_3$)$_2$). ^{13}C NMR (150.9 MHz, C$_6$D$_6$) δ 178.2 (C=O), 153.7, 153.6, 152.6, 143.7, 140.2, 137.0, 135.1, 134.6, 133.2, 132.9, 130.6, 128.9, 127.8, 127.2, 126.5, 126.0, 124.5, 124.1, 124.0, 121.5, 115.2 (aryl-C's), 28.8 (CH(CH$_3$)$_2$), 26.1 (CH(CH$_3$)$_2$), 24.8 (CH(CH$_3$)$_2$), 24.1 (CH(CH$_3$)$_2$), 6.3 (N(Si(CH$_3$)$_3$)$_2$). IR (KBr, cm^{-1}): 3449 (broad, s), 2960 (s), 1600 (w), 1576 (w), 1513 (s), 1461 (s), 1424 (w), 1258 (s), 1013 (w), 975 (w), 811 (s), 779 (w), 666 (w) cm^{-1}. MS (EI): 755 (M$^+$ - bipy). Anal. found (calcd for C$_{51}$H$_{68}$N$_5$OSi$_2$Y): C 66.02% (67.15%), N 7.22% (7.68%), H 7.23% (7.51%).

Synthesis of mono(N-2',6'-diisopropylphenyl(naphthyl)amidate)bis(2,6-diisopropylanilido)mono(2,2'-bipyridine)yttrium (5.19)

Inside a glovebox, a 20 mL glass vial was charged with mono(amidate) complex **5.14** (0.294 g, 0.361 mmol), 5 mL of THF and a stirbar. The reaction mixture was stirred until all solid was dissolved and 2,6-diisopropylaniline (0.1286 g, 0.725 mmol) diluted in 2 mL of tetrahydrofuran was added very slowly to the

stirring reaction mixture at room temperature. The reaction mixture turned a bright pale yellow colour and was stirred for 10 minutes. The solvent was then removed under vacuum, and the product was redissolved in 5 mL of hexanes. 2,2'-bipyridine (56.5 mg, 0.362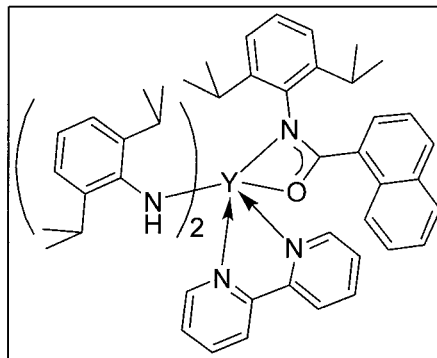 mmol) diluted in 2 mL of hexanes was added very slowly to the stirring reaction mixture at room temperature. Immediately the reaction mixture turns a dark purple colour and an red solid precipitates out of solution. The product was isolated by filtration through a fritted funnel and rinsed with hexanes. The product was recrystallized by dissolving in minimum amount

of toluene and then cooled to -30 °C to give red crystals. Yield: 0.2784 g, 83%. ^{1}H NMR

(300 MHz, C_6D_6) δ 9.15 (d, J = 4.4 Hz, 2H, aryl-H (bipy)), 7.53 (d, J = 9 Hz, 1H, *ortho-*

naphthyl-H), 7.44 (d, J = 9 Hz, 1H, aryl-H), 7.33 (d, J = 9 Hz, 1H, aryl-H), 7.26 (d, J = 9 Hz,

1H, aryl-H), 7.18-7.15 (m, 1H, aryl-H), 7.05 (m, 6H, aryl-H), 6.95 (t of d, ^3J = 9 Hz, ^4J = 1.2

Hz, 4H, aryl-H), 6.87 (t, J = 8 Hz, 4H, aryl-H), 6.71 (t, J = 8 Hz, 1H, aryl-H), 6.45 (t, J = 8

Hz, 2H, aryl-H), 5.42 (d, J = 1.4 Hz, 2H, N-H), 3.64 (septet, J = 6 Hz, 2H, CH(CH$_3$)$_2$), 3.15

(septet, J = 6 Hz, 4H, CH(CH$_3$)$_2$), 1.39 (d, J = 6 Hz, 6H, CH(CH_3)$_2$)), 1.25 (d, J = 6 Hz, 12H,

CH(CH_3)$_2$)), 1.15 (d, J = 6 Hz, 12H, CH(CH_3)$_2$)), 0.55 (d, J = 6 Hz, 6H, CH(CH_3)$_2$)). ^{13}C

NMR (150.9 MHz, C_6D_6) δ 179.7 (C=O), 153.4, 153.3, 152.2, 142.1, 141.8, 139.9, 134.9,

133.5, 133.3, 133.1, 132.6, 132.0, 130.1, 129.1, 127.5, 126.7, 125.9, 125.5, 125.1, 125.0,

124.7, 123.5, 121.5, 115.0 (aryl-C's), 30.4 (CH(CH$_3$)$_2$), 28.7 (CH(CH$_3$)$_2$), 25.8 (CH(CH$_3$)$_2$),

24.4 (CH(CH$_3$)$_2$), 24.3 (CH(CH$_3$)$_2$), 24.1 (CH(CH$_3$)$_2$). IR (KBr, cm^{-1}): 3449 (broad, s), 2960

(s), 1641 (w), 1591 (w), 1513 (s), 1422 (w), 1259 (s), 781 (w), 622 (w) cm^{-1}. Anal. found

(calcd for $C_{57}H_{68}N_5OY$): C 72.30% (73.77%), N 7.55% (7.47%), H 7.50% (7.39%).

5.7 References

(1)   Hazari, N.; Mountford, P. *Acc. Chem. Res.* **2005**, *38*, 839.

(2)   Zuckerman, R. L.; Krska, S. W.; Bergman, R. G. *J. Am. Chem. Soc.* **2000**, *122*, 751.

(3)   Eldred, S. E.; Stone, D. A.; Gellman, S. H.; Stahl, S. S. *J. Am. Chem. Soc.* **2003**, *125*, 3422.

(4)   Thomson, R. K.; Bexrud, J. A.; Schafer, L. L. *Organometallics* **2006**, *25*, 4069.

(5)   Hayton, T. W.; Boncella, J. M.; Scott, B. L.; Palmer, P. D.; Batista, E. R.; Hay, P. J. *Science* **2005**, *310*, 1941.

(6)   Graves, C. R.; Scott, B. L.; Morris, D. E.; Kiplinger, J. L. *J. Am. Chem. Soc.* **2007**, *129*, 11914.

(7)   Shannon, R. D. *Acta Crystallogr., Sect. A: Cryst. Phys., Diffr., Theor. Gen. Cryst.* **1976**, *32*, 751.

(8)   Giesbrecht, G. R.; Gordon, J. C. *Dalton Trans.* **2004**, 2387.

(9)   Masuda, J. D.; Jantunen, K. C.; Scott, B. L.; Kiplinger, J. L. *Organometallics* **2008**, *27*, 803.

(10)   Panda, T. K.; Randoll, S.; Hrib, C. G.; Jones, P. G.; Bannenberg, T.; Tamm, M. *Chem. Commun.* **2007**, 5007.

(11)   Chan, H. S.; Li, H. W.; Xie, Z. W. *Chem. Commun.* **2002**, 652.

(12)   Beetstra, D. J.; Meetsma, A.; Hessen, B.; Teuben, J. H. *Organometallics* **2003**, *22*, 4372.

(13)   Knight, L. K.; Piers, W. E.; McDonald, R. *Organometallics* **2006**, *25*, 3289.

(14)   Gordon, J. C.; Giesbrecht, G. R.; Clark, D. L.; Hay, P. J.; Keogh, D. W.; Poli, R.; Scott, B. L.; Watkin, J. G. *Organometallics* **2002**, *21*, 4726.

(15)   Liu, B.; Cui, D.; Ma, J.; Chen, X. S.; Jing, X. B. *Chem. Eur. J.* **2007**, *13*, 834.

(16)   Evans, W. J.; Ansari, M. A.; Ziller, J. W. *Inorg. Chem.* **1996**, *35*, 5435.

(17)   Booij, M.; Kiers, N. H.; Heeres, H. J.; Teuben, J. H. *J. Organomet. Chem.* **1989**, *364*, 79.

(18)   Gribkov, D. V.; Hultzsch, K. C. *Chem. Commun.* **2004**, 730.

(19)   Eppinger, J.; Spiegler, M.; Hieringer, W.; Herrmann, W. A.; Anwander, R. *J. Am. Chem. Soc.* **2000**, *122*, 3080.

(20)   Data was processed using the SQUEEZE function of the PLATON software to remove disordered pentane. Speck, A. L. *J. Appl. Cryst.* **2003**, **36**, 7.

(21)   Zhang, Z.; Leitch, D. C.; Lu, M.; Patrick, B. O.; Schafer, L. L. *Chem. Eur. J.* **2007**, *13*, 2012.

(22)   Data was processed using the SQUEEZE function of the PLATON software to remove residual THF. Speck, A. L. *J. Appl. Cryst.* **2003**, *36*, 7.

(23)   Bradley, D. C.; Ghotra, J. S.; Hart, F. A. *J. Chem. Soc., Dalton Trans.* **1973**, 1021.

(24)   Vitanova, D. V.; Hampel, F.; Hultzsch, K. C. *Dalton Trans.* **2005**, 1565.

Chapter 6. Conclusions and Future Work

6.1 Summary and Conclusions

The research in this thesis explores the chemistry involved with novel yttrium amidate complexes. These complexes can be synthesized in high yield from amide proligands and yttrium tris(bis(trimethylsilyl)amide). By changing the stoichiometry and reaction conditions, tris, bis and mono(amidate) yttrium complexes can be formed. A library of complexes with varied electronic and steric properties was prepared and their reactivity investigated.

All the yttrium complexes were found to be highly active initiators for the ring-opening polymerization of ε-caprolactone. The tris(amidate) complexes were the more controlled initiators to give poly(ε-caprolactone) in high yield with the narrowest polydispersity values. The amidate backbone did have an effect on initiation properties; complexes with ligands containing electron-withdrawing groups were not as efficient. The mechanism of initiation was studied and is proposed to go through a coordination-insertion mechanism. In addition, a detrimental side-reaction was postulated where ε-caprolactone may react with the yttrium amidate compound to form an enolate complex.

Another reaction explored was the hydroamination of aminoalkenes. The yttrium mono and bis(amidate) complexes were moderate catalysts for this transformation, whereas the tris(amidate) complexes did not catalyze the reaction at all. Electron-withdrawing groups on the amidate backbone had a large effect on reaction time, and complexes that contained an amidate ligand with one or more trifluoromethyl groups had the fastest reaction times.

A mono(amidate) yttrium complex was used in stoichiometric reactions to form anilido complexes. The anilido complexes were further reacted with large bulky donors, and bases in the hopes of forming a terminal yttrium imido complex. To date, attempts at α-H abstraction, and deprotonation have not proved successful in forming an isolable imido complex; however, these investigations are on-going in the hands of another doctoral student.

This thesis discusses an extension of amidate chemistry to group 3, a new area of research for the Schafer group. There is much more to discover using yttrium amidate complexes, and these compounds provide an important benchmark for lanthanide chemistry. Some suggestions that are extensions of this research or new research directions are recommended here.

6.2   Future Work

6.2.1 Yttrium Amidates as Polymerization Initiators for other Oxygen-containing Monomers

The mechanistic proposal in Chapter 3 suggests that to improve initiation for tris(amidate) complex **6.1** (**3.19** in Chapter 3), or any other amidate complex, the side-reaction to give an enolate complex needs to be minimized. The polymerization studies in Chapter 3 have also indicated that the substituents on the amidate backbone did have an effect on initiator ability. Taking advantage of the modularity that can be achieved in the amidate ligand, new complexes can be designed for ROP of ε-caprolactone.

6.1
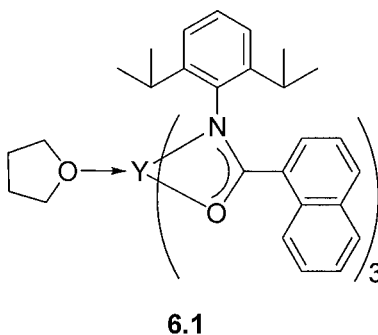
Figure 6.1. Tris(amidate) yttrium complex **6.1**.

It has been shown that adding electron-withdrawing groups to the amidate backbone is detrimental to polymerization. Perhaps, adding more electron-donating groups to the amidate backbone (such as OCH_3) could result in a more controlled polymerization. Another method could be to install more bulk on the amidate backbone, possibly by adding 2,6-di-*tert*-butyl groups on the nitrogen phenyl substituent. Future work will also involve utilizing the monomer lactide (**6.2**, Figure 6.2). Enolate formation may be sterically disfavoured in this case, due to the neighbouring CH_3 group.

6.2
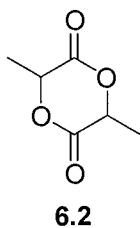
Figure 6.2. Structure of *rac*-lactide (**6.2**).

6.2.2 Intermolecular Hydroamination

In Chapter 4, yttrium bis and mono(amidate) complexes were found to be good precatalysts for hydroamination of aminoalkenes. Furthermore, by changing the electronic properties of the amidate ligand (such as adding a CF_3 group) the activity of the yttrium

precatalyst was enhanced. Although intermolecular hydroamination was not seen using the conditions presented in Chapter 4, it is an on-going research goal. The modular nature of the amide synthesis allows for further ligand design, in the hopes of creating a more reactive yttrium amidate complex. For example, the proposed proligand shown in Figure 6.3 combines steric properties at the nitrogen with an enhanced electron-withdrawing effect. The steric properties are necessary in order to obtain crystalline bis and mono(amidate) complexes, as mentioned in Chapter 2.

6.3
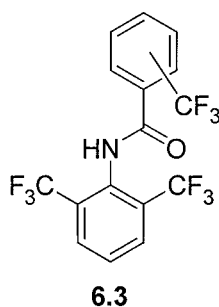
Figure 6.3. Potential new amide proligand.

Potentially, amide **6.3** will result in a highly active yttrium amidate complex that will catalyze intermolecular hydroamination under the conditions presented in Chapter 4. However, other reaction conditions for intermolecular hydroamination should also be attempted with all active yttrium amidate complexes. Examples of intermolecular hydroamination by Marks and coworkers have used n-propylamine with 1-butene and trimethyl(vinyl)silane.[1] Also, substituted styrene molecules have been effective for intermolecular hydroamination.[2] Screening both identity and concentration of reagents is key to discovering a working catalytic system.

R= F, CF$_3$, NMe$_2$, OMe
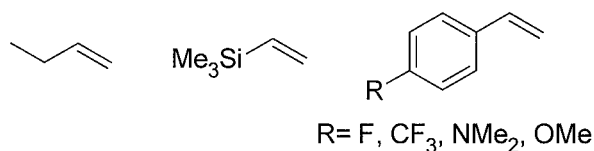
Figure 6.4. Possible alkene sources for intermolecular hydroamination.

6.2.3 Amidate Complexes as Imido Precursors

Chapter 5 explored preliminary reactivity into imido precursors starting with a mono(amidate) bis(amido) yttrium complex. Multiple avenues can be further investigated in the synthesis of the elusive terminal yttrium imido. Initial experiments using 2,2'-bipyridine (bipy), could be complemented with modifications to the bipy molecule, such as 4,4'-di-*tert*-butyl-2,2'-bipyridine or 2,2':6',2''-terpyridine.[3,4] These bulkier groups may be able to induce α-H abstraction on their own, or may be able to stabilize the complex during deprotonation with strong bases.

In Chapter 5, an yttrium aryl complex was used in the synthesis of an yttrium amidate complex. The further synthesis of the yttrium anilido complex proved to be difficult, likely due to the difficult separation of product and aryl amine by-product. A suggestion for future work would be to use a different starting material, such as the yttrium alkyl complex Y(CH$_2$SiMe$_3$)$_3$(THF)$_2$.[5] The removal of the tetramethylsilane by-product would be more facile; furthermore, the Y-C bond is more reactive than a Y-N bond and may be more successful for forming an yttrium imido complex by α-H abstraction or by deprotonation.

Another option in group 3 imido research is to change the metal centre entirely. Scandium has a similar ionic radius (Sc^{3+} = 0.745 Å) to that of Zr^{4+} (0.72 Å) and U^{5+} (0.76 Å).[6] Both zirconium and uranium terminal imido complexes have been successfully

synthesized;[7-9] the similar size of scandium makes it a good candidate for imido precursor synthesis.

6.2.4 Yttrium Amidates as Atomic Layer Deposition Precursors

The computer industry has led a large increase in research involving metal-oxide semiconductor field-effect transistors (MOSFET). The size of these transistors is becoming smaller with the improvements in technology. Traditionally, SiO_2 is used as a gate oxide in MOSFET, but shrinking the thickness of the SiO_2 layer has led to tunneling, and high leakage currents in the transistors.[10] Lanthanide oxides (typically Ln_2O_3) have a higher dielectric constant than SiO_2, which allows for gate oxide layers with less tunneling and current leakage. The most common method of forming these lanthanide oxide layer, is atomic layer deposition (ALD) of lanthanide complexes.[10] Many lanthanide complexes have been used as ALD precursors, and amidinate and acetoacetonate complexes are the most successful.[11-14] The key features of these complexes is that they are volatile, and typically contain alkyl groups on the ligand backbone. The amidate ligand is very similar to these ligand sets, as shown in Chapter 1, and could be used in the formation of lanthanide complexes for ALD precursors. The alkyl amide proligands introduced in Chapter 2 were used in preliminary reactions with yttrium, which were found to be inconclusive (Figure 6.5). Dimers or oligomers of yttrium were likely forming due to the lack of steric bulk at nitrogen, compared to the 2,6-dimethylphenyl or 2,6-diisopropylphenyl substituents. Dimer compounds of lutetium have shown to be volatile, so oligomers of yttrium may still be applicable in ALD.[14] These reactions were not optimized, and yttrium amidate complexes could be isolable and used as ALD precursors if research was continued.
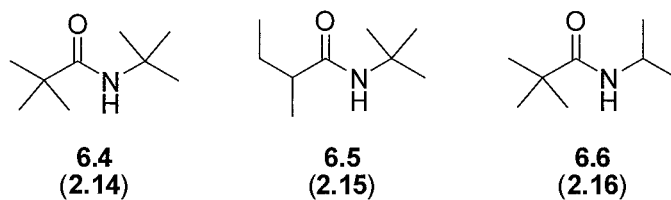
Figure 6.5. Amide proligands introduced in Chapter 2.

6.2.5 Imidates (O,N,O chelate) as a Ligand Set for Rare Earths

In Chapter 1 many different ligand sets for yttrium complexes were introduced. Many of these binding motifs formed a six-membered ring upon chelation, such as acetoacetonate,[15-18] and β-diketiminate ligands.[19-26] A similar binding motif to these ligand sets as well as the amidate ligand, is the imidate ligand. The only crystallographically determined O,N,O binding mode on yttrium results from isocyanate insertion into a yttrium caprolactamate.[27] The imidate ligand can be formed from the imide proligand, which has a similar synthesis to the amidate ligand set (Figure 6.6). One difference is that a primary amide is first formed by reaction of an acid chloride and ammonium hydroxide, and then further reacted with another acid chloride to obtain the imide proligand. Two examples, **6.10** and **6.11**, have been synthesized and fully characterized.
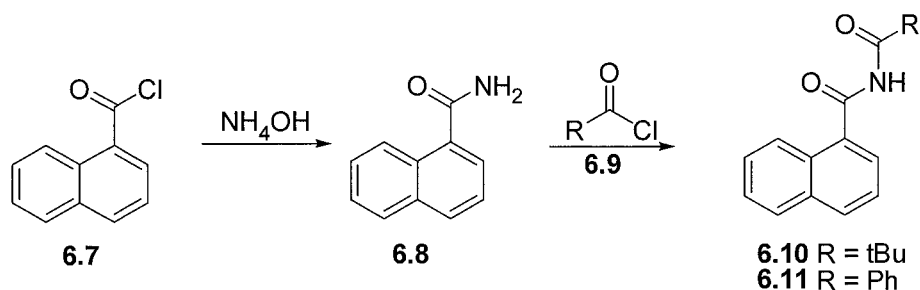
Figure 6.6. Synthesis of imide proligands **6.10** and **6.11**.

Initial experiments into preparation of an yttrium imidate complex followed the general procedure used for yttrium amidate formation. The reaction conditions were not optimized, and only a few attempts at synthesizing complex **6.12** were performed.
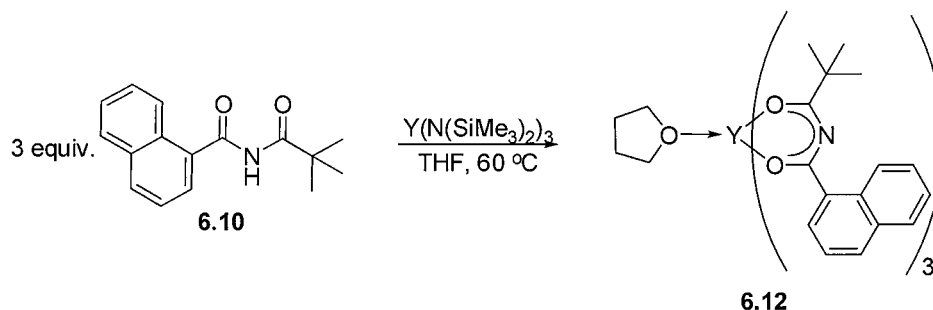
Figure 6.7. Synthesis of imidate complex **6.12**.

^{1}H NMR and IR spectra of complex **6.12** were obtained. Each possess similar features to amidate complexes. The ^{1}H NMR spectrum contained other very minor products that even after recrystallization were not removed. However, the spectrum did contain major peaks that correspond to complex **6.12**. Just as in the yttrium amidate synthesis, one molecule of THF is bound by the metal centre as evidenced by the THF signals in the ^{1}H NMR spectrum (δ 3.63 and 1.21), which are shifted slightly from unbound THF (δ 3.57 and 1.40).[28] The ^{1}H NMR spectrum contains the diagnostic *ortho*-naphthyl proton at δ 9.67, which is a large downfield shift from the proligand (*ortho*-naphthyl proton for **6.10** is at δ 8.18). Complex formation was confirmed by the lack of the N-*H* proton signal (δ 8.43 in **6.10**).

X-ray quality crystals were formed by dissolving **6.12** in a minimum amount of toluene and cooling to -30 °C. The solid-state molecular structure of complex **6.12** has a pseudo mono-capped octahedral geometry, with O2 and O6 as the axial ligands, and O5 as the

capping ligand (Figure 6.8, Table 6.1). The average C-N and C-O bond lengths in the imidate backbone are 1.345 Å and 1.259 Å, respectively, indicating delocalization through the chelate. The average Y-O bond for the imidate ligand is 2.264 Å, which is very similar to the yttrium amidate complexes. The average imidate bite angle (O-Y-O) is 72.44°, which is much larger than the 4-membered metallacycle for the yttrium amidate complexes.
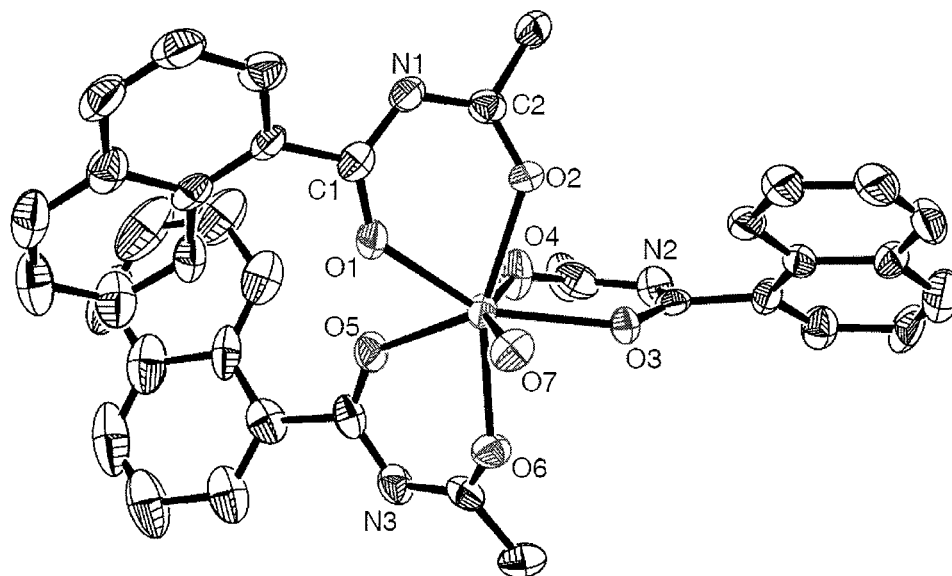
Figure 6.8. Solid-state molecular structure of complex **6.12**. THF methylene and *tert*-butyl methyl carbons have been removed for clarity.

Table 6.1. Selected bond lengths (Å) and angles (°) for complex **6.12**.

	Bond Length (Å)		Bond Angle(°)
Y1-O1	2.268(4)	Y1-O1-C1	136.3(4)
O1-C1	1.267(6)	O1-C1-N1	115.0(6)
C1-N1	1.332(7)	C1-N1-C2	120.6(5)
N1-C2	1.339(7)	N1-C2-O2	126.3(6)
C2-O2	1.264(6)	C2-O2-Y1	132.6(4)
O2-Y1	2.288(4)	O1-Y1-O2	71.19(14)
Y1-O3	2.286(4)	O3-Y1-O4	73.40(14)
Y1-O4	2.230(4)	O5-Y1-O6	72.73(14)
Y1-O5	2.264(4)		
Y1-O6	2.250(4)		
Y1-O7	2.349(4)		

There is still much to learn of this new class of yttrium compounds. The reaction conditions have not been optimized, and full characterization was not obtained. Synthesis of an yttrium imidate complex using imide **6.11** was also not optimized. Presumably imidate complex **6.12** can also initiate ε-caprolactone ring-opening polymerization (ROP), which has yet to be investigated. Furthermore, the synthesis of mono and bis(imidinate) yttrium complexes has not been attempted. Since these are a new class of yttrium compounds, the chemistry involved could extend to the range of reactivities explored in this thesis. The same investigations, such as ε-caprolactone ROP, hydroamination of aminoalkenes, and yttrium imido precursor synthesis could be performed with the analogous mono, bis and tris(imidate) yttrium complexes.

6.3   Summary

The research presented in this thesis is a new avenue in amidate chemistry for the Schafer group. It is merely the beginning of research into these group 3 amidate compounds, and already some continuing research into lactide polymerization has been initiated. The other research proposed in this section would extend the work in this thesis. Yttrium complexes are generally under-exploited in catalysis in spite of their low cost and promising reactivity trends in a range of transformations. The work presented here and subsequent proposed new directions take advantage of the modular amidate family of complexes. There are many accomplishments in this thesis and there are many more endeavors that can be explored from the foundations presented herein.

6.4 Experimental

6.4.1 Starting Materials and Reagents

All operations were performed under an inert atmosphere of nitrogen using standard Schlenk-line or glovebox techniques. THF, toluene, pentane, and hexanes were all purified by passage through an alumina column and sparged with nitrogen. $Y(N(SiMe_3)_2)_3$ was synthesized as described in literature,[29] or purchased from Aldrich and recrystallized from hexanes before use. All other chemicals were commercially available and used as received unless otherwise stated. ^1H and ^{13}C NMR spectra were recorded on Bruker AV300, AV400 and AV600 spectrometers. Shifts are reported in parts per million (ppm) relative to tetramethylsilane (TMS) and calibrated against residual solvent signal, coupling constants J are given in Hertz (Hz) (all couplings are ^3J unless otherwise stated). Infrared spectra were measured on a Nicolet 4700 spectrometer using KBr pellets and IR bands ν are reported in cm^{-1}. Elemental analyses and mass spectra were performed by the microanalytical laboratory of the Department of Chemistry at the University of British Columbia. X-ray crystallography was conducted at the University of British Columbia by Dr. Brian Patrick, Dr. Rob Thomson, or Neal Yonson.

6.4.2 Synthesis

Synthesis of *tert*-butyl(naphthyl) imide (6.10)

Under a flow of nitrogen, 1-Naphthoic chloride (6.00 mL, 40.0 mol) was added to a dry round bottom flask, equipped with a stir bar. An excess of ammonium hydroxide (100 mL) was added to the crude solid, in which a white gas was produced. The resultant mixture was stirred overnight and then filtered to
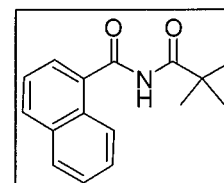
isolate a beige solid. The solid, 1-naphthoyl amide (**6.8**), was washed with water and then hexanes before use (Yield = 4.68 g, 68%). Lithium diisopropylamide (LDA) was prepared by adding n-butyllithium (22.7 mL, 1.60 M, 36.0 mmol) dropwise to a cooled (-78 °C) solution of diisopropylamine (5.10 mL, 36.0 mmol) in tetrahydrofuran (THF). The LDA solution was canula transferred to a solution of **6.8** (3.40 g, 20.0 mmol) in dry THF. The reaction mixture was stirred for 30 min at -78 °C, before trimethylacetyl chloride (2.45 mL, 20.0 mmol) was added via syringe. The colourless reaction mixture was warmed to room temperature and stirred overnight. The THF was removed in vacuo and the crude solid was redissolved in dichloromethane (DCM) and extracted with 1 x 30 mL 1 H aqueous HCl, 1 x 30 mL of 1 M aqueous NaOH, and 1 x 30 mL of brine. The DCM layer was then dried over $MgSO_4$, filtered and dried in vacuo to give a white solid. The solid was recrystallized by dissolving in minimum amount of DCM and adding hexanes until a white solid precipitated out of solution. Yield: 3.95 g, 78%. ^{1}H NMR (300 MHz, $CDCl_3$) δ 8.43 (broad s, 1H, N-*H*), 8.18 (d, *J* = 9 Hz, 1H, *ortho*-naphthyl-*H*), 7.96 (d, *J* = 9 Hz, 1H, aryl-*H*), 7.86 (m, 1H, aryl-*H*), 7.61-7.46 (m, 4H, aryl-*H*), 1.27 (s, 9H, C(C*H*$_3$)$_3$). ^{13}C NMR ($CDCl_3$, 75 MHz, 293K) δ 176.1 (*C*=O), 169.0 (*C*=O), 133.8, 133.1, 131.8, 129.9, 128.8, 127.7, 126.8, 125.7, 124.8, 40.5 (*C*(CH$_3$)$_3$), 27.2 (C(*C*H$_3$)$_3$). IR data (KBr, cm^{-1}): 3284 (s), 2971(s), 1733 (s), 1680 (w), 1511 (s), 1490 (s), 1248 (m), 1141 (w), 781 (w). EIMS (*m/z*): 255 [M]$^+$. Anal. found (calcd for $C_{16}H_{17}NO_2$): C 75.64% (75.27%), N 5.76% (5.49%), H 6.80% (6.71%).
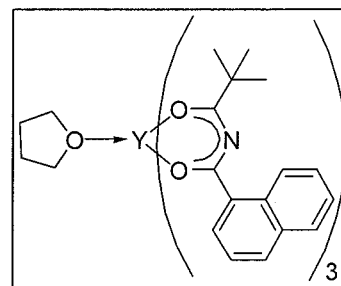
Synthesis of phenyl(naphthyl) imide (6.11)

The experimental method described for **6.10** was used in the preparation of **6.11** using n-butyllithium (7.50 mL, 1.53 M, 11.5 mmol), diisopropylamine (1.30 mL, 9.30 mmol), **6.8** (1.31 g, 7.66 mmol), and benzoyl chloride (1.07 mL, 9.23 mmol). Yield: 1.23 g, 58%. ^{1}H NMR (300 MHz, CDCl$_3$) δ 9.12 (broad s, 1H, N-H), 8.27 (d, J = 9 Hz, 1H, $ortho$-naphthyl-H), 7.97 (d, J = 9 Hz, 1H, aryl-H), 7.88 (m, 3H, aryl-H), 7.71 (d, J = 9 Hz, 1H, aryl-H), 7.60-7.42 (m, 6H, aryl-H). ^{13}C NMR (CDCl$_3$, 75 MHz, 293K) δ 168.7 (C=O), 165.5 (C=O), 133.6, 133.1, 132.8, 132.4, 131.9, 129.9, 128.8, 128.5, 127.8, 127.7, 126.6, 125.9, 124.7, 124.5. IR data (KBr, cm^{-1}): 3482 (br), 3235 (s), 1716 (s), 1671 (w), 1509 (s), 1499 (s), 1233 (m), 1198 (w), 780 (w). EIMS (m/z): 275 [M]$^+$. Anal. found (calcd for C$_{18}$H$_{13}$NO$_2$): C 78.14% (78.53%), N 5.00% (5.09%), H 4.80% (4.76%).
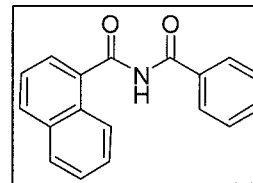
Synthesis of tris(*tert*-butyl(naphthyl)imidate)mono(tetrahydrofuran)yttrium (6.12)

Inside a nitrogen filled glovebox, a vial was charged yttrium tris(bis(trimethylsilyl)amide) (77.0 mg, 0.135 mmol) and a stirbar. To this, 5 mL of tetrahydrofuran (THF) was transferred to the reaction vessel at room temperature. Imide **6.10** (0.101 g, 0.396 mmol) was dissolved in 5 mL THF and transferred dropwise to the stirring solution of yttrium tris(bis(trimethylsilyl)amide in THF. The solution was stirred within the glovebox for 2 hours at 60 °C, and then filtered through Celite™ and concentrated under reduced pressure to a beige powder. The product was recrystallized by dissolving in a minimum amount of toluene and then left at -30 °C to yield colorless crystals. Yield: 0.102 g, 84%. X-

ray quality crystals were grown from cold toluene. Refer to Figure 6.8, Table 6.1 and Appendix III for crystallographic data. ^{1}H NMR (300 MHz, C_6D_6) δ 9.67 (broad s, 3H, *ortho*-naphthyl-*H*), 8.81 (d, *J* = 8 Hz, 3H, aryl-*H*), 7.64 (d, *J* = 8 Hz, 3H, aryl-*H*), 7.59 (d, *J* = 8 Hz, 3H, aryl-*H*), 7.23 (m, 6H, aryl-*H*), 7.02 (m, 3H, aryl-*H*), 3.63 (m, 4H, O-C*H₂*), 1.46 (s, 27H, C(C*H₃*)₃), 1.21 (m, 4H, O-CH₂C*H₂*). IR data (KBr, cm^{-1}): 3283 (w), 2956 (s), 1650 (s), 1558 (vs), 1408 (vs), 1376 (w), 1024 (w), 932 (s), 868 (w), 799 (s) cm^{-1}.

6.5 References

(1)   Ryu, J. S.; Li, G. Y.; Marks, T. J. *J. Am. Chem. Soc.* **2003**, *125*, 12584.

(2)   Ryu, J. S.; Marks, T. J.; McDonald, F. E. *Abstr. Pap. Am. Chem. Soc.* **2001**, *222*, U567.

(3)   Masuda, J. D.; Jantunen, K. C.; Scott, B. L.; Kiplinger, J. L. *Organometallics* **2008**, *27*, 1299.

(4)   Jantunen, K. C.; Scott, B. L.; Hay, P. J.; Gordon, J. C.; Kiplinger, J. L. *J. Am. Chem. Soc.* **2006**, *128*, 6322.

(5)   Arndt, S.; Voth, P.; Spaniol, T. P.; Okuda, J. *Organometallics* **2000**, *19*, 4690.

(6)   Shannon, R. D. *Acta Crystallogr., Sect. A* **1976**, *32*, 751.

(7)   Thomson, R. K.; Bexrud, J. A.; Schafer, L. L. *Organometallics* **2006**, *25*, 4069.

(8)   Graves, C. R.; Scott, B. L.; Morris, D. E.; Kiplinger, J. L. *J. Am. Chem. Soc.* **2007**, *129*, 11914.

(9)   Hayton, T. W.; Boncella, J. M.; Scott, B. L.; Palmer, P. D.; Batista, E. R.; Hay, P. J. *Science* **2005**, *310*, 1941.

(10)   Jones, A. C.; Aspinall, H. C.; Chalker, P. R.; Potter, R. J.; Kukli, K.; Rahtu, A.; Ritala, M.; Leskelä, M. *Mater. Sci. Eng., B* **2005**, *118*, 97.

(11)   Aspinall, H. C.; Bickley, J. F.; Gaskell, J. M.; Jones, A. C.; Labat, G.; Chalker, P. R.; Williams, P. A. *Inorg. Chem.* **2007**, *46*, 5852.

(12)   Kukli, K.; Ritala, M.; Pilvi, T.; Sajavaara, T.; Leskelae, M.; Jones, A. C.; Aspinall, H. C.; Gilmer, D. C.; Tobin, P. J. *Chem. Mat.* **2004**, *16*, 5162.

(13)   Paeivaesaari, J.; Dezelah, C. L. I. V.; Back, D.; El-Kaderi, H. M.; Heeg, M. J.; Putkonen, M.; Niinistoe, L.; Winter, C. H. *J. Mater. Chem.* **2005**, *15*, 4224.

(14)   Anwander, R.; Munck, F. C.; Priermeier, T.; Scherer, W.; Runte, O.; Herrmann, W. A. *Inorg. Chem.* **1997**, *36*, 3545.

(15)   Barash, E. H.; Coan, P. S.; Lobkovsky, E. B.; Streib, W. E.; Caulton, K. G. *Inorg. Chem.* **1993**, *32*, 497.

(16)   Liu, W.; Zhu, Y.; Tan, M. *J. Coord. Chem.* **1991**, *24*, 107.

(17)   Plaziak, A. S.; Zeng, C. H.; Costello, C. E.; Lis, S.; Elbanowski, M. *Inorg. Chim. Acta* **1991**, *184*, 229.

(18)   Wang, R.; Song, D.; Seward, C.; Tao, Y.; Wang, S. *Inorg. Chem.* **2002**, *41*, 5187.

(19)   Avent, A. G.; Caro, C. F.; Hitchcock, P. B.; Lappert, M. F.; Li, Z.; Wei, X.-H. *Dalton Trans.* **2004**, 1567.

(20)   Hayes, P. G.; Welch, G. C.; Emslie, D. J. H.; Noack, C. L.; Piers, W. E.; Parvez, M. *Organometallics* **2003**, *22*, 1577.

(21)   Liddle, S. T.; Arnold, P. L. *Dalton Trans.* **2007**, 3305.

(22)   Sanchez-Barba, L. F.; Hughes, D. L.; Humphrey, S. M.; Bochmann, M. *Organometallics* **2005**, *24*, 3792.

(23)   Sanchez-Barba, L. F.; Hughes, D. L.; Humphrey, S. M.; Bochmann, M. *Organometallics* **2006**, *25*, 1012.

(24)   Vitanova, D. V.; Hampel, F.; Hultzsch, K. C. *Dalton Trans.* **2005**, 1565.

(25)   Vitanova, D. V.; Hampel, F.; Hultzsch, K. C. *J. Organomet. Chem.* **2005**, *690*, 5182.

(26)   Wei, X.; Cheng, Y.; Hitchcock, P. B.; Lappert, M. F. *Dalton Trans.* **2008**, 5235.

(27)   Evans, W. J.; Fujimoto, C. H.; Ziller, J. W. *Organometallics* **2001**, *20*, 4529.

(28)   Gottlieb, H. E.; Kotlyar, V.; Nudelman, A. *J. Org. Chem.* **1997**, *62*, 7512.

(29)   Bradley, D. C.; Ghotra, J. S.; Hart, F. A. *J. Chem. Soc., Dalton Trans.* **1973**, 1021.

Appendix I

Crystallographic details for complexes **2.18**, **2.24**, **2.25**, **2.27** and **2.28** from Chapter 2.

	2.18	**2.24** (2 molecules tol)	**2.25**
Emperical Formula	$C_{73}H_{80}N_3O_4Y$	$C_{70}H_{90}N_3O_3Si_2Y$	$C_{50}H_{68}F_6N_3O_3Si_2Y$
f_w	1152.31	1166.54	1018.16
Morphology, colour,	Chip, colorless	Prism, colourless	Plate, colourless
Temperature (K)	173(2)	173(2)	173(2)
Wavelength (Å)	0.71073	0.71073	0.71073
Cryst. syst., space group	Monoclinic, $P\,2_1/c$	Monoclinic, $P\,2_1/n$	Triclinic, $P\,\text{-}1$
Unit cell dimensions a, b, c **(Å)**	13.7820(11), 33.598(3), 16.0575(12)	13.2111(8), 20.1020(14), 24.9192(17)	13.5055(5), 14.0512(4), 16.4069(6)
α, β, γ **(°)**	90, 98.762(3), 90	90, 101.524(2), 90	71.270(2), 73.207(2), 66.732(2)
Volume (Å³), Z	7348.7(10), 4	6484.4(7), 4	2661.40(16), 2
Calcd. Density (g/cm³)	1.042	1.195	1.271
Abs. coeff (mm⁻¹)	0.837	0.983	1.203
F **(000)**	2440	2488	1068
Cryst. size (mm)	0.25 x 0.20 x 0.20	0.30 x 0.25 x 0.20	0.50 x 0.20 x 0.070
Data collection θ range (°)	1.77 – 22.77	1.63 - 22.50	1.62 – 22.75
Limiting indices	-12 ≤ h ≤ 14, -36 ≤ k ≤ 36, -17 ≤ l ≤16	-14 ≤ h ≤ 13, -21 ≤ k ≤ 21, -26 ≤ l ≤ 26	-14 ≤ h ≤ 13, -15 ≤ k ≤ 15, -17 ≤ l ≤ 17
Reflections collected	43713	37610	18825
Indep. reflections	9816 [R(int) = 0.0735]	8456 [R(int) = 0.0636]	6783 [R(int) = 0.0837]
Completeness to max θ (%)	98.8	99.8	94.3
Abs. correction	Semi-empirical from equivalents	Semi-empirical from equivalents	Semi-empirical from equivalents
Max and min transmn	0.846 and 0.515	0.8215 and 0.3382	0.9192 and 0.6497
Refinement method	Full-matrix least squares on F^2	Full-matrix least squares on F^2	Full-matrix least squares on F^2
Data/restraints/param	9816/0/744	8456/0/728	6783/0/595
GOF on F^2	0.976	1.026	0.951
Final R indices [$I > 2\sigma(I)$]	R1 = 0.0614, wR2 = 0.1492	R1 = 0.0492, wR2 = 0.0980	R1 = 0.0475, wR2 = 0.0867
R indices (all data)	R1 = 0.1040, wR2 = 0.1649	R1 = 0.0844, wR2 = 0.1124	R1 = 0.1011, wR2 = 0.0969
Largest diff. peak and hole (e/Å³)	0.590 and -1.863	0.648 and -0.508	0.417 and -0.345

Complex	2.27	2.28
Emperical Formula	$C_{39}H_{68}N_3O_2Si_4Y$	$C_{33}H_{70}N_3O_2Si_4Y$
f_w	812.23	742.19
Morphology, colour,	Plate, colourless	Prism, colourless
Temperature (K)	173(2)	173(2)
Wavelength (Å)	0.71073	0.71073
Cryst. syst., space group	Orthorhombic, $P\,2_1\,2_1\,2_1$	Monoclinic, $C\,2/c$
Unit cell dimensions a, b, c (Å)	11.6377(14), 19.076(2), 20.423(2)	30.5629(9), 19.4095(4), 15.8674(4)
α, β, γ (°)	90, 90, 90	90, 115.7900(10), 90
Volume (Å^3), Z	4534.1(9), 4	8475.2(4), 8
Calcd. Density (g/cm^3)	1.190	1.163
Abs. coeff (mm^{-1})	1.425	1.519
F (000)	1736	3200
Cryst. size (mm)	0.35 x 0.20 x 0.08	0.20 x 0.20 x 0.10
Data collection θ range (°)	1.99 – 28.12	1.48 – 25.43
Limiting indices	$-15 \le h \le 14, -22 \le k \le 25, -26 \le l \le 14$	$-36 \le h \le 36, -15 \le k \le 23, -19 \le l \le 19$
Reflections collected	34857	37105
Indep. reflections	10974 [R(int) = 0.0616]	7770 [R(int) = 0.0447]
Completeness to max θ (%)	99.3	99.2
Abs. correction	Semi-empirical from equivalents	Semi-empirical from equivalents
Max and min transmn	0.8945 and 0.6354	0.8642 and 0.6766
Refinement method	Full-matrix least squares on F^2	Full-matrix least squares on F^2
Data/restraints/param	10974/0/488	7770/0/503
GOF on F^2	0.998	1.014
Final R indices [$I >$ $2\sigma(I)$]	R1 = 0.0466, wR2 = 0.0787	R1 = 0.0669, wR2 = 0.1581
R indices (all data)	R1 = 0.0877, wR2 = 0.0890	R1 = 0.1082, wR2 = 0.1935
Largest diff. peak and hole (e/Å^3)	0.335 and -0.294	1.067 and -1.160

Appendix II

Crystallographic details for complexes **5.16**, and **5.18** from Chapter 5.

	5.16	**5.18**
Emperical Formula	$C_{45}H_{68}N_3O_2Si_2Y$	$C_{51}H_{68}N_5OSi_2Y$
f_w	828.11	912.19
Morphology, colour,	Prism, yellow	Prism, red
Temperature (K)	173(2)	173(2)
Wavelength (Å)	0.71073	0.71073
Cryst. syst., space group	Triclinic, P-1	Monoclinic, $P\,1\,2_1/n\,1$
Unit cell dimensions a, b, c (Å)	12.3861(7), 12.4287(7), 17.5174(10)	16.2277(17), 23.826(3), 16.7482(18)
α, β, γ (°)	73.689(3), 72.551(3), 77.253(3)	90, 100.624(4), 90
Volume (Å^3), Z	2441.5(2), 2	6364.6(12), 4
Calcd. Density (g/cm^3)	1.126	0.952
Abs. coeff (mm^{-1})	1.278	0.985
F (000)	884	1936
Cryst. size (mm)	0.25 x 0.20 x 0.15	0.40 x 0.15 x 0.06
Data collection θ range (°)	1.73 – 28.37	1.71 - 22.60
Limiting indices	$-16 \le h \le 16, -16 \le k \le 15, -23 \le l \le 21$	$-17 \le h \le 16, -25 \le k \le 25, -15 \le l \le 18$
Reflections collected	48561	38602
Indep. reflections	11827 [R(int) = 0.0444]	8359 [R(int) = 0.1049]
Completeness to max θ (%)	96.6	99.1
Abs. correction	Semi-empirical from equivalents	Semi-empirical from equivalents
Max and min transmn	0.8256 and 0.6967	0.9432 and 0.6939
Refinement method	Full-matrix least squares on F^2	Full-matrix least squares on F^2
Data/restraints/param	11827/0/491	8359/0/559
GOF on F^2	1.048	0.905
Final R indices [$I > 2\sigma(I)$]	R1 = 0.0424, wR2 = 0.1056	R1 = 0.0497, wR2 = 0.1002
R indices (all data)	R1 = 0.0590, wR2 = 0.1100	R1 = 0.1068, wR2 = 0.1116
Largest diff. peak and hole (e/Å^3)	0.582 and -0.491	0.333 and -0.502

201

Appendix III

Crystallographic details for complex **6.12** from Chapter 6.

	6.12
Emperical Formula	$C_{52}H_{56}N_3O_7Y$
f$_w$	923.91
Morphology, colour,	Prism, yellow
Temperature (K)	173(2)
Wavelength (Å)	0.71073
Cryst. syst., space group	Monoclinic, $P\,2_1/\,c$
Unit cell dimensions a, b, c **(Å)**	22.593(3), 9.1237(10), 23.576(2)
α, β, γ (°)	90, 101.846(4), 90
Volume (Å^3), Z	4756.2(9), 4
Calcd. Density (g/cm^3)	1.290
Abs. coeff (mm^{-1})	1.280
F (000)	1936
Cryst. size (mm)	0.30 x 0.20 x 0.20
Data collection θ range (°)	1.82 – 22.56
Limiting indices	$-24 \leq h \leq 24$, $-9 \leq k \leq 9$, $-25 \leq l \leq 24$
Reflections collected	27337
Indep. reflections	6210 [R(int) = 0.1239]
Completeness to max θ (%)	99.2
Abs. correction	Semi-empirical from equivalents
Max and min transmn	0.774 and 0.617
Refinement method	Full-matrix least squares on F^2
Data/restraints/param	6210/0/577
GOF on F^2	0.999
Final R indices [$I > 2\sigma(I)$]	R1 = 0.0543, wR2 = 0.1022
R indices (all data)	R1 = 0.1286, wR2 = 0.1256
Largest diff. peak and hole (e/Å^3)	0.548 and -0.307